REPUBLIC OF KENYA

MINISTRY OF ENERGY

Geological, volcanological and hydrogeological controls on the occurrence of geothermal activity in the area surrounding Lake Naivasha, Kenya

1990

Geological, volcanological and hydrogeological controls on the occurrence of geothermal activity in the area surrounding Lake Naivasha, Kenya

MINISTRY OF ENERGY

Geological, volcanological and hydrogeological controls on the occurrence of geothermal activity in the area surrounding Lake Naivasha, Kenya

with coloured 1:250 000 geological maps

M. C. G. Clarke, D. G. Woodhall, D. Allen and G. Darling

with contributions by

J. K. Kinyariro, F. M. Mwagongo, J. P. Ndogo, W. Burgess, K. Ball, S. Scott, N. J. Fortey
B. Beddoe-Stephens, A. Milodowski, P. H. A. Nancarrow and L. A. J. Williams

NAIROBI 1990

CONTENTS

PLATES (pages 49–54 and 81–85)

TABLES

EXECUTIVE SUMMARY

Geothermal power is a very important form of indigenous energy in Kenya and is planned to be harnessed to generate a much greater proportion of the country's electricity in the coming decades than is the case at present. To prepare for this increase the Ministry of Energy is working with foreign institutions in both development and exploration programmes. This report gives the results of the first phase of one exploration programme, carried out with the assistance of the British Geological Survey under the terms of the Government of Kenya–United Kingdom Technical Cooperation Agreement and in conjunction with the UNDP who funded work in adjacent areas.

The initial task was the detailed geological and geothermal mapping of the Longonot volcano and surroundings in the central Rift Valley, and also reconnaissance sampling of surface waters over the whole length of the rift; no drilling was envisaged. At an early stage it was decided to include the areas previously explored in detail at Olkaria and Eburru as there were no modern maps showing the setting of these important geothermal resource areas within the broader geology of the rift and it was considered important to be able to compare relevant features of the three volcanoes. The detailed observations are summarised in this text and on the two 1:100 000 scale coloured maps included with this text.

The text is divided into six sections—**Section One** gives more details of the future economic importance attached to the development of geothermal power in Kenya and the relationship of the various institutions involved.

Section Two summarises the global and regional geological and geophysical setting of the Rift Valley which is seen to be part of a worldwide network of seismically and volcanically active belts which include most of the important geothermal regions of the world. These belts have a high 'geothermal gradient' due to the presence of hot magma at shallow depths and volcanoes are formed when this magma is released at the earth's surface. The geological and geophysical data shows that the central rift valley is particularly favourable for the probability of shallow heat sources which form one of the two essential prerequisites for the localisation of exploitable geothermal fields. The second prerequisite is the presence of sufficient underground water in the hot rock areas to allow the formation of the large quantities of steam needed to drive the turbines which generate electricity. Section Two therefore also outlines the regional natural water circulation pattern (Hydrology).

Section Three gives details of the physical form and make-up of the various volcanic features in the map area. These geological and geovolcanological studies involved prolonged fieldwork including the climbing of steep crater walls and traversing areas of bush sometimes inhabited by buffolo, lion and leopard. This work has revealed the history of volcanic events which occurred at the three major centres—Longonot, Olkaria and Eburru and the relationship of the minor volcanic features in the Elmenteita/Badlands, Ndabibi and Akira plains areas. The single most important feature at both Longonot and Olkaria is the presence of geothermally active major volcanic ring structures. These indicate the probability of very widespread shallow heat sources. Radiocarbon dating of specific layers in the volcanic products has allowed absolute ages to be assigned to the volcanic activity, much of which at both Longonot and Olkaria has occurred in the last 9000 years and some in the last 300 years. Such ages mean that these volcanoes are dormant rather than extinct and emphasise the continued presence of shallow heat sources.

Section Four reports and interprets results of laboratory examination and analysis of samples of the various rock formations which typify the various volcanic centres. An important result of the microscope examination was the recognition of 'solution porosity' apparently caused by the hot gases and fluids trapped in the cooling volcanic rocks. Rocks of high porosity have a better geothermal potential than those with low porosity due to an increased ability to allow water to travel through them. This feature was seen in a suite of rock fragments which has been erupted from Longonot and it is recommended that further study is made of this phenomenon.

Rock chemical analysis shows that Longonot, Olkaria and Eburru each have distinct chemistry, although they all are highly alkaline. Olkaria rocks contain much higher average contents of some trace elements such as Uranium and Thorium, this may be an important factor controlling the localisation of a major crustal heat anomaly.

Section Five gives the results of geothermal mapping and some studies of soil and fumarole gas. The accurate positioning and recording of all known and newly located thermal sites including hot springs, steam jets, steaming ground, ground with signs of past thermal activity plus the sites and yields of water boreholes with above-ambient temperatures was part of the routine fieldwork and forms much of the content of the geotherm map. The numerous fumaroles within Longonot crater were mapped systematically for the first time together with newly located sites to the south of the crater. Previously known data from west Olkaria were integrated with the new data from east of the gorge in the Domes area. Some new sites were located at Eburru and add to the data for that area.

The most important single result was the recognition that the Olkaria activity, i.e. shallow heat source, extends east of the Njorowa gorge as part of a major volcanic ring structure. This effectively increases the area of geothermal potential for the Olkaria Complex alone, by 30 square km.

Exploration for geothermal activity concealed by recent ash falls was initiated using soilgas carbon dioxide and radon detection. This proved that the Mt Margaret area and the Longonot ring fracture are possibly thermally active even though there is little or no surface indication.

A study of comparative carbon dioxide/radon ratios in fumarole gas showed that although the former is always present, radon at Olkaria and, to a lesser extent, Eburru, is much higher than at Longonot, Suswa and Mt Margaret. It is suspected that high radon levels signify higher permeability and therefore, using this factor alone, that Longonot and Suswa have less potential.

Section Six describes the many physical and chemical hydrogeological studies carried out as part of the project. Records from 596 water boreholes were used to construct a map of the water table surface which shows that water flows south from Lake Naivasha through the Olkaria Field. A smaller northward flow under Eburru is also indicated. Permeabilities (the ability for underground flow) are relatively low but the presence of numerous faults longitudenal to the Rift may assist water movement and may account for the presence of warm water issuing at Magadi, far from any obvious heat source. Water balance studies do not indicate that extraction of steam at the Olkaria geothermal field will affect Lake Naivasha water levels.

This section includes much new chemical data from most of the larger springs and lakes in the Rift and from the Bala springs at Homa Mountain, Western Kenya, but in no case does the hydrogeological data alone indicate the presence of a previously unknown geothermal area. Chemical studies included the collection of much oxygen and hydrogen isotope data which throw light on the past history of the waters. Interpretation of these data indicates that all the fluids sampled from wells could be derived from a mixture of rain falling on the rift wall and water from rift lakes. There is no evidence of a deep thermal water as proposed by previous studies.

Gases in the geothermal fluids are dominated by crustally derived carbon dioxide, usually followed by methane. Helium and hydrogen have been detected at Eburru and Longonot indicating venting from deep magma bodies. A disappointing aspect was the lack of much viable data from the geothermometer studies. Detailed discussion is reported of new and previous hydrochemical data for the Olkaria Well field and for Lake Magadi.

GENERAL CONCLUSIONS ON AREAS WITH GEOTHERMAL POTENTIAL

1. Areas with the highest geothermal potential lie within or adjacent to large ring structures at Olkaria and Longonot. These structures indicate the presence of large shallow magma bodies (heat sources) of geologically very young age.

2. These heat sources lie south of Lake Naivasha and across the presumed path of water flowing underground out of that lake.

3. The Olkaria ring structure has the most apparent potential as it localises very numerous young volcanic subcentres, has the greater number of fumaroles and has a far higher radon emission.

4. The south-west quadrant of the Longonot caldera also has potential but surface indications are largely masked by a later blanket of ash.

5. The coincidence of high values of soilgas carbon dioxide with the tectono-volcano axis running from Longonot crater in the area of Mt Margaret also indicates a possible potential resource area.

6. The relatively narrow thermal zone at Eburru together with the lack of a recogniseable thermally active ring structure would, on the criteria used above, indicate that this area might have a lower potential than the unexplored parts of Olkaria, or even Longonot.

RECOMMENDATIONS

The following areas, in order, should be considered for exploration scout drilling:

i The area occupied by the Olkaria ring structure lying immediately east of the Njorowa Gorge and sometimes called the Domes area, plus its extention to the southeast.

ii The southeast quadrant of the Longonot Caldera.

iii The area between the Satellite Station on the Narok road, and Mt Margaret.

1 Introduction

1.1 PREVIOUS EXPLORATION FOR, AND PRESENT STATUS OF, GEOTHERMAL ENERGY IN KENYA

Over 30 years ago it was recognised that the Central Rift Valley, in particular the Olkaria area, might contain a geothermal energy resource. In 1956 two wells were drilled and the second, X2, located approximately 3 km north-west of the present production field, reached a depth of 1035 m with temperatures up to 235°C. This promising result was not followed up until 1970, when the Government of Kenya (GOK), together with the United Nations Development Programme (UNDP), commenced a detailed surface investigation of the Olkaria, Eburru and Bogoria areas. The geological, geothermal geophysical and hydrological data were reviewed in 1972 and top priority was given to the Olkaria area (GENZL, 1986) on the basis of the following three important factors:

1 The occurrence of high natural heat flow (e 400 MW (t))—similar to that at Wairakei, New Zealand—a well known proven resource.

2 The presence of a high-temperature sodium chloride water at relatively shallow depths (1100 m), again similar to that at Wairakei,where it had been successfully exploited for electricity generation.

3 The possibility that some parts of the Olkaria system were steam dominated with similar physical properties as those at Lardarello in Italy, another successfully exploited geothermal system.

A programme of exploration drilling began in 1973 and lead to the establishment, by 1981, of a production field immediately west of the Hell's Gate Gorge. Although individual wells have a lower than average power production (in world terms), power generation has been successful and at present stands at 45 MW installed, from an area of approximately 1.5 km^2.

Exploration drilling has been, and continues to be, undertaken to the north and west of the production field. Two of these wells are better producers than those in the presently exploited field, and enhance the potential of Olkaria as a future major energy resource.

In the early 1980s, attention was again focused on Eburru and a detailed re-investigation of the surface phenomena was carried out by the GOK with the assistance of Japan International Co-operation Agency (JICA). Plans have been made to drill six holes at Eburru with the aid of water from Lake Naivasha.

As a result of the success of the Olkaria project and the assumed high potential at Eburru the possibility of a future expansion in geothermal energy generation was taken very seriously and now forms an important element of the future energy resources identified in the recent National Power Development Plan (Acres, 1987). This provides GOK with a comprehensive master plan for the orderly and economic expansion of generation and transmission facilities in Kenya.

1.2 THE NATIONAL (KENYAN) EXPLORATION FOR GEOTHERMAL ENERGY PROJECT

The National Project's objectives are to undertake geothermal reconnaissance in the Rift Valley in order to inventorise geothermal resources and to identify priority areas for future development, given that geothermal resources are scheduled to produce 280 MW electrical energy by 2006 (Acres, 1987). Table 1 outlines the important role expected of geothermal energy in the future.

The UK project, the results of which are described in this memoir, was formulated to complement a larger input funded by UNDP, and close liaison on work programs and priorities was maintained between the UK team, the Kenyan Project Team Leader and the UN Co-ordinator. The combined input of these three institutions comprised the National (Kenyan) Exploration for Geothermal Energy Project.

During 1985–87 a combination of Kenyan, British and United Nations Development Programme personnel covered the area between Lake Bogoria in the North and Lake Magadi in the South (Figure 1). Exploration was extended to the young volcanoes north of Lake Baringo during a new GOK-UK project phase commenced in 1988.

The 1985–87 detailed reconnaissance work comprised three sub-areas: Suswa Volcano and surrounds (surveyed by UNDP); Longonot–Olkaria–Elmentaita (BGS), the results of which are summarised here, and Menengai–

Table 1.1 Econometric summary

1987 Kenya generation capacity

351 MW Hydro	(74.5%)	471 MW
75 MW Thermal	(16.0%)	
45 MW Geothermal	(9.5%)	

Predicted future demand:

Year	Peak load	
1990	517 MW	i.e. 5.6%/yr growth
1995	670 MW	
2000	871 MW	
2005	1123 MW	

Comparative costs of new projects:

Hydro	1.0–1.4 KSh/KWh
Thermal	1.0 KSh/KWh
Geothermal	0.6 KSh/KWh (Best = $0.036)

Planned new capacity

Hydro (in construction)	250 MW
Hydro (identified)	50 MW
Thermal	+ 200 MW
Geothermal (not proved)	280 MW

Estimated proportion of new investment to 2006

Hydro	15%	Total is several 100s million $US
Thermal	35%	
Geothermal	50%	

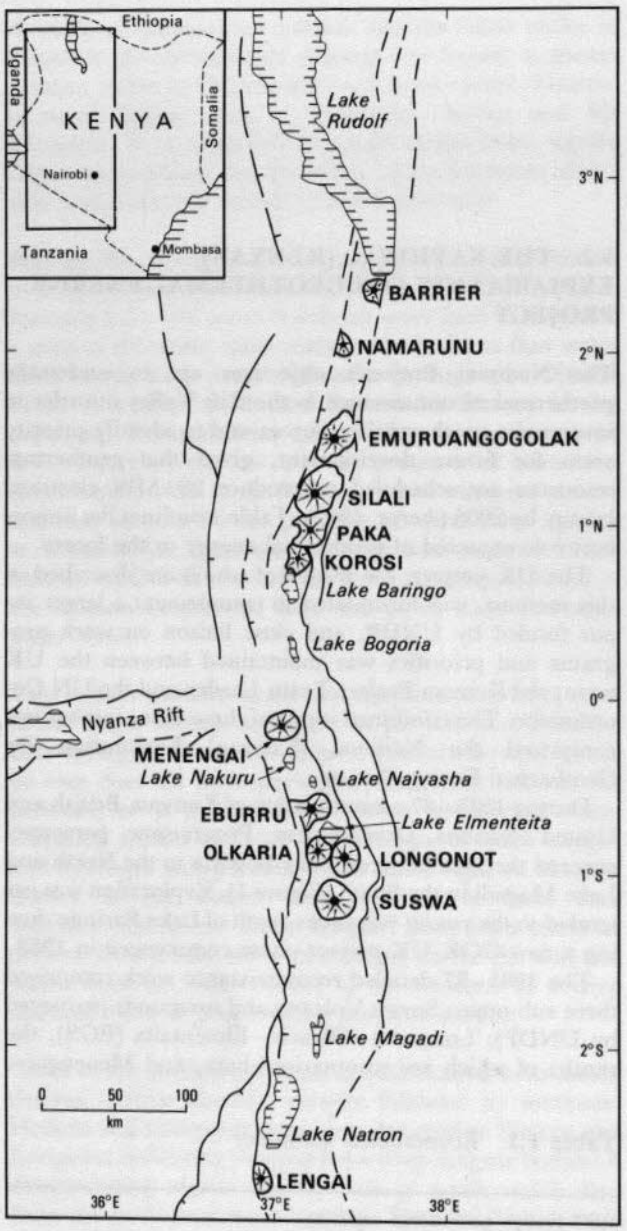

Figure 1.1 Kenya (Gregory) Rift Valley showing boundary faults, lakes and Recent volcanoes.

Bogoria (UNDP contractors GEOTERMICA ITALIANA). In addition, BGS made a study of the hot springs at Lake Magadi, which lies to the south of Suswa and also, for comparative purposes, some springs from Bogoria northwards. At a later stage, resistivity and gravity surveys over parts of each area were carried out by the UNDP contractor.

1.3 INSTITUTIONAL FRAMEWORK AND SUMMARY INPUT OF THE UK FUNDED PROJECT

In 1985 a Project Memorandum was signed by GOK and the UK Government concerning assistance in the field of Geothermal Exploration in terms of the bilateral Technical Co-operation agreement. The local institution was the Ministry of Energy and Regional Development, Geothermal Section. The UK scientific institution involved was the British Geological Survey, funded through the British Government's Overseas Development Administration (ODA). Close contacts in Nairobi were maintained with the East African Development Division (EADD), a regional office of ODA, and the British High Commission.

The UK personnel input consisted of two experts, residential for two years plus short term visiting specialists in various aspects of hydrogeology and geochemistry. Considerable laboratory and analytical work was also funded and vehicles and camp equipment provided for the fieldwork. Additionally funding was made available for six months work by an independent consultant, Dr L A J Williams, of Lancaster University UK.

The residential period terminated at the end of November 1987 but further funding was provided in UK for final report writing and the preparation of coloured maps for publication.

The UK work programme included the following activities:

1 Encouragement and training of local counterpart professional and technical staff, both in the field and office. By September 1987, it had been arranged that two counterpart geologists started a two year MSc course in UK. This course included economic geology and earth

Table 1.2 Reports submitted previous to this memoir (The following BGS reports have been submitted to the GOK authorities and copies distributed to other relevant bodies.)

a Eight Quarterly Reports including highlights and progress.

b Nine Project Technical Reports as follows:

BGS GEN/KEN/1	Bibliography of the geology of the Kenya Valley, with emphasis on the geothermal potential (submitted December 1985)
BGS GEN/KEN/2	Geological and Geothermal mapping (Progress Report for TRM January 1986)
BGS GEN/KEN/3	Regional Hydrogeological Investigations (Progress Report for TRM January 1986)
BGS GEN/KEN/4*	Compilation and interpretation of rock geochemical data for the Longonot Volcano and the Greater Olkaria Volcanic complex (submitted 7 September 1987)
BGS GEN/KEN/5*	The geology of Longonot Volcano, the Greater Olkaria Volcanic Complex and adjacent areas (submitted 7 September 1987)
BGS GEN/KEN/6*	Rn/CO_2 investigations at Longonot, and Olkaria and surrounding areas (submitted 5 November 1987)
BGS GEN/KEN/7*	Hydrogeology Progress Report, March–August 1987 (submitted 7 September 1987)
BGS GEN/KEN/9	Petrography and Mineralogy of lithic clasts and other rock specimens from the Longonot area, Kenya (submitted May 1988)
BGS SD/89/1	Geothermics and hydrogeology of the southern part of the Kenya Rift Valley. BGS Hydrogeology Series Research Report (submitted 1989)

* Advances copies also make available for contractors use. (Also submitted in September 1987 were draft geological and geothermal maps of the Longonot, Olkaria and adjacent areas).

resources exploration and was sucessfully completed by the two candidates in 1989.

2 Preparation of a bibliography, with abstracts, as a reference source concerning previous project related work on the Rift Valley. This was of immediate use to the other components of the national project.

3 Geological and volcanological investigation of an area of 3000 km^2 in the Rift Valley and its borders between Lake Elmenteita and the south slopes of Longonot. This area includes three major volcanic centres — Eburru, Olkaria and Longonot.

4 Exploration and investigation of geothermal surface manifestations of the above area.

5 Compilation of each of the above data sets as 1:50 000 map sheets, with additional cross sections.

6 Collection of rock samples for chemical analysis and petrographic studies and integration of this new data with that pre-existing in order to compare and contrast the magma composition and evolution at each of the main volcanoes.

7 Sampling of surface waters for chemical analysis and stable isotope determination. Stable isotope data for the UNDP geochemical studies were also provided.

8 Compilation and statistical analysis of physical hydrogeological data (mainly from water boreholes) between Lake Nakuru and Lake Magadi.

9 Investigation of radon/CO_2 in soil gas and fumaroles using rapid field methods.

10 Investigations of gas geochemical parameters including CH_4, C_2H_6 and $\delta^{13}C$.

11 Preparation of an integrated report on the geology and stratigraphy of the rift between the equator and 1°. north for which 1:125 000 scale geological maps had previously been published (EAGRU project maps). This report was compiled by the consultant, Dr Williams with the assistance of Dr Greg Chapman, BGS.

12 Preparation of Technical Reports for distribution and discussion at Technical Review Meetings, (TRM) held in Nairobi under the auspices of GOK and UNDP in February 1986 and November 1987 and for incorporation in the UNDP Project Final Report September 1987. (Table 2).

13 Preparation of published coloured geological and geothermal maps of the 1985–87 project area at a scale of 1:100 000.

2 Regional setting

2.1 INTRODUCTION

Hot springs (the most common surface indication of geothermal activity) are found in a number of places in Kenya both inside and outside the Rift Valley (Tole, 1986). However, preliminary work indicates that the enthalpy (relative energy potential) of occurrences outside the Rift Valley, is generally quite low and that subsurface temperatures do not reach the 200–230°c required as one of the prerequisites for electricity generation, within economic drilling depths. These 'low enthalpy' geothermal occurrences may well have potential as heat sources for, e.g. drying of agricultural or industrial products, baking, medicinal uses or local mineral water bottling but are not considered further in this report. High enthalpy geothermal resources, on present information, are present only within the Rift Valley (Figure 1.1).

2.2 PLATE TECTONIC CONSIDERATIONS AND GEOPHYSICAL EVIDENCE

The Rift Valley is part of a worldwide system of sublinear belts of active seismicity, volcanicity and heat flux defining the edges of lithospheric plates.

Three classes of plate margin are recognised, each one of which may localise geothermal resources:

(a) Constructive — Where oceanic crust is created at spreading centres, e.g. Red Sea; Mid Atlantic Ridge, including Iceland.

(b) Destructive — Where crust is consumed in subduction zones, e.g. Java–Sumatra Trench.

(c) Conservative — Where plates move relative to one another without creating or destroying crust, e.g. Transform margins as the San Andreas system.

The Kenyan Rift Valley conforms most closely with an incipient or early stage of type (a). It continues northwards through Ethiopia to the Afar region where it forms a 'triple junction' with the Red Sea and Gulf of Aden spreading axes where new crust is being generated (Figure 2.1).

In Kenya, however, separation is not complete although geophysical evidence strongly suggests that the lithosphere is anomalously thin representing the incipient nature of the breakup process (Wendland and Morgan, 1982).

In continental areas away from Rift zones and high mountain belts, the lithosphere consists of an upper layer of crustal rocks averaging 40 km in thickness underlain by 100 km of relatively rigid mantle. At the base of this is a seismic discontinuity marking the transition to less dense partially melted mantle (the low velocity zone of the asthenosphere), (Windley, 1984). A combination of gravity, seismic and heat flow data indicates that in the East African Rift system relatively normal crustal thickness characterises the Rift shoulders but that within the Rift this is reduced to 20 km. Furthermore the seismic data can be interpreted as indicating that the zone of partial melting (top of asthenosphere) may be in direct contact with the lower crust. (See Figure 2.2, after Fairhead, 1986). The general effect is of an approach to breakup involving 'necking' of the lithosphere and a greatly increased thermal gradient.

At the time of writing an important research programme (KRISP) is underway, aimed at further elucidation of the geodynamic processes taking place, by means of the deep seismic refraction method, (Khan et al.,1988).

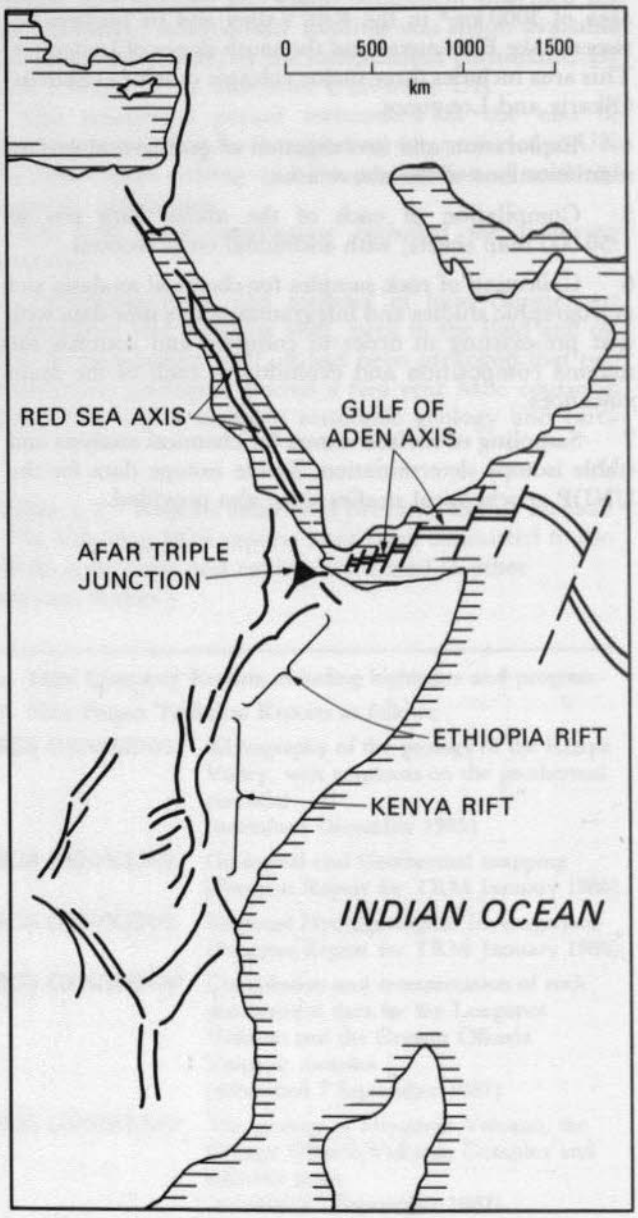

Figure 2.1 Relation of Kenya/Ethiopia Rift to the Red Sea and Gulf of Aden spreading axes.

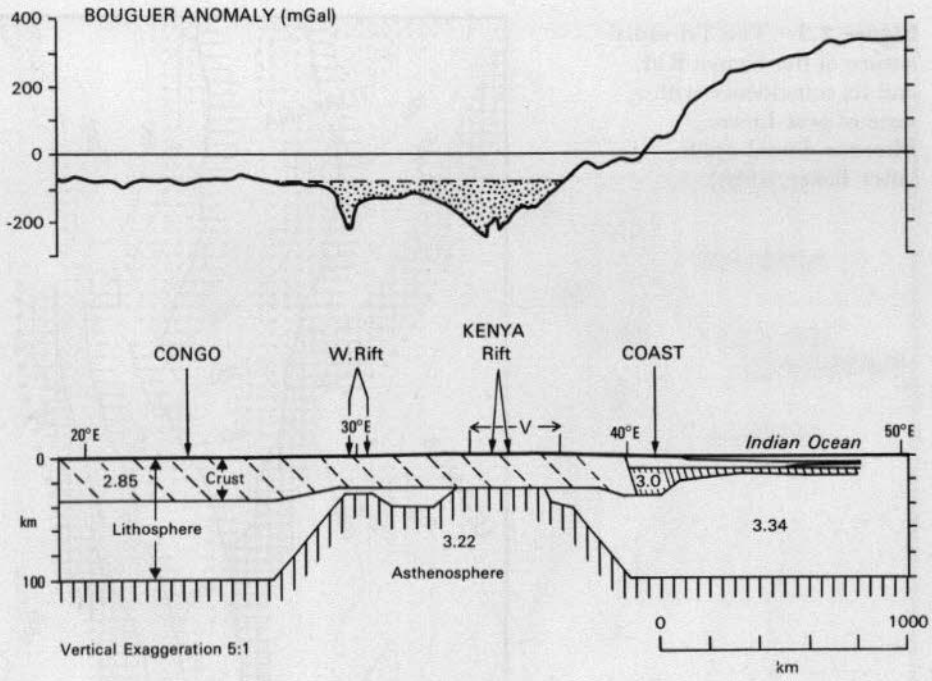

Figure 2.2 Regional E–W bouguer anomaly profile and lithospheric model through Central and Eastern Africa, (after Fairhead, 1986).

2.3 THE KENYA DOME AND THE TRI-RADIAL NATURE OF THE RIFT IN KENYA

In the past many of the syntheses explaining the present structure of the Kenya Rift, invoke the concept of a broad domal or shield structure as an integral stage in its development. The present day gross topography mirrors that dome with highlands 3000, and 4000 m asl between 2° north and south flanking the Rift and decreasing in altitude radially. The broad zone of high ground is cut by a prominent, generally north–south, fault-bounded trench—the Rift Valley.

Quite near to the culmination of this domal feature the generally north–south linearity of the Rift boundary faults shows a distinct elbow, changing from east of north in the Baringo–Suguta sector to east of south in the more southerly Nakuru–Naivasha sector (Figure 2.3).

From this inflection, a third graben feature extends westwards to Lake Victoria—this is the Nyanza Rift, thus illustrating the tri-radial nature of the Kenya Rift system.

This arm of the Rift differs from the other two, in that associated volcanicity is mostly pre-Quaternary in age and of carbonatite/nephelinite character (Le Bas, 1978) and does not include the highly salic compositions characteristic of the North and South arms of the Rift system.

The floor of the rift is highest in the central portion between Lake Nakuru and Lake Naivasha where it is almost 2000 m asl and decreases in altitude northwards towards Lake Turkana (300 m asl) and southwards towards Lake Magadi (600 m asl). Although the eastern portion of the Nyanza Rift, (see below), is overwhelmed by Plio-Pleistocene volcanics, further west its floor too conforms to the radial pattern, passing below the level of Lake Victoria at Kisumu to form the Winam Gulf.

The evidence for structural doming was based on quite scattered occurrences of Miocene sediments which in turn lead to the concept of a pre-Miocene erosion surface (Shackleton, 1951; Pulfrey, 1960) which was believed to show a gradual rise towards the Rift with a relatively sharp reversal of dip on the shoulders (Figure 2.3).

This domal structure and another coinciding with the Ethiopian Highlands are frequently related to explanations of some of the broad gravity anomalies of the region (Figure 2.4, after Fairhead, 1986). Refinement of the gravity database however, shows that the Rift axis coincides with a linear zone of higher gravity within this regional gravity low, (Figure 2.5).

The concept of a broad structural dome has been the subject of considerable discussion. King (1978) believed that there was a gentle basement arch over the Kenya Rift region, but that it developed earlier as a continental watershed consequent on the breakup of Gondwanaland. Williams, (1978), argues that much of the pre-Miocene topography near the Rift consisted of basement high ground, i.e. was not reduced to the pre-Miocene bevel required by earlier reconstructions.

The interpretation preferred here is that the present broad zone of high relief, characterising central Kenya and traversed by Rift faults, is in most part due to greater thicknesses of volcanics erupted in the central sections, i.e. the area might be considered analogous to a giant volcanic shield.

The zone where the three Rift arms meet has been considered to be a classic triple rift junction overlying a mantle plume (Geotermica Italiana, 1987, after Burke and Dewey, 1973) and initially lead to hypotheses that the junction area should be the most thermally anomalous part of the the present day rift system. However, the Geothermica mapping confirmed earlier observations, that the western (or Nyanzian) arm of the Rift has been inactive in the Pleistocene thus reducing the importance of the presumed triple junction as a control on present day volcanicity and therefore, geothermal activity.

During the Pliocene (5–2 Ma Bp) the junction area may well have been the locus of highest mantle activity and therefore volcanism. It can be argued, however, that by the later Pleistocene, and continuing to the present, the locus of most intense mantle activity has moved south and now corresponds to the western side of the Rift in the Elmenteita–Naivasha area. The following facts support this view:

1 The Rift floor reaches its highest elevation (near 2000 m) in the Elmenteita–Naivasha sector.

2 The Western Rift escarpment (Mau) reaches its highest elevation due West of Lake Naivasha.

3 Three large (and highly evolved) volcanic complexes

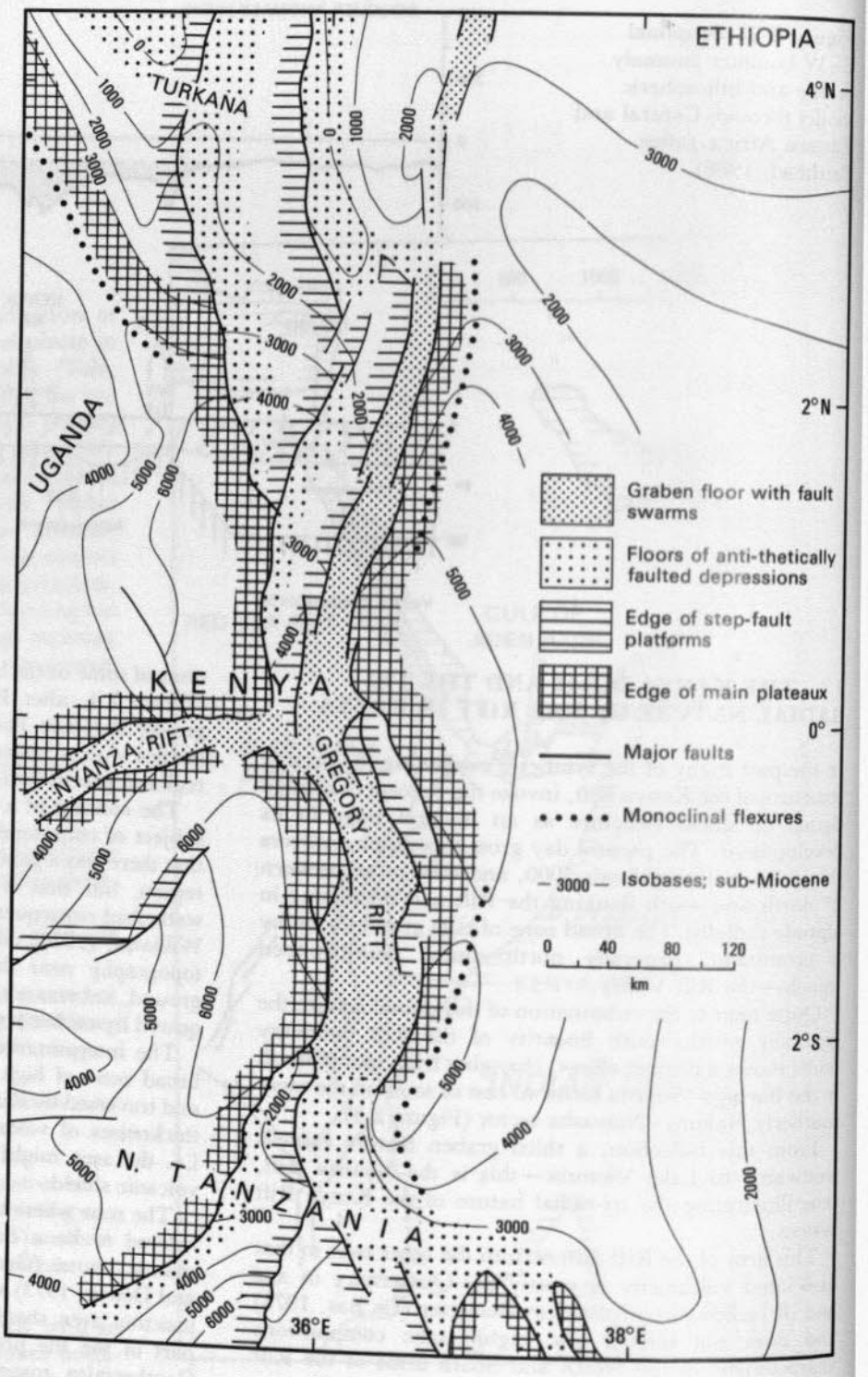

Figure 2.3 The Tri-radial nature of the Kenya Rift, and its coincidence with a zone of post-Lower Miocene domal uplift, (after Baker, 1988).

(Longonot, Olkaria and Eburru) occur around Lake Naivasha within an area of 50 × 30 km—a much greater concentration of Pleistocene to Recent volcanoes than exists elsewhere in the Rift.

4 The regional gravity minimum corresponds with the highest portion of the Mau escarpment (Figure 2.4) and therefore, with the Olkaria and Eburru centres.

5 Olkaria and Eburru are the only Late Quaternary (i.e. still active), centres in the Rift where rhyolitic volcanism is present. Rhyolites represent the most evolved compositions in terms of fractional cystallisation or alternatively, (see later discussion—Section 4), may result from partial melting.

It is a fact that the two geothermal fields currently chosen for exploitation are associated with the centre of this topographic and gravimetric anomaly and are of the most evolved composition known in the region.

2.4 OUTLINE OF THE STRUCTURAL AND PETROLOGICAL EVOLUTION OF THE KENYA RIFT REGION

A very large amount of work has been carried out on these aspects and much of it, particularly the petrology, very fully reviewed in a recent book (Fitton and Upton, 1987). The following brief summary owes much to these authorities but incorporates some Project experience since the published works draw no geothermal inferences.

It is generally agreed that the tectonic and volcanic regimes which have formed the Kenya Rift as we know it today commenced in the early to mid-Miocene, i.e. approximately 25–30 Ma and only since 4 Ma has there been a graben. From about 1.7 Ma an inner narrow trough developed within which the well-preserved and still-active central volcanoes are located (Figure 1.1).

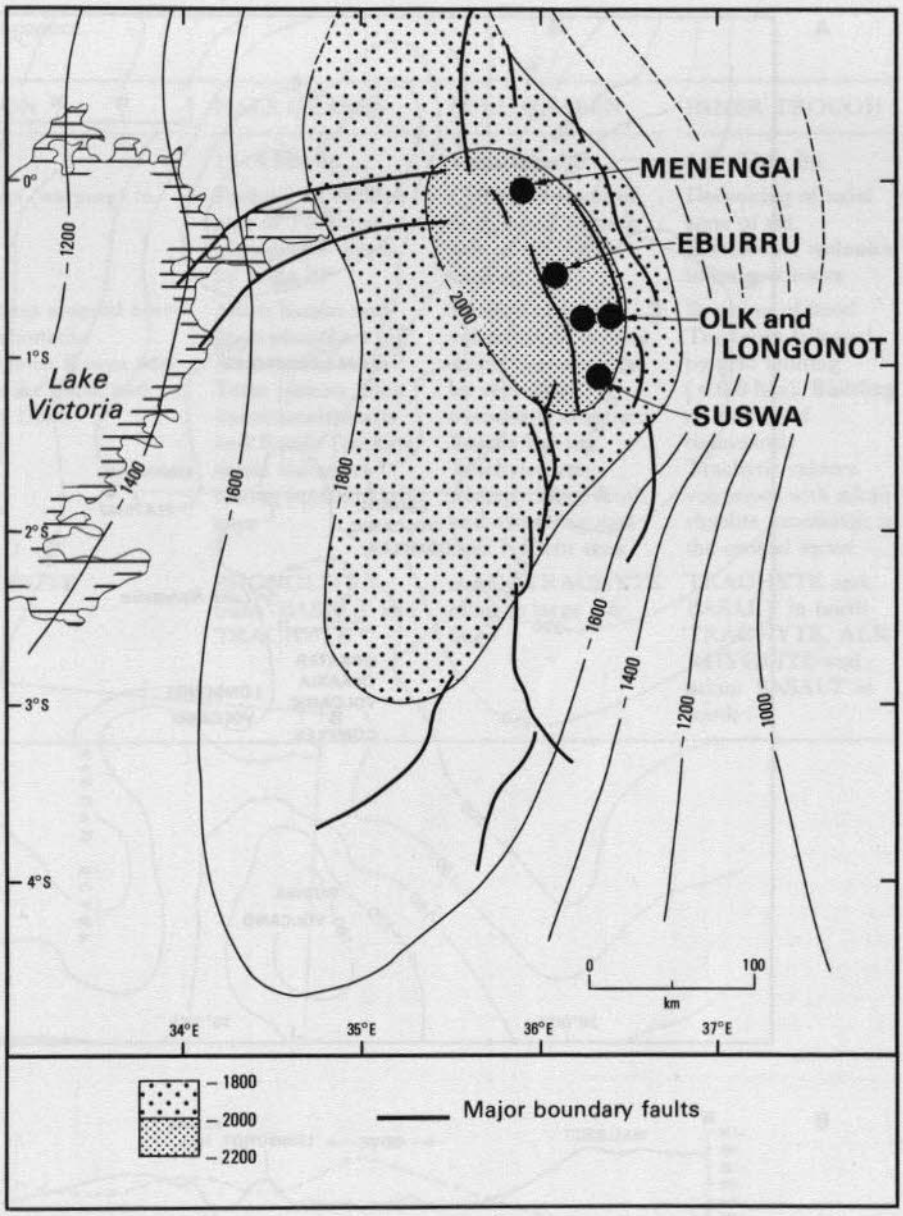

Figure 2.4 Regional bouguer anomaly over the Kenyan Rift contoured at 200 gu intervals, showing location of Recent volcanoes.

Characteristic magmatism changed from nephelinitic through phonolitic to trachytic and sometimes peralkaline salic, with basalt accompanying all stages but tending to change from alkali to transitional type.

The main stages of rift development are summarised in Table 2.1.

The majority of geothermal surface manifestations are associated with the zone of young and geologically still-active volcanoes situated within the inner trough. Available data on the warm and hot springs in other parts of Kenya indicate that these are of lower enthalpy, (Tole, 1987).

It is the young and still-active centres which comprised the initial focal points of the recent geothermal exploration project but it was also recognised that these centres were not the only potential resource areas. Exploration was directed at the whole of the inner graben to some degree and particularly at the linear tectono-volcano axes (TVAs) which often emanate from the young centres but which may in fact be the surface expressions of the on-going regional extensional tectonics.

The highly thermally active areas of Lakes Magadi and Bogoria are a third style of target being associated neither with the youngest volcanic axes nor with actual centres. They probably result from the surface discharge of previously heated axially derived groundwater possibly some distance from the actual heat source.

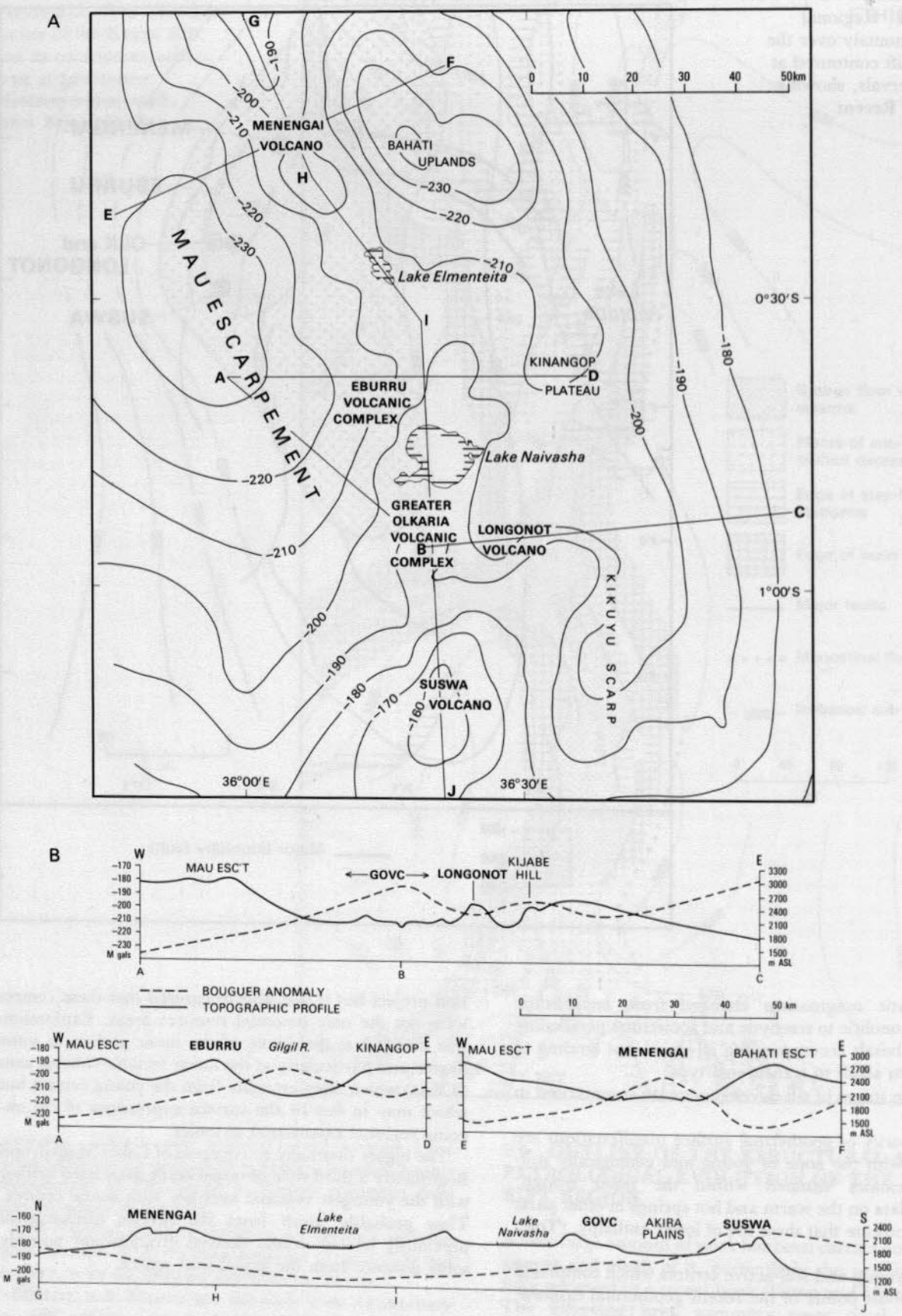

Figure 2.5A Bouguer anomaly contours at 10 mg intervals for central Kenya Rift.
B Profiles of above.

Table 2.1 Main stages of rift development

STAGE	PRE-RIFT DEPRESSION	HALF GRABEN	FULL GRABEN	INNER TROUGH
AGE	25–12 Ma Bp	12–4 Ma Bp	4–1.7 Ma BP	1.7–0 Ma Bp
TECTONIC STYLE	Broad shallow depressions (warping) in the Turkana region	Faulting in western part of Turkana, extending S-wards by 7 Ma BP	Commencement of faulting on Eastern side of rift. Grid faulting	Deepening of axial zone of rift. Extensional tectonics in narrow zones
VOLCANISM	Alkali Basalts and basanites erupted over wide areas in north. Carbonatite-nephelinite volcanism in west Kenya and the southern rift, i.e. on the south and west flanks of the Kenya Dome	Alkali basalts and-flood phonolites e.g. Uasin-gishu and Yatta plateau, then transitional basalts and Basalt/Trachyte shield volcanoes having marked Daly gaps	Basalt/Trachyte volcanism in central sector characterised by very large pyroclastic eruptions. Basalts less but Trachytes very widespread in south and extending east over Nairobi area	Eruption of flood Trachytes followed by grid faulting (<0.8 Ma). Building of a chain of dominantly Trachytic caldera volcanoes with alkali-rhyolite prominent in the central sector
SUMMARY	BASALT and NEPHELINITE	PHONOLITE, trans. BASALT and TRACHYTE	mainly TRACHYTE often as large ash flows	TRACHYTE and BASALT in north. TRACHYTE, ALK. RHYOLITE and minor BASALT in south

2.5 OUTLINE OF THE REGIONAL HYDROGEOLOGIC PATTERN

As stated above, the floor of the Rift Valley has its highest elevation in the area of Lake Naivasha, generally falling both to the north and south. There is thus a potential hydraulic gradient within the Rift in these, axial, directions. The often steep and markedly elevated boundary escarpments, however, develope the greatest head and lateral flow into the Rift from these highland areas must be extremely important. These highlands support well developed tropical rain forest, e.g. the Aberdares, Mau and Kikuyu escarpments, indicating that local recharge must be higher than in the Rift where the vegetation is of semiarid character (Figure 2.6).

Meteorological records confirm this difference—the escarpments having an annual rainfall of 1200–1500 mm with similar to lower evapotranspiration rates while the lower rainfall within the Rift (430 mm at Magadi, 980 mm at Nakuru), is accompanied by potential transpiration rates often many times the rainfall.

A combination of intrarift faulting and the occurrence of recent volcanic activity has resulted in localised drainage basin development. A number of these basins are the site of present day Rift Valley lakes most of which show clear indications of being much larger in the past.

The high evaporation/precipitation ratio prevailing in the floor of the rift combined with the closed nature of the basins results in these lakes being of generally brackish to saline character. An exception to this general pattern, is Lake Naivasha, which is the freshest of the lakes and as such supports an increasing horticultural industry on its banks. Its low salinity coupled with the fact that it has no surface outlet indicates that underground outflow must occur. The opposite case is exemplified by Lake Magadi which has no outlet, is fed on all sides by springs which are themselves saline and much of whose surface is covered with a thick trona deposit which forms the basis of an important chemical industry.

Examination of water borehole records shows that the piezometric surface generally follows the surface contours, i.e. underground movement of water is occurring both AXIALLY along the Rift, and LATERALLY from the bounding highlands into the Rift. The data support flow both north and south from Naivasha, with a steeper fall to the south. As the presently operating power station of Olkaria lies only 3 km south of the south-west shore of the lake it is therefore possible that at least some of the water forming the aquifer exploited at Olkaria is derived from the lake, however, a significant proportion, at least in the west, is probably derived laterally from the Mau Escarpment.

One of the key chemical parameters investigated during the present project was the variation of stable O and H isotopes in surface waters and condensates—these data providing much information on the probable involvement of these waters in the geothermal regime. Early in the project the stable O and H isotope characteristics of rainfall in the Kenya Rift and bounding area was investigated to allow comparison with values from surface springs etc., (Chapter 6). The results define a Meteoric Line distinctly shallower than that proposed as the typical world value (Craig, 1963). The Kenya Line (Figure 6.5) is defined as:

$$\delta^2H = 5.56\ \delta_{18}O + 2.04$$

The shallower slope is believed to reflect evaporation while the rain is falling. The data also indicates that there is an altitude control, for every 100 m increase in height $\delta^{18}O$ decreases 0.29‰ and δ^2H decreases by 1.5‰, i.e. (as elsewhere in the world) there is an increase in the proportion of heavy isotopes with decreasing altitude. The hypothesis of a latitude dependent effect is however, inadequately supported by the new data, as is systematic variation from one side of the Rift to the other.

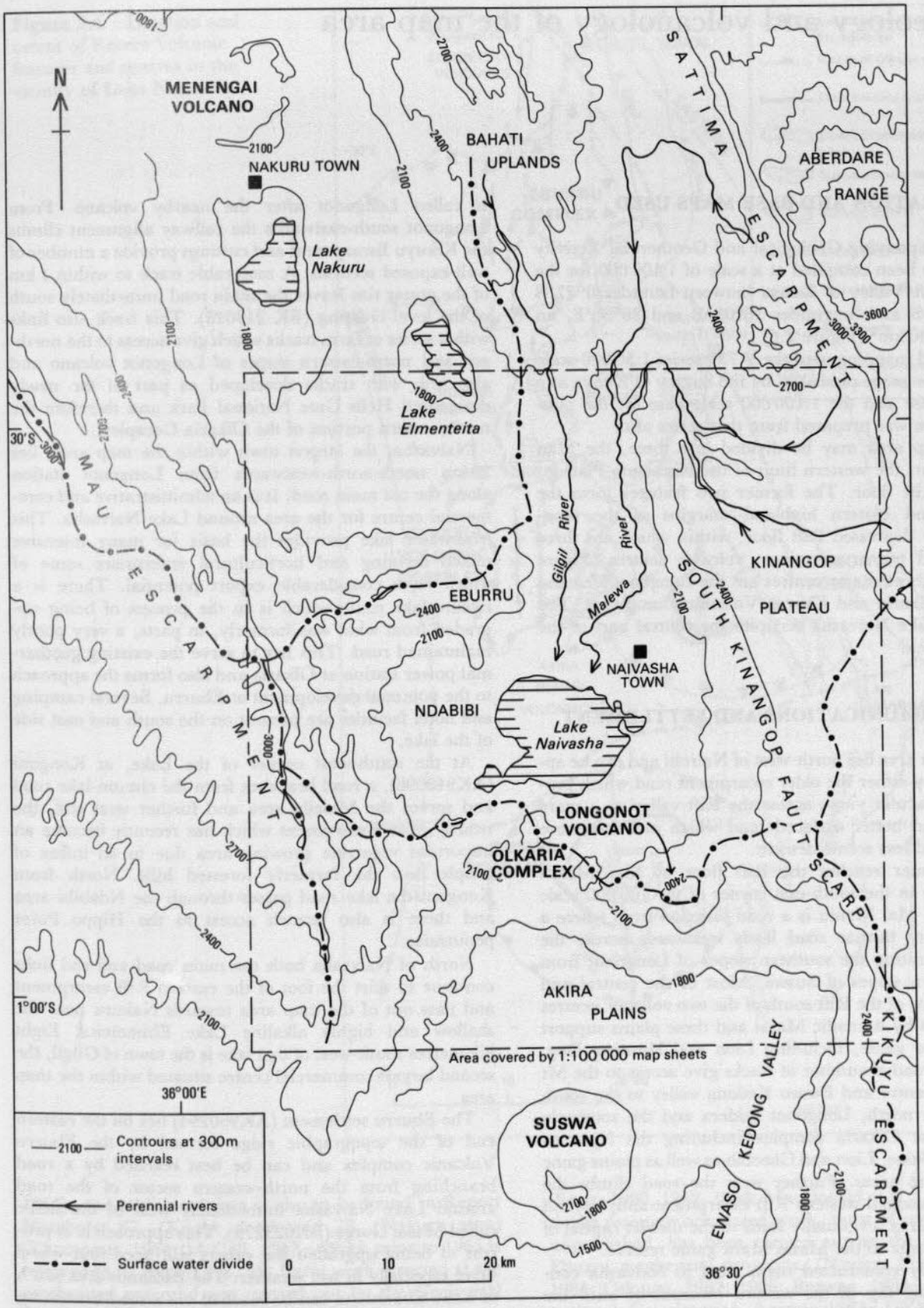

Figure 2.6 Physiography of the central Rift.

3 Geology and volcanology of the map area

3.1 LOCATION AND BASE MAPS USED

The accompanying Geological and Geothermal Activity maps have been compiled at a scale of 1:100 000 for the central Rift Valley of Kenya between latitudes 0°27′S and 1°03′S and longitudes 36°09′E and 36°38′E, an area of 3540 km² (Figure 2.6).

The field mapping used the Y 731 series 1:50 000-scale topographic maps published by the Survey of Kenya as a plotting base and the 1:100 000 scale base for the published maps was prepared from that series also.

The map area may be divided into three, the Mau Escarpment; the western limit of the Kinangop Plateau; and the Rift floor. The former two features form the western and eastern highland margins of the topographically depressed Rift floor, within which are three major, and numerous minor, volcanic centres (Figure 3.1). The three major centres are the Longonot Volcano and the Olkaria and Eburru Volcanic Complexes. The 200 km² Lake Naivasha occupies the central part of the mapped area.

3.2 COMMUNICATIONS AND SETTLEMENT

The project area lies north-west of Nairobi and can be approached by either the older escarpment road which provides spectacular views across the Rift valley or a more modern and better surfaced road which makes a more gradual and less scenic descent.

The former reaches the Rift floor at Mai Mahiu (BJ312915) in the south-east corner of the 100 000 scale map sheet. Mai Mahiu is a road junction from where a good quality tarmac road leads westwards across the plains separating the southern slopes of Longonot from the northern slopes of Suswa. Most of the central and western floor of the Rift south of the two volcanic centres is inhabited by nomadic Masai and these plains support considerable game, including Lion and Hunting Dog. From this road a number of tracks give access to the Mt Margaret centre and Ewaso Kedong valley to the south and, to the north, Longonot caldera and the southerly parts of the Olkaria complex including the Njorowa Gorge. Buffaloe, Lion and Cheetah as well as plains game inhabit these areas. Further west the road climbs the relatively subdued western Rift escarpment and, beyond the project area, eventually leads to the district capital of Narok en route to the Masai Mara game reserve.

The newly constructed main road to Naivasha continues on the top of the eastern escarpment until the latitude of Lake Naivasha when it makes a gradual descent to the Rift floor and the town of Naivasha. The eastern Kinangop plateau can be reached from a junction near Magumu (BK 270053).

The old main road to western Kenya and Uganda runs north-westwards from Mai Mahiu as an often markedly potholed route frequented by heavy goods traffic. Fourteen kilometres north-west of the junction this road is crossed by the main railway route from Nairobi and a small settlement has developed around the station which is called Longonot after the nearby volcano. From Longonot south-eastwards the railway alignment climbs the Kikuyu Escarpment and cuttings provide a number of well-exposed sections. A motorable track to within 1 km of the crater rim leaves the main road immediately south of the level crossing (BK 219018). This track also links with a series of farm tracks which give access to the northern and north-eastern slopes of Longonot volcano and also link with tracks developed as part of the newly designated Hells Gate National Park and therefore the north-eastern portion of the Olkaria Complex.

Naivasha, the largest town within the map area, lies 20 km north-north-westwards from Longonot station along the old main road. It is an administrative and commercial centre for the area around Lake Naivasha. This freshwater lake provides the basis for many intensive mixed farming and horticultural enterprises some of which have considerable export potential. There is a circum-lake route which is in the process of being upgraded from what was formerly, in parts, a very poorly maintained road. This has to serve the existing geothermal power station at Olkaria and also forms the approach to the potential development at Eburru. Several camping and hotel facilities are present on the south and east side of the lake.

At the south-west corner of the Lake, at Kongoni (AK948096), a road branches from the circum-lake road and serves the Maiella area and further west still, the nearby Mau Escarpment which has recently become an important vegetable growing area due to an influx of people into the formerly forested hills. North from Kongoni the lake road passes through the Ndabibi area and there is also branch access to the Hippo Point peninsular.

North of Naivasha both the main road and rail links continue to skirt the foot of the eastern Rift escarpment and pass out of the map area towards Nakuru near the shallow and highly alkaline Lake Elmenteita. Eight kilometres south-west of that lake is the town of Gilgil, the second largest commercial centre situated within the map area.

The Eburru settlement (AK950294) lies on the eastern end of the topographic ridge formed by the Eburru Volcanic complex and can be best reached by a road branching from the north-western sector of the road around Lake Naivasha immediately west of the defile called Masai Gorge (BK023279). This approach is in process of being upgraded but others still need four-wheel drive especially in wet weather. The Badlands area sou h of Lake Elmenteita can be reached via a road branching from the main Naivasha–Nakuru road 4 km north of Gilgil (AK984479) or a seasonal track from a junction near Gilgil (BK008454).

3.3 PREVIOUS WORK

Previous systematic geological survey of the project area is covered in Report Number 55, (Naivasha area), of the Geological Survey of Kenya, (Thompson and Dodson,

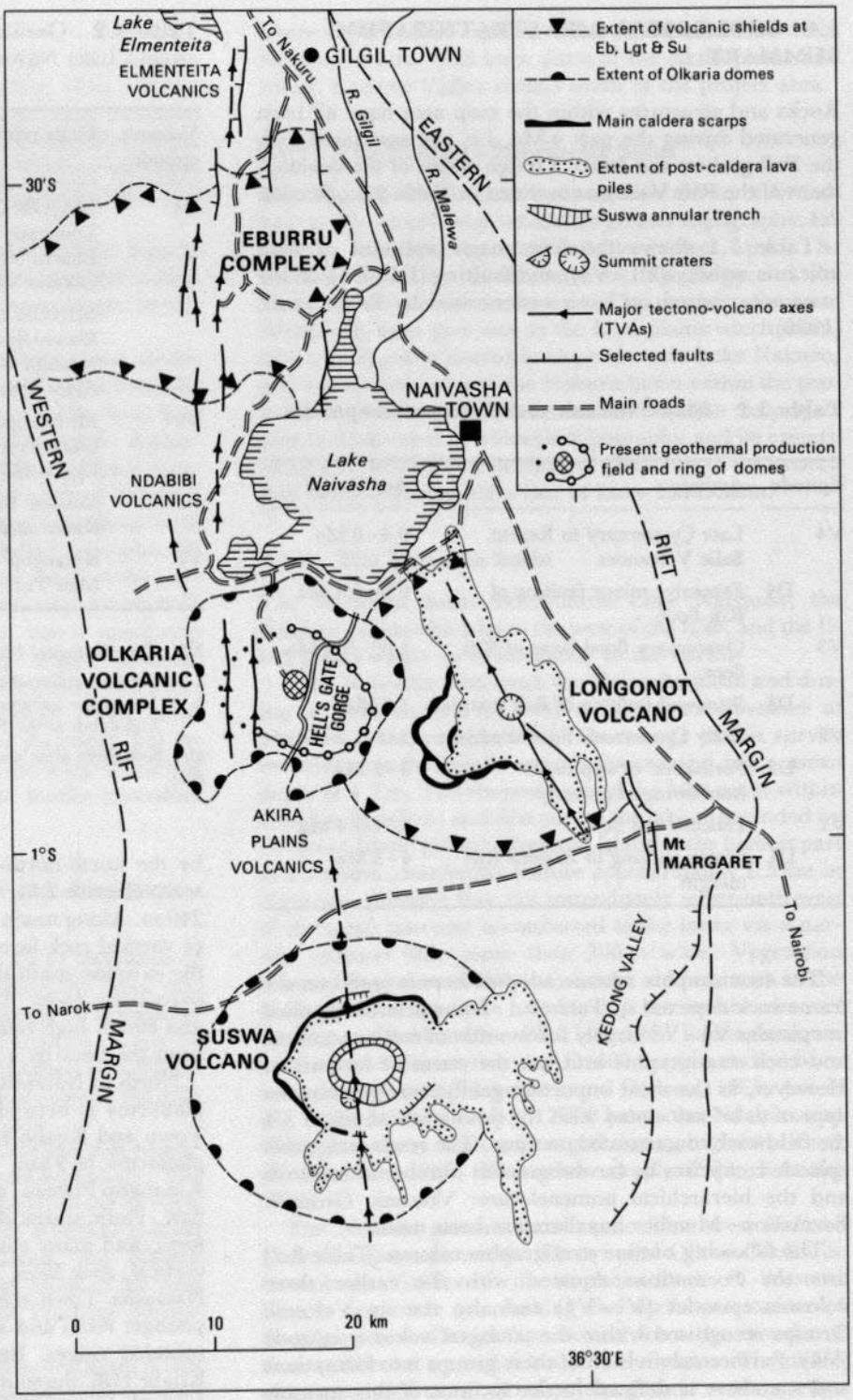

Figure 3.1 Location and extent of Recent volcanic features and centres in the vicinity of Lake Naivasha.

1963), and additional data is also to be found in Report Numbers: 67, (Kijabe area) and 78, (Nakuru area) (Thompson, 1964; McCall, 1967). Work prior to 1963 is referred to in Report No. 55. Early work directed at the geothermal potential was carried out by the Geological Survey and Mines Dept.,(Mason, 1967).

More recently parts of the area, particularly Longonot Volcano, (Scott, 1977), and the Olkaria Volcanic Complex, (Bliss, 1979; Bone 1988), have been the subject of postgraduate research studies. Research on the Olkaria Volcanic Complex has also included the adjacent Ndabibi plains, (Bliss, 1979) and Akira plains, (Bone, 1988). The Mount Margaret and Kijabe Hill areas have been the subject of a separate dissertation, (Kagasi, 1983). Results of some of the above research have been published, (Scott, 1980, 1982, 1984; MacDonald et al., 1987). Additional resource orientated work, most of which remains unpublished, has been carried out on the Olkaria and Eburru geothermal prospects, (Naylor, 1972; Ndombi, 1981; Odongo, 1982, 1986; Browne, 1984, Japan International Co-operation Agency 1983, GENZL, 1986). The results of other research include details of the petrography and mineralogy of rocks from Eburru (Sutherland, 1974), the results of radiometric dating, (Baker and Mitchell, 1976, 1988) and aspects of the geology and geography of Lakes Naivasha, (Richardson, 1966; Kamau, 1974; Ase et al., 1986) and Nakuru/Elmenteita, (Washbourn-Kamau, 1970; Richardson et al., 1972; Butzer et al., 1972).

3.4 GEOLOGICAL AND STRATIGRAPHIC SUMMARY

Rocks and structures within the map area have all been generated during the past 4 Ma, i.e. are associated with the Full graben and Inner Trough stages of the development of the Rift Valley as outlined in Table 2.1., Section 2.4.

Table 3.1 shows the four major episodes of both volcanic activity (V1–V4), and faulting (D1–D4), in the map area, based on work summarised by Baker et al. (1988):

Table 3.1 Major volcanic and deformation episodes

Episode	Activity	Age Range
V4	Late Quaternary to Recent Salic Volcanoes	0.4–0 Ma
D4	Extensive minor faulting of Rift floor	0.8–0.4 Ma
V3	Quaternary flood lavas of Rift floor	1.65–0.9 Ma
D3	Renewed faulting of Rift margins	1.7 Ma
V2	Early Quaternary flood trachytes	2.0–1.8 Ma
D2	Formation of step faults (narrowing of graben)	3–2 Ma
V1	Pliocene ash flows	3.7–3.4 Ma
D1	Major faulting of Eastern Rift margin	4–3 Ma

The stratigraphic scheme adopted here is based on the framework depicted in Table 3.1. Nomenclature applied to episodes V1–V3 largely follows that of earlier accounts and each stratigraphic unit has the status of formation. However, as the most important geothermal phenomena appear to be associated with the young volcanoes of V4 the fieldwork concentrated on these. The result is that this episode comprises by far the greatest number of subunits and the hierarchical nomenclature: Volcanic Group–Formation–Member has therefore been used.

The following outline stratigraphic column (Table 3.2) lists the Formations equated with the earlier three volcanic episodes (V1–V3) and also the six Volcanic Groups recognised within the youngest volcanic episode (V4). Further subdivision of these groups into formations and members is defined in the sections of this memoir dealing with individual Volcanic Centres or Complexes.

Table 3.2 Outline volcanic stratigraphy of the area around Lake Naivasha

Volcanic episode	Units represented
V4	MAJOR CENTRES OR COMPLEXES Longonot Volcanic Group Eburru Volcanic Group Olkaria Volcanic Group MINOR CENTRES Elmenteita Volcanic Group Ndabibi Volcanic Group Akira Volcanic Group
V3	Mt Margaret Formation (Mt) Gilgil Trachyte Formation (Trg) Kijabe Hill Formation (Kb)
V2	Limuru Trachyte Formation (Tr) Karati and Ol Mogogo Basalt Formation (Trb)
V1	Kinangop Tuff Formation (Tk) Mau Tuff Formation (Tkm)

NB The Geological Map also depicts two further units:

a = Fluvio—colluvial deposits, by reworking of the volcanics.

ls = Lacustrine sediments—deposited during the previous lake highstands in the Naivasha–Elmenteita–Nakuru Basin.

nb Both these units are interdigitated with or overlie rocks of V4 age.

3.5 THE RIFT MARGINS

3.5.1 Geomorphology

The Kinangop Plateau (eastern margin)

The name Kinangop Plateau is used in the Geological Survey of Kenya report on the "Naivasha Area", (Thompson and Dodson, 1963). The authors however state that it could be more accurately referred to as a shelf or plain, and in some cases it has been referred to as the Kinangop Platform, (Williams, 1978; Baker et al., 1988).

Only the westernmost part of the Kinangop Plateau occurs within the project area where it attains a maximum elevation of about 2740 m. Its western margin is defined by the north-north-west-trending South Kinangop fault scarp (Figure 2.6), which ranges in height from 100 m to 240 m. Along much of its length, this scarp has very steep or vertical rock faces above less steep talus slopes, but in the extreme south the scarp has been buried by younger pyroclastic rocks. The crest of the scarp is between 500 and 600 m high relative to the rift floor, but is separated from the floor by a series of downfaulted platforms.

North of Naivasha Town, the combined width of these platforms is between 2.5 and 5 km. Between Naivasha Town and Kijabe Hill however, the total width of these platforms is 9 km, and their surfaces, like that of the Kinangop Plateau, are gently sloping in a northerly direction. Fault scarps define the western edge of each platform, and many consist, at least in part, of very steep or vertical, rock faces, sometimes up to 80 m high. South of Naivasha Town these scarps have been buried beneath younger rocks and are apparent as either gentle slopes or rounded ridges. Immediately north and north west of Kijabe Hill, the southern termination of these platforms is topographically complex due to the crosscutting of west-north-west and predominately north-trending fault scarps. These scarps are up to 180 m high.

Kijabe Hill is a volcanic cone which probably formed on a narrow downfaulted platform adjacent to the Kinangop Plateau. The cone attains a maximum elevation of 2660 m and is 700 m above the nearby rift floor.

Between Kijabe Hill and Kijabe Town, the southern continuation of the Kinangop Plateau fault scarp is a steep, highly dissected slope, up to 460 m high. This slope dies out immediately east and south-east of Kijabe Town and is replaced by the near north-trending Kikuyu Escarpment. Relative to the rift floor in the Mount Margaret area, the crest of the Kikuyu Escarpment is between 600 and 700 m high. However, the intervening ground also comprises several platforms separated by step faults.

The Mau Escarpment (western margin)
NB for localities cited see geological map
The north- to north-north-west-trending Mau Escarpment forms the western edge of the project area. It attains a maximum elevation of just over 3080 m due West of the Ndabibi Estate, but is over 3000 m for 36 km of its length within the map area, decreasing in height both north and south.

The Escarpment is between 1000 and 1100 m high in relation to the rift floor at Ndabibi, and is over 800 m high east of Nairagie Ngare which lies on the southern border of the mapped area.

As in the case of the Kinangop Escarpment downfaulted platforms separate the Mau Escarpment from the rift floor proper and range in combined width from 8 to 11 km in areas to the north and south of Sakutiek. A maximum width of 13 km occurs in the Nairagie Ngare area. The platforms adjacent to Eburru and south of Sakutiek are highly dissected and in these areas, marginal fault scarps are indistinct. Elsewhere the platform margins are defined by fault scarps which often have steep and variably dissected slopes. The most westerly (main) fault scarp building the Mau Escarpment, has a maximum elevation of over 300 m. The scarp height however, decreases southwards to just over 200 m near Sakutiek, and this height persists into the Nairagie Ngare area. Steep talus slopes occur along much of its length, but for 13 km in the north, the lowest part of the scarp is marked by a very steep or vertical rock face locally exceeding 100 m in height.

3.5.2 Geology of the Rift Margins and older parts of the floor

The Rift Margins expose an older (V1) sequence of trachytic, often ignimbritic, pyroclastics (the Mau and Kinangop Tuff Formations) and a younger (V2) thick sequence of trachytic flood lavas (the Limuru Trachytic Formation). Minor basalts, the Ol Mogogo and Karati Formations, are associated with the upper part of the tuffs and all these rocks are older than 1.7 Ma.

Subsequent faulting (D3) produced the stepped escarpments described in the section on geomorphology. The Kijabe basalt formation was later erupted on one of these platforms while on the floor of the Rift a further episode (V3) of trachytic magmatism occurred, the Plateau Trachytes. These are most widespread south of the map area but are represented by the Gilgil Trachyte Formation within the area discribed here.

One of the characteristics of the plateau trachytes is that they predate the last major faulting episode (D4) to affect the Rift floor.

The Mt Margaret Formation is also correlated with the V3 episode but has the form of a small central volcano which is still associated with fumarolic activity.

It is assumed that equivalents of all these formations underlie the younger centres of Longonot, Olkaria and Eburru and are therefore depicted as so doing on the cross-sections accompanying the 1:100 000-scale map.

More details of these formations are given in Table 3.3.

3.6 RIFT FLOOR PLAINS

The project area includes four large areas of rift floor plains; the Nakuru–Elmenteita basin in the north, the Naivasha basin, the Akira plains in the south, and the Ewaso Kedong Valley in the south-east. Only the southernmost part of the Nakuru–Elmenteita basin lies within the project area, and large parts of the Akira plains and Ewaso Kedong Valley extend south of the project area.

3.6.1 The Nakuru–Elmenteita basin

The Nakuru–Elmenteita basin is bisected by a broad, low, north–south ridge which has greater topographic expression immediately north of the project area. The Nakuru basin lies to the west of this ridge and the Elmenteita basin lies to the east. The northern flanks of Western Eburru give way to the Kiwi plains which maintain a very gentle northerly slope towards Lake Nakuru, and are the only part of the Nakuru basin within the project area. Most of the Elmenteita basin within the project area is dominated by volcanic topography and its eastern margin is defined by downfaulted platforms of the eastern Rift margin immediately east of Lake Elmenteita.

3.6.2 The Naivasha basin

The Naivasha basin incorporates Lake Naivasha, the Ndabibi plains which lie to the west of the lake, and the Ilkek plains which lie immediately to the north.

Lake Naivasha dominates the Naivasha basin and during a 1983 survey its level stood at an elevation of 1889.3 m (Ase, et al., 1986). The results of this survey revealed that the lake is smooth floored and has a mean depth of 4.7 m. The deepest parts of the lake occur within Oloiden Bay (9 m) and that part of the lake surrounded by Crescent Island (17 m). Crescent Island is the highest part of a volcanic cone/crater feature approximately 1.5 km in diameter. Oloiden Bay lies immediately west-south-west of the main lake and is connected to the latter via a narrow channel little more than 300 m wide. Vegetation (mainly Papyrus and Salvina) occurs around much of the shore of the main lake and extends across the channel leading to Oloiden Bay. Past lake level fluctuations are known and the most recent (AD1880 to present day) have been documented (Thompson and Dodson, 1963; Ase et al., 1986) Within the last 12 000 years the Ndabibi and Ilkek plains have been submerged during high lake levels (Richardson, 1966, Richardson et al, 1972; Kamau, 1974).

The Ndabibi plains extend up to 9 km west of Lake Naivasha and separate the Eburru and Olkaria Volcanic Complexes. Gullies on the southern flanks of Western Eburru terminate on reaching the north-west corner of the plains and alluvial fans extend from the mouths of these gullies for up to 1.5 km onto the plains. The plains are about 1980 m in elevation along their western edge and slope very gently eastwards towards the lake.

The Ilkek plains extend up to 23 km north of Lake Naivasha and they range in width from a maximum of 13 km in the south, near Naivasha Town, to a minimum of 4 km in the extreme north near Gilgil Town. The plains slope gently southwards from a maximum elevation of just below 2000 m in the north. Waterloo Ridge defines most of the western margin, and fault scarps along the lowest of the rift platforms below the Kinangop Plateau define the eastern margin. Ridges formed of volcanic rock occur at and east of the Ilkek settlement, and several have prominent fault scarps along their western sides. The Marula Estate offices and Manera Farm are situated on the southern part of the plain which has the form of a delta fan up to 9 km wide associated with the Malewa River.

Table 3.3 Details of the formations other than those comprising the recent volcanic group (*oldest unit at top*)

Name of formation (Fmn) or member (Mem)	Map symbol	Type area/section	Age	Major outcrops	Lithology
Kinangop Tuff Fmn	Tk	N. of Kijabe Hill BK 270020	3.4–4.5 Ma BP	Eastern rift margin	Ignimbrite succession; mostly welded tuffs, palaesols & weathered zones at top of most beds
Mau Tuff Fmn	Tkm	W of Nderit River AK 748382		Western rift margin	Ignimbrite succession — dominated by welded tuff
Karati Basalt Fmn	Tlb	Road section, adj. N. Karati settlement BK 201191	2.6 ± 0.4 Ma BP	Adj N Karati settlement, very small o/c's adj. Naivasha Town & 15–18 km SSE of town	Olivine basalt lava, feldspar /olivine phen. in small o/c's. Scoriaceous blocks & lapilli in o/c's SSE of Naivasha Town (e.g. BK 197074 & BK 222059). Pyroclastics = possible remnants of cones
Ol Mogogo Basalt Fmn	Tlb	Adj. Ol Mogogo settlement in Kinangop Plateau fault scarp BK 138380		Adj. Ol Mogogo settlement & in Turasha River — adj. Turasha settlement	Lava with abundant feldspar, olivine & pyroxene phen. Bedded scoriaceous lapilli = remnants of cone
Limuru Trachyte Fmn	Tl	Old Naivasha Rd. SE of Mai Mahiu BJ 326905	1.66–2.65 Ma BP	Eastern rift margin especially on old Naivasha road down Kikuyu escarpment	Lava flows of trachyte & rhyolite composition. Some flows have abundant feldspar phenocrysts
Gilgil Trachyte Fmn	Tlg	E. of Nderit River AK 754365		N & NE of Eburru Volc & on E side of Waterloo Ridge	Lava — sometimes with abundant feldspar phen. Trachyte composition
Kijabe Hill Basalt Fmn	Kb	Kijabe Hill	<1 Ma BP	Kijabe Hill (well seen in railway cuttings)	Pahoehoe & some aa lava, basaltic with abund. v large tabular feldspar phenocrysts
Mt Margaret Volcanic Fmn	Mt	Mt Margaret		Mt Margaret & low ridge immed. to W	Bedded pumice lapilli/blocks &/or ash — grades up into welded scoriaceous lapilli; in turn grades up to banded lava. Bedded ash (fine to coarse) within former crater & on ridge W of Mt Margaret
Lake sediments	ls	Naivasha Town at BK 139228		Ilkek Basin, Elmenteita basin, Ndabibi, Oserian Farm, Sulmac Estate	Pumiceous granule — pebble gravel, coarse sand, gravelly sand, silt & clay
Alluvial deposits	a	Malewa River Valley e.g. at BK 130282, BK 125283, BK 091264		Gullies & small internally draining basins, Akira plains	Silt, fine sand, some ferruginous coarse sand. Boulder gravel within Hell's Gate & locally on Akira plains

Table 3.3 Continued

Thickness in m a = max exposed b = max indicated bed	Volcanological interpretation or depositional environment	Underlain by	Overlain by	Notes
a150	Emplacement of widespread ignimbrites from centre or centres unknown poss. within area of rift floor now covered by younger volcanics	?	Tl, TLg	Aged based on rad. dates by Baker et al., 1988 & Kagasi, 1983
a100	as for Tk	?	Tl	Correlated with Kinangop Tuff
b3	Products of hawiian &/or strombolian eruptions — lava extrusion dominant	Tk		Age from Baker et al., 1988
b8	As for Karati Basalt	Tk	Tk/Tl?	Age assumed similar to above
a100	Extrusion from centre/centres unknown — presum. in area now covered by much younger rift floor volcanics	Tk, Tlb		Interbedded with Tk in Naivasha town area
	As for Limuru Trachyte	Tk	Erw/ls	Correlated with Plateau Trachytes of Baker et al., 1988
	Product of hawiian type volcanism	Tk, Tl	Lpk	Has eroded crater at summit
	Bedded pyroclastics form bulk of now eroded cone, flanks of latter mantled by welded scoria & banded lava. Latter interpreted as being rheomorphic welded fall tuff. Bedded ash — probably fall deposit, within former crater, but dominated by surge deposits on ridge W of Mt Margaret	?	Lpk	Eroded nature indicates older age than fumarole & high CO_2 associated with N–S faulting
a15	Re-working of pyroclastics in shallow lakes	Ba, Kp, Er[2], LpK	Lp7? Lp8	Exposures in Sulmac Estate at BK 033073 indicate Ls & Lp5 (+ Op3) interfinger
	Gully floor & basin (small) deposits, latter possibly interbedded with ls, alluvial fans e.g. Akira plains, Ndabibi & N of Naivasha Town			Probably interbedded with ls in Ilkek Basin (E area)

3.6.3 The Akira plains

The Akira plains are mainly formed of numerous very gently sloping alluvial fans which have reworked the various airfall units and extend southwards from the mouths of gullies on the south-west flanks of Longonot Volcano, the south flanks of the Olkaria Volcanic Complex, and from the mouths of gullies that terminate on reaching the plains after having traversed downfaulted platforms of the western Rift margin in the Lolonito and Kepise areas. By far the largest of these 'gullies' is the Ol Njorowa Gorge. A braided channel network is apparent on aerial photographs of the plains in the area between Tandamara, Sibet and Loirogwa. The plains merge imperceptably with the outer very low dipping south and south-west sectors of the Longonot shield.

3.6.4 The Ewaso Kedong Valley

The Ewaso Kedong Valley separates the eastern and south-eastern flanks of Longonot Volcano from the rift platforms of the eastern rift margin. At its northernmost extent, between Longonot Volcano and Kijabe Hill, the valley is 3 km wide, but south of Kijabe Hill widens rapidly to just over 10 km and this width is maintained southwards. The valley floor slopes in a southerly direction from an elevation of just over 2100 m in the extreme north to less than 1700 m in the south. Gullies formed by southwards draining ephemeral streams and a number of, mostly buried, fault scarps, are the only topographic features on the valley floor other than the Mt Margaret volcanic centre. The fault scarps define a north–south fault zone which defines a shallow graben extending 5 km north, and 3 km south, of Mt Margaret. A 600 m wide valley separates the western side of Mt Margaret from a prominent 2.25 km long fault scarp, which unlike others in the area has not been buried beneath later rocks. The northern half of this fault scarp occurs as an east facing rock face 5 m in height.

The only volcanic centre in the Ewaso Kedong Valley is Mt Margaret, which is situated 5 km west of the lowest of the downfaulted platforms of the eastern rift margin and 13.5 km south-east of the summit crater of Longonot Volcano. Mt Margaret averages 1.6 km across and stands 120 m above the surrounding plains.

3.7 LONGONOT VOLCANO

3.7.1 Introduction and morphology

Longonot Volcano has a well-developed cone with a summit crater and shows evidence of an earlier calderic stage. It is formed of (often perakaline), trachytic pyroclastic rocks and lava flows, but in some cases, there is evidence of the mixing of magmas of alkali basalt and trachyte compositions. (Scott, 1977, 1980 and 1984).

Longonot Volcano occupies an area of approximately 350 km^2 on the eastern rift floor, and attains a maximum elevation of 2776 m asl. It is about 880 m high relative to Lake Naivasha in the north, but is over 1000 m high relative to the Akira plains which lie immediately south-west of the volcano. The cone covers an area of about 45 km^2, and the 2 km diameter summit crater has a smooth floor, surrounded by very steep to vertical walls which vary in height between 350 m in the west, and 75 m in the east.

Numerous ephemeral streams have dissected unconsolidated pyroclastic deposits which mantle the flanks of the cone. Arcuate lava flow fronts up to 40 m high form distinct topographic features on its northern, eastern and southern slopes, and where lava flows extend beyond these slopes onto adjacent parts of the rift floor, similar flow fronts also occur on the south-east flanks.

Arcuate to cuspate ridges extend around the western and southern side of the cone, and are the topographic expression of the rim of the caldera within which the cone has formed. Burial of the original caldera rim by younger pyroclastic deposits has resulted in ridges which are rounded in profile, but which still retain steeper slopes on the inner (scarp) side. The buried caldera rim, west of the cone is up to 140 m high relative to the caldera floor. In contrast the south-west caldera rim is defined by very subdued ridges with only slight topographic expression. The caldera scarp south of the cone is rarely more than 40 m high, but, unlike other sectors, vertical rock faces occur intermittently along 1.5 km of its length.

Longonot caldera formed at the summit of a large volcanic shield with slopes frequently less than 5°. Steeper slopes (10–15°) occur in the immediate vicinity of the caldera rim. The middle and upper slopes of the shield beyond the caldera rim have been dissected by ephemeral streams. Gullies, mostly 10–20 m deep, terminate close to the crests of the caldera rim ridges, but two gullies up to 40 m deep have breached the very subdued south-west caldera rim ridges.

On the lower south-west and south slopes, gullies give way to very gently sloping alluvial fans which are most apparent on air photographs. The northern slopes have been only locally dissected by ephemeral streams.

3.7.2 Geology

The products of the Longonot Volcano constitute the Longonot Volcanic Group which incorporates seven formations. The relationship of stratigraphy to major events in the volcanic history of Longonot, is shown below in outline and in Figure 3.2. The main events in its history are:

1 *Building of an early shield*
Represented by the Olongonot Volcanic Formation —poorly exposed pyroclastics and lavas in boreholes.

2 *Caldera formation*
Represented by the (dominently ignimbritic) Kedong Valley Tuff Formation.

3 *Building of a pyroclastic and lava cone*
Represented by the Akira (often plinian) Pumice Formation. This comprises six members, the early ones including surge beds, the later—ashfalls.

Later stages of cone building are dominated by lava—the Longonot Trachyte Formation. The Longonot Mixed Lava Formation was erupted on the northern lower flanks at this time also.

4 *Formation of a summit crater*
Preceded or accompanied by the Longonot Ash Formation

5 *Flank and craterfloor lava eruption*
Represented by the Upper Trachyte Member (flanks) and Upper Mixed Lava Member (crater).

More details of the stratigraphy are given in Table 3.4. Measured sections including Longonot tephra are shown on Foldout No. 1. Tables 3.5 and 3.6 give details of the syn-caldera formation Lpk at two localities outside the map area.

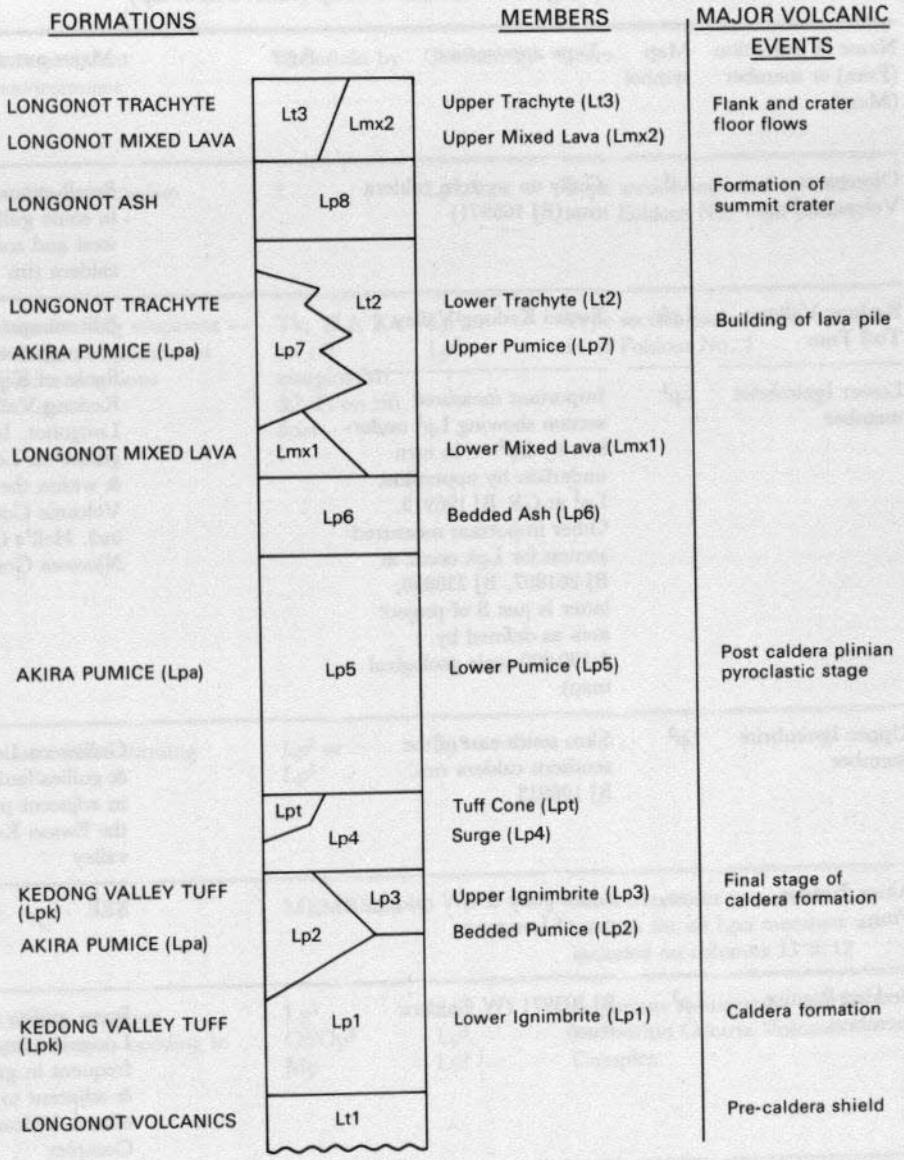

Figure 3.2 Summary of the stratigraphy of Longonot Volcano.

3.7.3 Age of the volcano

No K-Ar age determinations have been successfully carried out on Longonot rocks (Kagasi, 1983), but the earliest activity may have commenced no more that about 0.4 Ma (Scott, 1977 and 1980). Radiocarbon dates (Harkness, pers. com., 1987), carried out as part of the present project, indicate that a substantial part of the post-caldera volcanism is no older than 9150 ± 110 BP, and that the summit crater is less than 3500 ± 120 BP. The last eruptions may have occurred only a century or two ago (Richard et al., 1957). Fumarole activity occurs within the summit crater, along part of the southern caldera rim, and at isolated localities on the south-east flanks.

3.8 THE GREATER OLKARIA VOLCANIC COMPLEX

3.8.1 Introduction and morphology

The Greater Olkaria Volcanic Complex (GOVC) is a multicentered volcanic field, 240 km² in area, which lies west of Longonot Volcano—between the latter and the western margin of the rift. Some previous work on this area refers to these volcanics as the 'Naivasha Complex', (Macdonald et al., 1987) but the name Olkaria is preferred due to the close association of these rocks with the well-known geothermal field of the same name.

Whereas volcanic activity at Longonot has formed a single, large and topographically distinct volcanic centre of dominantly trachyte composition, the activity of the GOVC has been such that at least 80, much smaller, volcanic centres have formed, (hence the term 'Complex'). The characteristic composition of surface exposures at Olkaria is comendite or peralkaline rhyolite. Most Olkaria centres occur as either steep sided domes, formed of lava and/or pyroclastic rock, or as thick lava flows of restricted lateral extent(Figure 3.3). Individual domes range from being small topographic features less than 500 m in basal diameter and no more than 50 m high, to prominent features such as Olkaria Hill which is 340 m high, and has a basal diameter of 2 km.

Groups of coalesced domes and lava flows form distinct topographic features in several parts of the complex. The largest of these is the Gorge Farm–Kibikoni Farm group of hills which is 8 km long in a northerly direction, and up to 5 km wide. Immediately east of Olkaria Hill is a ridge, with a 2.5 fissure system along which there is a series of narrow, deep craters. The Ololbutot lava, which originates from the southern part of this fissure, is the youngest flow within the complex and its surface remains

Table 3.4 Details of the Longonot Volcanic Group (*oldest unit at top*)

Name of formation (Fmn) or member (Mem)	Map symbol	Type area/section	Age	Major outcrops	Lithology
Olongonot Volcanics Fmn	Lt^1	Gully on western caldera rim (BJ 105971)		Small exposures only in some gullies on west and south caldera rim	Pumice, ash and welded beds in surface exposures, but trachyte lava as well as pyroclastics in boreholes
Kedong Valley Tuff Fmn	Lpk	Ewaso Kedong Valley		Rift margin NE & E of Longonot incl. flanks of Kijabe Hill. Kedong Valley SE of Longonot. In some gullies on Longonot & within the Olkaria Volcanic Complex — incl. Hell's Gate/Ol Njorowa Gorge	At least 5 ignimbrite units each with weathered zone & palaeosol (reddish-brown) at top. Lowest ignimbrite is welded, rest partly welded or unwelded tuffs. Some coigimbrite ash fall & some with ground layer of pumice lapilli & ash fall. Lithologically distinct unit of pumice lapilli (base) & accretionary lapilli ash fall in exposures NE of Longonot
Lower Ignimbrite member	Lp^1	Important measured section showing Lp^3 underlain by Lp^2 — in turn underlain by uppermost Lp^1 at GR BJ 196913. Other important measured section for Lpk occur at BJ 261887, BJ 238808; latter is just S of project area as defined by 1:100 000 scale geological map)			
Upper Ignimbrite member	Lp^3	5 km south-east of the southern caldera rim. BJ 196913		Gullies on Longonot & gullies/fault scarps in adjacent parts of the Ewaso Kedong valley	Single unit of partly welded tuff, locally with scoriacieons blocks at top. Has reddish brown weathered zone & palaeosol at top
Akira Pumice Fmn	Lpa	Akira gully & SW caldera rim of Longonot		SEE	INFORMATION
Bedded Pumice member	Lp^2	BJ 105971 (W Caldera Rim)		Some gullies on Longonot, more frequent in gullies on & adjacent to the olkaria Volcanic Complex	Single unit of bedded pumice lapilli (grey) & ash, latter more frequent towards top
Surge member	Lp^4	BJ 109943, BJ 119945 (Akira gully)		Gullies on Longonot & within & adjacent to the Olkaria Volcanic Group	3, sometimes 4 pumice lapilli & ash beds each with brown top. Lowest bed is lithic rich pumice lapilli deposit but higher beds are dominated by ash with accretionary lapilli & large scale cross bedding
Lower pumice member	Lp^5	BJ 119945, BJ 119957 (Akira gully)	C^{14} date of 9150 ± 110 years BP on palaesol below Lp^5	Most gullies on Longonot, many within & adjacent & to Olkaria Volcanic Complex. Also present on N & NW flanks of Suswa	At least 13 beds of grey pumice lapilli each with brown palaesol &/or weathered zone at top. With syenite, obsidian trachyte 'lava' lithics. Many show upward increase in lithic contents. Lowest beds contain pumice blocks
Bedded Ash member	Lp^6	BJ 122957 (Akira gully)		Most gullies on Longonot, some within the Olkaria Volcanic Complex	Single bed of laminated fine to coarse grey ash, with basal grey pumice lapilli, grades up into a weathered zone & palaeosol
Upper pumice member	Lp^7	BJ 119957 (Akira gully)		Some gullies on Longonot, some occurrences in E & NE parts of the Olkaria Volcanic Complex	Up to 5, but usually no more than 3, beds of grey pumice lapilli & ash with weathered zone & palaeosol at top of each. Includes blocky cone forming pyroclastics on Longonot

Table 3.4 Continued

Thickness in m a = max exposed b = max indicated bed	Volcanological interpretation or depositional environment	Underlain by	Overlain by	Notes
[a]5	Products of pre-caldera volcanism	?	Lp^2, Lpa	Type section included on column 11 of Foldout No. 1 (in pocket)
[b]11	Products of caldera forming eruptions — presence of >5 distinct ingnimbrites suggests >5 separate eruptions	Tk, Tl & Kb on rift margins Mt &? Tt on rift floor	Lp^2 or Lp^3	Type section included on column 14 of Foldout No. 1
[a/b]15	Product of the last caldera forming eruption	Lp^2 or Lp^1	Lp^4	
FOR	INDIVIDUAL	MEMBERS		Most important measured sections for all Lpa members are included on columns 11 & 12
[a/b]18	Fall deposit of plinian eruption, accretionary lapilli & cross bedding in some ash beds	Lp^1 O^2/Op^2 Mp	Lp^3 Lp^4, Lp^5	Important stratigraphic marker bed within Olkaria Volcanic Complex
[a]11 [b]4	Fall deposits of plinian eruprions, all but lowest bed followed by ash surge deposits	Lp^3 Lp^2	Lp^5	Within Olkaria Volcanic Complex this member is represented only by the lowest lithic rich pumice lapilli bed
[a]65 [b]16	Fall deposits of plinian eruptions. Eruption centre(s) buried beneath lavas of Longonot Trachyte	Lp^4 Lp^2	Lp^6 Lp^7 Lp^8	Interbedded with O^3/Op^3 within Olkaria Volcanic Complex. C^{14} sample site at BJ 119945
[a/b]5	Fall deposit: initial magmatic (plinian or subplinian) eruption of pumice lapilli followed by phreato-magmatic eruptions of ash	Lp^5	Lp^7 Lp^8	Is locally useful stratigraphic marker bed within the Olkaria Volcanic Complex
[a]10 [b]2.5	Pumice lapilli = product of magmatic (plinian or subplinian) eruptions. Ash = product of phreato-magnetic eruptions. All are fall deposits. Cone pyroclastics include welded fall tuff	Lp^6 Op^4	Lp^8	Where Lp^7 & Lt^2 exposed together, former underlies the latter. Overlies boulder gravel in Hell's Gate (BK 044033) & Lake Sediments in the Sulmac Estate (BK 030078)

Table 3.4 Continued

Name of formation (Fmn) or member (Mem)	Map symbol	Type area/section	Age	Major outcrops	Lithology
Tuff cones	Lpt	WSW end of Obsidian Ridge (BK 115058)		W end of Obsidian Ridge & Crescent Island	Tuff & lapilli-tuff, possibly with veneer of scoriaceous blocks & lapilli. Lithic blocks of trachyte welded tuff & porphyritic basalt
Longonot mixed lava Fmn	Lmx			N flanks of Longonot, Obsidian Ridge, & near S shore of Lake Naivasha	Lava, basic in appearance, & feldspar, olivine & pyroxene-phyric. Cone pyroclastics consist of welded scoriaceous blocks & bombs
Lower mixed lava member	Lmx^1	Crater on N flanks of Longonot at BK 143043			
Upper mixed lava member	Lmx^2	Longonot summit crater (BJ 163999)			Basaltic lava, some scoriaceous lapilli on rim of summit crater
Longonot Trachyte Fmn	Lt	Longonot cone		Forms steep sided cone of Longonot.	
Lower Trachyte mem	Lt^2	Side gully from Akira gully BJ 123957		Outcrops restricted to arcuate flow fronts & gullies owing to an Lp^8 cover	Trachyte lava flows with blocky flow surfaces, & at least some with basal agglutinate (lithic-rich)
Upper Trachyte mem	Lt^3	North slopes Longonot cone BK 165013		occurs as two flows, on N flanks, & SW flanks of Longonot	Trachyte lava with blocky flow surfaces, but pahoehoe lava close to vents. Cone pyroclastics assoc. with N flow
Longonot Ash Fmn	Lp^8	Longnot summit crater (NW wall, BJ 163999)	C_{14} date; 3280 ± 120 years BP from palaesol immed. below Lp^8	Widespread on Longonot, best exposed in gullies & in upper walls of the summit crater. Also occurs within the Olkaria Volcanic Group	Summit crater walls; lower half consists of pumice lapilli & blocks, upper half = bedded ash. Elsewhere, bedded ash overlies thin basal pumice lapilli

very blocky and only lightly vegetated. The Olenguruoni Hills are a group of domes which lie along the north to north-west edge of the complex. In the eastern part of the complex, the hills of Broad Acres Farm are formed of lava flows, rather than domes.

In eastern and southern parts of the complex, many domes have a topographically distinct arcuate alignment. In the south and south-west, they have coalesced to form a ridge, the highest point of which is known as Ol Orugo.

These arcuate aligned domes, together with the Ol Orugo Ridge, partly enclose a depression which is centrally situated within the Olkaria Volcanic Complex as a whole. The depression's full extent has been obscured by the Olobutot ridge and the Gorge Farm hills. Other isolated hills occur within the depression near its eastern side.

The above mentioned depression is bisected by an erosional channel, which formed during southward overflow of Lake Naivasha when the lake level was much higher that at present. The northern half of this feature, hereafter referred to as 'Hells Gate', is a sinuous flat floored feature which extends south-westwards from the north-east side of the volcanic complex. Cliffs up to 120 m high occur where lava flows have been eroded.

Pinnacles known as Fischer's Tower in the north (BK064051), and Central Tower (BK019013), which lies 6 km to the south-west, are volcanic necks revealed by the erosion of surrounding pyroclastic rocks. In the vicinity of Central Tower the smooth floor gives way southwards to a narrow, deeply incised gorge which marks the southward transition into what is hereafter referred to as the Ol Njorowa Gorge. About 1.5 km south of Central Tower, the narrow, deeply incised gorge gives way to that with a smooth floor up to 300 m wide, but which in contrast to Hell's Gate, has walls up to 200 m high.

The Ol Njorowa Gorge is at its deepest where it cuts through the southern arcuate margin of the volcanic complex, and from there southwards, its walls decrease rapidly in height and it merges with the westerly part of the Akira Plains (Figure 3.5).

The Hells Gate–Ol Njorowa Gorge is 16 km in total length and isolates about 56 km^2 of the eastern part of the volcanic complex, from the remainder. Within this 'East Domes' area the above mentioned arcuate aligned domes

Table 3.4 Continued

Thickness in m a = max exposed b = max indicated bed	Volcanological interpretation or depositional environment	Underlain by	Overlain by	Notes
	Products of phreato-magmatic/surtseyan eruptions, scoriaceas veneer probably of late stage magmatic (strombolian) eruptions	?	?	Obsidian Ridge cone possible = Lp^5 Crescent Island is pre — Lp^5
^{a}14^a	Eruptions probably of strombolian/hawiian nature, minimal production of pyroclastics	Lp^6/Lp^7?	Lp^8	Overlies Lake Sediment in boreholes C 910 at BK 096082 (Scott, 1977, 1980)
		Lp^2/Lp^8		
^{a}300 ^{b}100	Agglutinate at base of some flows, suggests lava was 'fountain-fed' during strombolian/hawaiian type eruptions	Lp^6 or Lp^7	Lp^8	
$^{a/b}$5	Hawaiian (SW flow) & strombolian hawaiian (N flow) eruptions on flanks	Lp^8		
Summit crater $^{a/b}$60 Elsewhere $^{a/b}$10	Initial magmatic eruption (plinian or subplinian) produced pumice lapilli fall, followed by phreato-magmatic eruptions-produced ash fall	Lt^2 or Lp^7 or Lp^6	Lt^3 Lmx^2	C^{14} sample site at Ak 994038

have their most prominent topographic expression (Figure 3.3).

Other topographic features within the volcanic complex are a number of small, smooth-floored, intervolcanic alluvial basins which occur to the north, west and south of Olkaria hill.

3.8.2 Geology

On the basis of surface outcrops the main products of volcanism within the Olkaria Volcanic Complex (termed the Olkaria Volcanic Group) have been alkali rhyolite (comendite) lava and pyroclastic rocks. Trachyte and basalt-hawaiite lava have been minor products, but wide spread trachytic pyroclastics to the north-west, west and south-west of the complex are believed to have been erupted from vents within the complex.

This belief is supported by the abundance of trachytic volcanic rocks encountered in more than 30 geothermal boreholes which have been drilled to depths of between 1000 and 2500 m below the surface. Rhyolitic and basaltic volcanic rocks have also been encountered in these boreholes.

The presence of a previously established Longonot Tephra succession in the area east of the gorge has allowed a subdivision of the Olkaria Volcanic Group into five formations one of which, the Olkaria Comendite Formation, comprises four members (Figure 3.4). This in turn has lead to a multistage model for the development of the most recent events at Olkaria. The stages proposed, with associated units, are:

1 *Dominantly trachytic lava and pumice pile*
Represented by the Maiella (plinian) pumice formation (Mp) and the Olkaria Trachyte (lava) formation (Ot).

2 *Caldera fracture*
Represented by the Ol Njorowa (welded) Pantellerite formation. (01)

3 *Early post-caldera activity*
Represented by the Lower Comendite member of the Olkaria Comendite formation, in the form of lava and pyroclastic facies. (02)

4 *Ring Dome formation*
Represented by the Middle Comendite member which is

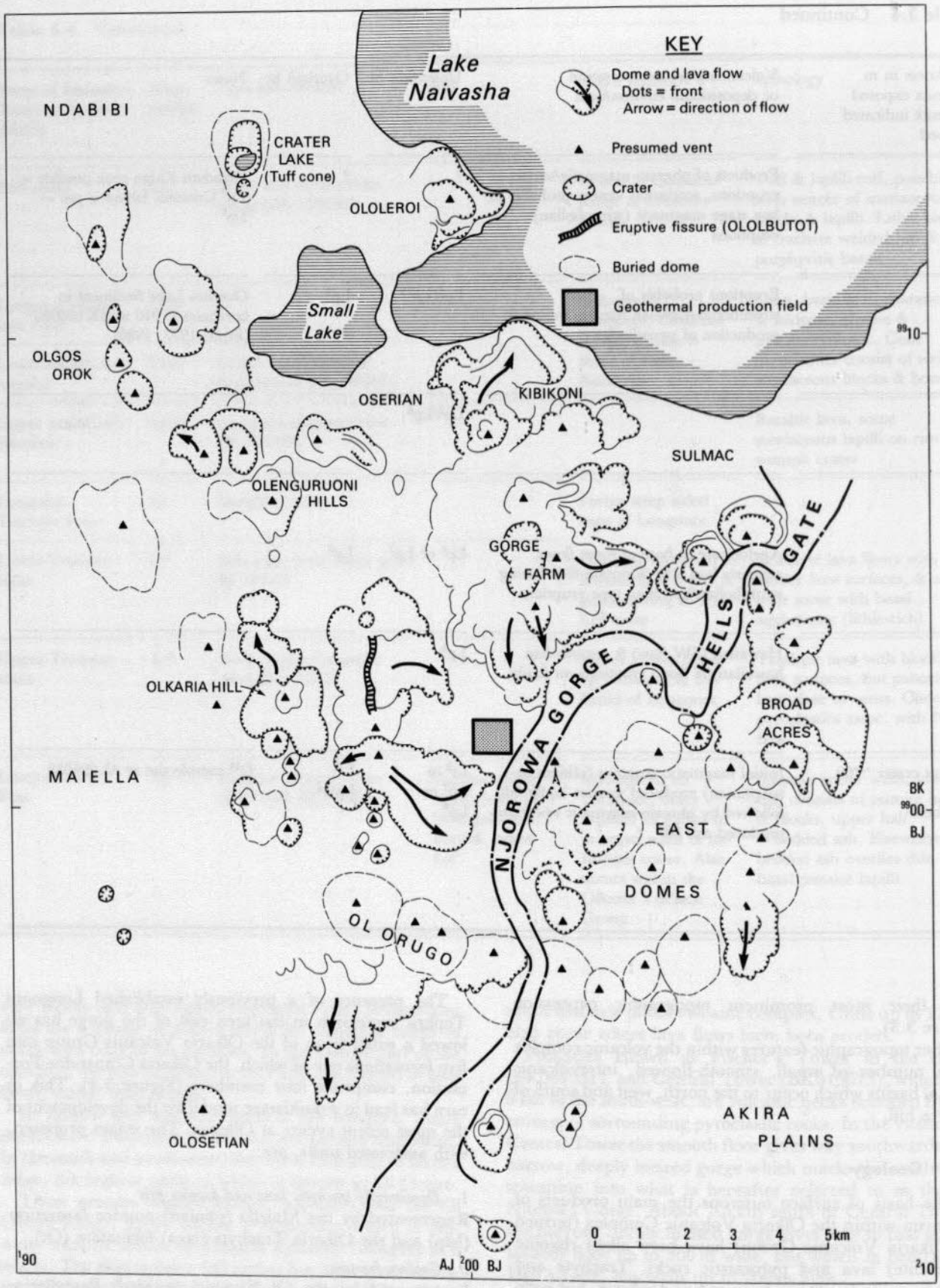

Figure 3.3 Main surface features of the Greater Olkaria Volcanic Complex.

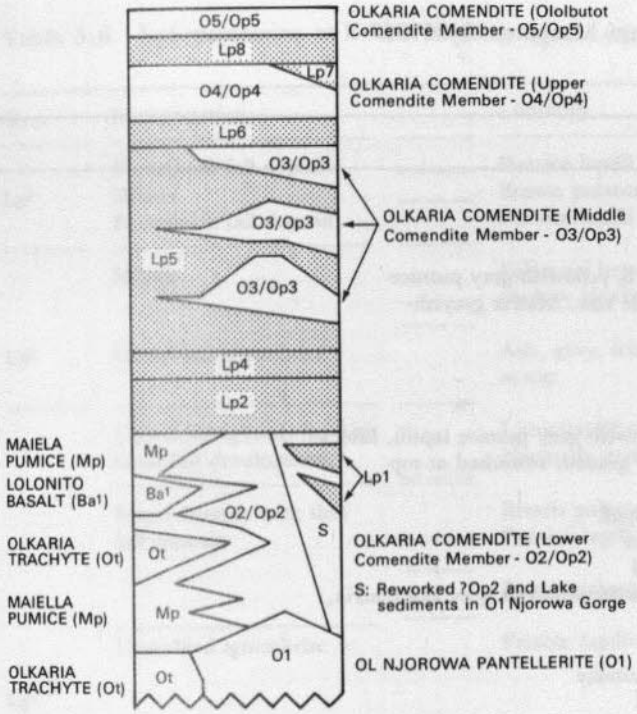

N.B. Longonot Stratigraphic Units (stippled) as follows;

Lp1: Kedong Valley Tuff
Lp2: Bedded Pumice Member of Akira Pumice
Lp4: Surge Member of Akira Pumice
Lp5: Lower Pumice Member of Akira Pumice
Lp6: Bedded Ash Member of Akira Pumice
Lp7: Upper Pumice Member of Akira Pumice
Lp8: Longonot Ash

Figure 3.4 Summary of Olkaria stratigraphy showing its relationship to Longonot pyroclastic sequences.

often dome building, eg the arcuate domes of east of the gorge. Thick surge beds also characterise this stage. (03)

5 *General resurgence*

Represented by the Upper Comendite member which builds superincumbent short thick flows which are particularly well developed at the northern entrance to Hells Gate. (04)

6 *North-south fissure activity*

Represented by the Ololbutot Comendite member whose most striking expression is a very thick, very young flow within the depression formed by the ring domes. (05)

Details of the stratigraphy deriving from the present work are given in Table 3.7 and a selection of measured sections in Foldout No. 1.

Details of the subsurface geology are known from cuttings and cores obtained from production wells which define the Olkaria Geothermal Field, and from exploration wells drilled elsewhere in the Olkaria Volcanic Complex. Recent examination of the above mentioned cores and cuttings (Browne, 1984; Odongo, 1982, 1984; GENZL, 1986), has shown that the subsurface geology consists of at least 2600 m of subaerially erupted rhyolitic, trachytic and basaltic lava, and associated pyroclastic rocks. Lava flows predominate in the production wells, but pyroclastics are more frequent in the exploration wells in western areas. No lithological marker horizons have been identified even within the closely spaced production wells (Browne, 1984).

3.8.3 Age

An age of 0.45 Ma has been obtained from a sample taken from a depth of 1000 m in the "most recent" borehole near Olkaria hill (B C King, pers. comm. in Bliss, 1979). The number and location of this borehole is not known.

The two ^{14}C dates reported from the Longonot succession can be also used to bracket the younger Olkaria events. The Lower Comendite member is more than 9150 ± 110 BP while the Middle member, that associated with the prominent ring dome event, is younger than that date but older than 3280 ± 120 BP. Carbonised tree branches from a pumice flow associated with the Olubutot lavaflow gave an age of 180 ± 50 BP.

3.9 THE EBURRU VOLCANIC COMPLEX

3.9.1 Introduction and morphology

The Eburru Volcanic Complex is located to the northwest of Lake Naivasha and forms the drainage divide be-

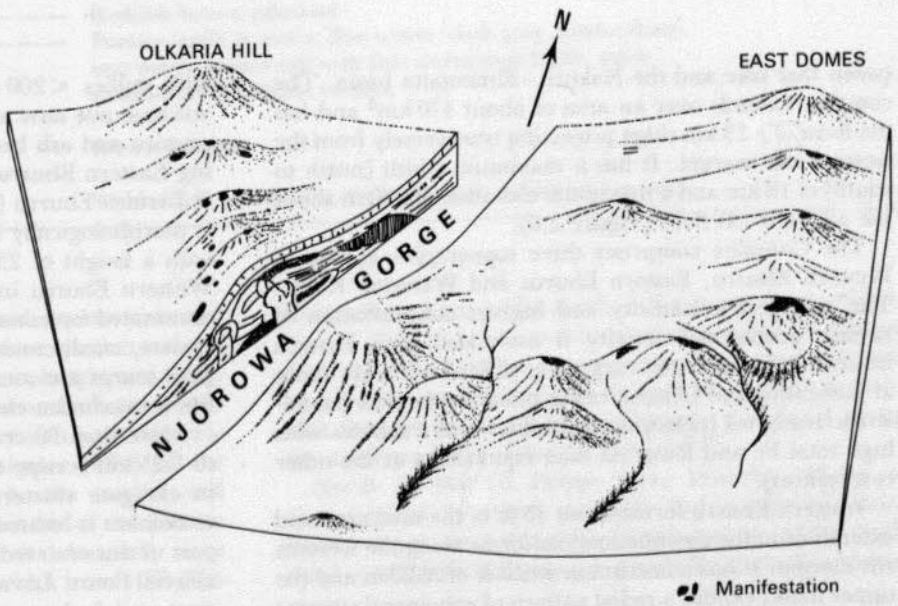

Figure 3.5 Relation of East Domes arc to domes west of Njorowa Gorge.

Table 3.5 LpK succession in gully immediately W of Mount Margaret: BJ261887 (Total thickness 22 m) (*youngest at top*)

Strat	Interpretation	Lithology
	Unwelded (? reworked) ignimbrite	Grey, friable ash with pumice lapilli & lithics
Lp^3	Ignimbrite	Partly welded tuff, grey & yellowish-grey pumice lapilli, lithics up to cobble size. Matrix greyish-yellow/brown tuff
		Brown palaeosol
	Pyrolcastic fall deposits	Grey, grey-green & yellowish grey pumice lapilli, lithics incl. obsidian. Normally graded, reworked at top
Lp^1 &/or Lp^2		Reddish-brown — palaeosol Pumice lapilli — compact Reddish-brown palaeosol
	?ignimbrite	Pumice lapilli & lithics, with yellowish grey ash matrix, reworked
	Unwelded ignimbrite	Friable ash (grey) with pumice lapilli & lithics, unsorted
	Pyroclastic fall deposits	Bedded pumice lapili, grading up into ash
Lp^1	Hiatus	Palaeosol, grey-brown (lower) to reddish-brown (upper), derived lithics in lower part. Trace layer of pale yellowish-brown ash
	Unwelded ignimbrite	Friable ash (grey) with pumice lapilli & lithics unsorted, but normal grading of lithics with trachyte, welded tuff obsidian & syenite pebbles towards base & reversed grading of pumice lapilli
	Fall &/or surge deposits	Laminated ash & pumice lapilli
	Hiatus	Brown palaeosol
?	Fall deposits	Grey pumice lapilli
	Hiatus	Yellowish-brown palaeosol
		Angular unconformity
Mt	Fall deposits	Bedded ash & lapilli

tween that lake and the Nakuru–Elmentaita basin. The complex extends over an area of about 470 km² and has the form of a 23 km ridge projecting transversely from the western rift margin. It has a maximum width (north to south) of 18 km and a maximum elevation of 980 m above the adjacent rift floor (Figure 2.6).

The Complex comprises three topographic entities—Western Eburru, Eastern Eburru and Waterloo Ridge. The youngest volcanicity and highest concentration of surface geothermal activity is associated with Eastern Eburru. Characteristic rock types differ both from those at Longonot and Olkaria being pantellerites and pantelleritic trachytes (peralkaline rhyolites and trachytes with high total Fe and lower Al than equivalents at the other two centres).

Western Eburru forms about 35% of the total area and extends onto the downfaulted platforms along the western rift margin. It has a maximum altitude of 2820 m and the upper flanks exhibit a radial pattern of ephemeral streams with gullies <200 m deep. It is interpreted as an older volcanic pile now almost completely blanketed with thick pumice and ash beds from the younger centres comprising Eastern Eburru.

Eastern Eburru (approximately 57% of the total area) is morphologically linked to Western Eburru by a saddle with a height of 2520 m. Eastern Eburru contrasts with Western Eburru in that it is much less dissected and is dominated by constructional volcanic landforms such as craters, small cones, lava flows and domes. Very young fault scarps are conspicuous on its northern flanks. It too has a maximum elevation of 2820 m.

More than 50 craters ranging in diameter from 200 m to 1.25 km occupy the summit area above 2600 m; many in elongate clusters aligned north–south. The Eburru settlement is located within the eastern and north-eastern part of this cratered area. The larger craters have smooth alluvial floors. Lava flows with steep sided fronts are common and fault scarps occur within a 3–4 km wide zone

Table 3.6 Lpk succession at Ewaso Kedong ..... (*youngest at top*)

Strat	Interpretation	Lithology
	Pyroclastic fall deposit	Pumice lapilli, reworked
Lp^5	Hiatus	Brown palaeosol, abundant pumice
	Pyroclastic fall deposit	Pumice lapilli grey, trachyte & syenite lithics
	Hiatus	Palaeosol brown to yellowish-brown, grey-green cindery blocks at base
Lp^3	Unwelded ignimbrite	Ash, grey, friable, dark grey cindery blocks at top
	Unwelded ignimbrite with basal fall development	Lithic/lapilli-tuff, greenish-grey, drifts of pumice lapilli in lower part Normally graded pumice layer at base, brown weathered at top
	Major hiatus, with thin fall deposits	Brown palaeosol Pumice lapilli, grey, carbonate cement in patches
		Brown palaeosol
	Unwelded ignimbrite	Friable lapilli-ash, greenish-grey to yellowish-grey
Lp^1		Lithic/lapilli-ash, brown weathered, forms persistent layer
	Unwelded ignimbrite	Compact lithic/lapilli-ash, greenish-grey. Lithics incl. grey trachyte, yellow/pale brown tuff. Some drifts of pumice lapilli. Abundant pebble to cobble sized lithics of syenite, varicoloured trachyte, obsidian & red altered rock in basal 0.7 m
	Hiatus	Brown-orange palaeosol
	Fall deposits	Bluish-grey ash, very fine at top reversely graded pumice lapilli layer in middle, normally graded pumice lapilli at base
	Hiatus	Brown palaeosol, abundant pumice
Lp or Suswa	Unwelded ignimbrite	Pumice-rich lapilli-ash, compact resistent, pale brown to purple, dark green-grey pumice lapilli, lithics up to pebble size, pumice blocks at base
	Fall deposits	Two layers of reversely graded ash & pumice lapilli
	Hiatus	Reddish-brown palaeosol, compact, some carbonate nodules
Probably Suswa	Fall deposits	Pumice lapilli, brownish or reddish-grey, compact
	Hiatus	Reddish-brown palaeosol
	Ignimbrite	Pumice lapilli & scoria, fine-coarse, dark grey, grades down into partly welded tuff with fine scoriaceous lapilli, sand-sized lithics & feldspar crystals
	Hiatus	Brown palaesol
	Welded ignimbrite	Welded tuff, scoriaceous blocks & lapilli & feldspar crystals

extending northwards from the cratered summit area and corresponding with the zone of surface geothermal activity. Most scarps rarely exceed 10 m in height and range in length from 300 m to 3.5 km. Some fault scarps do occur on the southern flanks but are much less common.

Waterloo Ridge forms the remainder (8%) of the Eburru Volcanic Complex and lies to the east of, and topographically lower than, the remainder of the Eburru massif. The 19.5 km long ridge is elongate in a north–south direction and varies in width from 1.5 km in the south to 3 km in the north. It has a maximum elevation of 2160 m in the northern section which is divided from the southern by a young lava from the Ol Bonge cone on the south-east flanks of Eastern Eburru. An erosion channel known as Masai Gorge is developed along the northern front of the Ol Bonge flow.

North of the Ol Bonge lava, Waterloo Ridge is characterised by steep, probably fault-controlled, east-facing slopes, and the ridge crest is up to 160 m high relative to the Ilkek Plains, (northern Naivasha Basin) im-

Table 3.7 Details of the Olkaria Volcanic Group (*oldest units at top*)

Name of formation (Fmn) or member (Mem)	Map symbol	Type area/section	Age	Major outcrops	Lithology
Maiella Pumice Fmn	Mp	Gully & roadside exposures in the Maiella area between the Ngati & Ngunyumu settlements. AK 879072, AK 874065		Widespread immediately W & SW of the Olkaria Volcanic Complex, confined to gullies in W part of the complex itself. May be present within Ol Njorowa but not seen any further east	Grey pumice lapilli & ash beds with palaeosol &/or weathered zone at top of most beds. Some pale grey & bluish-grey beds, are yellowish-grey due to alteration in areas of geothermal activity. Occasional vertical colour changes may be due to compositional zoning. In S areas some beds contain many discrete feldspar crystals &/or feldspar phenocrysts in the lapilli
Olkaria Trachyte Fmn	Ot	Gullies immediately S of Ol Orugo e.g. AJ 983975, AJ 985968		Gullies & ridges S & SW of Ol Orugo	Highly feldspar porphyritic crystalline lava & obsidian, flow banded & brecciated towards & at top. Also has basal breccia. Includes small exposure of welded scoriaceous lapilli & block tuff, at base of Mp in gully of Ol Orugo
Lolonito Basalt Fmn	B^1	Gullies E & NE of Loirogwa e.g. AJ 960937, AJ 958941, AJ 957946		Gullies E & NE of Loirogwa, Kepise area SE of Loirogwa & Sibet Hill in Erusia area S of Loirogwa	Basic vesicular lava with aa and occasional pahoehoe flow surfaces, flow banded 'trachy basalt' & 'trachybasalt' auto breccia. Basic lava only in Kepise & Erusia areas; scoria cone forms W side of Sibet Hill
Ol Njorowa Pantellerite Fmn	O^1	Lower parts of walls on either side of the deepest part of Ol Njorowa Gorge e.g. BJ 009955		Ol Njorowa Gorge only	Densely welded block pyroclastics
Reworked pyroclastics & lake sediments	S	Ol Njorowa Gorge e.g. BK 014007 & around		Ol Njorowa Gorge	Sand/sandstone, siltstone some carbonate & siliceous concretions, reworked pumice lapilli & ash, some diatomaceous
Olkaria Comendite Fmn (Comprises 4 members $O^{2\text{-}5}$ as below, each with pyroclastic facies $Op^{2\text{-}5}$)	O/Op	Olkaria Hill, Ololbutot & area immediately E of Central Tower. Measured section at AK 949020 shows interrelations of 3 Op units & 2 Longonot units			Lava flows crystalline (? devitrified glass), flow banded & interbedded with obsidian towards top, blocky flow surfaces. Domes (mostly O^3), otherwise similar to the lava, except where altered by geothermal activity. Plugs & dykes exposed in Hell's Gate/Ol Njorowa gorge

Table 3.7 Continued

Thickness in m a = max exposed b = max indicated bed	Volcanological interpretation or depositional environment	Underlain by	Overlain by	Notes
[a]?100 [b]10	Fall deposits—probably products of plinian eruptions. Centres not known but assumed to be within Olkaria Volcanic Complex but buried beneath later rocks (e.g. O/Op)	Tl Tmm	Lp^2	Interbedded with O^2/Op^2 & B^1 N.B. Longonot origin for some pumice beds cannot be ruled out. Fluvial sand & gravel occurs in places e.g. AK 874065 & between AJ 921954 & AJ 935932. Measured sections are included in solumns 2 & 3 in Foldout (in back pocket)
[a](b?)10	Lava extruded from centre at or very close to Ol Orugo	Mp O^2	Mp Lp^2	Measured section included in column 5 in Foldout
[a/b]5	Basic lavas probably are products of hawaiian/strombolian eruptions—from minor volcanic centres S of Olkaria Volcanic Complex in case of Kepise & Erusia occurrences	Mp	Mp	Measured section & stratagraphic relation included in column 6 in Foldout
[a]100	Welded fall or ignimbrite proximal facies	?	O^2/Op^2	
[a]55	Shallow lacustrine—frequent influxes of pyroclastic material including Longonot ignimbrites	O^1 Op^2/O^2	Lp^1	Measured section included in column 9 in Foldout
lava flows [b]60	Violent (vulcanian?) eruptions of pumice & lithic material preceeded the eruption of either short thick lava flows or domes			Columns 7, 8 & 9 in Foldout include many sections. Ages given are interpretations of C^{14} dates obtained relative to Longonot Tephra

Table 3.7 Continued

Name of formation (Fmn) or member (Mem)	Map symbol	Type area/section	Age	Major outcrops	Lithology
Lower comendite member	O^2/ Op^2	Lava—BK 025034 Proximal Op^2 AJ 950943	>9150 BP	Within & W of Hell's Gate–Ol Njorowa Gorge, rarely exposed E of gorge. Olenguruoni hills & Kibikoni Farm (Op^2), gullies in central & SW parts of Olkaria Volcanic Complex (Op^2, some O^2)	Pyroclastics (Op2–5): fall deposits composed of pumice & lithic blocks (proximal) or pumice lapilli & ash (intermed. distal). Some 'breadcrust' bombs; pumice is either very pale grey or white (contrasts with Longonot Akira pumice & most Maiella pumice); surge deposits (Op^3 only) consist of pumice lapilli & ash with dune & parallel bedding, plus accretionary lapilli. Pyroclastic flow deposits (Op^5 only) occur on floor of Ol Njorowa Gorge
Middle comendite member	O^3/ Op^3	Lava (O^3)—BJ 062976 Surge (Op^3)—BK 019012 & BJ 059938	<9150 >3280 BP	Gorge farm, central & E parts of Olkaria Volcanic Complex. incl. Arcuate Domes	
Upper comendite member	O^4/ Op^4	Lavas well exposed in walls of Hell's Gate & in nearby Fischer's Tower Plug. BK 063052. Proximal facies of Op^4 at AK 965029. Distal facies at AK 996033	>3280 BP	Broad Acres Farm Hell's Gate (inc. Fischer's & Central Towers, Ololbutot area, adjacent to Olkaria Mtn, along E edge of Ol Njorowa Gorge. Locally on Western rim of Longonot Caldera	
Olobutot comendite member	O^5/ Op^5	Flow front well exposed at AK 006006 & pumice flow at BJ 009982	C^{14} date of 180 ± 50 BP	Olobutot area W & S of the Olkaria geothermal field	

mediately to the east. Steep slopes only occur very locally on the west side of the ridge. South of the Ol Bonge lava the ridge has less steep, east-facing slopes, and in places it is relatively symmetrical in profile.

3.9.2 Geology

The Eburru Volcanic Complex is characterised by highly evolved trachytic and rhyolitic compositions which differ in detail from those erupted at Longonot and Olkaria in that they are richer in total iron and generally lower in alumina and often have higher peralkaline indices. The high silica varieties are pantellerites rather than comendites as at Olkaria.

The three subareas discribed in the previous section correspond with three separate stages of the evolution of the Eburru Volcanic Complex as a whole. An outline of the stages proposed, with associated formations is given below:

1 *Building of a volcanic pile at Western Eburru*
Very little of this is exposed due to subsequent blanketing by products of Eastern Eburru but a number of small outcrops exist on the northern lower slopes (Kiambogo Pantellerite Formation) as well as some near the summit (Western Eburru Pantellerite Formation).

2 *Eruption of Waterloo Ridge fissure zone*
Waterloo Ridge is interpreted as the product of a series of dominantly pyroclastic eruptions whose origin was an elongate fracture associated with north–south faulting. Welding of pumices is frequent but often is of fall rather than flow origin. A product of this activity is the Waterloo Ridge Pantellerite Formation.

3 *Building of a volcanic pile at Eastern Eburru*
Most of the earlier products of this stage are concealed by younger deposits. Much of the activity was probably pyroclastic (Eburru Pumice Formation) the youngest expression of which are the numerous craters of the Eburru summit area. The upper eastern flanks of Eburru are dominated by lava flows and (often welded) cone pyroclastics of the Eburru Trachyte Formation.

4 *Axial activity at Eastern Eburru*
The Eburru Pantellerite Formation builds a marked north-south elongate zone of lava flows and cratered pyroclastic cones to the west of the Eburru Trachyte outcrops. These outcrops generally straddle the Western Eburru pile, running from the low ground at Ndabibi in the south over the eastern termination of the Eburru ridge and down the northern flanks to the Elmenteita area in the north.

More details of the stratigraphic units are given in Table 3.8.

Table 3.7 Continued

Thickness in m a = max exposed b = max indicated bed	Volcanological interpretation or depositional environment	Underlain by	Overlain by	Notes
Pyroclastics [b]21	Dispersal of pyroclastic fall deposits much less than that of the Akira & Maiella Pumice Formations	Mp O[1]	Lp2 Ot	Up to 5 distinct beds, interbedded with Mp, in gully exposure of Loirogwa. Measured sections included in columns 4 & 5 of Foldout Distinction from Mp not always clear
	Thick surge horizons are products of phreatomagmatic volcanism (Op[3])	Lp[2] Lp[4-5]	Lp[5-6]	Up to 3 distinct beds within Lp[5] in a gully exposure adj. to Olkaria Mountain. Measured sections included in columns 7, 9 & 10 of Foldout
		Lp[6]	Lp[7] Lp[8]	On W rim of Longonot caldera bed occurs between Lp[6] & Lp[7]
		Lp[8]		[14]C age on carbonised tree from Op[5] (BJ 009982)

3.9.3 Age

No specific data are available but the comparable lack of erosion and associated vegetation cover indicates that the youngest activity must be similar in age to that at Longonot and Olkaria, i.e. is Recent, and probably only hundreds of years old.

The distribution of the majority of fumarolic activity coincides with many of the summit craters and the northern portion of the Eastern Eburru Pantellerite Formation, perhaps indicating that these areas have been active most recently.

3.10 THE ELMENTEITA, NDABIBI AND AKIRA VOLCANIC GROUPS

These three groups comprise the products of the youngest phases of volcanism in the following 3 areas:

3.10.1 The Elementeita basin

Volcanism in the Elmenteita basin, between Eburru and Lake Elmenteita, has taken place in structural continuity with that of Eastern Eburru, but unlike the latter has been basaltic in composition. During periods of low lake levels the volcanism has been magmatic in nature and consequently small scoria cones have formed in association with the extrusion of basaltic lava. During periods of higher lake levels the volcanism had a phreatomagmatic nature and built a series of relatively large tuff cones, few of which have been associated with lava extrusion.

The cones are distributed in an 8 km-wide zone which extends northwards from the foot of Eastern Eburru to the southern shore of Lake Elmenteita. Karterit and Losiwire are the only named cones in the area and are the largest. Losiwire has a basal diameter of 1.4 km and a maximum height of 120 m along parts of the rim of a 900 m diameter crater. Faults traverse the cone in a north–south direction and the majority have formed scarps no more than 20 m high. One fault zone however has formed a 50 m-deep notch. Karterit is 2.6 km long in a north–south direction and is up to 2 km wide. It has a 1.5 km-wide crater in the north which has coalesced with a much smaller crater to the south. The above cones do not appear to have formed in association with lava extrusion. The large craters relative to the overall size of the cones is consistent with them having formed as tuff cones (Wohletz and Sheridan, 1983), probably during periods of high lake level.

The remaining cones in the area occur either within or around the edges of a very young lava flow which forms the Otutu or Badlands area, and which extends for nearly 11 km in a west-north-west direction at the foot of Eastern Eburru. Lava tubes are a feature of this area. A 60 m-

Table 3.8 Details of the Eburru Volcanic Group (*oldest units at top*)

Name of formation (Fmn) or member (Mem)	Map symbol	Type area/section	Age	Major outcrops on map	Lithology
Waterloo Ridge Pantellerite Fmn	Erw	Masai Gorge-type section BK 033285. Important other exposures at BK 025286 & BK 042229		Waterloo Ridge & smaller fault bounded ridges to the W	Strongly banded 'lava'. Unwelded pyroclastics composed of pale bluish-grey pumice blocks & lapilli & lithics (lava & obsidian) with interbeds of eutaxitic welded tuff with obsidian fiamme in a yellow tuff matrix. Some welded tuff with feldspar crystals & fine lapilli
Kiambogo Pantellerite Fmn	Erk	Kiambogo Farm AK 816378		Kiambogo Farm, Ol Jorrai Ranch & Soysambu	Mostly banded 'lava' like that of Erw, but welded pyroclastic rock, with traces of flattened lapilli, occurs in Kiambogo Farm
Western Eburru Pantellerite Fmn	Er^1	Summit area of western Eburru. Important measured section at AK 855285 very thick lava at AK 857284		Summit area of W Eburru	Feldspar porphyritic banded lava. Unwelded pyroclastics composed of pale yellowish-grey pumice lapilli, blocks & obsidian lithics. Obsidian layer at top of unwelded pyroclastics
Eburru Pumice Fmn	Ep	Kiambogo Gully — important measured sections at AK 795261, AK 796289, AK 811293. Other important measured sections outside type area at AK 927299 & AK 994394		Widespread over Western Eburru extending onto the adjacent Mau Escarpment. Also present on Eastern Eburru & Waterloo Ridge	Grey pumice lapilli &/or ash beds most of which have a palaesol &/or weathered zone at the top. Blocky pumice deposits occur in the cratered summit area of Eastern Eburru. Pumice accompanied by obsidian & trachyte lava lithics. Occasional beds rich in feldspar crystals, & highly feldspar porphyritic lapilli. Some bedded ash deposits low in the exposed succession
Eburru trachyte Fmn	Et				
Older mem	Et^1	Eburru Farm BK 001310		Eastern Eburru only, Ol Jorrai Ranch, Kianugu, Lion & Ol O'bonge hills & adjacent areas	Trachyte lava flows, usually feldspar porphyritic. Cones of pumiceous & scoriaceous blocks occur as Lion and Ol O'bonge hills. Kianugu hill is formed of densely welded pyroclastic rock
Younger mem	Et^2	Masai Gorge BK 034284			
Eastern Eburru Pantellerite Fmn	Er			Eastern Eburru only, N, Central & S areas	Obsidian lava flows; massive, vesicular, sparsely to highly feldspar porphyritic. Some thick flows consist of crystalline lava with obsidian at the surface. Welded pyroclastic rock forms ridges in N area & may form part or all of cones in the S area
Older mem	Er^2	Crater at AK 927299			
Younger mem	Er^3	Cedar Hill area AK 955325			

Table 3.8 Continued

Thickness in m a = max exposed b = max indicated bed	Volcanological interpretation or depositional environment	Underlain by	Overlain by	Notes
[a]~20	Lava may be at least in part a rheomorphic welded pyroclastic fall. Associated unwelded blocky pyroclastics are proximal fall deposits — interbedded with obsidian-rich welded fall tuff. Welded tuff with fine lapilli is probably an ignimbrite	ls at base, on Tlg	Ep	
?	Lava may be a rheomorphic welded pyroclastic fall. Welded pyroclastic rock in Kiambogo Farm may also be of fall origin	?	ls	
lava [b]70 tephra, [b]10 obsidian, [b]1.75	Unwelded pyroclastics represent proximal fall deposit. Obsidian layer may be a welded deposit composed of obsidian pyroclastic	?	Ep	
a 120, b 20	Fall deposits representing the products of plinian eruptions. At least some eruptions took place within the cratered summit of Eastern Ebburu	Er^1	Et & Er	Interbedded with Et
?	Volcanism dominated by extrusion of lava, some cone pyroclastics formed around vents	Ep	Ep &/or Er	Et^2 differs from Et^1 only by lack of Ep cover
b 30	Volcanism dominated by lava extrusion — youngest flow (Er^3) accompanied/preceeded by eruption of pumice blocks & lapilli dispersed westwards. Cedar Hill is obsidian flow/dome	Ep	Ep &/or Et	

high cone, with a basal diameter of 400 m and a 150 m diameter crater, at the south-east corner of the flow (AK943375), is assumed to be its source. The Otutu flow has surrounded other cones. Other unnamed cones lie at or close to the edge of the Otutu flow. Another very similar flow extends northwards between Losiwire and Karterit and terminates on a broad front about 1.5 km from the southern shore of Lake Elmenteita. Older lava occurs in a wide area south-west, west and north of Losiwire and extends to the southern shore of the lake. The highest parts of the lava form extensive rocky outcrops whereas intervening depressions are smooth, and sediment floored.

Older lavas outcrop on the Gilgil ridge and Ilkek plains to the east of Elmenteita and also to the west and south-west of that lake. In these cases the lavas are best exposed in fault scarps.

The products of volcanism in the Elmenteita basin form the Elmenteita Volcanic Group, of which the Elmenteita Basalt and Tuff Cones are formations. (Table 3.9)

3.10.2 The Ndabibl plains

The Ndabibi plains form an 11 km wide low-lying area between the Eburru and Olkaria Volcanic Complexes.

Volcanism on the Ndabibi plains has occurred between, and in structural continuity with, that of Eastern Eburru to the north and the Olkaria Volcanic Complex to the south. Unlike in the Elmenteita basin both rhyolitic and basaltic volcanism has occurred on the Ndabibi plains but in common with the Elmenteita basin varying lake levels have influenced the nature of volcanism (e.g. magmatic or phreatomagmatic). The rhyolite occurs mainly as domes and lava flows with some some pyroclastic cones. Most of the rhyolite is comenditic, as at the Olkaria Volcanic Complex, but some pantellerite similar to that of the Eburru Volcanic Complex, has also been erupted.

The basaltic centres consist of cratered volcanic cones, similar to those of Losiwire and Karterit in the Elmenteita area. The largest contains Crater Lake. The Crater Lake cone is 2 km long in a north–south direction, is up to 1 km wide, and reaches a maximum height of just over 60 m above the surrounding plains.

The group of centres north of the Crater Lake cone includes several steep sided comendite domes rising to 160 m above the adjacent plains. East of Crater Lake, the Ololeri Farm is located on a broad pantellerite dome which is 2.5 km long in a west-north-west direction, and which attains a maximum height of just over 160 m relative to Lake Naivasha. A group of comendite domes occurs on the southern part of the Ndabibi plains in an area known as Olgos Orok. The steep-sided 220 m high dome known as Mulla has a small summit crater and is the largest of this group of 5 domes which are aligned in a near-northerly direction.

The products of the Ndabibi plains volcanism form the Ndabibi Volcanic Group, of which the Ndabibi Basalt, Tuff Cones, Ndabibi Comendite and Ndabibi Pantellerite are formations.(Table 3.9)

3.10.3 The Akira plains

Basaltic, trachytic and rhyolitic volcanism, which has occurred on the Akira plains,, probably defines structural continuity between the Olkaria Volcanic Complex and Suswa Volcano, which lies immediately south of the area mapped in detail.

A small 40 m-high steep-sided basic pyroclastic cone with a basal diameter of 250 m, and with a crater less that 100 m across, lies on the plains approximately 3 km south of the entrance to Ol Njorowa Gorge. One of the largest centres on the Akira plains is the 80 m high ridge known as Tandamara (or Olomoroj) which lies just over 6 km south-south-east of the entrance to Ol Njorowa Gorge. Tandamara is 900 m long in a north-north-east direction and attains a maximum width of just over 500 m. Small ridges between 1 and 3.5 km south and south-west of Tandamara may be erosional remnants of other volcanic centres. A 1 km long and 850 m wide ridge known as Sibet lies on the western edge of the Akira plains, 7 km west-south-west of Tandamara and incorporates a volcanic cone on its western side.

The products of the Akira plains volcanism constitute the Akira Volcanic Group, of which the Tandamara Trachyte and Akira Basalt are recognised as formations, (Table 3.9). Although rhyolitic volcanism has occurred on the plains close to the Ol Njorowa Gorge entrance the products of this volcanism are more conveniently included in the Olkaria Volcanic Group.

3.11 SEDIMENTARY ROCKS

3.11.1 Lake sediments (ls)

Lake sediments form a large part of the floor of the Naivasha basin and are exposed in gullies, road sections and small quarries on the Ilkek plains and around the northern side of the Olkaria Volcanic Complex.

The Gilgil river gully exposes (at BK061344) a 15 m succession dominated by grey to brownish grey silt and clay. Gravel composed of well-rounded, pebble-sized, pumice clasts is exposed alongside the Nakuru highway at BK084328, but finer gravel together with silty sand, and some white clay occurs in other roadside exposures. Further north pale grey silty gravel with drifts of pumice, underlies lava of the Elmenteita Basalt at BK039403, and overlies banded rhyolite and obsidian of the Waterloo Ridge Pantellerite (Eburru Volcanic Group). Silty clay, pumice gravel and sand and gravel of possible deltaic rather lacustrine origin occur in the Karati Gully, North of Naivasha Town. 3 m of the clay overlies a palaeosol at BK145243 developed at the top of a 1.5 m thick grey-green lithic lapilli-tuff which is correlated with Kedong Valley (Longonot Volcanic Group) Tuff ignimbrite and is underlain by up to 5 m of deltaic sand and gravel.

Sand and pebble beds dominate exposures of lake sediments around the northern side of the Olkaria Volcanic Complex. Gravel composed of rounded pumice clasts is common, and in some cases it also contains subrounded comendite clasts. Deposition in a high-energy, possible fluvial, environment is indicated by well-bedded sand dominated sequences which show large-scale cross-bedding and channel development (e.g. between AK994094 and BK003094 and between BK038078 and BK031078). In a quarry near the Elsamere Conservation Centre (BK018097) lacustrine sands and gravels composed of subrounded comendite pebbles and cobbles, overlie lava of the Olkaria Comendite (Lower Comendite Member-02), and underlie the Longonot Ash (Lp8). Quarry exposures at BK021089 show 2.5 m of lake sediments overlying a thick (2 m +) bed of grey pumice lapilli.

Gully exposures immediately west of the Sulmac Estate (e.g. BK033073) show interbeds of lake sediments and the

Lower Pumice Member (Lp5) (Longonot Volcanic Group).

In the Nakuru–Elmenteita basin the most extensive exposures occur on downfaulted platforms in the Kariandus area, but those in the Kariandus diatomite mine described by McCall (1967) lie just north of the project area. White diatomite is exposed alongside and adjacent to the Nakuru highway south of Kariandus (e.g. between AK983481 and AK979484). It overlies the brecciated surface of a lava flow of the Gilgil Trachyte (Eg AK983481), and thin beds of olive-green ash and grey pumice lapilli occur within the diatomite. The olive-green ash is believed to be a distal product of tuff cone eruptions which have taken place south of Lake Elmenteita. The pumice beds range in thickness from 0.05 m to 0.4 m and reversed grading is apparent in the thicker beds. They probably correlate with part of the Eburru Pumice. The diatomite is overlain by silt, sand and gravel. Within the Nakuru–Elmenteita basin proper lake sediments are exposed on the floor of a deep fault-induced valley incised into the northern rim of Losiwire crater (AK931449). Cobble and boulder gravel, composed of rounded tuff clasts, overlies a fine grey pumice gravel which inturn overlies friable very pale grey-brown silt. In a road section on the eastern side of the Kiambogo gully, bedded, cross-bedded and channelled sand and gravel, probably deposited in a fluvial environment, overly pumice gravel which may have been lake deposited. Near the south-western edge of the basin, exposures in the Nderit Valley, at AK757397, consist of distal Eburru Pumice ash overlying approximately 20 m of pumice rich gravel and sand, which inturn overlies an Eburru Pumice succession. Clay, silty clay and coarse sand with pumice fragments underlies the Eburru Pumice succession. In contrast no sediments are exposed on the opposite (south) side of the valley at AK760394, where numerous beds, 1 to 4 m thick of the Eburru Pumice are exposed.

3.11.2 Alluvial deposits (a)

Many of the gullies that have dissected parts of the Longonot Volcano, and the Olkaria and Eburru Volcanic Complexes, have smooth floors as a result of the deposition of alluvial sediments. Renewed downcutting in gullies on Longonot Volcano and the Olkaria Volcanic Complex has revealed that these alluvial deposits are dominated by sand and gravel.

Alluvial deposits associated with the Malewa river are dominated by greyish brown silt and fine sand within which there are intervals of reddish brown ferruginous coarse sand and granule gravel, and pale grey clay (e.g. BK116399, BK130282, BK125283 and BK091264). The pale grey clay usually occurs in very thin (0.25 m) beds and may have been lake deposited. Large-scale cross-bedding in other parts of the succession indicate deposition in a high energy environment.

Boulder gravel, composed predominantly of sub-angular to subrounded clasts of comendite lava, is exposed intermittently on the smooth floor of Hell's Gate. It fills small channels that have been eroded into ignimbrite of the Kedong Valley Tuff (Longonot Volcanic Group) at the top of a west-north-west-trending, south-facing, scarp (e.g. BK054033). It is overlain by grey pumice lapilli, which may correlate with the Upper Pumice Member (Lp7) of the Akira Pumice, and the Longonot Ash (Lp8). Further south (e.g. BK017017) the gravel contains boulders of ignimbrite, similar to that mentioned above, and comendite.

Talus associated with the fault scarps along the eastern rift margin is well exposed in the south in sections along the old Naivasha road (e.g. BJ330898, BJ331895, BJ330840 and BJ331825). It is composed of angular, sub-angular and subrounded pebbles, cobbles and boulders of trachyte lava, similar to that exposed in-situ in adjacent road sections.

3.12 AGE RELATIONSHIPS

The new radiocarbon dates for Longonot volcanic rocks, which show maximum ages of 3280 ± 120 yr BP for the base of the Longonot Ash (Lp8) and 9150 ± 110 yr BP for the base of the Lower Pumice Member (Lp5) of the Akira Pumice, also indicate maximum and minimum ages for the Middle(03/0p3) and upper (04/0p4) Comendite members of the Olkaria Comendite. The former occurs interbedded with the Lower Pumice Member (Lp5) of the Akira Pumice and the latter underlies the Longonot Ash (Lp8).

Further constraints on the timing of some events in the volcanic history of Longonot Volcano and the Olkaria Volcanic Complex are provided by radiocarbon dates obtained from a Lake Naivasha sediment core (Richardson, 1966; Butzer et al., 1972) which were as follows:

1a 3000 ± 60 yr BP; sample immediately above 'dessicated' layer.
1b 3040 ± 60 yr BP; sample immediately below 'dessicated' layer.
2 5650 ± 120 yr BP.
3 9200 ± 160 yr BP.

This core was taken from that part of the lake enclosed by Crescent Island and which is the deepest part of the lake as a whole. The 9200 ± 160 yr BP date was obtained from sediment which indicated a high lake level, and the 5650 ± 120 yr BP date was from sediment deposited at the end of a prolonged period of high lake level. The c.3000 yr BP dates were from sediments which indicate a small lake with fluctuating levels. During the highest lake level a shoreline existed close to the 2000 m contour compared with the a shoreline at about 1885 m in 1983 (Ase et al., 1986). During the period of high lake level overflow took place via the Hell's Gate Ol Njorowa Gorge, and according to Butzer et al., (1972) this overflow lasted until about 5600 years ago.

The probable timing of the latest events in the history of Longonot Volcano and the Olkaria Volcanic Complex, relative to that of overflow and variations in level of Lake Naivasha are shown in Figure 3.6. The oldest of the above sediment dates approximates closely to the Akira Pumice, and therefore the abundant pumice gravel in lake sediments exposed around the northern side of the Olkaria Volcanic Complex may have at least in part formed as a result of the erosion and reworking of pumice produced during Lower Pumice Member (Lp5) eruptions. Erosion as a result of overflow through the Hell's Gate–Ol Njorowa Gorge has affected lava flows of the Upper Comendite Member (04) of the Olkaria Comendite which therefore cannot be younger than about 5600 years. On the northern flanks of Longonot Volcano lake sediments are not well exposed but some boreholes show lake sediments, equated with the 5600 yr BP highstand, underlying the lower member (Lmx1) of the Longonot Mixed Lavas (Scott, 1980) which therefore must be younger than 5600 years. This interpretation means that the steep-sided cone of Longonot Volcano, which is

Table 3.9 Details of the Elmenteita, Ndabibi and Akira Volcanic Groups (*oldest unit at top*)

Name of formation (Fmn) or member (Mem)	Map symbol	Type area/section	Age	Major outcrops	Lithology
Elmenteita Basalt Fmn			All Fmns are late Pleistocene to recent age	Soysambu, Otutu, Nagum & Malura areas, & in N part of Ilkek basin	Mostly basalt lava, but youngest (Otutu) lava is of mugearite/benmoreite composition. Oldest lavas (Malura & Ilkek basin) are highly prophyritic. Scoria &/or spatter is cone forming at vents
Older member	Be^1	Nakuru BK 038404 Otutu area AK 927380			
Younger member	Be^2				
Tuff Cones Fmn				Elmenteita & Ndabibi areas	
Surtseyan type	kBt	Exposure adjacent to Elmenteita road at AK 918468		Sopysambu area, incl. Karterit & Losiriwe craters, area immed. E & SE of Karterit crater. Nadabibi area incl. Crater Lake. Horseshoe Hill adj. to Loldia Estate. In Maiella/Kongoni farm area SW of Ndabibi	Lithic-rich block &/or lapilli ash when cone forming (KBt)
Distal Tuff member	kBtm	N edge of Otutu flow. AK 915412			Fine to coarse ash & fine lapilli ash mantles pre-existing rocks in adjacent areas
Transitional member	Bt	Exposure on E side of cone, adj. Moi North Lake road—AK 957162		Ndabibi area	Scoriaceous ash & Lapilli with pebble sized lithics, interbedded fine, accretionary—lapilli ash & coarse scoriaceous lapilli. All above lithologies are cone forming
Ndabibi Basalt Fmn	Bn	Quarry at AK 886186 in Ndabibi Estate		Ndabibi, Matuya & Loldia Estates, immediately E of S end of Waterloo Ridge & in Maiella area SSW of Ndabibi	Lava of basalt, hawaiite or mugaerite composition; flow units interbedded with scoria & spatter in type section. Cone forming scoria & spatter in Loldia Estate at AK 995214
Ndabibi comendite Fmn	N	Ndabibi Estate— AK 945195—lava AK 931085—cone		Ndabibi Estate, Ololeri area & Kongoni Farm	Variably vesicular (occas. pumiceous), feldspar porphyritic comendite, crystalline & obsidian (with devitrifed bands). Obsidian locally highly spherulitic. Banding & layering sometimes suggestive of welded pyroclastic rock rather than a lava. Some undoubted pyroclastic rock composed of pumice & lithic lapilli & blocks forms cones W of Ololeri Farm & in N part of Ndabibi
Ndabibi Pantellerite Fmn	P	Ololeri Farm/Hippo Point BK 006127		Ololeri Farm/Hippo Point, Ndabibi Estate	Obsidian with devitrified bands & phenocrysts of feldspar and quartz
Akira Basalt Fmn	Ba^2	Akira Plains (S of entrance to Ol Njorowa Gorge) AJ 991911		Akira Plains	Lava, basaltic in appearance, but of mugearite/benmoreite compositions. Scoria & spatter forms prominent cone immed. S of entrance to Ol Njorowa Gorge
Tandamara Trachyte Fmn	Tt	Tandamara BJ 028875		Tandamara, Lolkidongoe & smaller ridges to the SSW & SW of Tandamara	Welded scoriaceous lapilli & some banded 'lava' on Tandamara, elsewhere welded scoriaceous lapilli & blocks

Table 3.9 Continued

Thickness in m a = max exposed b = max indicated bed	Volcanological interpretation or depositional environment	Underlain by	Overlain by	Notes
[b]4	Products of hawaiian &/or strombolian eruptions—lava extrusion dominant	ls, kBt/ kBtm, Er[2], Erw, Tlg	ls	ls overlies all but the youngest flows in type area. Older ls occurs between Be & Erw at BK 039402
	Products of Surtseyan volcanism—due to interaction between lake &/or ground water & magma. Mostly fall deposits, but surge deposits occur locally in Ndabibi area (e.g. AK 953156) & are conspicuous in gully exposures of the Maiella/Kongoni Farm outcrop (e.g. AK 885060)	ls, Tlg, Er[2]	Ba/Bn, ls	Distal ash (kBtm) occurs interbedded with ls in Kariandus area (e.g. AK 980484)
	Products of volcanism ranging from strombolian to surtsevan in nature during each eruption	ls, Op N, Mp	ls?	
[a]12	Products of hawaiian &/or strombolian eruptions—lava extrusion probably dominant	kBtm	ls, ?Ep	
	Extrusion of comendite as domes, domes ± lava (obsidian) & pyroclastic cones. Steep sided cratered 'domes' e.g. Mulla, possibly formed of welded pyroclastics & not lava. (AK 931085)	?	ls ?Lp/Mp	
	Extrusion of Obsidian flow, no evidence of any associated pyroclastics	?	Lp[a]/Op ls	
	Product of hawaiian &/or strombolian volcanism—lava extrusion dominant	?Lp[a]	a	Partly overlain by alluvial deposits incl. outwash from Ol Njorowa Gorge. Older lava occurs (?uplifted) on N side of Tandamara. Ba[1] (Lolonito Basalt) is probably related
	Non violent extrusion (?Strombolian) of pyroclastics at high temp. forming welded deposits. Lava on Tandamara may be rheomorphic pyroclastic fall	LpK, Ba[2]		Uplift & tilting of large areas of Lpk + Ba[2] prior to and during extrusion at Tandamara

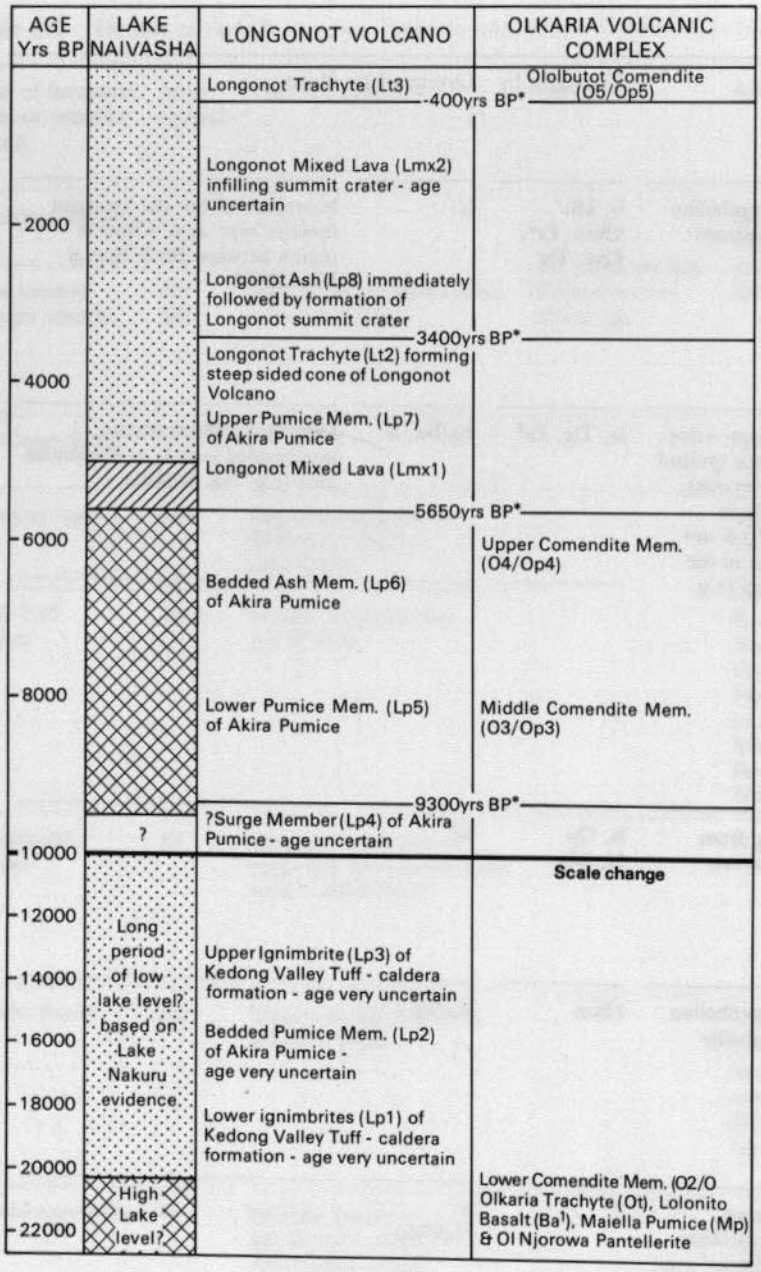

Figure 3.6 Age relations between Lake Naivasha lake levels and Longonot and Olkaria volcanic sequences.

formed mostly of lava flows of the Longonot Trachyte (Lt2) was built between 5600 and 3300 years BP.

No precise time constraints can be placed on Longonot and Olkaria Volcanic events before the c.9300 yr BP onset of eruptions of Longonot Volcano which produced the Lower Pumice Member (Lp5) of the Akira Pumice. The pre-c.9350 yr BP history of Lake Naivasha is not known, but if events were similar to those experienced in other lakes such as Nakuru and Elmenteita then a prolonged period of low lake level may have followed an earlier highstand at c.21 000 yr BP (Butzer et al., 1972). Exposures in the Karati gully, north of Naivasha town, show palaeosols separating a distal ignimbrite of the Kedong Valley Tuff from overlying lacustrine clay and underlying fluviodeltaic (?) sand and gravel. If the clay was deposited during the c.9350 to 5600 yr BP highstand of Lake Naivasha then the ignimbrite was emplaced sometime during the preceeding period of low lake level, that is between c.9350 and 21 000 yr BP. Kedong Valley Tuff ignimbrites occur immediately above and within a thick sequence, which includes probable lake deposited sediments, exposed within the upper part of the Ol Njorowa Gorge. These lake sediments are clearly older than those associated with the c.9350 to 5600 yr BP highstand of Lake Naivasha, but may correlate with the c.21 000 yr BP, highstand deduced at the Elmenteita area.

No age data is available for rocks of the Eburru and Elmenteita Volcanic Groups, but some correlation with events in the histories of the Nakuru–Elmenteita and Naivasha basins is however possible. Occasional thin, probably Eburru derived, pyroclastics occur interbedded with lake sediments exposed alonside the Gilgil river (e.g. BK061344) and the Nakuru highway (e.g. BK092287). The sediments include both relatively thin (0.5 to 2 m) beds of colour-graded clays that may have been deposited during a period of fluctuating lake level (e.g. c.3000 yr BP to present), and unbedded clay which may have been deposited in a more stable period when a higher lake level may have prevailed (e.g. c.9350 to 5600 yr BP). These exposures therefore merely show pyroclastics from Eburru have been dispersed over the Ilkek basin within the last c.9000 years.

Lake sediments on the Karterit crater have yielded a radiocarbon date of 9650 ± 250 yr BP (Butzer et al., 1972), which is therefore a minimum age for this tuff cone. These sediments, together with those that occur within the fault induced notch on the northern side of Losiwire crater and which may be similar in age, were probably deposited during a c.8000 to 10 000 yr BP highstand of Lakes Nakuru and Elmenteita (Butzer er al., 1972). Low lake levels occur between this and the earlier, c.21 000 yr BP, highstand. Eburru Pumice sequences exposed in the Nagum area of Eastern Eburru, and in the Nderit Valley south of the Miti Mingi settlement have laterally equivalent reworked and/or lake deposited pumice gravels exposed nearby. In each case the Eburru Pumice sequences are among the oldest exposed and the pumice gravels may correlate with either the c.21 000 yr BP, or an older highstand.

Because of the intervening Naivasha basin, and its widespread lake sediments, no undoubted interbedded relationship between Eburru pyroclastics and those derived from Longonot Volcano and the Olkaria Volcanic Complex has been found.

3.13 STRUCTURE

The main structural features in the project area are shown on the 1:100 000-scale geothermal map and are as follows:

1 Faults defining the Rift flanks, margin and floor.
2 A north–south major volcanic alignment extending from Lake Elmenteita, through the Eburru and Olkaria Volcanic Complexes, to the Akira plains.
3 A major north-north-west–south-south-east alignment of flank eruption centres and fissures on Longonot Volcano, which passes through the summit crater. (Tectono-volcano axis or TVA).
4 Numerous minor volcanic alignments (usually as elements within 2 and 3 above).
5 Ring fracture aligned centres in the Olkaria Volcanic Complex, possibly controlled by a former caldera trace.
6 Caldera development centred on Longonot cone.

North- to north-west-trending faults define the eastern and western rift margins, and most of this faulting has probably occurred prior to the development of the volcanic centres on the rift floor. At least three distinct periods of faulting have occurred within the period 0.4 to 4 Ma, and these followed the periods of volcanism that gave rise to the Kinangop Tuff, Limuru Trachyte and Gilgil Trachyte.

Post-0.4 Ma faults are associated with parts of the Eburru–Olkaria major volcanic alignment, and are conspicuous on the northern flanks of Eastern Eburru. Reactivation of some rift margin faults has occurred, and may be also post 0.4 Ma in age. Such faulting has been seen in road sections alongside the Naivasha highway, near the Magumu settlement, at BK274048, and alongside the Narok road in the Nairagie Ngare area at AJ795791, AJ841795 and AJ847788. The Narok road sections lie south-east of the project area, but indicate reactivation of faults which continue into the project area where they are deeply buried by pyroclastic rocks derived from the young Rift floor volcanoes.

The major Eburru–Olkaria volcanic alignment incorporates the volcanic centres of the Elmenteita basin and the Ndabibi and Akira plains, together with the young eruption centres on Eastern Eburru and in the western part of the Olkaria Volcanic Complex. It is indicated on the geothermal 1:100 000-scale map as a shaded zone. Numerous centres are concentrated within a 5 to 7 km-wide belt, and many occur in groups which form, mostly north-trending but occasionally north-west or north-east-trending, minor alignments. A line of vents and small domes passing through Olkaria hill together with the Ololbutot fissure zone are two prominent and adjacent, north-trending minor alignments, which form part of the zone in the western part of the Olkaria Volcanic Complex.

A continuation of the major tectono-volcano axis south of the map border is indicated by the distribution of young features and active geothermal manifestations on Suswa Volcano. (Torfarson, 1987).

The Longonot major volcanic alignment (the smaller shaded area on Map 2) may extend as far north as Crescent Island on the south-east shore of Lake Naivasha, and its southernmost expression is marked by the group of centres (minor alignment) from which the Mlima Panya lavas were erupted.

Minor alignments on Longonot Volcano also include eruption centres situated on fissures radially aligned relative to the summit crater. The most prominent radial fissure is that from which very recent lava (Upper

Trachyte Member-Lt3) was erupted onto the south-western flanks of the steep sided cone.

Within the Eburru Complex a number of eruption centres are inferred on the southern part of Waterloo Ridge and support the possibility that this also is a fissure zone.

The eastern and southern part of the Olkaria Volcanic Complex includes an arcuate group of eruption centres. The centres of the Gorge Farm and Olkaria hill and other similar centres lie on a possible continuation of this arc and would therefore define a ring feature. This interpretation is indicated on the 1:100 000-scale map. The western portion of this ring is cut by the younger Olobutot fissure zone.

The more recent structures' relationship with surface geothermal indications and possible control on subsurface extent of geothermal reservoirs is discussed in more detail in Chapter 5.

4 Petrology

4.1 INTRODUCTION

Scott (1977) and Bliss (1979) have presented detailed accounts of the petrography of lavas and pyroclastic rocks from Longonot Volcano and the Olkaria Volcanic Complex. Much of the Bliss data has been published by MacDonald et al. (1987). For this reason only limited petrographic studies have been undertaken during this project. In contrast less petrographic (and geochemical) data was available for Eburru (e.g. Sutherland, 1974) and a relatively large number of samples therefore studied.

A detailed petrographic and mineralogical investigation was carried out on samples of lithic material, collected from Longonot and Olkaria pyroclastic rocks (Fortey et al., 1988). The lithics probably include material derived from early, and/or pre-Longonot volcanic rocks, and the object of the investigation was to ascertain whether any interaction with a possible geothermal aquifer had taken place (see 4.2.2).

A large amount of rock geochemical data was also available for both Longonot and Olkaria but this was added to in order to assist the mapping as it was found that individual phases of activity at Olkaria have distinctive geochemistry. A further suite of unpublished Longonot analyses were made available (Scott, personal communication, 1987) and has been incorporated in the compilations plotted here.

4.2 PETROGRAPHY

4.2.1 Rift margins

The welded ignimbrites of the **Kinangop Tuff** are composed of pyroclasts, pyrogenic crystals and lithics which occur in a matrix which is often either semi-opaque or opaque. The pyroclasts are often elongate and are composed of spherulitic aggregates of alkali feldspar, amphibole and quartz. Alkali feldspar and amphibole sometimes also occur as microphenocrysts. The most common pyrogenic crystals are alkali feldspar, and these are sometimes accompanied by green clinopyroxene, aenigmatite(?), and in rare instances, brown pleochroic biotite. The most conspicuous lithics are those which are holocrystalline and formed of alkali feldspar, amphibole pyroxene and aenigmatite. The matrix, when semiopaque, is predominantly cryptocrystalline. A strongly banded/laminate texture occurs in some rocks and may be due to the presence of abundant large flattened pyroclasts. In some cases many of the laminae consist of highly elongate cavities lined with radiating aggregates of alkali feldspar and alkali amphibole (riebeckite/arfvedsonite) which are probably products of vapour phase crystallisation.

Karati Basalt samples are composed of abundant phenocrysts and microphenocrysts of olivine, which are sometimes accompanied by those of plagioclase, clinopyroxene and opaque oxide, and which occur in a coarsely textured groundmass composed of plagioclase, olivine, clinopyroxene and opaque oxide. Biotite occurs as a late stage mineral in a sample from north of Longonot settlement (BK198073), and calcite occurs in irregular cavities in a sample from just east of Naivasha town (BK165207).

The **Limuru and Gilgil Trachytes** are petrographically similar and contain numerous phenocrysts of alkali feldspar, less frequent phenocrysts of clinopyroxene (sodic?), and occasional phenocrysts of oxide-rimmed/replaced olivine (fayalitic?) and opaque oxide. The latter may include olivine phenocrysts that have been wholly replaced by oxide. The groundmass is composed of abundant alkali feldspar, which is accompanied by alkali pyroxene and/or alkali amphibole, aenigmatite, and in some cases an opaque mineral and quartz. Quartz is most frequent in the groundmass of Limuru Trachyte samples, and in one instance occurs as phenocrysts. Glass is abundant in the groundmass of some samples. Calcite, possibly representing products of vapour phase crystallization, and hydrothermally deposited zeolite(?) are rare occurrences. Chlorite and oxide occur in some samples as irregular patches in the groundmass and may be an alteration product.

4.2.2 The Longonot Volcanic Group

Calcified ignimbrites of the **Kedong Valley Tuff**, from near the Mai Mahiu and Munyu settlements (BJ294907 and BK255045), are composed of abundant glass shards, fibrous pumice pyroclasts, pyrogenic alkali feldspar crystals, and holocrystalline and glassy microlithics. All but the pyrogenic feldspar crystals and microlithics have been replaced by calcite which sometimes is apparent as large, irregular and uniformly extinguishing crystals. In some cases the interiors of the largest pumice pyroclasts remain uncalcified. Partly welded and welded ignimbrites of the Kedong Valley Tuff are petrographically similar to the welded ignimbrites of the Kinangop Tuff described above.

A suite of lithics, collected from pumice beds of the **Akira Pumice** (Lower Pumice Member Lp5), were submitted to detailed investigation (Fortey et al., 1988) and consist of trachyte, syenite and "agglomerate." In the trachyte and syenite lithics phenocryst contents and the coarseness of the groundmass vary considerably. The phenocrysts include anorthoclase, augite, sodalite, magnetite and rare subhedral fayalite, and the groundmass is composed of glass, anorthoclase, sodic plagioclase (in syenite), subpoikilitic aegerine-augite, magnetite and apatite. A range of deuteric, pneumatolytic and possibly hydrothermal features were noted. The deuteric stage is seen in the precipitation of interstitial/poikilitic minerals (fayalite, aegerine, arfvedsonite and aenigmatite). In the syenite lithics the prevalent intergrown feldspar mesh may be deuteric rather than pneumatolytic in origin, and interstitial aegerine-augite and katophorite also formed at this stage. Pneumatolytic (vapour-phase) effects include the extensive development of dissolution porosity and minor veining. Minerals precipitated at this stage include aegerine, biotite, arfvedsonite, aenigmatite, monazite, quartz, ilmenite and RE silicates. Lower temperature minerals probably deposited from mixed meteoric/juvenile aqueous fluids include analcite, tourmaline,

fluorite and fine decussate biotite. Additonal formation of dissolution porosity took place at this stage, e.g. in analcite-rich altered agglomerate. SEM studies show that porosity may total <10% by volume of the rock. There is thus the possibility that such rocks may have enhanced geothermal potential compared with those with no porosity. Goethitic oxidation and minor calcite, quartz, trona and fluorite developed late, possibly in situ, after the eruptions which produced the agglomerates.

This study included microprobe analysis of a number of phases—pyroxenes, amphiboles, feldspars, olivine, aenigmatite, sodalite, analcite and biotite, (Fortey et al., 1988). Pyroxenes are typically zoned to sodic margins, (Figure 4.1a). Amphiboles are soda-rich with compositions near arfedsonite and katophorite (Figure 4.1b). The former often contains 2–3% F. Two feldspars are often present-andesine and anorthoclase, (Figure 4.1c).

An additional 46 lithic samples from pyroclastic deposits of the Surge and Lower Pumice Members (Lp4 and Lp5) of the Akira Pumice were subjected to petrographic examination in Kenya. Thin sections were made at the Mines and Geological Survey Department (Ministry of Environment and Natural Resources), Nairobi. The majority (29) consisted of trachyte, with phenocrysts of alkali feldspar, sodalite, fayalitic olivine, clinopyroxene (soda hedenbergite), alkali pyroxene (aegerine-augite), and an opaque mineral, in a groundmass composed of alkali feldspar, alkali pyroxene (aegerine-augite/aegerine), aenigmatite, arfvedsonite, and an opaque mineral. Sodalite occurs in about 70% of the trachyte lithics examined and sometimes has alkali pyroxene coronas. This mineral has not been recorded in any of the surface trachyte lavas.

According to Scott (1977, 1982) the lavas of the Longonot Trachyte contain 0 to 8% phenocrysts of anorthoclase, fayalitic olivine, iron rich clinopyroxene and titanomagnetite, which occur in a groundmass composed of alkali feldspar, alkali clinopyroxene, aenigmatite, alkali amphibole, and, in some early flows, titanomagnetite. The lavas are unaltered, but fine grained carbonate sometimes occurs interstitially with respect to groundmass feldspar, pyroxene, aenigmatite and amphibole. Scott (1982) interpreted the carbonate as being a primary, residual crystallisation product of a $C0_2$-rich vapour phase. Carbonate also occurs as one of a series of minerals replacing some olivine phenocrysts.

The lavas of the **Longonot Mixed Lava** either consist of two separate groundmass components one of which is basaltic, the other trachytic, or a single groundmass which contains both basaltic phenocrysts (sodic plagioclase feldspar, opaque oxide and pyroxene) and trachytic phenocrysts (alkali feldspar, sodic pyroxene, aenigmatite, and an opaque mineral), (Scott, 1984).

4.2.3 The Olkaria Volcanic Group

According to MacDonald et al. (1987) comendites from the Naivasha area are variably porphyritic (0.5 to 11%) and the phenocryst minerals are sanidine, quartz, ferrohedenbergite, fayalite, titanomagnetite, ilmenite, biotite, riebeckite/arfvedsonite, aenigmatite and zircon.

In support of new geochemical analyses, petrographic study was carried out on a suite of 23 samples from the lower (O2), middle (O3) and upper (O4) members of the **Olkaria Comendite**. Quartz phenocrysts occur in the majority of samples together with those of alkali feldspar. Less frequent in some samples were phenocrysts of olivine (probably fayalitic), clinopyroxene (sodic?), alkali amphibole and an opaque mineral. In some cases the groundmass consists of very finely crystalline alkali feldspar and quartz which may be a product of the devitrification of glass. Isotropic glass occurs in some samples, which may also contain patches or bands of devitrified glass. Spherulites, probably formed of fibrous crystals of quartz and feldspar, are abundant in the groundmass in many of the samples. Opaque oxide and alkali amphibole (arfvedsonite?) are groundmass minerals in most samples, and the latter sometimes occurs as acicular crystals in variolitic aggregates.

Samples, of basaltic and trachybasaltic appearance in hand specimen, from the **Lolonito Basalt**, contain phenocrysts of alkali feldspar, olivine, clinopyroxene and opaque oxide. Clinopyroxene and oxide phenocrysts occur mostly in rocks of trachybasalt appearance, while those of olivine are somewhat less frequent. Some 'Trachybasalts' contain sieve-textured and/or embayed phenocrysts/xenocrysts of alkali feldspar.

Two samples of lava from the **Olkaria Trachyte** contain numerous phenocrysts of alkali feldspar, clinopyroxene (sodic?) and opaque oxide, together with occasional oxide rimmed/replaced olivine (fayalitic?) phenocrysts, in a groundmass composed of alkali feldspar, clinopyroxene (sodic?), aenigmatite and glass.

4.2.4 The Eburru Volcanic Group

The strongly banded **Waterloo Ridge and Kiambogo Pantellerites** are microcrystalline rocks composed of alkali feldspar, quartz and alkali amphibole. The banding is defined by alternating laminae of varying grain size. Phenocrysts of alkali feldspar and alkali amphibole are usually present, but not abundant. Rare quartz phenocrysts occur in some rocks. Flow-orientated feldspar laths occur in the groundmass of some rocks, but in many cases the groundmass is patchy in appearance (ophimottled texture) owing to the presence of numerous small oikocrysts of quartz and feldspar. The groundmass quartz and feldspar are sometimes present as microgranophyric intergrowths, which in turn sometimes have a radiating appearance suggesting that they formed as incipient spherulites. An ophimottled texture is in some cases defined by minute oikocrysts of a dark blue-black, pleochroic, amphibole which may be riebeckite. It is considered possible that these rocks have developed by rheomorphism of agglutinated pyroclastic deposits.

The banded rocks of the **Kiambogo Pantellerite** differ from those of the Waterloo Ridge Pantellerite in that the banding is more commonly defined by concentrations of minute granular amphibole crystals, spherulites composed of feldspar and/or amphibole, and in some cases by concentrations of elongate, flow orientated, crystals of feldspar and amphibole. Quartz is much less apparent in the Kiambogo Pantellerite, but may be common as minute groundmass crystals accompanying those of alkali feldspar and amphibole. The latter includes greenish brown to very dark blue pleochroic riebeckite/arfvedsonite, and a brown to dark brown pleochroic mineral which may also be an amphibole (katophorite? ferrorichterite?, Sutherland, 1974).

A single sample of lava of the **Western Eburru Pantellerite** contains numerous phenocrysts of alkali feldspar, together with less frequent amphibole and quartz phenocrysts, in a banded microcrystalline groundmass composed of alkali feldspar, amphibole and quartz. The banding is defined by concentrations of minute granular amphibole crystals, and abundant flow orien-

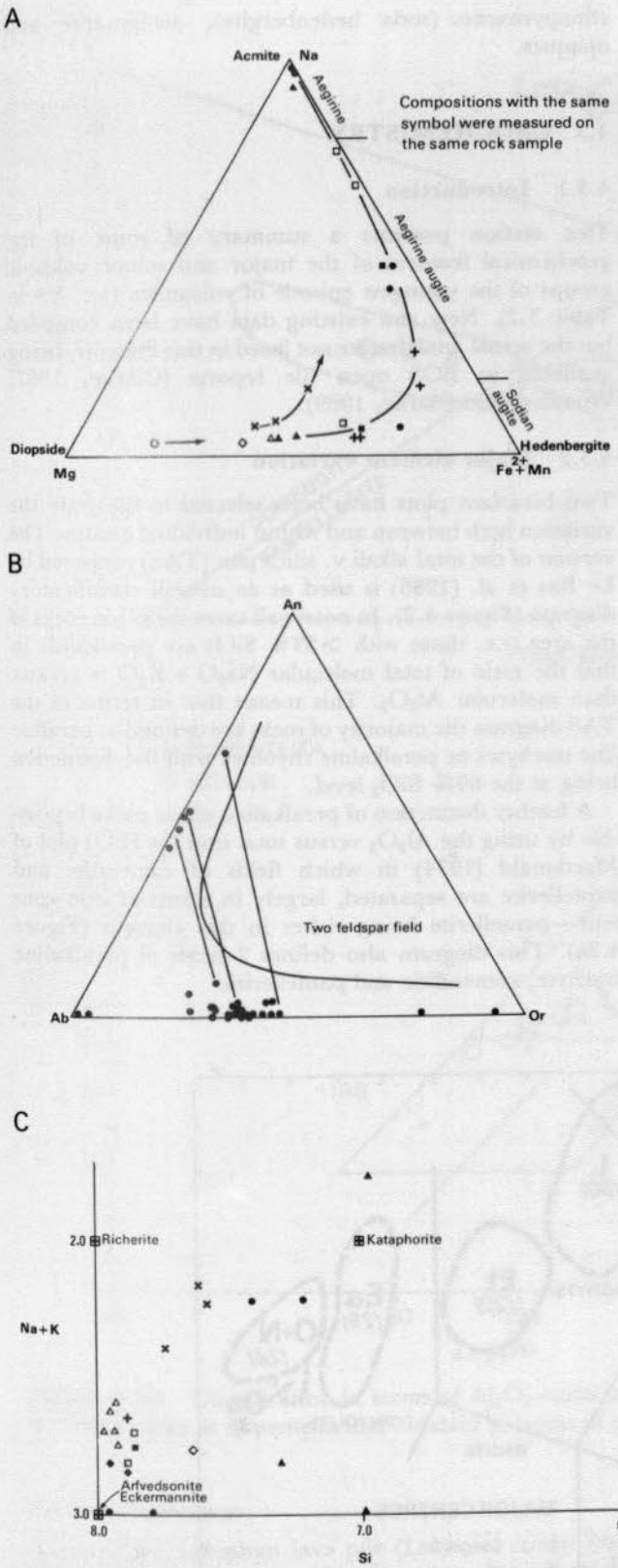

Figure 4.1 Mineral compositions determined by microprobe. a) pyroxenes, b) feldspars, c) amphiboles.

tated feldspar laths. The amphibole has blue to bluish brown pleochroism and probably therefore of reibeckite/arfvedsonite composition.

The lavas of the **Eburru Trachyte** are porphyritic, holo- and hypocrystalline rocks. Alkali feldspar is the dominant phenocryst phase, and in some rocks this is accompanied by rare, oxide-rimmed/replaced, olivine phenocrysts, clinopyroxene, aenigmatite, amphibole and an opaque mineral. Colour and pleochroicsm in the clinopyroxene phenocrysts indicate probable soda hedenbergite (pale green, nonpleochroic) and aegerine-augite (blue-green, pleochroic). Alkali feldspar, aegerine-augite and aenigmatite are the main crystalline phases in the groundmass. Alkali amphibole (arfvedsonite?) is sometimes present as a deuteric mineral.

The lavas of the **Eastern Eburru Pantellerite** differ from those of the Eburru Trachyte in that they are predominantly glassy, and in some cases carry quartz phenocrysts. Quartz sometimes occurs as microgranophyric intergrowths. Elongate, subhedral to anhedral, phenocrysts of a dark greenish brown/opaque, pleochroic amphibole occur in most rocks, sometimes accompanied by rare phenocrysts of pale green clinopyroxene. Crystals and microlites of alkali feldspar and amphibole occur in the glassy groundmass. The latter is sometimes partly or wholly devitrified, and very abundant fine vesicles give some rocks a fibrous or pumiceous appearance. In other instances feldspar (?) microlites define a flow texture which is sometimes so highly irregular and convolute that the groundmass is pyroclastic in appearance. The latter is sometimes emphasized by the presence of patches packed with minute opaque microlites. The above mentioned groundmass textures may be a result of some rocks having formed as welded accumulations of glassy and sometimes highly vesicular pyroclasts, which may undergone subsequent rheomorphism.

4.2.5 The Elementeita Volcanic Group

The lavas of the Elmenteita Basalt contain phenocrysts and/or glomerocrysts of plagioclase feldspar, olivine, clinopyroxene and opaque oxide in a mostly holocrystalline groundmass. Phenocrysts of plagioclase and olivine occur in most rocks whereas those of clinopyroxene and opaque oxide are usually infrequent or absent. The glomerocrysts are mostly aggregates of feldspar and olivine, but in some cases also include clinopyroxene. Oxide phenocrysts are most readily apparent when they occur as inclusions in olivine and/or feldspar phenocrysts. Some rocks have a glomeroporphyritic texture. The groundmass is composed of plagioclase feldspar, olivine, clinopyroxene and opaque oxide. The groundmass of the most recent lava flow of the Elmenteita Basalt (Otutu flow) is hypocrystalline, and the glass occupies most, or all, of the wedge-shaped interstices between feldspar laths thus defining an intersertal texture. The glass is usually packed with semi-opaque mafic(?) minerals and/or oxide grains. The clinopyroxene is mostly very pale brown (non-pleochroic) in colour but is darker brown (titan-augite) in some of the oldest lavas, and is occasionally pale green (augite?) in the most recent lava.

Amygdaloidal calcite occurs in the lava exposed alongside the Kiambogo road (e.g. AK960368) west of Kianugu hill.

The pyroclastic deposits which form the **Tuff Cones** are composed of isotropic, brown to yellowish brown (palagonitised), pyroclasts the largest of which commonly contain numerous rounded or lobate vesicles and in some cases microphenocrysts of olivine, augite and feldspar. Feldspar and augite also occur as, often glass coated, pyrogenic crystals. The finest pyroclasts sometimes form a matrix, but in other instances pore spaces occur between the coarser pyroclasts and may be either lined or filled with calcite and zeolite. Calcite-filled amygdales occur in some of the coarser pyroclasts. The lithic fragments include highly recrystallized welded tuff, holocrystalline rhyolite composed of feldspar laths and amphibole, and

basalt which is petrographically similar to that of the Elmenteita Basalt described above.

4.2.6 The Ndabibi Volcanic Group

Basalt lavas and basaltic blocks from tuff cones at Ndabibi are petrographically very similar to those of the Elmenteita Basalt.

The **Ndabibi Comendite** is composed of alkali feldspar, quartz, amphibole, rare clinopyroxene and an opaque mineral. The alkali feldspar occurs mainly as phenocrysts and monomineralic glomerocrysts, but is also present as minute crystals in an otherwise glassy groundmass. Quartz sometimes occurs as phenocrysts, and may accompany alkali feldspar in groundmass spherulites. The amphibole occurs in some rocks as brown to very dark bluish brown, pleochroic, granular crystals and is probably riebeckite/arfvedsonite. The clinopyroxene is represented by occasional bluish green microphenocrysts of aegerine-augite, and an opaque mineral which may be oxide replaced crystals of fayalitic olivine.

The **Ndabibi Pantellerite** is composed of microphenocrysts, and occasional larger phenocrysts, of alkali feldspar, which are accompanied by, and sometimes intergrown with, those of clinopyroxene/amphibole(?), and which occur in a microcrytalline groundmass composed of alkali feldspar, amphibole, quartz and aenigmatite.

4.2.7 The Akira Volcanic Group

In outlying occurrences (e.g. BJ001859 and BJ024862) the **Tandamara Trachyte** is composed of phenocrysts and glomerocrysts of alkali feldspar, pale green clinopyroxene, oxide rimmed fayalitic olivine and an opaque mineral, which occur in a groundmass of alkali feldspar, clinopyroxene (soda hedenbergite), aenigmatite and opaques.

4.3 GEOCHEMISTRY

4.3.1 Introduction

This section presents a summary of some of the geochemical features of the major and minor volcanic groups of the youngest episode of volcanism (i.e. V4 in Table 3.2). New and existing data have been compiled but the actual analyses are not listed in this memoir, being available as BGS open file reports (Clarke, 1987; Woodhall and Clarke, 1989).

4.3.2 Major element variation

Two bivariant plots have been selected to illustrate the variation both between and within individual groups. The version of the total alkali v. silica plot (TAS) proposed by Le Bas et al. (1986) is used as an overall classificatory diagram (Figure 4.2). In nearly all cases the silicic rocks of the area (i.e. those with >59% SiO) are peralkaline in that the ratio of total molecular $Na_2O + K_2O$ is greater than molecular Al_2O_3. This means that in terms of the TAS diagram the majority of rocks are defined as peralkaline trachytes or peralkaline rhyolites with the distinction being at the 69% SiO_2 level.

A further distinction of peralkaline silicic rocks is possible by using the Al_2O_3 versus total iron (as FeO) plot of Macdonald (1974) in which fields of comendite and pantellerite are separated, largely in terms of iron content—pantellerite being richer in this element (Figure 4.3a). This diagram also defines 2 fields of peralkaline trachyte, comenditic and pantelleritic.

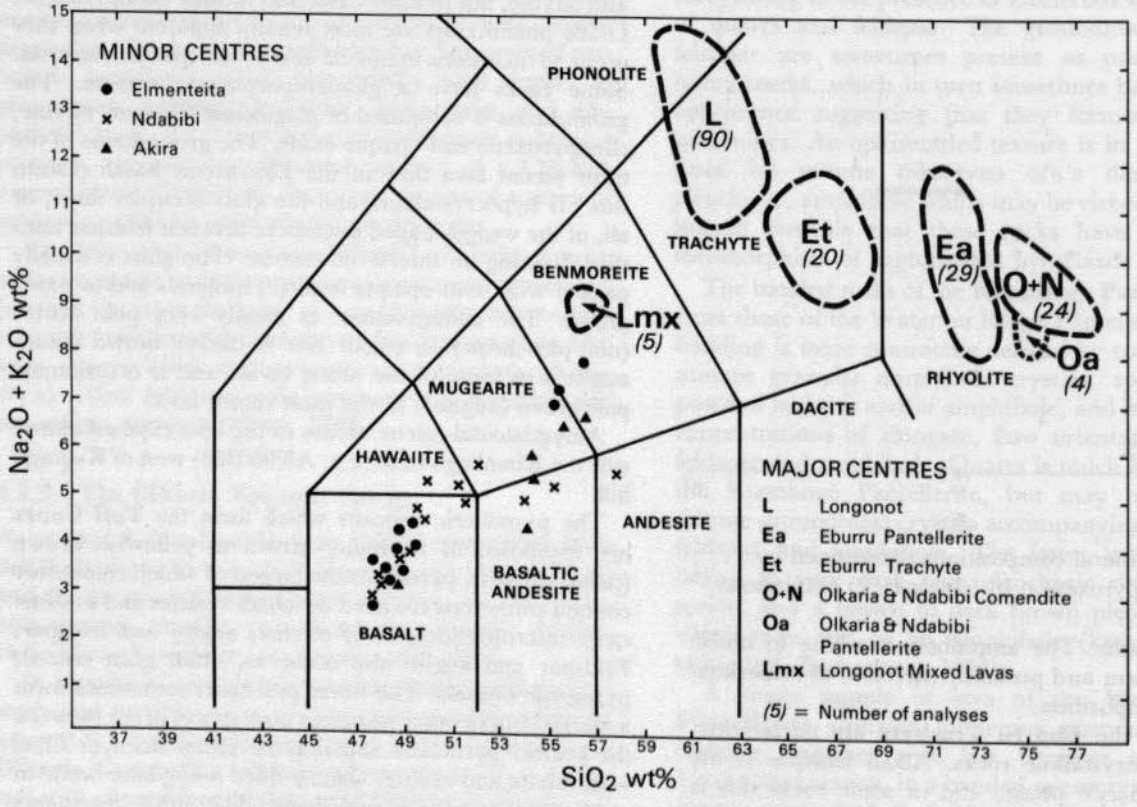

Figure 4.2 Classification of Recent volcanic groups in relation to the total alkali–silica diagram, (LeBas et al., 1987).

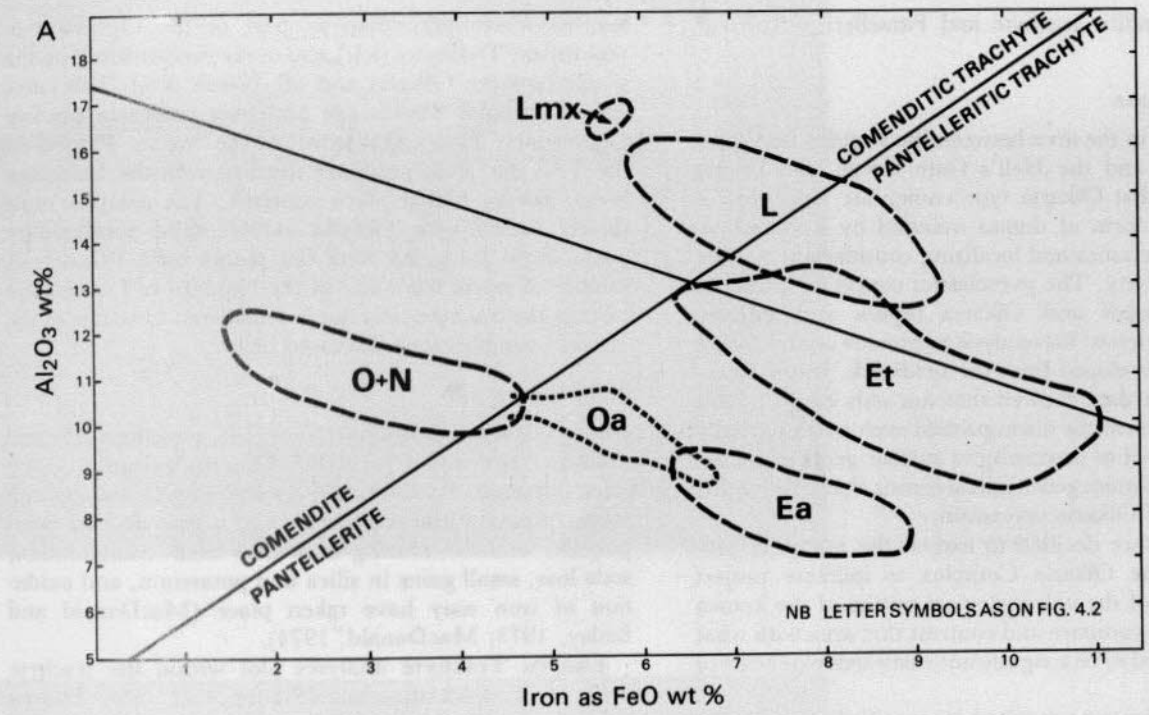

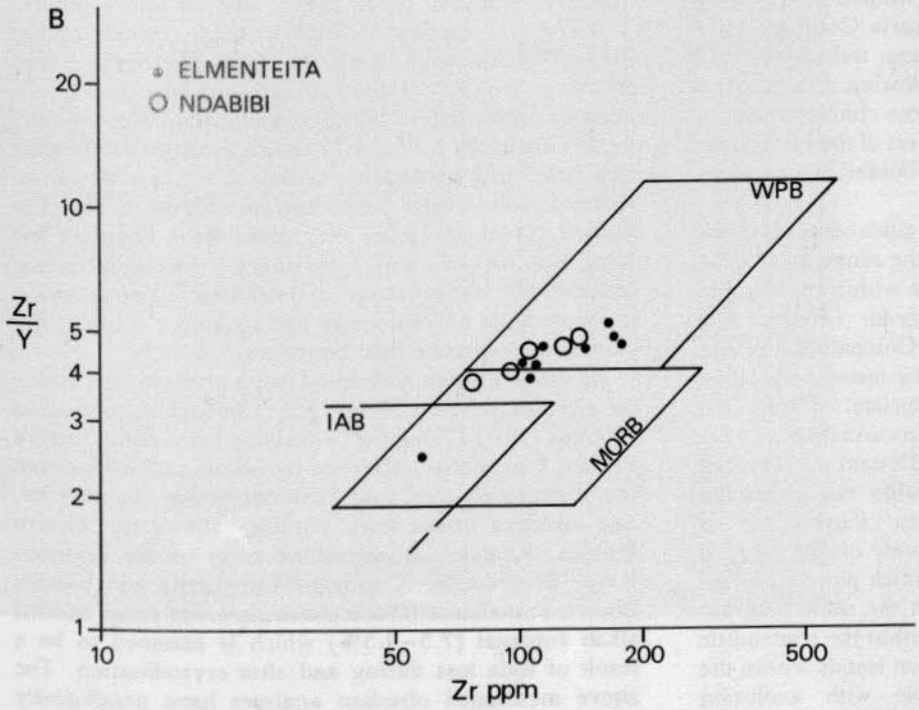

Figure 4.3A Classification in terms of Al_2O_3–total iron as FeO diagram, (Macdonald, 1974).
B Basic rocks at Elmenteita and Ndabibi in terms of plate tectonic settings defined by Pearce and Norry (1979).

4.3.2.1 Longonot

Lavas of the Longonot lava pile (Lt2) and recent flank flows (Lt3) all fall in a restricted portion of the Trachyte field of the TAS diagram. Silica percentages are between 61–64% and the greater variation in total alkali may result, in part, from soda loss during deuteric or even meteoric processes. There is sufficient excess of alkali over alumina to make the Peralkalinity Index greater than unity and therefore these are peralkaline trachytes.

Lavas of the northern plain (Lmx1) plot in a similar position but with slightly lower silica. Previous work has shown that these are in fact 'mixed' lavas, having a subordinate basic component as microscopic tongues and blebs, (Scott, 1986). The crater-floor lavas, together with samples of the coeval bombs and cinders on the crater rim (Lmx2) also show a restricted but separate composition, plotting in the Benmoreite field of the TAS diagram. This group are of mixed basic-trachyte composition also.

Analyses of pumice fragments from the **Kedong Valley Tuff, Akira Pumice and Longonot Ash** have major element variations similar to those of the lavas, and therefore mostly plot within the trachyte field on the total alkalis-silica diagram. Some however have lower silica (59–61%) and higher alkalis (up to 14.5%) than the trachyte lavas and plot within the phonolite field (Figure 4.2). Using the classification scheme for oversaturated peralkaline volcanic rocks proposed by MacDonald (1974) which is based on alumina and total iron (as FeO) contents, all Longonot analyses, plot within the adjacent

fields of comenditic trachyte and Pantelleritic trachyte, (Figure 4.3a).

4.3.2.2 Olkaria

Field mapping in the area between the western Longonot Caldera scarp and the Hell's Gate Gorge (the Domes area) showed that Olkaria type comendite volcanism is present in the form of domes mantled by a varied sequence of pyroclastics and localising considerable surface geothermal activity. The pyroclastics consist of interbeds of both Longonot and Olkaria tephra and initially samples were selected for analysis to provide confirmation of the model developed from the fieldwork. Initial interpretation of the data showed that not only could tephra from the two centres be distinguished even when partially altered as a result of proximity to surface geothermal activity but that distinct geochemical trends characterise different phases of Olkaria volcanism.

It was therefore decided to extend the mapping program across the Olkaria Complex to increase project understanding of the volcanological setting of the known resource and to compare and contrast that area with what is now concluded to be a significant eastwards extention of the resource.

These investigations resulted in a unified stratigraphy being established for the whole Olkaria Complex by a combination of classic field mapping techniques and geochemical finger printing. The following data displays and discussion apply to all of the area characterised by comendite volcanism both east and west of the Hells Gate Gorge and includes discussion of the Ndabibi comendites also.

Olkaria Comendite analyses have silica contents in the range 73–78%, and total alkalis in the range 9–11.5%, and therefore plot in a restricted area within the rhyolite field on a total alkalis-silica diagram (Figure 4.2) Peralkalinity indices for the Olkaria Comendite analyses are in excess of unity and therefore the terms peralkaline rhyolite or comendite are appropriate. Using the classification scheme, based on alumina and total iron (as FeO) contents, proposed by MacDonald (1974), all Olkaria Comendite analyses plot within the comendite field (Figure 4.3a). The Olkaria Pantellerite is distinguished from the comendite purely on the basis of unpublished analyses (Bone, 1988) which plot within the pantellerite field on Figure 4.3a. On the same diagram the Olkaria Trachyte analyses plot within the comenditic trachyte field. Major element variation trends within the Olkaria Comendite are compatible with evolution towards increasing peralkalinity. This trend is accompanied by slight decreases in silica and alumina contents, and more marked increases in iron (total) and alkalis.

This increase in iron and alkalies, together with decrease in alumina, is reflected by the appearance of phases such as aegerine-augite and arfvedsonite, often prominently displayed in small late stage vugs as acicular (vapour phase?) aggregates.

The TAS plots show that samples from the Ndabibi area exhibit relatively small variation and have generally higher percentages of silica compared with the Olkaria comendites.

An important observation is that the two groups of data, from Olkaria and Longonot, plot as quite separate fields on the TAS diagram perhaps indicating no direct petrogenetic relationship.

There are trachytes associated with the Olkaria complex, particularly on the southern flanks of the main ring feature where they map as part of the O_2 phase of volcanism. Trachytes (s.l.) also occur further south on the plains between Olkaria and the Narok road. The latter are of probably earlier age and may represent pre-late Quaternary 'Flood Trachytes' of the region. Plotted on the TAS dia. both pairs are distinct from the Longonot lavas, having higher silica contents. The samples most closely linked with Olkaria exhibit mild peralkalinity while those from the southern plains have P.I.<1. A sample of scoria from one of the Ndabibi tuff cones also plots in the trachyte field but is considered to be one of the 'mixed' compositions discussed below.

4.3.2.3 Eburru

New analyses of crystalline lavas (34), obsidians (15) and pumice fragments (22) of the Eburru Volcanic Group were obtained. Analyses of crystalline lavas and pumice fragments may not be indicative of a true magma composition because, during and after their consolidation, soda loss, small gains in silica and potassium, and oxidation of iron may have taken place (MacDonald and Bailey, 1973; MacDonald, 1974).

Eburru Trachyte analyses plot within the trachyte field on a TAS diagram (Figure 4.2). The Eburru Trachyte analyses differ from those of the Longonot Trachyte in having a higher silica content range (64–69%) but lower alkalis (9–12%). The range in total alkalis is probably a function of soda loss during and possibly immediately after crystallisation. Peralkalinity indices are in the 1.12 to 1.72 range. A trend of increasing total iron with decreasing alumina is apparent on an alumina versus total iron diagram (Figure 4.3a). The Eburru Trachyte lavas, etc, differ from those of the Longonot, Olkaria and Tandamara trachytes in having considerably higher range of total iron contents and a lower alumina content range and straddle the trachyte–peralkaline–rhyolite field boundary.

All other Eburru Volcanic Group analyses plot within the rhyolite field on Figure 4.2. The highest total alkali contents (10–12%) occur in obsidian lavas of the Eastern Eburru Pantellerite, obsidian pyroclasts and lithics from the Western Eburru, and Waterloo Ridge, Pantellerite, and obsidian lithics from pumice beds of the Eburru Pumice. Analyses of crystalline rocks of the Waterloo Ridge Pantellerite, Kiambogo Pantellerite and Eastern Eburru Pantellerite have a distinctly lower range in total alkali contents (7.5–9.5%) which is assumed to be a result of soda loss during and after crystallisation. The above mentioned obsidian analyses have peralkalinity indices in the 1.20 to 2.47 range. Total iron and, in particular, alumina contents in Eastern Eburru, Western Eburru, Kiambogo and Waterloo Ridge Pantellerites, are less than in the Eburru Trachyte, and consequently on an alumina versus total iron diagram all plot well within the **pantellerite** field (Figure 4.3a). A trend of increasing total iron, with decreasing alumina, similar to that shown by the Eburru Trachyte is also apparent on the above diagram.

4.3.2.4 Minor Volcanic Groups

Analyses of the 3 minor volcanic groups reflect the field observation that the compositions present are dominantly basic with many samples plotting as basalts on the TAS diagram. However, a number of samples are intermediate in composition indicating either fractional crystallisation or, more likely on textural evidence–magma mixing. (Figure 4.2). The basalts have a dominantly

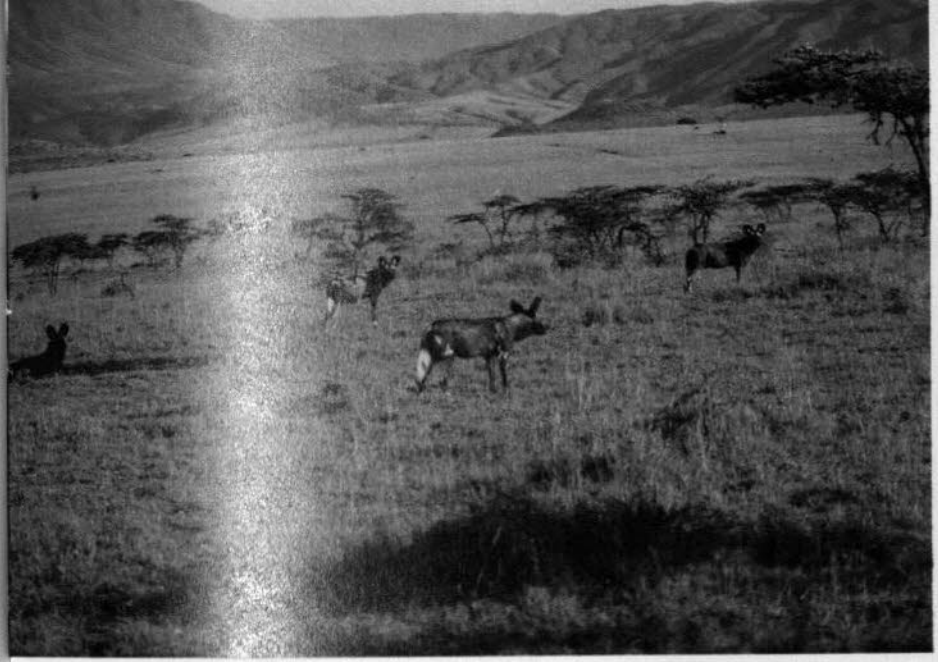

Plate 1 The Akira Plains, here seen with wild dog, form the rift floor south of Longonot and the Olkaria Complex. On the right is the southern flank of the latter, while forming the skyline is the western rift margin—the Mau Escarpment.

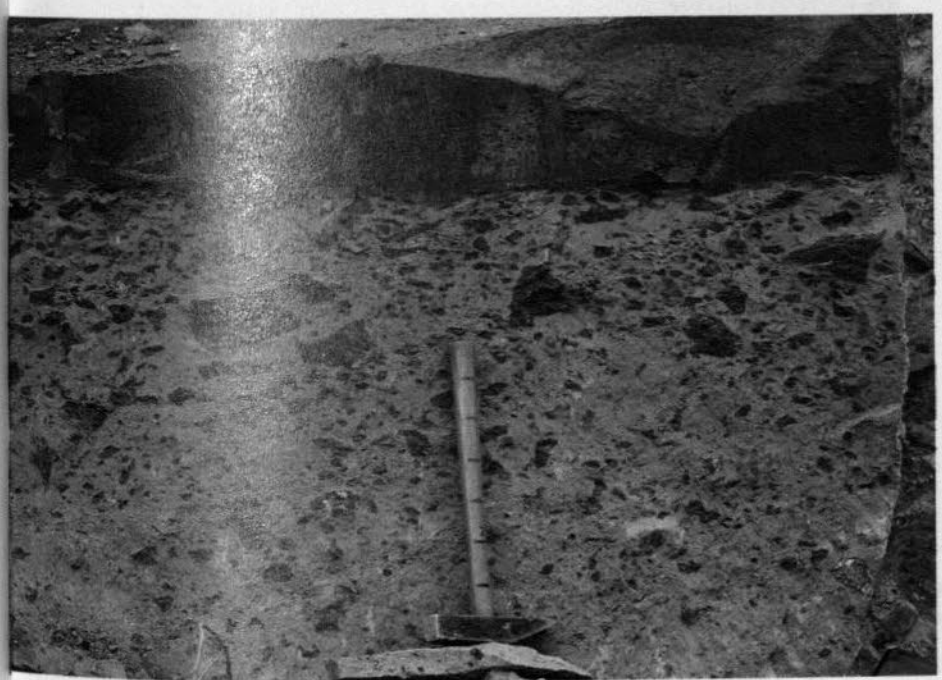

Plate 2 Two ignimbrite flow units in the Mau Tuff near Narok, showing reversely graded pumice clasts.

Plate 3 Longonot Volcano viewed from the east and showing the summit crater rim. Previous to this work all known thermal activity was within the crater.

Plate 4 Longonot Volcano. A 25 km tectono-volcano alignment (TVA), associated with weak thermal activity and subsidiary young minor eruption centres, runs through the main edifice and extends northwards to Crescent Island and southwards to the Narok road. This view shows the manifestation of this alignment on the north flanks of the main cone.

Plate 5 Longonot Caldera Escarpment, southern sector. The crags near the base of the eroded scarp are welded pyroclastics hosting small fumaroles.

Plate 6 Fumarole as noted in the previous photo, maximum temperature recorded in this sector was 64°C.

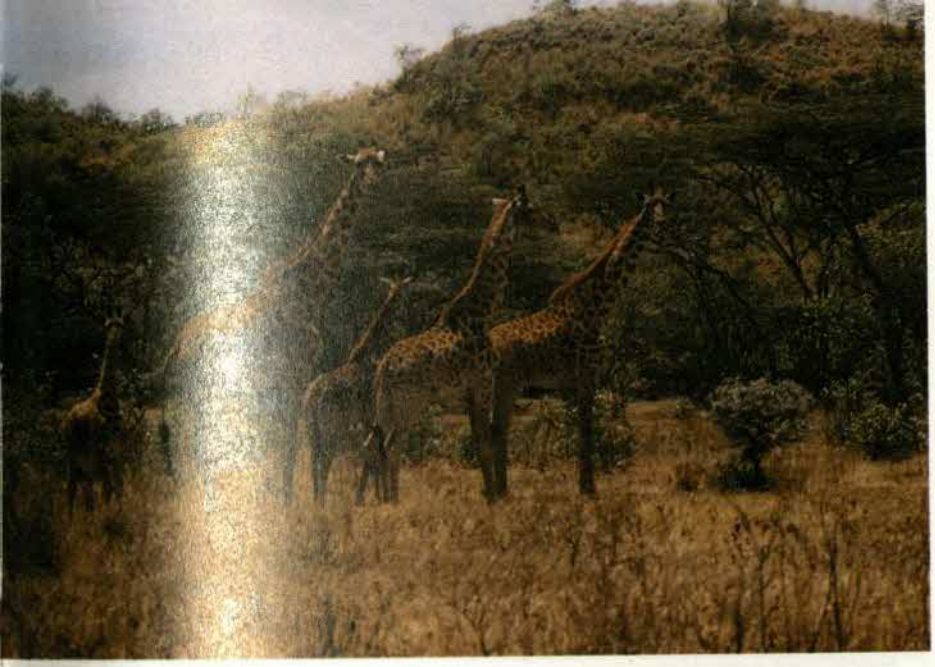

Plate 7 Wild life. The southern and eastern flanks of Longonot; the eastern Domes, Hells Gate and Njorowa Gorge areas of Olkaria; and both the Longonot Farm and Akira Ranch plains currently support a large concentration of game. During the present survey numerous antelope, zebra and giraffe were encountered as well as buffalo, lion, cheetah and wild dog. The authorities have recognised the importance of the wildlife by designating two areas as Game Parks: a) the cone of Longonot Volcano and b) much of the area occupied by the Olkaria Complex.

Plate 8 Longonot Volcano, Akira Pumice Formation, plinian beds of the Lower Pumice Member separated by thin weathered ash fall and underlain by the pale-coloured Surge Member.

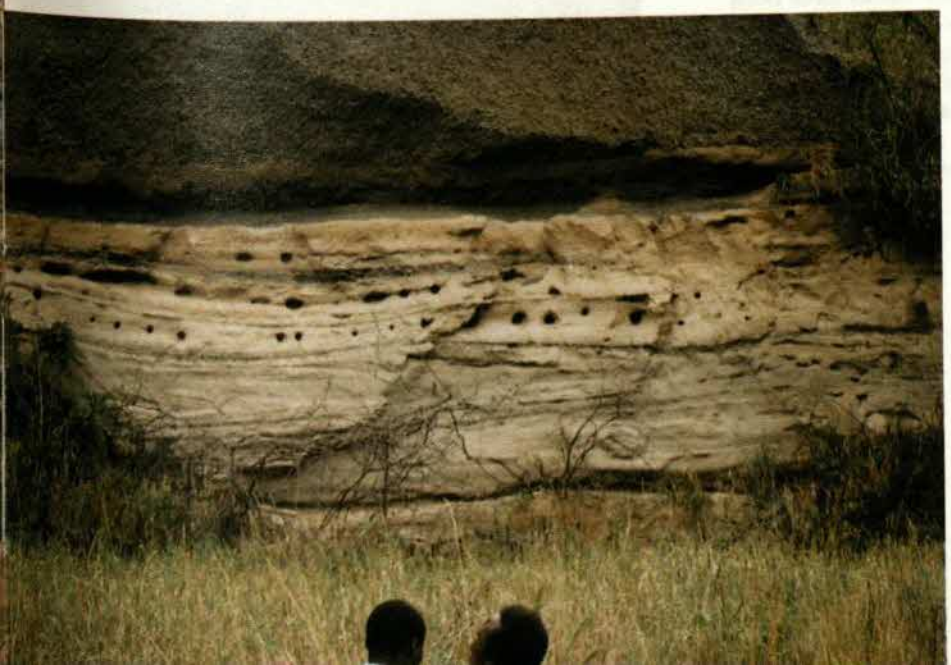

Plate 9 Closer view of surge member showing laminar and dune bedding, often picked out by thin pumice beds and with horizons of accretionary lapilli.

Plate 16 Olkaria Volcanic Complex. An Upper Comendite Member pumice unit formed by three plinian beds overlying eroded lava of Middle Comendite age.

Plate 17 Olkaria Volcanic Complex. Laminated and dune-bedded surge deposits of Middle Comendite age.

Plate 18 Armoured and accretionary lapilli within the above unit.

'within plate'-tectonic setting using the criteria of Pearce and Norry (Figure 4.3b).

Basic and intermediate compositions also occur within the main Olkaria Complex, e.g. in S. Hellsgate and at Central Tower, in both cases being macroscopically texturally mixed with O4 comendites.

4.3.3 Trace element variation

4.3.3.1 Nb v. Zr plots

Longonot

Despite the very restricted major element variation between units Lmx1. Lt2 and Lt3 the trace element data from Longonot e.g. Nb/Zr content, varies considerably, (Figure 4.4a). This is so both between units and within Lt2. The recent flank flows (Lt3) appear compositionally equivalent to the more evolved portions of the lava-pile, while Lmx1 have much lower incompatable element (ICE) content than the more 'basic' Lmx2 suite.

It is assumed that increasing totals of incompatable trace elements (ICE), e.g. Zr, indicate more highly evolved compositions.

It is possible to devide the main Longonot lava pile lavas (Lt2) into 4 subgroups based on their relative extent and age, (Figure 4.6a). The earlier, more widespread lavas (Lt2a and 2b) are lowest in Nb and Zr content while the later lavas of the pile (including the post-crater flank flows Lt3) are highest in Nb and Zr (Figure 4.6b). This pattern can be interpreted as indicating that the earlier less evolved lavas were more fluid than those later and more evolved.

Compositional variation in the Longonot pyroclastic sequence using Nb/Zr ratios indicates that:

1 There ia a generally wider intra-unit variation in the pyroclastics than in the lavas.
2 The pyroclastic eruptions were generally tapping more evolved magma, i.e. magma with greater ICE content than in lavas.
3 The decrease in ICE from bottom to top of some Plinian beds of Lp5, is an indication of magma chamber zonation revealed during a large explosive eruption, (cf Fisher and Schmincke, 1985, Table 2-2).
4 The overlying beds sometimes contain pumice of more evolved nature than the upper (i.e. last) part of the previous eruption. This indicates that the magma chamber had refractionated and therefore a time lapse occurred between these two plinian events. The presence of an intervening palaeosol supports this deduction.
5 There is a general decrease of ICE content from early to late Lp5 events, superimposed on the intrabed variation noted in 3 above. This correlates with a general decrease in bed thickness and clast size.
6 The later beds of Lp5 have similar contents of Zr to those of the most evolved Lt2 and 3 lavas (i.e. ~1000 ppm).

Broad correlation of ICE content with volcanic events is illustrated in Figure 4.7. It can be seen that higher ICE contents characterise i), units in which ignimbrites are prominent, i.e. Lp1 and Lp3, ii), the earlier part of the Lp5 plinian sequence and iii), (highest of all) the Lp4 base-surge

Volcanological inferences can also be drawn from the cyclical nature of the Zr levels versus time and eruptive style. The three troughs may represent tapping of relatively unfractionated (less evolved) magma, following caldera collapse or crater formation. The relatively high Zr levels present in the most recent flows perhaps signal that pyroclastic activity is to be expected in the (volcanological) near future.

On a Nb/Zr diagram pre-, syn- and post-caldera rocks of Suswa Volcano (Torfason, Skilling, unpublished analyses) define a trend which is entirely separate and distinct from that of Longonot rocks. All new analyses, including some by Scott (unpublished), of pyroclasts from ignimbrites exposed in the Ewaso Kedong Valley plot along the Longonot trend and for this reason these ignimbrites are assigned to the Kedong Valley Tuff. Kinangop Tuff analyses however are inseparable from those of the Kedong Valley Tuff, and other Longonot Volcanic Group analyses, on the basis of Nb and Zr variation.

Olkaria

As in the case of Longonot Volcano incompatable trace elements show a much greater variation than major elements. On a Nb versus Zr bivariant plot (Figure 4.4b) the following features are immediately apparent:

1 There is much greater compositional variation than in Longonot Volcanic Group rocks.
2 Three separate Olkaria Volcanic Group trends are apparent, and distinguish a) Lower Comendite Member rocks (O2/Op2), b) Middle Comendite Member rocks (O3/Op3) and c) Upper Comendite and Ololbutot Member rocks (O4/Op4 and O5/Op5).
3 The upper range in the Middle Comendite Member (O3/Op3) trend is greatly extended, with Zr contents of almost 4000 ppm and over 1000 ppm Nb.
4 The Nb versus Zr plot does not permit a clearcut distinction between Olkaria and Longonot analyses.

The three separate Nb/Zr trends mentioned above where intially defined using the new analyses, but existing analyses (MacDonald et al., 1987) clarify these trends and enable reclassification of the older data using the new stratigraphy (Table 3.7), which has been substantiated by the above trends. Olkaria Pantellerite analyses plot along the Lower Comendite Member (O2/Op2) trend (Figure 4.4b). On a Nb/Zr diagram analyses by Bone (unpublished) of rhyolites from Olkaria geothermal boreholes plot together with those of the Lower Comendite Member (O2/Op2).

Comendites from the Ndabibi area plot in a very restricted field at the least ICE-enriched portion of the plot. It appears that the Ndabibi volcanism was of different character geochemically and, judging by the low ICE contents, was not particularly evolved, (see later discussion of Figure 4.9).

Eburru

Nb and Zr data for rocks of the Eburru Volcanic Group are plotted as Figure 4.4c, and the following observations are possible:

1 The Eburru Trachyte Formation is the least-evolved unit at Eburru in terms of general levels of incompatable trace element content as exemplified by Nb and Zr.
2 The Eburru Trachyte and Younger Pantellerite formations have mainly very similar Nb versus Zr ratios whereas the Waterloo Ridge and Older Pantellerites generally lie on a separate trend, with a slightly higher Zr/Nb ratio.
3 The two older formations are generally more enriched in the incompatable elements, probably related to the more explosive nature of their emplacement.
4 Eburru Pumice analyses do not relate exclusively to either of the two trends. This is not surprising as this

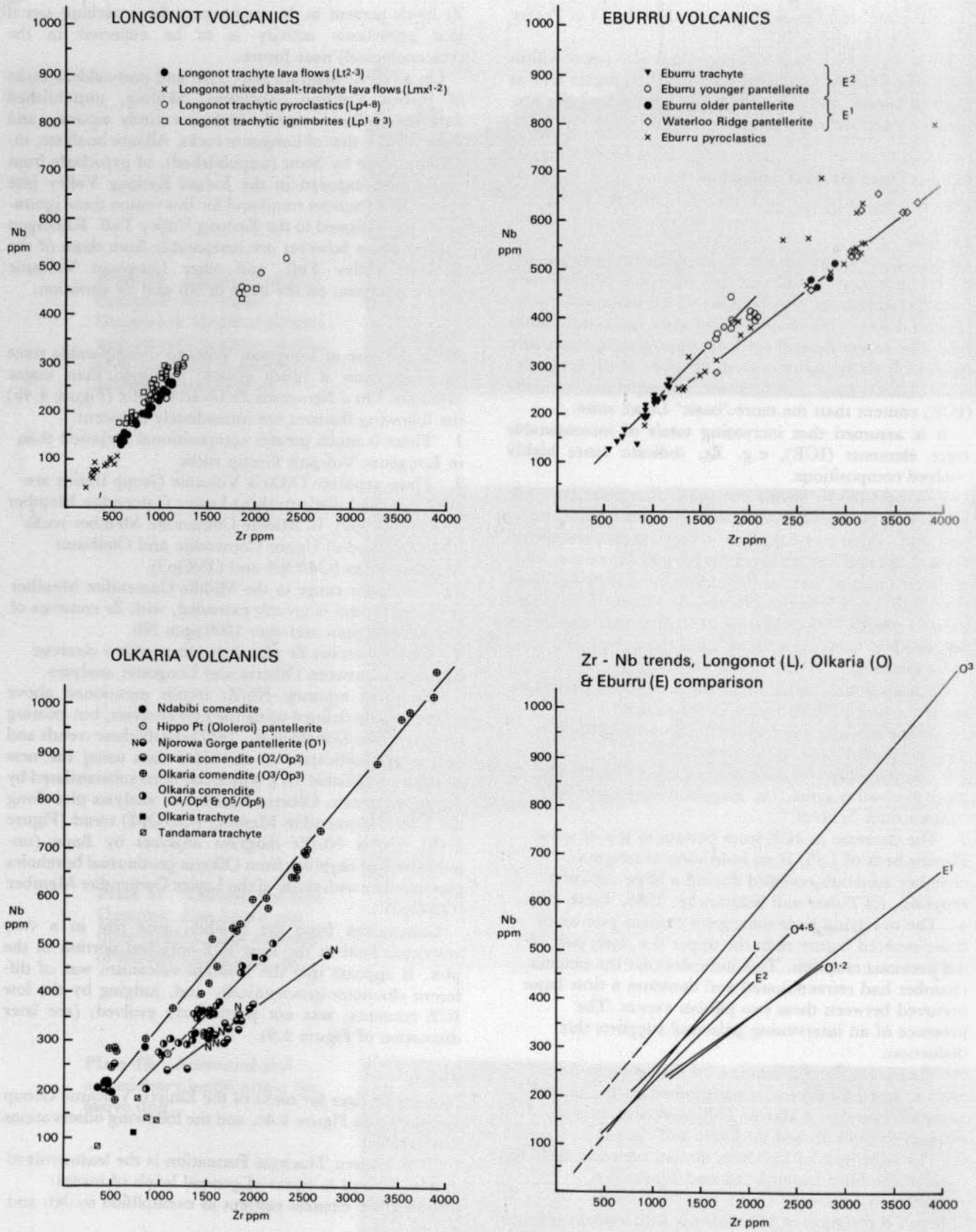

Figure 4.4 Niobium and zirconium variation within and between Longonot, Eburru and Olkaria volcanic groups.

Formation includes all pumices on Eburru of whatever age. Further work would probably show that geochemical fingerprinting, as established for the Olkaria Volcanic Group, could subdivide this unit.

4.3.3.2 Nb v. Th plots (Figure 4.5)

Although Nb/Zr ratios clearly differentiate between phases of Olkaria activity there is complete overlap of Olkaria, Longonot and Eburru (Figure 4.4d) data. A number of other ratios were therefore scanned and it was found that a plot of Th v. Zr also separates the various Olkaria volcanic phases but in addition allows distinction of Longonot compositions, but not however Longonot from Eburru.

These relationships are displayed in Figure 4.5 for the same data set plotted on Figure 4.4. Almost identical Olkaria groupings and trends result but Longonot and Eburru samples show a consistent much lower Th/Zr ratio compared to all the Olkaria trends. The extremely high absolute levels of ICE present in some O3 samples, particularly pyroclastics, is again demonstrated by Figure 4.5.

4.3.3.3 Th v. U plots

Figure 4.8 includes values >240 ppm Th and 43 ppm U from Olkaria samples indicating that the Olkaria complex rocks have a much higher absolute content of radioactive elements (RAE) than is the case at either Longonot or Eburru.

Other aspects of Th and U variation in the Longonot and Olkaria complexes are illustrated in Figure 4.8 where 3 groups of pumice data are plotted. A colinear relationship exists irrespective of overall composition or phase of volcanism. Relative depletion of RAE at Longonot is clear. The extremely enriched nature of many O3 compositions and relative restricted compositional variation within O4 are clearly displayed.

Compositional variation related to style of volcanism is illustrated in Figure 4.9 again using Th/U ratios as indicative of ICE content and therefore degree of evolvement. The sample suite plotted comprises all available BGS O3 data. The least evolved compositions are all from domes while the most evolved are all pumice. Intermediate compositions are either of pumice or lavaflows. It is concluded that there is a close relationship between ICE content (degree of magma evolution), and increasing volatility of eruption, i.e. ICE contents increase from highly viscous dome formation through lava emission to increasingly explosive eruptions including base surges. It is speculated that the most highly evolved compositions represent material from the upper most fractionated part of a large magma chamber.

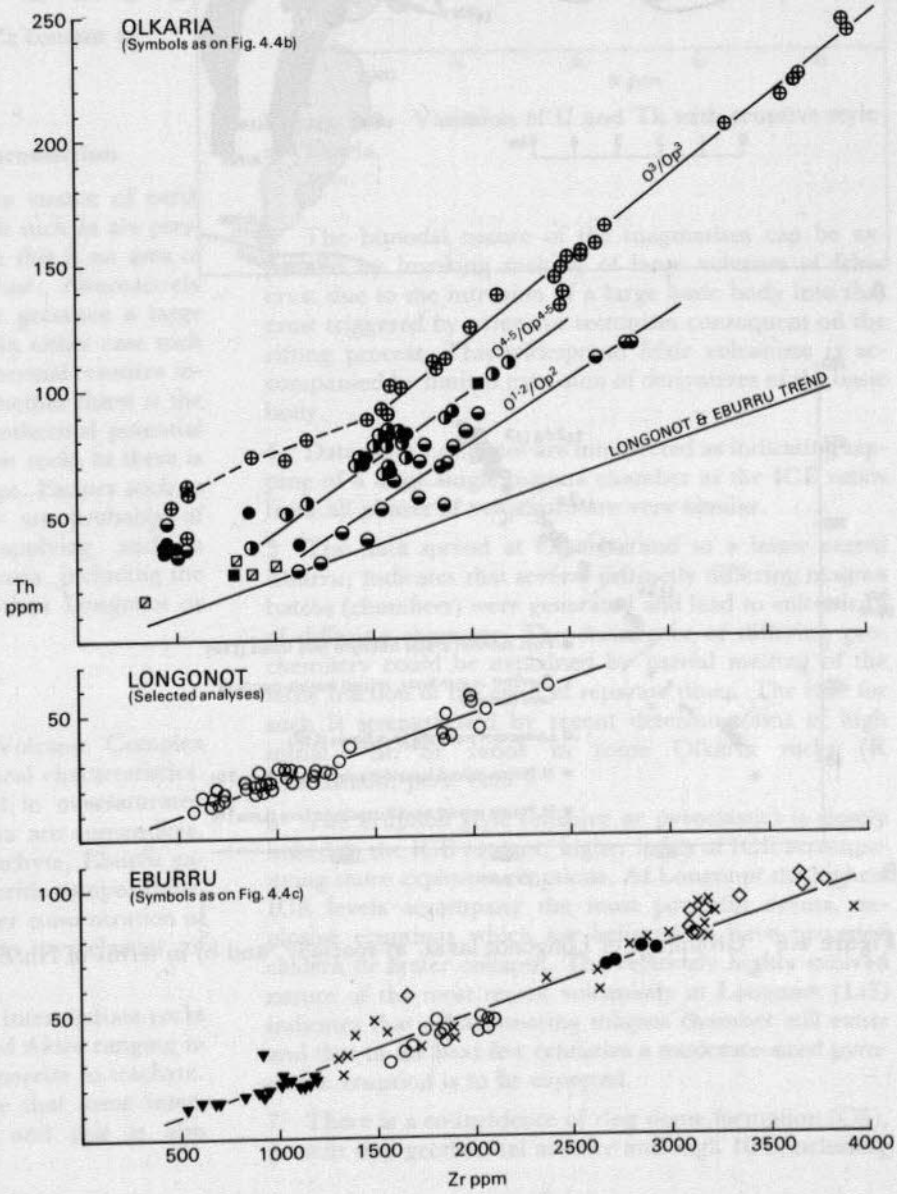

Figure 4.5 Thorium and zirconium variation within and between Longonot, Eburru and Olkaria volcanic groups.

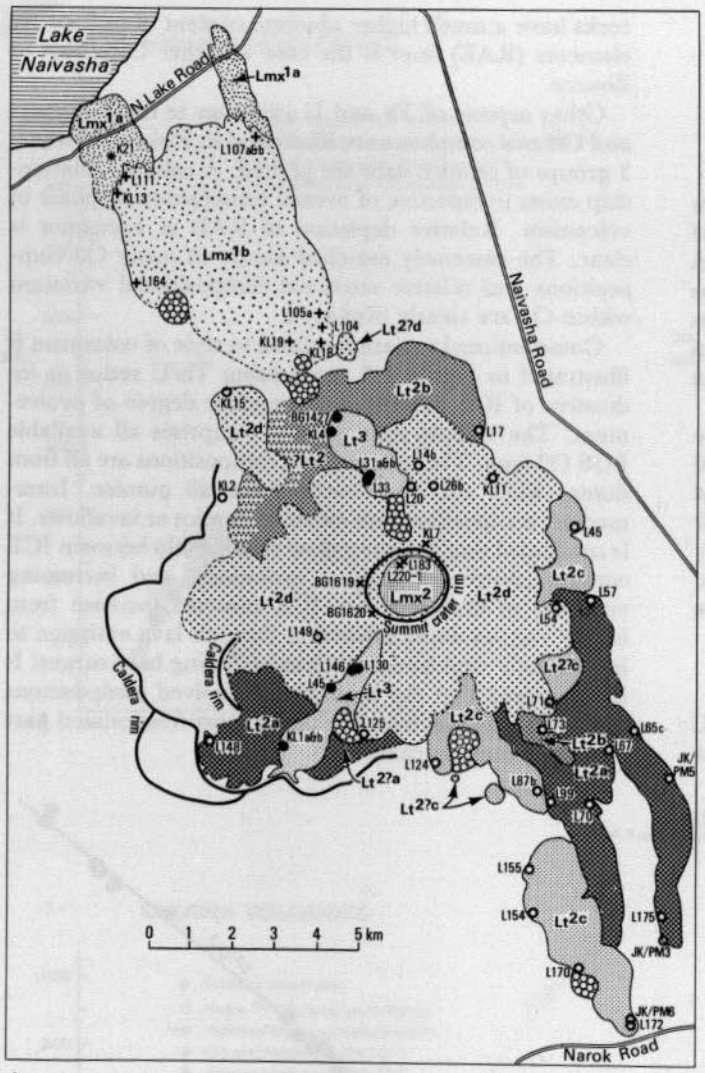

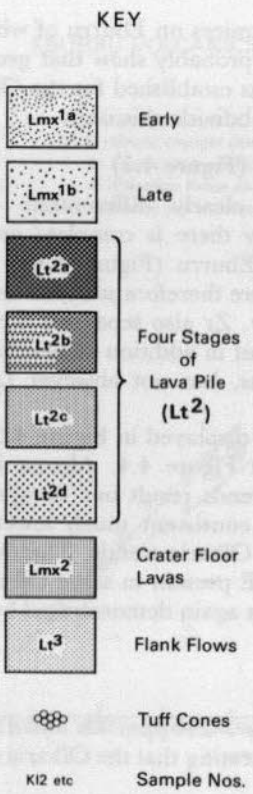

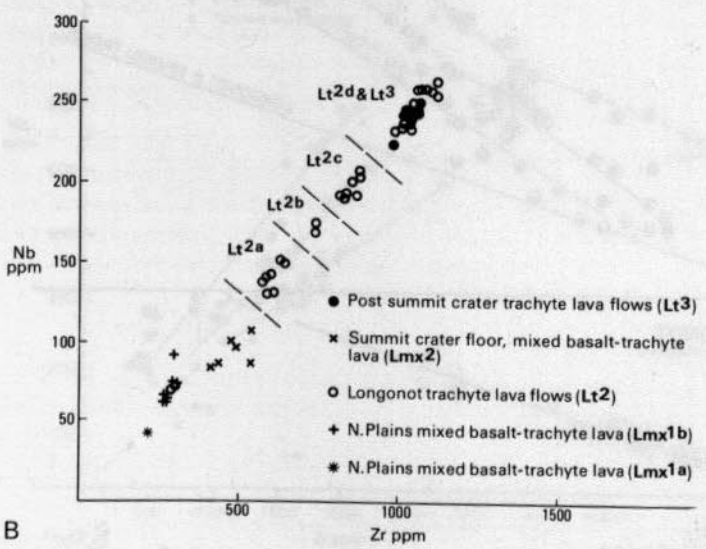

Figure 4.6 Groupings of Longonot lavas, a) spacially, and b) in terms of Nb/Zr content.

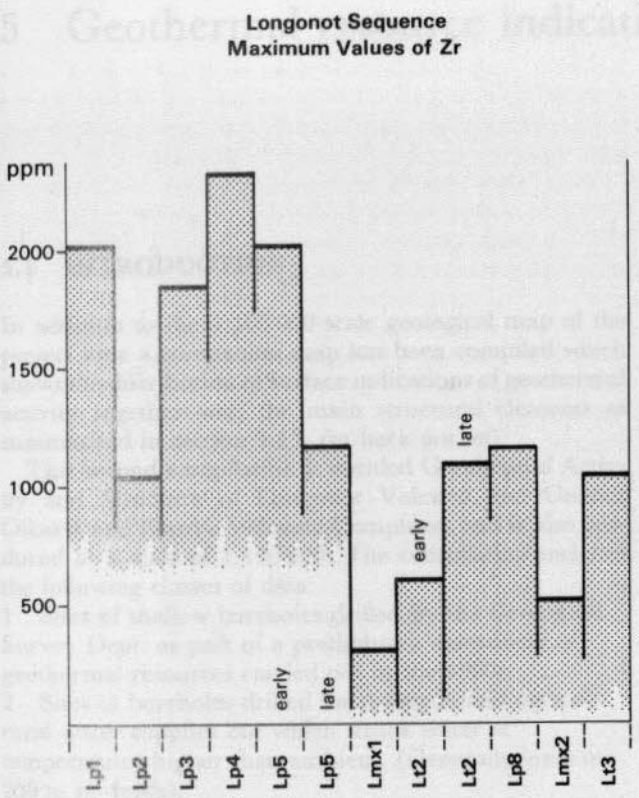

Figure 4.7 Variation of maximum Zr content at Longonot.

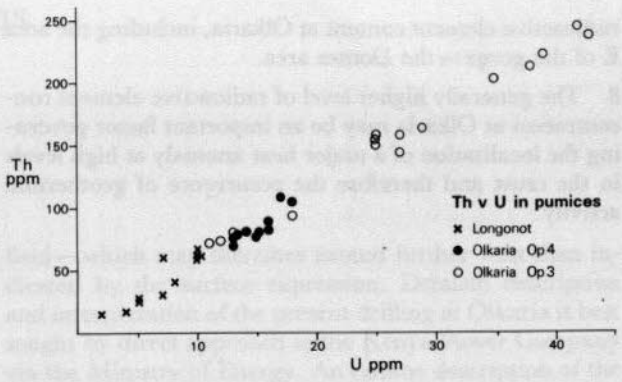

Figure 4.8 Comparison of U and Th contents of pumice at Longonot and Olkaria.

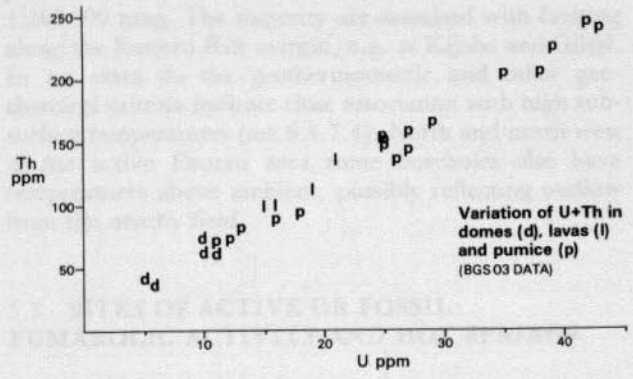

Figure 4.9 Variation of U and Th with eruptive style at Olkaria.

4.3.4 U and Th content and heat production

Radioactive elements are the ultimate source of earth heat. High concentrations of U and Th such as are present at Olkaria may be indications that this is an area of particularly thermally anomalous crust. Alternatively these high contents may indicate the presence a large highly fractionated magma chamber. In either case such areas would seem appropriate for geothermal resource investigation. It is not clear however whether there is the same positive relationship between geothermal potential and radioactive element content of host rocks as there is using the hot dry (granite) rock concept. Factors such as aquifer occurrence and permeability are probably of greater importance. Nevertheless applying such a criterion alone would suggest that Olkaria, including the Domes area, has a greater potential than Longonot or Eburru.

4.3.5 Conclusions

1 Longonot, the Greater Olkaria Volcanic Complex and Eburru have distinctive geochemical characteristics. Longonot compositions are saturated to oversaturated peralkaline trachytes, those at Olkaria are comendites, i.e. alkali rhyolites, but with some trachyte, Eburru exhibits both quartz trachyte and pantelleritic compositions. A striking difference is the much higher concentration of incompatible elements (ICE) in the pyroclastics of Olkaria compared with the other two.

2 Subordinate volumes of basic and intermediate rocks are exposed at Elmenteita, Ndabibi and Akira ranging in composition from basalt through benmoreite to trachyte. At Longonot there is strong evidence that some intermediate rocks result from mixing and this is also suspected at Olkaria.

3 The bimodal nature of the magmatism can be explained by invoking melting of large volumes of felsic crust due to the intrusion of a large basic body into that crust triggered by extensive tectonism consequent on the rifting process. This widespread felsic volcanism is accompanied by limited extrusion of derivatives of the basic body.

4 Data from Longonot are interpreted as indicating tapping of a large single magma chamber as the ICE ratios from all phases of volcanism are very similar.

5 The data spread at Olkaria, and to a lesser extent Eburru, indicates that several distinctly differing magma batchs (chambers) were generated and lead to volcanicity of differing character. The occurrence of differing geochemistry could be explained by partial melting of the felsic fraction of the crust at separate times. The case for such is strengthened by recent determinations of high initial $^{87}Sr/^{86}Sr$ ratios in some Olkaria rocks (R Macdonald, pers. com.).

6 The eruption style (effusive or pyroclastic) is closely linked to the ICE content, higher levels of ICE accompanying more explosive eruptions. At Longonot the highest ICE levels accompany the most powerful events, explosive eruptions which are believed to have preceded caldera or crater collapse. The relatively highly evolved nature of the most recent volcanicity at Longonot (Lt3) indicates that a fractionating magma chamber still exists and that in the next few centuries a moderate-sized pyroclastic eruption is to be expected.

7 There is a co-incidence of ring dome formation (O3), present day geothermal activity and high ICE,including

radioactive element content at Olkaria, including the area E of the gorge—the Domes area.

8 The generally higher level of radioactive element concentration at Olkaria may be an important factor governing the localisation of a major heat anomaly at high levels in the crust and therefore the occurrence of geothermal activity.

5 Geothermal resource indications

5.1 INTRODUCTION

In addition to the 1:100 000-scale geological map of the project area a companion map has been compiled which shows the distribution of surface indications of geothermal activity together with the main structural elements as summarised in section 3.13, (in back pocket).

This second compilation is entitled Geothermal Activity and Structure of Longonot Volcano, the Greater Olkaria and Eburru Volcanic Complexes and is also produced at a scale of 1:100 000. The compilation includes the following classes of data:

1 Sites of shallow boreholes drilled by the Geological Survey Dept. as part of a preliminary assessment of geothermal resources carried out in the 1960s.

2 Sites of boreholes drilled for domestic and agricultural water supplies but which struck water at temperatures higher than ambient. (Generally less than 250 m in depth).

3 Sites of deep (>800 m) production and exploration boreholes drilled as part of the ongoing development at Olkaria.

4 Locations of active or fossil fumarolic activity.

5 Location of hot springs and seeps.

6 Locations of soil-gas and fumarole field determinations of CO_2 and radon carried out using Orsat and Emanometer apparati.

7 Sites where rainwaters, surface waters and borehole waters and fumaroles were sampled for a wide spectrum of geochemical criteria. (The results of these determinations are discussed in the following section (6)).

5.2 PREVIOUS WORK AND EXISTING DATA

Shallow geothermal exploration drilling carried out in the 1960s consisted of 27 holes of maximum recorded depth of 61 m. These were drilled on the southern flanks of the Olkaria Complex and on the low ground separating Olkaria and Suswa Volcano. Almost all the holes recorded temperatures of >40°C and steam was noted in some (Mason, 1967). With the exception of those closest to Olkaria (Nos 4, 4A and 4B) and at the south entrance to the Njorowa Gorge (Nos1,1A and 1B) no surface indication is present and soil gas exploration undertaken as part of the present project showed no elevated values of CO_2 in the area.

In the same area steam was struck in two holes drilled for water, C1524 (South Njorowa Gorge) and C1402 (Akira Ranch), 98 and 231 m deep respectively. This is now piped to the surface and discharges at the local boiling point.

There is thus evidence of water and steam above boiling point at quite shallow levels in the area south of Olkaria and south-west of Longonot Caldera. In the latter area there are no natural surface indications.

The exploration and production wells drilled at Olkaria are all within the field delineated by natural surface geothermal features (fumaroles), however borehole OW601 is right on the north-west margin of the field—which may therefore extend further west than indicated by the surface expression. Detailed description and interpretation of the present drilling at Olkaria is best sought by direct approach to the Kenya Power Company via the Ministry of Energy. An outline description of the hydrogeology and geothermal style of the known field is given in section 6.5.

Several holes drilled for water in other parts of the project area have elevated temperatures and are shown on the 1:100 000 map. The majority are associatd with faulting along the Eastern Rift margin, e.g. at Kijabe and Gilgil. In no cases do the geothermometric and other geochemical criteria indicate close association with high subsurface temperatures (see 6.4.7.4). North and north-west of the active Eburru area some boreholes also have temperatures above ambient, possibly reflecting outflow from the nearby field.

5.3 SITES OF ACTIVE OR FOSSIL FUMAROLIC ACTIVITY AND HOT SPRINGS

5.3.1 General description

In addition to conventional geological mapping the field investigations included the search for surface indications of geothermal activity. The most wide spread form of such are areas where the rock is altered, frequently to a cream-yellow to reddish pink coloured clay. Limited mineralogical investigations indicate that the commonest phase present is halloysite $Al_4S_4(OH)_8\ O_{10}.8H_2O$ a disordered form of kaolin. Lesser amounts of chlorite, smectite and kaolin may also be present. Haematite and alunite also occur, the intense red color of many examples suggests significant amorphous ferric oxide is present also.

Temperatures of such clays are frequently above ambient, in some cases near or at the local boiling point. In these cases they are very damp and visible steam may be present, sometimes from distinct orifices or fumaroles. Steam emission is best seen when the air temperature is low for example in the early morning, or immediately after heavy rain.

Although in many places the alteration is visible from a distance of several hundreds of metres some significant localities are completely concealed either by vegetation or by talus. Initial discovery of such areas resulted from frequent use of probes, equipped with <0.5 m-long metal protrusions which are temperature sensors connected to a digital read-out. These can be used by unskilled personnel and provide a rapid means of assessing areas with no visible manifestation.

Although no true solfatara are present a limited number of fumaroles have been observed around which small-scale precipitation of sulphur is occurring.

Silicification, in the form of chalcedony, is also common accompanying fossil fumarolic areas, i.e. areas of alteration which are no longer hot or active. These have probably suffered some erosion to reveal the silica which generally appears to have precipitated at shallow depths

beneath the surface. Erosion may reveal silica cementing individual clasts in a tuff or producing a swarm of subvertical pipes by alteration of fine ash. Deeper levels of erosion may reveal silica veins up to several centimetres wide.

5.3.2 Longonot volcano

It has been long known that fumaroles existed in the Longonot summit crater but no systematic map had been produced prior to this project. There was no record of fumaroles outside of the crater.

Areas of fumarolic activity occur on talus slopes at the foot of the vertical crater walls, and in these areas steam percolates through the talus and the finer fragments are altered. The alteration products include reddish brown iron-oxide and white kaolin. A limited amount of deposition of yellow sulphur has taken place (Figure 5.1). Steam emission can sometimes be induced by shallow excavations into the altered talus.

Individual fumaroles are also associated with fractures and joints in the lava which forms the lower and middle parts of the crater walls. In the north-west wall of the crater several fumaroles appear to be situated along linear fractures of various trends. Very little alteration and deposition occurs in association with these fumaroles, but there are areas of green/brown algal growth where the steam has been condensing against the lava.

Several inconspicuous fumaroles in the eastern part of the crater are situated along the edge of the recent lava which forms the crater floor. Their presence is usually indicated by luxuriant growths of ferns.

Temperature measurements of many of the above mentioned fumaroles were in the 44 to 93°C range, and those in excess of 85°C were mostly commonly recorded in the fumarolic areas where extensive alteration of talus, and sulphur deposition, occurs.

Isolated fumaroles are present outside of the summit crater to the south. Three occur in the walls of the southern caldera rim 3 to 3.5 km south-south-west of the crater, and another on the northern edge of a flat topped, 400 m-diameter, lava dome which lies 4.25 km south-south-east of the crater. The fumaroles on the southern caldera wall are associated with fractures in welded pyroclastic rock with minor alteration only. The maximum temperature recorded was 64°C. The fumarole on the dome consists of patches of steaming ground within ash, (Lp8), which overlies the dome forming lava (Lt2). The ash has been altered to reddish grey and red clay and there are traces of yellow sulpur deposits. The maximum temperature recorded was 74°C.

A small thermal area is located on the surface of the Mlima Panya lava flow, 600 m north of the Narok road. Condensation and some algal growth occurs but no alteration of the lava has taken place. The maximum temperature recorded was 48.7°C. This manifestation occurs where one of a series of prominent open fissures on the lava flow surface intersects a south- to south-east-facing flow front. Other fissures on the southern half of the flow were examined but no further manifestations found.

Both active and fossil fumarolic zones occur around the rims of two pyroclastic cones that have formed along the northern post-summit crater eruptive fissure. Temperatures in a small localised area of residual activity on the northern rim of the large scoria cone reached 55°C. Pyroclastic rock in the small remaining area of residual activity has been altered to soft red, brown, orange and green clays but in the inactive areas exposures of consolidated and unconsolidated pyroclastic material has a distinct red colouration and some traces of yellow sulphur occur. Some of the consolidated pyroclastic material consists of lapilli loosely cemented by silica(?).

In general geothermal manifestations at Longonot either lie within the summit crater or on the main alignment of flank eruption centres and fissures, which passes through the summit crater, or along the rim of the caldera. The manifestations along the latter occur in the south where pre-caldera rocks are exposed beneath a somewhat thinner pyroclastic cover, and where it is believed that the topographic caldera rim lies very close to the ring-fracture. The lack of manifestations elsewhere along the rim can be accounted for by a thicker pyroclastic cover.

5.3.3 Mount Margaret

Highly altered (silicified) pyroclastic rocks crop out along arcuate ridges around the eastern and northern side of Mount Margaret, and indicate a widespread, but now extinct, area of geothermal surface activity. Some activity however does persist in the form of a small fumarole at the southern extremity of the zone of alteration. This activity is associated with a north-trending fault zone along which erosion by a southward draining stream has formed a prominent gully. The fumarolic area is about 10 m above the gully floor on its western side and steam issues from fractures in a vertical face formed of silicified pyroclastic rock. Algal growth has occurred where the steam has condensed on the rock-face and fine talus immediately below has been altered to reddish brown clay. The maximum temperature recorded was 89°C.

5.3.4 Kijabe and the eastern rift margin

A warm spring is located adjacent to the stream known as Tongitongi at the foot of the main rift escarpment, just below the railway, about 1.2 km south-east of Kijabe railway station. The source of the spring water is near the top of an accumulation of talus, about 10 m above the stream bed on its southern side. A temperature of 44.5°C was recorded in water artificially ponded around the spring.

An area of hydrothermally altered rock, indicating an extinct geothermal manifestation occurs at the foot of the escarpment along the edge of the Kijabe terrace, 3 km south-west of Kijabe railway station. The area is approximately 75 m long in a north-west–south-east direction and consists of two main outcrops of pale grey-weathering porphyritic lava which resembles that which outcrops in the escarpment except that it is yellow or white in colour due to the alteration, rather than the usual dark grey. The yellow colouration is probably associated with sulphur deposits. The two outcrops are separated by an area of horizontally bedded, coarse ash, some of which is a reddish brown colour. No temperatures distinctly higher than ambient were recorded.

A number of hot springs are known in the Rift Valley and particularly near the shores of, and within some of, the low-lying lakes, for example, Magadi and Bogoria. Within the area surveyed in detail during the present project hot spring activity is mainly limited to the east Rift margin, the southern extention of Lake Elmenteita and the Njorowa Gorge.

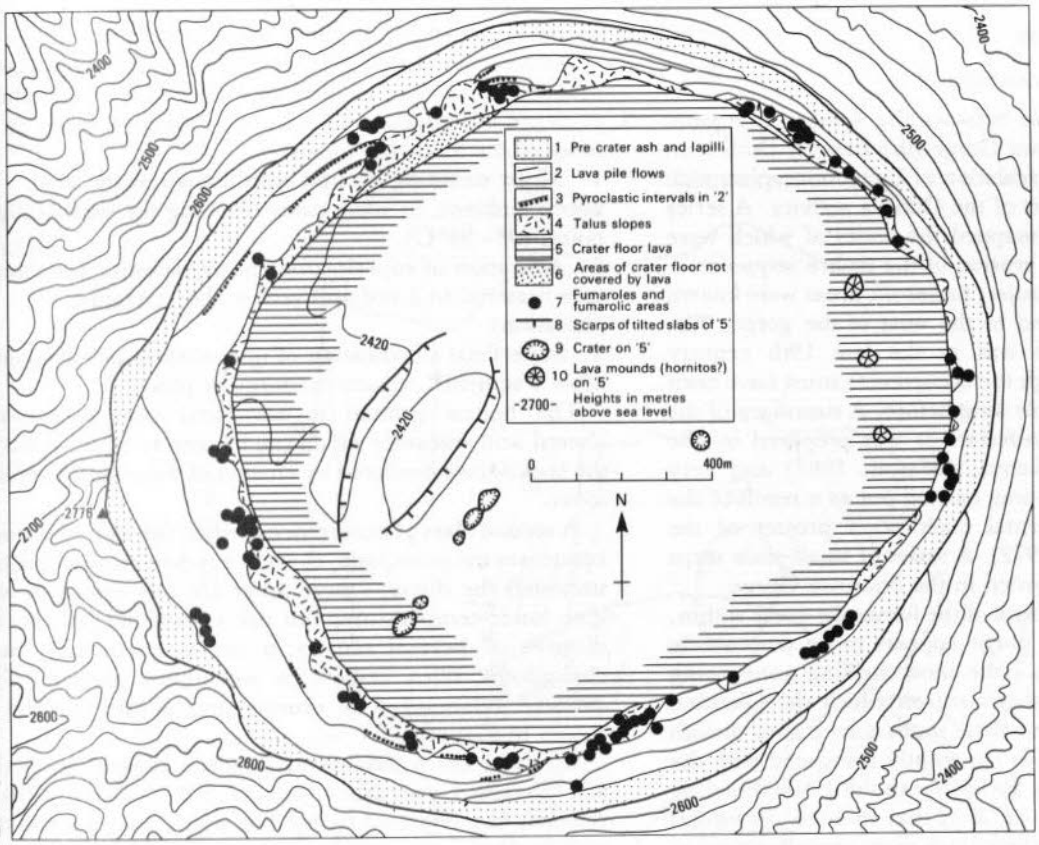

a)

Figure 5.1a Location of fumaroles in Longonot crater.

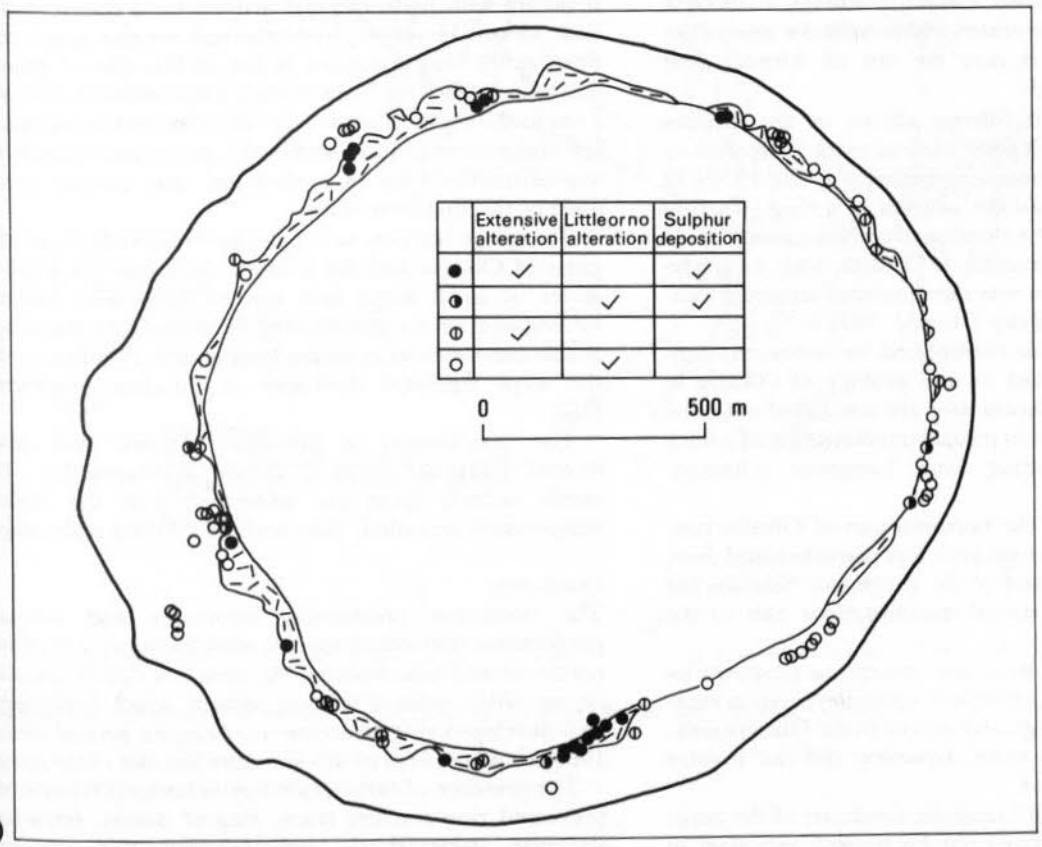

b)

Figure 5.1b Degree of alteration and presence of sulphur in fumaroles in Longonot crater.

5.3.5 **Olkaria complex**

5.3.5.1 General description

Examination of the area between the western Longonot Caldera and the Njorowa Gorge (the Eastern Domes on Figure 3.3) proved intercalation of Longonot tephra with those originating as part of the Olkaria activity. A series of arcuate domes was mapped the cones of which were sometimes revealed by erosion of the tephra sequence.

Prior to the present project fumarolic areas were known to be widespread in and to the west of the gorge. The earliest written record was in the late 19th century (Fischer, 1985), although the occurrences must have been known to the local people long before. A summary of the characters of these manifestations was prepared by the geological survey of Kenya, (Mason, 1967) and very detailed geological mapping carried out as a result of the UNDP-assisted geothermal exploration project of the early 1970s, (Naylor, 1972). A series of small-scale seeps have been recently recorded in the Njorowa Gorge.

Overall structural control of the fumarolic areas within, and to the west of the gorge appears to be dominantly orientated north–south—the most striking zone being the fissure and crater alignment on which the Ololubot Lava vent lies. Another north–south zone passes though Olkaria hill and a third is apparently associated with the gorge itself (Figure 5.2). Referring to the 1:100 000-scale geothermal map it can be seen that these north–south features are components of a much more extensive zone of young activity extending from Elmenteita, across eastern Eburru, through Ndabibi and southwards across Olkaria.

However there are no previous references to geothermal manifestations east of the gorge and presumably for this reason all detailed feasibility studies at Olkaria have tended to be concentrated within or to the west of the gorge and that area is now the site of Africa's first geothermal power plant.

The relative lack of interest shown in the Eastern Domes area following Naylor's initial work is typified by the comments of the consulting geologist to the 1970–72 project, who agreed that the concept of a ring structure was feasible but that the dominantly north–south structures and youngest volcanism at Olkaria, with its apparent extension to Eburru was the dominant structure controlling geothermal activity (Healey, 1972).

That doubt persists is exemplified by comments contained in a recent report on the geology of Olkaria in which the hills of the Domes area are concluded not to be ash or pumice cones but to result from dissection of a thick pyroclastic fall emanating from Longonot (Odongo, 1983).

A doctoral thesis on the northern part of Olkaria contains much relevant petrographic and petrochemical data, especially of the area west of the gorge and Ndabibi but did not mention geothermal manifestations east of the gorge (Bliss, 1979).

Support for the ring structure concept, as proposed by Naylor, is given in a geological summary map accompanying the results of a gravity survey of the Olkaria area, (Ndombi, 1981). This work, however, did not involve any fresh geological data.

The first indication of fumarolic areas east of the gorge resulted from work carried out by project personnel in conjunction with Dr S. C. Scott of Plymouth Polytechnic. Dr Scott spent the month of January 1986 working on Longonot pyroclastics as part of a sabbatical from his lectureship at Plymouth Polytechnic, UK. During a joint aerial reconnaissance areas of altered ground were seen on the flanks of two of the Eastern Domes.

Subsequent detailed examination of the pyroclastic mantled domes east of the gorge showed that ten exhibit evidence of hydothermal activity. This may take one or more of the following forms:

1 Moist steaming ground with temperatures well above ambient, in some cases reaching the local boiling point, (93–94°C).
2 Alteration of superincumbent pyroclastics and dome core material to a red and yellow clay. (Argillic alteration).
3 Superficial silicification of near-surface pumice and lithic fragments, sometimes forming pipes.

The hottest ground is associated with extensively altered acid volcanics which can be seen to be the cores of the lava domes unroofed by erosion of the younger tephra cover.

A second class of occurrence is when the altered ground comprises the pyroclastic cover, i.e. when erosion has not unroofed the dome—these areas are less extensive and give lower temperatures but are considered no less indicative of thermal activity at depth, particularly as a chalcedonic silica cement is sometimes present. The deduced relationship of erosion and altered ground is shown in Figure.5.3.

Seven of the hydrothermally active domes lie on the arc, discussed previously, section 3.8.1, which is truncated by the Njorowa Gorge but which continues to the west as a very similar topographic and geological feature. Previous (1972) work had located hydrothermal activity both on this ridge west of the gorge and in the adjacent gorge walls (Figures 3.4 and 5.2).

There is thus a very strong coincidence of the ring structure with hydrothermal activity for a distance of at least 15 km. However, hydrothermal activity is not confined to the ring structure as hot and/or altered ground has been located on Domes lying 2 km inside the arc and 3 km to the south (Figure 5.2). The distribution of steaming and altered ground within the gorge also extends for approximately 4 km in a direction near normal to the trace of the ring structure.

The gorge bottom, being at a lower altitude than other parts of Olkaria has the greatest discharge potential. A series of small seeps and springs have been recently located and are the physical expressions of such discharge. Stable isotope determination (section 6.5.2) indicates that the seeps represent discharge of the deep geothermal fluid.

The distribution of previously known and newly located fumarolic areas is shown on Figure 5.2. The newly located areas are annotated with the highest temperature recorded. (See also the 100 000 scale map).

Conclusions

The dominant present-day structures and volcanic phenomena controlling surface manifestations are mostly north–south linear features but these are clearly imposed on an older volcano-tectonic system which included a well-developed ring structure involving an area of almost 100 km^2, 40 per cent of this structure lies east of the gorge.

The presence of early welded pyroclastics (O1) near the presumed ring fracture trace, ring of domes, intra-ring structure volcaniclastic sedimentation and apparent resurgent activity within the ring structure (O5) are all characters shared by some calderas. (e.g. Valles). Calderas indicate the probable presence of former large magma chambers.

Indirect support for the caldera concept at Olkaria

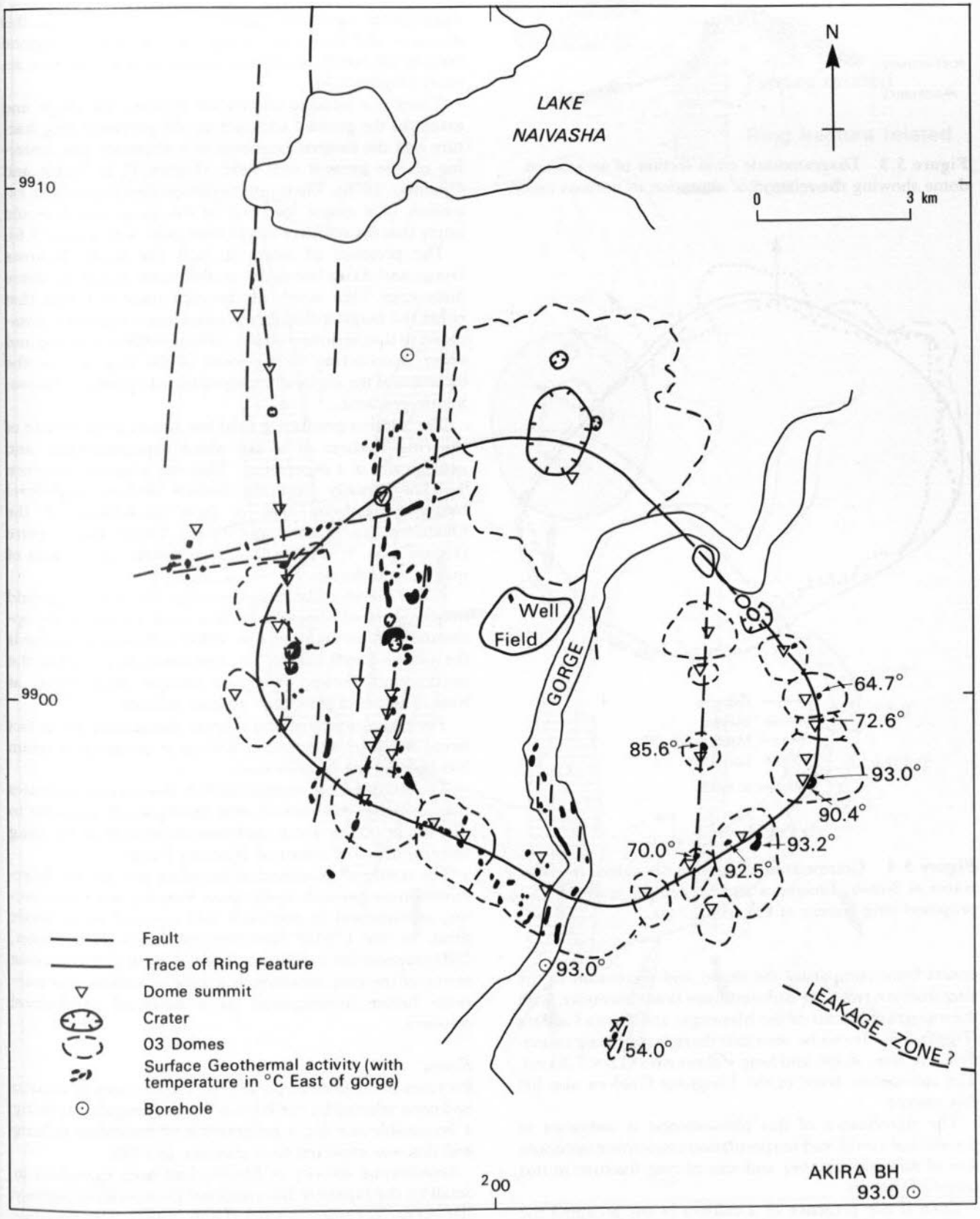

Figure 5.2 Relation of fumarole distribution to structure at the Olkaria Complex.

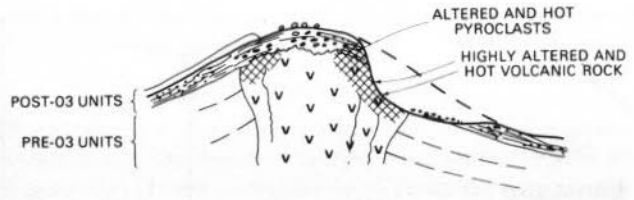

Figure 5.3 Diagrammatic cross section of an eastern dome showing the relation of alteration to various units.

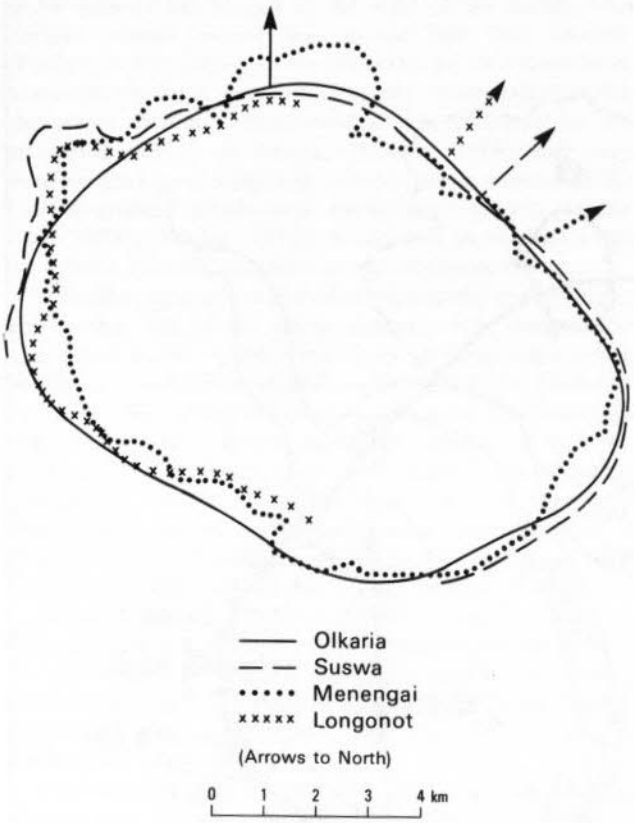

Figure 5.4 Comparison of the size of caldera fracture traces at Suswa, Longonot and Menengai, with the proposed ring feature at Olkaria.

comes from comparing the shape and dimension of the ring fracture trace, as deduced from dome summits, with the topographic trace of the Menengai and Suswa Caldera (Figure 5.4). It can be seen that there is a striking coincidence in size, shape and long v.short axes (11 × 7.5 km). The incomplete trace of the Longonot Caldera also fits this pattern.

The significance of this phenomenon is unknown at present but could lead to speculation concerning optimum size of magma chamber and size of ring fracture in this sector of the rift.

Even if the presence of a caldera is not accepted the evidence of very young activity, together with the comenditic nature and widespread vent distribution at the Olkaria Complex indicates that an extensive, shallow, highly differentiated magma chamber exists.

Much of the length of this ring structure on the west, south and east sectors, is still geothermally active at the surface. Several areas, additional to the western north–south fissure zones of Olkaria Hill and Ololbutot, within the ring structure, notably the bottom of the Njorowa Gorge, are also thermally active. It is therefore reasonable to suppose that a shallow heat source underlies much of the area encompassed by, and adjacent to, this structure and that areas of highest heat flow correspond both to the north–south and arcuate zones of surface activity (Figure 5.5).

There is a striking correlation between the shape and extent of the ground enclosed by the proposed ring fracture and the eastern extention of a resistivity low centering on the present well field, (Figure 12 in Noble and Ojiambo, 1976). Their interpretation clearly shows an extension of a major low east of the gorge which would imply that the resource might exist there also (Figure 5.6).

The presence of steam in both the south Njorowa Gorge and Akira boreholes as well as the fumarolic dome discovered 3 km south of the ring trace indicates that either the magma chamber is much more extensive, compared to that assumed above, or that outflow of steam and water is occurring to the south of the ring, i.e. in the direction of the regional topographic and presumed piezometric gradient.

The present producing field lies almost at the centre of the ring features at a site which topographically and geologically is a depression. This site is located between 1–3 km laterally from the nearest deduced high-level magma chambers, that is those underlying a) the Ololbutot fissure zone and b) the Gorge Farm centre (Figure 5.5). It may in fact be situated over an area of magma withdrawal.

It can therefore be suggested that the producing field may be situated within an outflow zone, i.e. not at the optimum location and that sites either to the north, towards the Gorge Farm centre, or west,towards or within the north–south fissure zone, are obvious alternatives, at least in terms of proximity to heat sources.

The above northern and western alternatives are in fact being tested by exploration drilling at present and steam has been struck in both cases.

The information summarised in this section indicates that a further prospective area exists, which amounts to the whole of the south and eastern sectors of the ring feature, much of it east of Njorowa Gorge.

The results of geochemical sampling and isotope determination on gas and condensates from the south-east sector, summarised in section 6 and reported on in more detail by the UNDP Geochemical Team (Armansson, 1987) support the suggestion that the south and south-east sector of the ring structure is a zone of upflow and warrants futher investigation as a potential geothermal resource.

Eburru

Previous to the present project the summit area of Eburru had been selected by the Kenya Power Company as being a favourable site for a programme of feasibility drilling and this was expected to commence in 1989.

Geothermal activity at Eburru had been examined in detail by the Japanese International Co-operation Agency (JICA) project prior to 1985 (JICA, 1983). The distribution of fumarolic areas given on the 1:100 000-scale compilation is mainly derived from the Japanese work with a few exceptions. The northernmost fumaroles were discovered during the 1986 work of the British-assisted project as was a series of fossil fumarole locations associated with the Waterloo Ridge Pantellerite outcrops.

The recent project field work concentrated on remapping and classifying the young volcanic rocks (section 4) to assist comparisons with Longonot and Olkaria.

By comparing the two 1:100 000-scale maps it can be seen that the fumarolic activity occupies an elongate zone

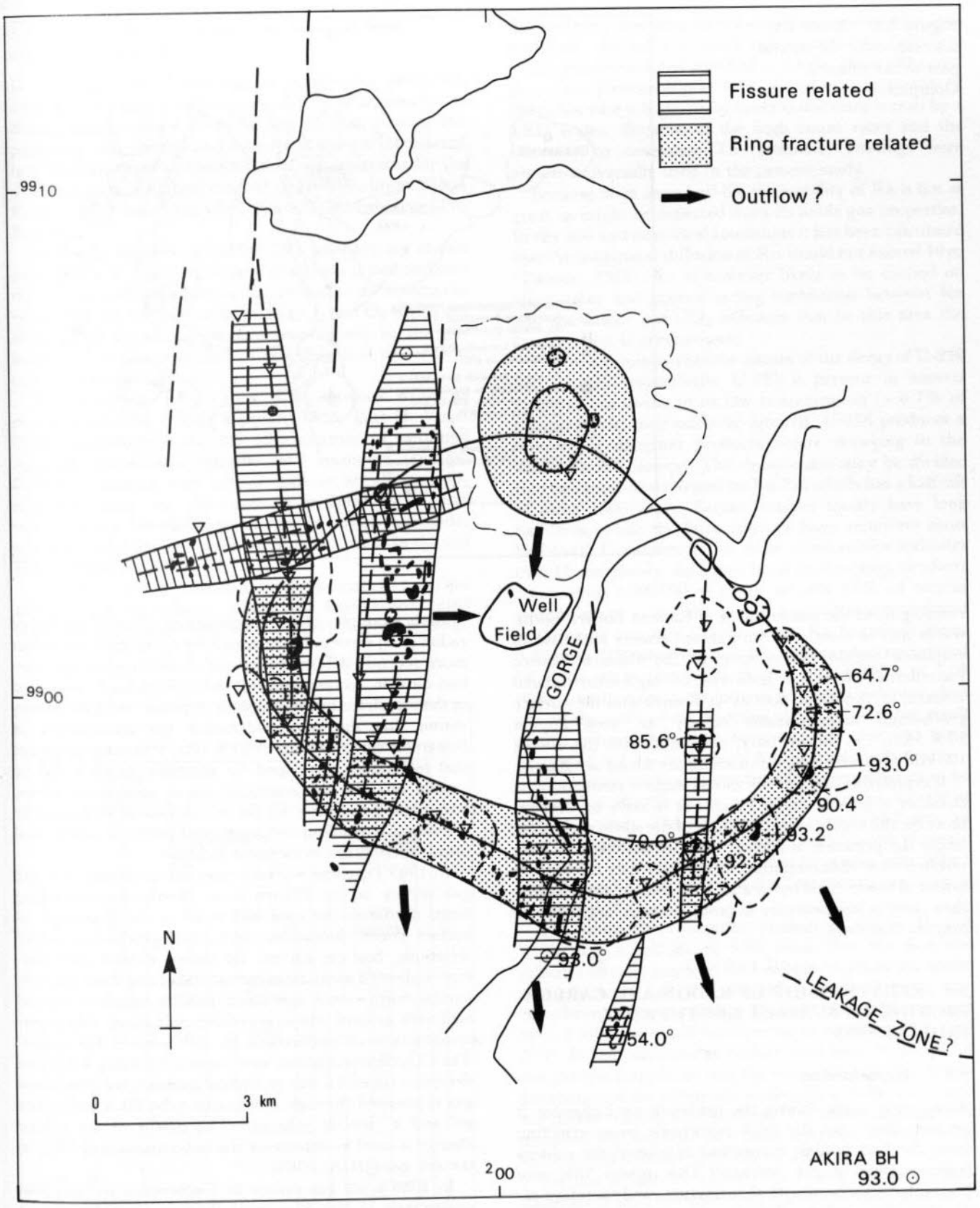

Figure 5.5 Cartoon of shallow heat sources at Olkaria.

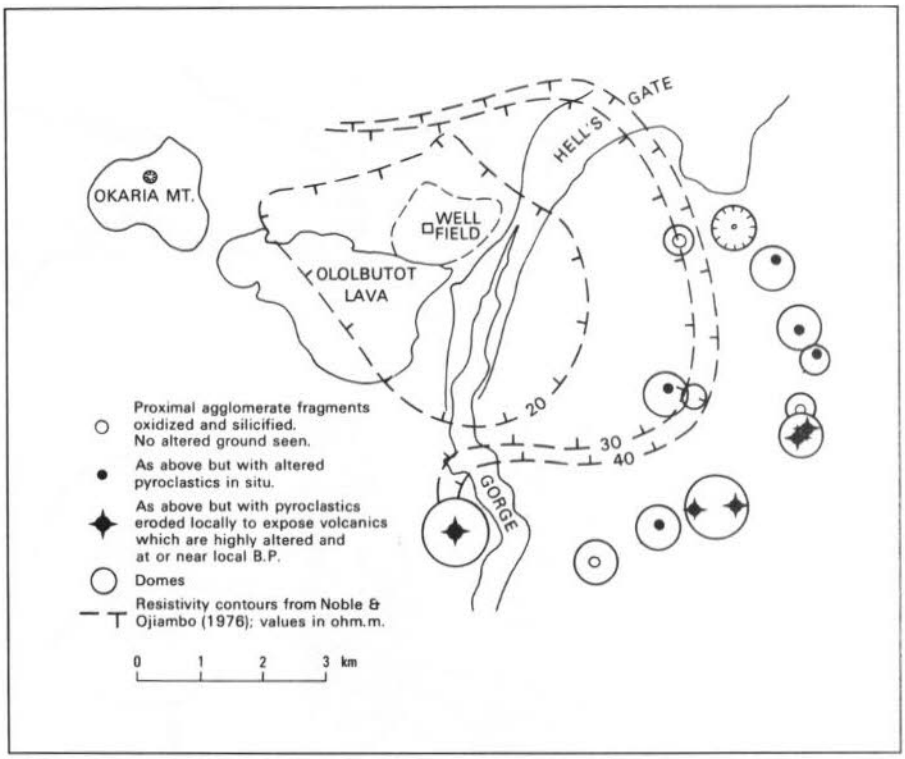

Figure 5.6 Resistivity anomaly over the central part of the Olkaria Complex.

running from the summit area of Eastern Eburru northwards and is associated with recent craters and fissures emplaced within the outcrop of the Eastern Eburru Pantellerite. There is no indication of ring fracture related volcanic or fumarolic activity at Eburru and the surface geothermal manifestations occupy an area approx 10×3 km, i.e. 30 km^2 only, compared with the almost 100 km^2 area over which fumaroles are found at Olkaria.

It is probable that no widespread shallow young magma chamber is present under Eburru as is likely at Olkaria, however the highly evolved nature of the silicic rocks does imply the presence of such if they are assumed to have resulted from differentiation. If however they result from fusion of lower crust by contact with basic mantle diapirs then there is less necessity to postulate such large shallow magma chambers.

5.4 RELATIONSHIP OF RADON AND CARBON DIOXIDE TO SURFACE GEOTHERMAL INDICATIONS

5.4.1 Introduction

At an early stage during the fieldwork on Longonot it became clear that the thick pyroclastic cover resulting from the Lp5 plinian events had blanketed the caldera fracture west of the volcano. This meant that any fumaroles associated with that fracture, and therefore indicative of a geothermal resource more widespread than presently known, would be buried and have little or no surface expression.

It is well known that the commonest gas emitted from fumaroles is often carbon dioxide which may form 95% of the non-condensable fraction, followed by sulphur dioxide, hydrogen sulphide, nitrogen, hydrogen, argon, helium and methane.

It was therefore decided to adapt certain soil gas geochemical methods which had been previously developed for the exploration of mineral deposits.

Early examples of such applications included the use of radon (Rn) surveys in the search for uranium deposits but more recently determinations of common gases e.g. carbon dioxide, oxygen and sulphide species have been used in the search for buried sulphide deposits. With the observation that the non-condensable gas components of fumaroles contained up to 95% CO_2 it became apparent that techniques developed for minerals search could be readily adapted for investigations of geothermal areas, and might be suitable for the search for buried fumarolic activity or to confirm the presence of potential geothermal areas where other evidence is lacking.

In 1983 Japanese workers reported the results of a soil gas survey in the Eburru area. North–south-trending faults dominate the area and result in the alignment of surface cones, fumaroles, and other geothermal manifestations. Soil gas surveys for carbon dioxide and mercury indicated anomalous concentrations of these gases in similar north–south zones and the CO_2 results correlated well with ground temperature determinations. Hg determinations were undertaken by the Scintrex Hg meter. The CO_2 determinations were carried out using Kitagawa detection tubes. In this procedure a known volume of soil gas is pumped through a detection tube filled with silica gel and a 'special reagent'. The extent of the colour change is used to determine the concentration of CO_2 in the soil gas (JICA, 1983).

In 1986 a soil gas survey by Geotermica Italiana was undertaken in the Menengai Bogoria area. Confining their attention to CO_2 they collected samples from a meter depth, into evacuated glass containers, prior to transportation to a laboratory for analysis by gas chromatography. The results were generally of a lower magnitude to those obtained by the Japanese workers or in the current study. The sample spacing was 150–300 m. Significant anomalies were detected on axes of recent volcanic cones and at caldera rim faults, (Geotermica Final Rep., 1987).

5.4.2 Methods of sample collection and field analysis used by BGS

In the field sampling of soil or overburden gases was undertaken using a hollow spike driven to a convenient depth, usually about 0.6 m. Using suitable pumps, the pathways were purged and samples of soil gas transferred into the burette of an ORSAT analysis apparatus for the determination of carbon dioxide and oxygen and a radon Emanometer for radon (Rn, Em-222) and thoron (Tn, Em-220).

The main features of the ORSAT analyser are shown on Figure 5.7. A known volume of soil gas is pumped into the burette and subsequently transferred to the absorption vessels for the selective removal of CO_2 and O_2 which are determined by changes in volume shown in the gas burette. The practical limit of determination under field conditions is about 0.1%.

The absorbent for CO_2 is 40% aqueous KOH as recommended by British Standard 1756, Part II. Vogel (1961) recommends the use of a mixture of saturated aqueous ammonium chloride and ammonia (sp. gr. 0.880) in contact with copper coils as an effective O_2 absorber since its efficiency is maintained at low temperatures. Interfering gases such as carbon monoxide, ethylene and acetylene were not found to occur in the soil atmospheres investigated.

The Rn level is determined by transference of a soil gas sample from the spike by means of a flexible hose fitted with a hand pump with a non-return valve, into the Emanometer counting chamber which consists of a conical flask, the walls of which are coated with ZnS, and with a photomultiplier attached to the clear base. The output of the photomultiplier is displayed by a ratemeter (if the count rate is high) or for lower count rates is read by a LED scaler. Because of the high count rates and the necessity to determine Tn, ratemeter readings were almost universally used in the present study.

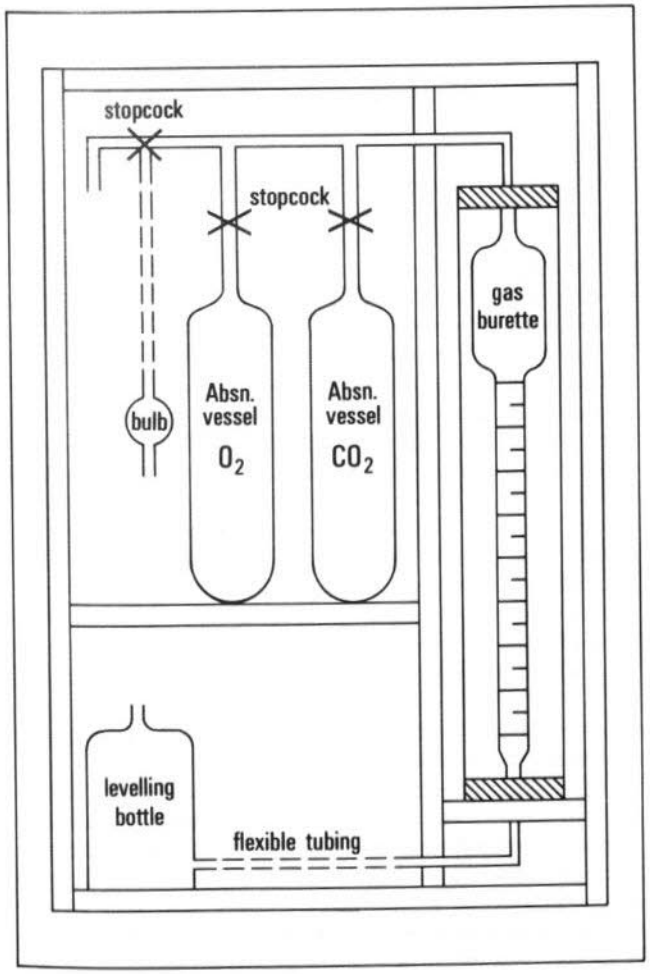

Figure 5.7 Main features of Orsat apparatus.

Because of its short half-life the mobility of Rn is not as great as might be expected from its noble gas properties. In dry soil and near ideal conditions it has been calculated that the maximum diffusion of Rn would not exceed 10 m (Tanner, 1964). Rn is however likely to be carried on other gases and general strong correlation between Rn and the major gas CO_2 indicates that in this area the carrier effect is predominant.

Figure 5.8 summarises the nature of the decay of U-238 and Th-232 respectively. U-235 is present in natural uranium but owing to its low concentration (= 0.7% of natural levels) may safely be ignored. U-238 produces a number of daughter products before decaying to the stable Pb-206 isotope. The decay chain may be divided into two sections separated by Ra-226 which has a half-life of some 1600 years. Earlier isotopes mostly have long half-lives, while the later isotopes have relatively short half-lives. Consideration of these relationships indicates that U completely separated from its daughter products takes some 1 000 000 years to achieve 91% of secular equilibrium, i.e. that the daughter products are produced at the same rate that U-238 decays. Rn has a half-life of 3.82 days. The shorter-lived daughter products produced by alpha decay (especially Po-218 with half-life of 3.05 mins) usually exist in the form of aerosols which may plate out on the walls of the counting chamber. The net result of this behaviour is that the count rate observed for a sample of soil gas containing Rn increases with time.

In contrast the time taken for secular equilibrium to be achieved in the Th decay series is very much shorter at about 70 years. The half-life of Tn is only 54.7 secs. so that by repeating counts at 1 min. intervals the presence of Tn may be identified easily. Problems may arise where both Rn and Tn occur and in this case corrections have to be applied.

The immediate daughter product of Rn is Po-218 which has a half-life of 3.05 mins. For the first few minutes after a sample of Rn has been obtained the count rate increases as the Po-218 isotope breeds into equilibrium. The percentage increase after 1 Minute and after 2 minutes would be expected to be about 20% and 35%. In the particular procedure used here the sample of soil gas was introduced into the instrument by continuous pumping and the ratemeter reading (RnO) observed until a constant reading was obtained. The count rate was then observed and recorded at minute intervals sometimes for as long as 8 minutes (RnO-8, in Table 5.1).

Tn has a half-life of only 54.7 secs. Its immediate daughter is Po-216 which has a half-life of only 0.16 secs. This means that the count-rate contribution from Tn is amplified by equivalent counts from the Po-216. The count rate after one minute declines to slightly less than 50% if the sample consists only of Tn.

Where both Rn and Tn occur the relative proportions contributing to the alpha activity can be calculated. Calibration with a pure Rn source enables corrections to be made for the contribution from Tn and Rn to the total alpha activity of the soil gas.

A total count after one minute is recorded and then sequentially at minute intervals. During each minute

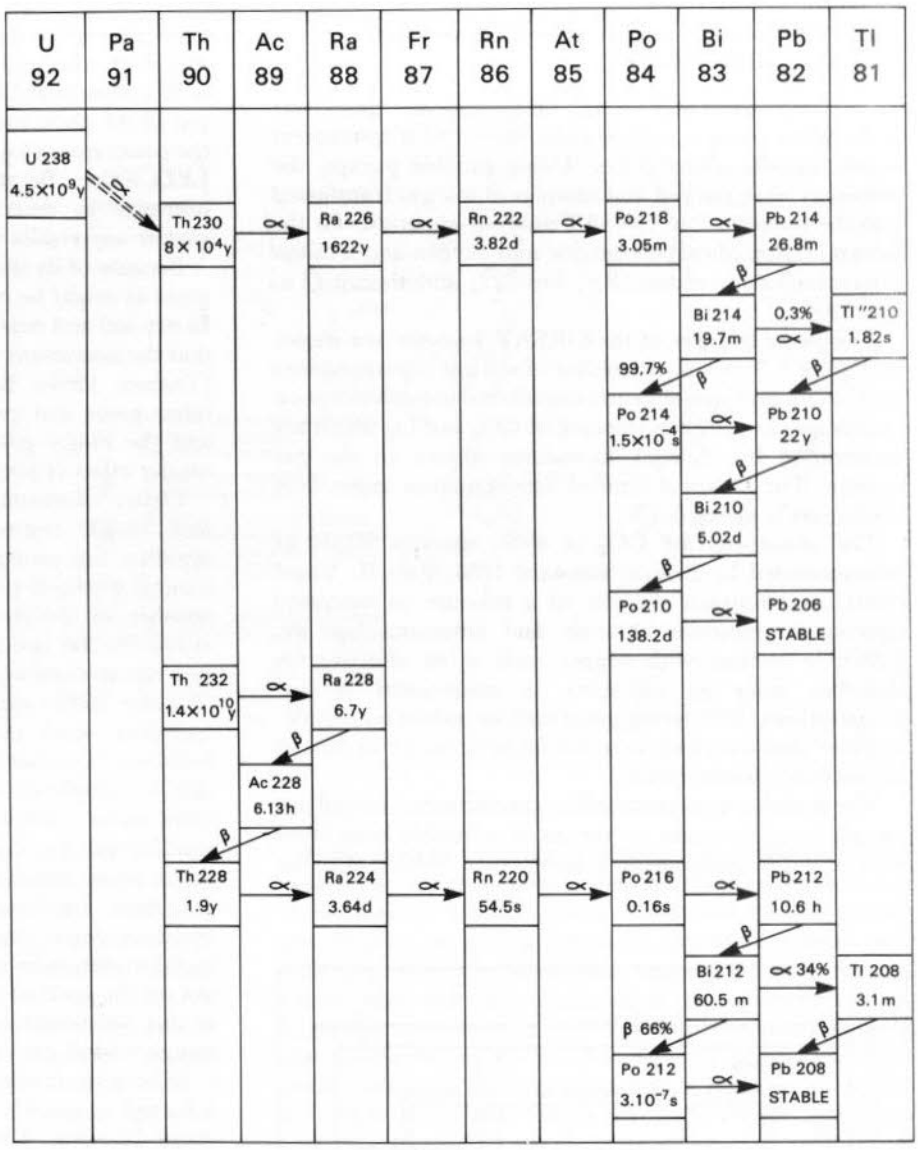

Figure 5.8 U-238 and Th-232 decay series.

therefore a quantity of Po-218 will have bred in. If the count rates at minutes one to three are given as C1, C2 and C3 then the cpm due to Rn can be calculated as $= 0.87C3 + 0.32C2 - 0.34C1$. Cpm due to Tn is thus simply the net cpm minus the above.

5.4.3 **Orientation and preliminary assessment**

5.4.3.1 Olkaria

The first area to be investigated was on one of the eastern 'Domes'. Here an intensely altered area had been identified having at least three sub-areas of fumarolic activity. The immediate fumarolic area is characterised by the presence of only sparse vegetation and conspicuous shallow erosion. The general vegetation in the area is grass and sedge, with rare thorn (*Acacia* sp.) trees. Comendite domes were originally buried by a drape of airfall volcanic ash. In places erosion has removed about 2 m of this ash exposing the altered comendite lavas. Fumaroles are most common within or adjacent to the lava exposures.

The area was investigated on two traverses at right angles crossing from ground with no visible alterations, across strongly altered ground and back to unaltered ground. These and other soil gas profiles are located on the 1:100 000-scale geothermal map as SG1 and SG2.

The first (east–west) traverse, although crossing an eroded area, was carefully sited so as not to overlie an area of steam emission. Figure 5.9. shows the Rn profile for this traverse. A zone of high values is observed in the central part of the traverse in which there are two particularly high portions at about – 100 m and at 60–90 m. The CO_2 values show a similar distribution but with values approaching background in between the two CO_2 peaks. Similar highs are observed for temperature at 30 cms depth. The O_2 values are particularly interesting as they maintain a 'normal' or close to atmospheric level throughout, allowing for a slight dilution by high concentrations of CO_2. The gas geochemical results show evidence for a widespread halo of high CO_2 and Rn values extending for at least 100 m outside the areas of visual alteration, and coincide closely in this area with zones of high thermal flux. Profiles for CO_2, O_2 and temperature are also shown on Figure 5.9.

The second (north–south) traverse intesected the first at 60 m and crosses a zone of exposed comendite lava and steaming ground between 10 m and 30 m. Otherwise normal vegetation for the area is observed. The CO_2, Rn and soil temperature readings peak over the area of the fumaroles but high values extend to nearly 100 m. Temporal analysis of the Rn readings gives a modified count rate for Rn, the pattern for which is identical to the total count. The Tn concentration is relatively low, but the

Table 5.1 Rn + CO_2 results for fumaroles

Site	Notes	Temp	CO_2	Tot	O2	RBG	R-0	R-1	R-2	R-3	R-4	R-5	R-6	R-7	R-8
Longonot crater (all sampled with spike and condensor)															
FL1.1	(F23)	91.7	45.2	67.7	22.5	10	63	65	73	70	77	80	87		
FL1.2		88.0	9.9	27.5	17.6	0.1	80	65	60		45	35	35		
FL1.3		91.7	2.1	22.2	20.1	0	1.75	1.75	1.75	1.75	1.75	1.75	1.75		
FL2.1	(Below main peak)	75.5	7.7	26.1	18.4	10	60	56	45	45	47	45	46		
FL2.2		72.8	5.3	24.1	18.8	40	5	2	2	0	0	0	0		
FL2.3			7.9	26.1	18.4	40	7	3	3	−2	9	0	0		
FL3.1	(F24)	88.3	28.4	42.2	13.8	0	100	90	95	95	95	102	100		
FL3.2		87.9	25.5	39.9	14.4	7.5	102.5	92.5	89.5	85.5	82.5	85.5	85.5		
FL3.3		88.6	24.3	39.2	14.9	13.5	97.5	76.5	71.5	68.5	69.5	76.5	76.5		
FL4.1	(F26) NW part of Mlima-	68.0	1.0		20.2		29	25	25	23	22	24			
FL4.2	Panya zone	68.0	2.0		19.8		30	29.5	30	31	31	30			
FL4.3		67.0	2.0		19.8		32	27	25	27	25	26			
Mount Margaret (F27)															
FM1	Used funnel & condensor	86.5	85.0		0	70	65	58	58	65	68	65	74		
FM2	80 ml air as dilution in	85.8	83.0		5.6	35	87	77	83	85	82	85	87		
FM3	M1 & M2, & 60 ml in M3	86.9	46.0		18.0	18	82	72	70	69	62	62	62		
Suswa outer Caldera wall — north sector															
FSC1.1	(F3)	92.2	9.0	27.8	18.8	45	315	345	385	405	415	425	445		
FSC1.2		86.0	6.0	25.4	19.4	110	215	220	230	240	250	260	250		
FSC1.3		84.2	1.4	21.8	20.4	170	10	0	−10	−20	−20	−20	−30		
FSC2.1	(F7)	91.9	2.5	22.6	20.1	0.8	175	170	170	190	195	207	210		
FSC2.2		92.1	11.0	29.2	18.2	12	498	528	563	588	628	648	678		
FSC2.3		91.5	10.1	28.6	18.5	50	470	510	560	575	600	610	640		
FSC3.1	(F11)	85.0	1.9	21.8	19.9	65	145	115	120	125	120	125	130	120	135
FSC3.2		87.8	1.9	21.5	19.6	60	150	120	125	120	130	120	120	125	
FSC3.3		85.6	1.4	21.4	20	50	104	100	98	98	100	102	100		
FSC4.1	100 m N of F11	83.6	1.4	21.6	20.2	48	48	52		54	56	62	61		
FSC4.2		83.7	1.3	21.8	20.5	35	67	65	67	70	75	75	75		
FSC5.1	200 m E of F11	90.5	8.9	27.3	18.4	7	193	183	191	193	193	192	192	192	
FSC5.2		90.0	1.8	22.0	20.2	32	41	40	43	44	45	45	44		
Suswa — Trench floor															
FST1.1	0.75 km NW of FST4	77.2	6.4	25.5	19.1	3	37	39	39	44	44	45	44		
FST1.2		78.8	5.9	25.2	19.3	12	40	36	38	42	42	44	43		
FST1.3		78.3	6.2	25.5	19.3	25	37	35	33	37	41	40	43		
FST2.1	Below lookout (F8)	91.1	8.0	25.4	17.4	35	265	265	245	245	255	255	265		
FST2.2		91.2	6.7	25.8	19.1	65	180	175	165	165	175	175	185		
FST2.3		90.5	0.5	21.2	20.7	100	−10	−8	−15	−17	−30	−30	−30		
FST3.1	(F13) Sulphur present	93.5	38.5			1	119	94	91	91	96	103	103		
FST3.2a	60 ml air dilution	94.2	24.8	37.2	12.5										
FST3.2b	no dilution	94.2	31.9	44.2	12.3	9	36	31	37	34	39	36	38		
FST4.1	(F14) on line of recent	81.1	8.5	26.5	18	5	10	7.5	7	5.5	6	6.5	5.5		
FST4.2	volcanic axis	75.5	5.7	24.4	18.7	4	9	7	6.5	5.5	7	7.5	8		
FST4.3		82.1	9.8	27.4	17.6	4	11	9	8.5	8	9.5	9.5	10.5		
Eastern Olkaria domes															
FD1.1	(F15)	93.0	10.5	28.9	18.4		530	570	610	640	640	680	710		
FD1.2		93.0	13.5	31.2	17.7		970	1070	1170	1220	1270	1320			
FD2.1	(F16)	87.1	11.9		18.3		700	700	720	750	760	760			
FD2.2		68.4	16.4		15.2		480	540	590	630	680	700			
FD3.1	(F17)	92.4	7.7	26.6	18.9	0.3	800	725	720	725	740	720	780		
FD3.2		92.4	6.8	26.2	19.4	65	785	695	685	675	695	705	735	755	
FD3.3		91.3	6.1	24.8	18.7	95	535	505	515	525	535	545	580	615	600
FD4.1	(F21)	91.3	4.0	22.7	18.7	100	450	470	490	520	550	570	580		
FD4.2		86.6	2.7	21.9	19.2	95	355	355	275	385	395	415	415	425	425
FD4.3		92.2	4.0	23.1	19.1	100	450	430	450	450	470	500	510		
Olkaria west of Hell's Gate															
FO1.1	in production field	93.3	2.2	22.5	20.3	3	267	247	212	217	212	212	227	237	232
FO1.2		94.4	2.9	21.7	18.8	20	255	270	305	315	330	330	345		
FO1.3		94.3	~50			10	410	420	450	465	485	510	525		
FO2.1	(F18) S Hell's Gate	95.0	42.0		12	0.5	2350	2400	2600	2900	3000	off scale			
FO2.2		94.8	22.5		15.3	350	750	850	850	900	950	1000	1050		
FO2.3		94.8	3.8		19.5		650	700	700	725	750	775	800	800	
FO3.1	Button flow, N end of	94.0	6.2	25.5	19.3	1.5	950	875	860	900	950	975	950	1000	
FO3.2	Olubutot fissure zone	94.0	12.4	29.2	16.8	275	1925	2125	2275	2425	2525	2675			
FO3.3			23.2	37.9	14.7	250	600	500	580	620	650	670	680	720	
FO4.1	S end Olubutot zone	93.5	34.6		13.3		930	930	880	930	1030	1060	1080		
FO4.2		93.5	30.6		15		3000 +	i.e. off scale							
Eburru settlement area															
E1.1	Near big condensor	92.2	87.0			30	1020	970	970	985	995	990	1005	1000	
E1.2		92.2	41.5	33.1	10.5	90	770	690	720	750	780	810	820		
E2.1	Kaolin mine	92.3	~50			160	1440	1020	840	760	740	750	740	750	
E2.2		92.0	~70			160	890	790	840	830	830	820	820		
E3.1	Opposite shops	92.1	3.9	23.9	20	175	200	195	200	200	200	204	205	205	
E3.2		92.5	38.5			175	625	695	775	715	745	790	805		

F11 etc refer to fumaroles previously sampled for geochemistry by UNDP (HA)

Sampled by: K Ball, B Macharia, P Mwangi, R Fordyce and M Clarke, August and September 1987

Tot—Total gas; RBG—Radon background

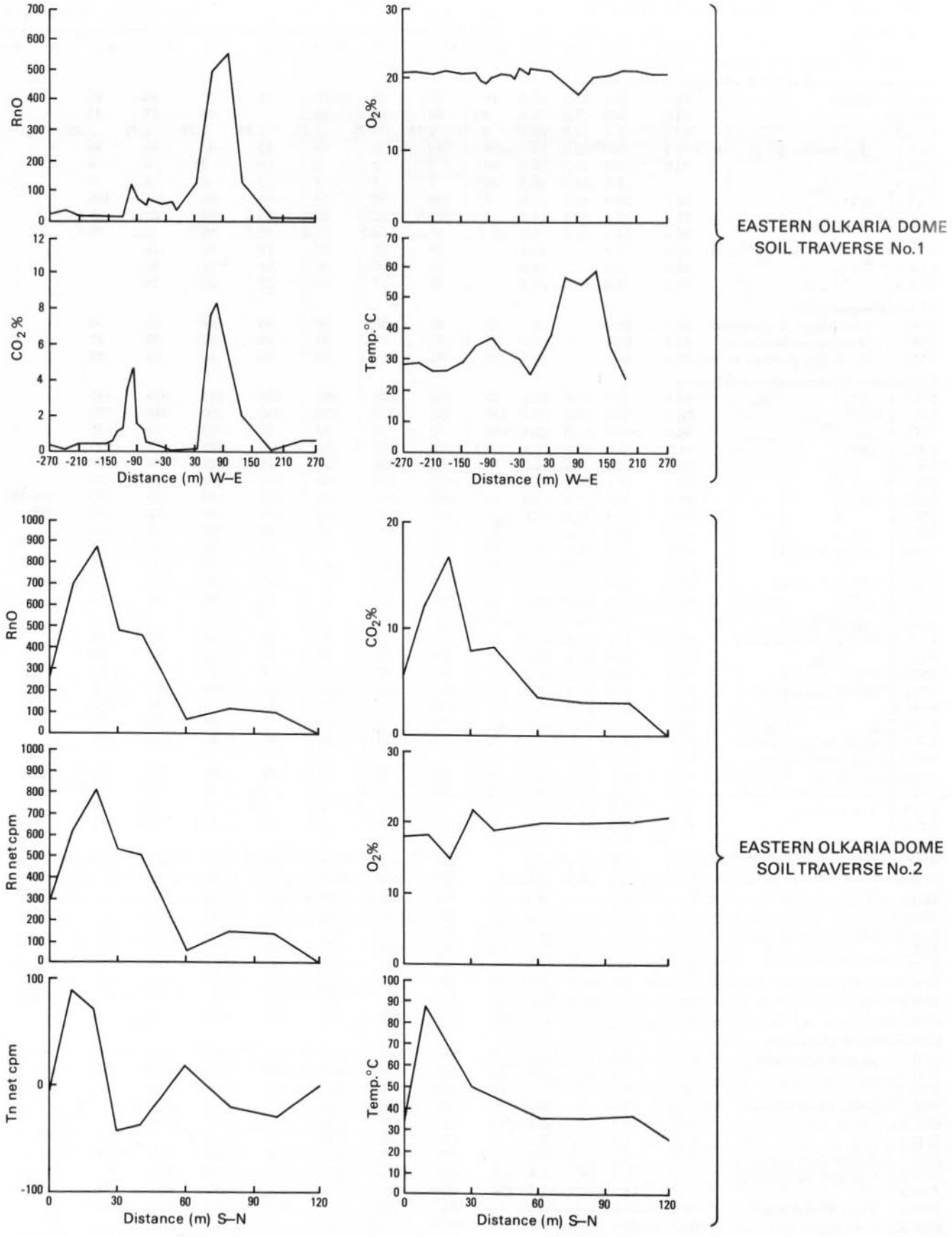

Figure 5.9 Radon, CO_2 and temperature variation across a fumarolic area in the Eastern Domes.

highest values correspond to the areas where the Rn flux is highest.

The data show clearly that there is strong correlation between CO_2, radon and elevated temperature and that this can be detected outside of areas of visible surface alteration. The general increase in alpha activity relative to the early readings shows that the main radioactive gas is radon, rather than thoron.

5.4.3.2 Longonot

This area differs from the Olkaria and Domes area by being underlain by volcanic rocks of trachytic composition. The area examined represents an exposed sector of the Longonot Caldera fracture.

Preliminary investigations of the south caldera wall had identified some fumarolic activity (c.40–50°C) in the scarp so the 3 traverses (SG 3,4 and 5) were aligned at a high angle to this in order to cross the likely position of the caldera fault.

The parallel traverses identified a high CO_2 zone at approximately the same position relative to the cliff face (Figure 5.10). In all these traverses the O_2 concentration is similar to atmospheric allowing for the dilution with high concentrations of CO_2. Half-life considerations of the alpha activity in soil gas indicates that the main alpha emitting gaseous component is Tn.

To the west of the cliff forming the south caldera wall, is an area of low relief which may be crossed by the original arcuate caldera fault. Two traverses (SG 6 and 7, Figure 5.11) separated by 30 m were investigated to determine whether there was a gas-emitting structure in the area and whether the postulated caldera fault was thermally active. Any fault is likely to be buried by 30 m or more of ash.

Again Tn is the major alpha-emitting gas. There is a subdued peak in the CO_2 profiles but neither is near the arcuate feature. It is concluded that the high CO_2 zone represents the more distant expression of the thermally active fault indicated in traverses 3–5.

The investigation of the southern caldera scarp showed that it may be possible to identify buried caldera faults by detecting gas leaking from them. More generally—the orientation survey at Olkaria and Longonot showed that emission and CO_2 vary widely over the area.

5.4.4 Exploration of specific structures

5.4.4.1 Longonot West Caldera, Soil Traverses 8 and 9

The purpose of this part of the investigation was to study the distribution of gases in soils overlying a portion of the Longonot Caldera Rim for which there had been no recorded instances of geothermal manifestations. The two

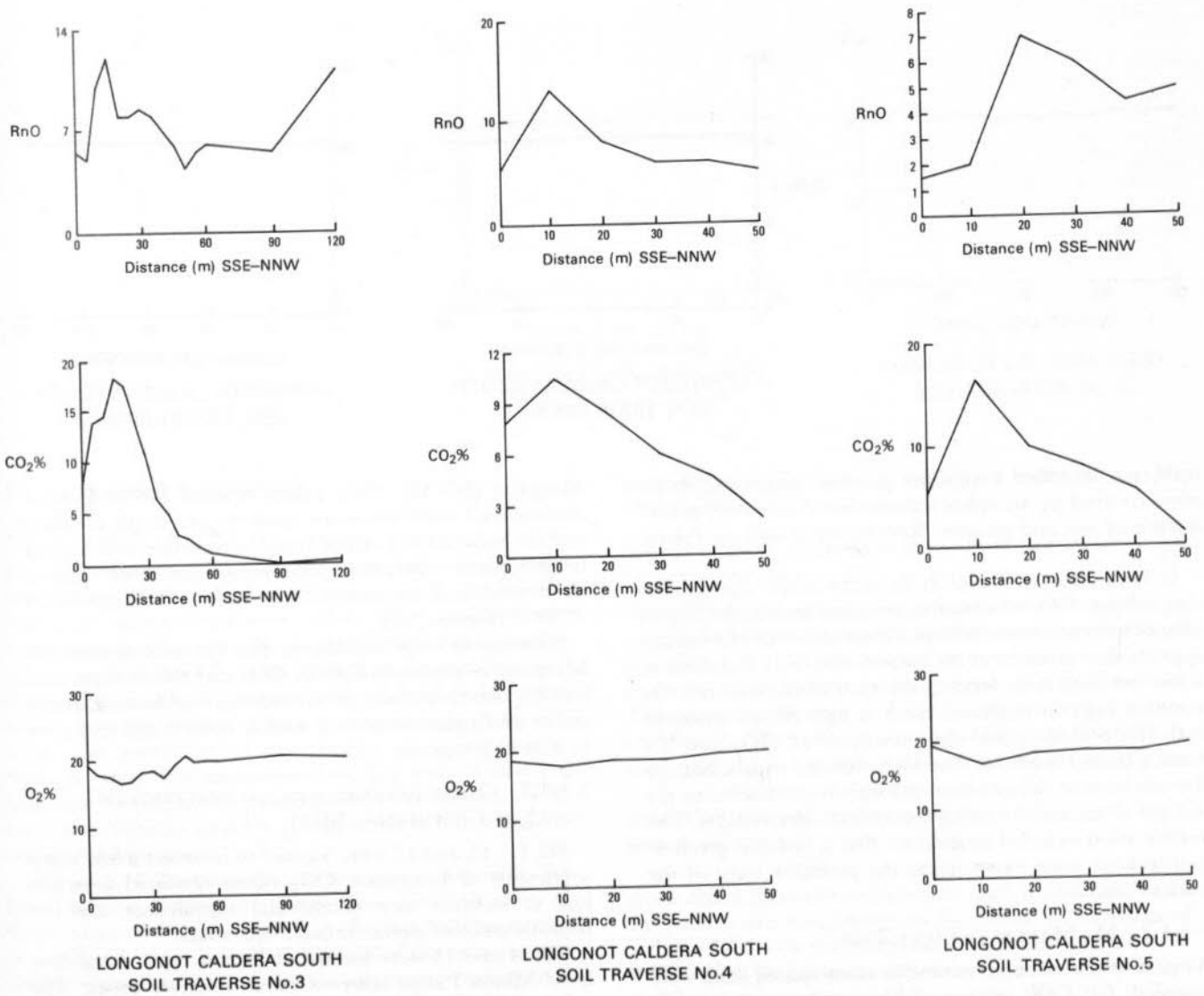

Figure 5.10 Soil gas variation across the Longonot south caldera fracture (SCF).

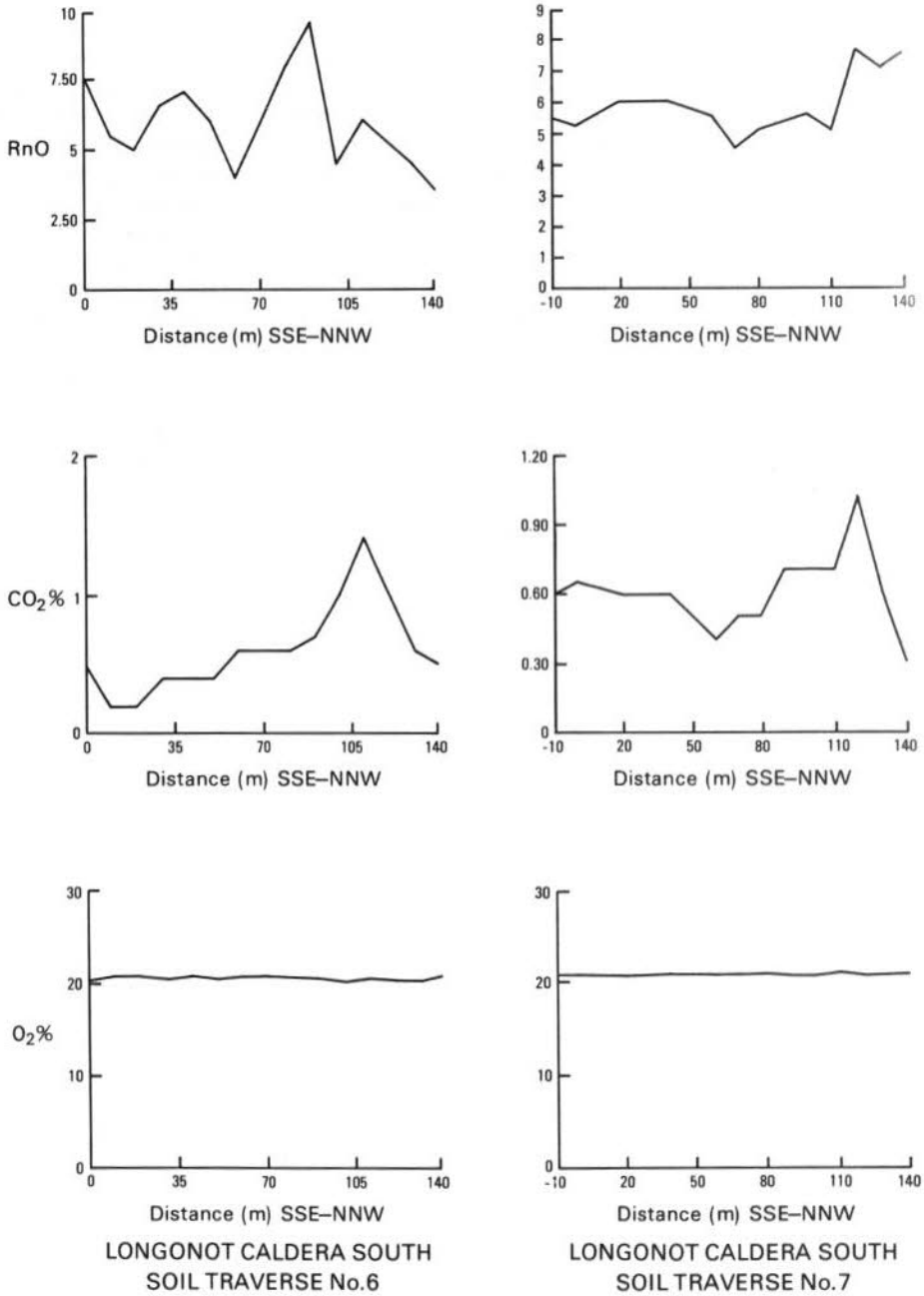

Figure 5.11 Soil gas variation across a concealed extention of the Longonot SCF.

traverses described here cross possible outgassing structures covered by an indeterminate but thick (>30 m) sequence of ash and pumice. Results are shown on Figure 5.12.

In both lines (SG8 and 9) Tn is the major alpha emitting soil gas. CO_2 is below the detection limit at the beginning of both traverses, rises to a measurable level from the approximate position of the caldera rim fault and stays at a low but detectable level to the ends of the traverse. O_2 remains high throughout. Such a pattern is consistent with the evolution and slow transport of CO_2 and Tn from a buried fracture. The CO_2 diffuses widely but the Tn has time to decay away, the only contribution to the soil gas alpha activity being from locally derived Tn. The results are concluded to indicate that a possible geothermal leakage zone exists along the probable trace of the caldera fault.

5.4.4.2 Mt Margaret Fault Zone

As part of the orientation studies close-spaced sites were sampled for CO_2 over a 0.5 km wide north–south-trending fault zone immediately south-west of Mt Margaret (SG 10). CO_2 values reached 3.8%. Further close-spaced traverses were made to the north of SG10 and the highest CO_2 values found to correlate with highest temperatures. Detailed resampling and then pitting discovered local values of $CO_2 < 35\%$ and temperatures $<50°C$ (Figure 5.13).

Subsequent work has shown that the area around Mt Margaret is generally high in CO_2 and this is supported by CO_2 determinations on the only active fumarole at this centre and alpha emission is similar in level and character to that at Longonot.

5.4.4.3 Other detailed soil gas traverses (SG 11–15 on Geothermal Map)

SG 11, 12 and 13 were located to intersect a low scarp south-west of Longonot. CO_2 values obtained were too low to indicate any geothermal significance and no measurement of alpha emission was made.

SG 14 and 15 were located as lines normal to the flow front Mlima Panya where a small fumarole exists. The only anomalous values of CO_2 were in the immediate vicinity of this fumarole.

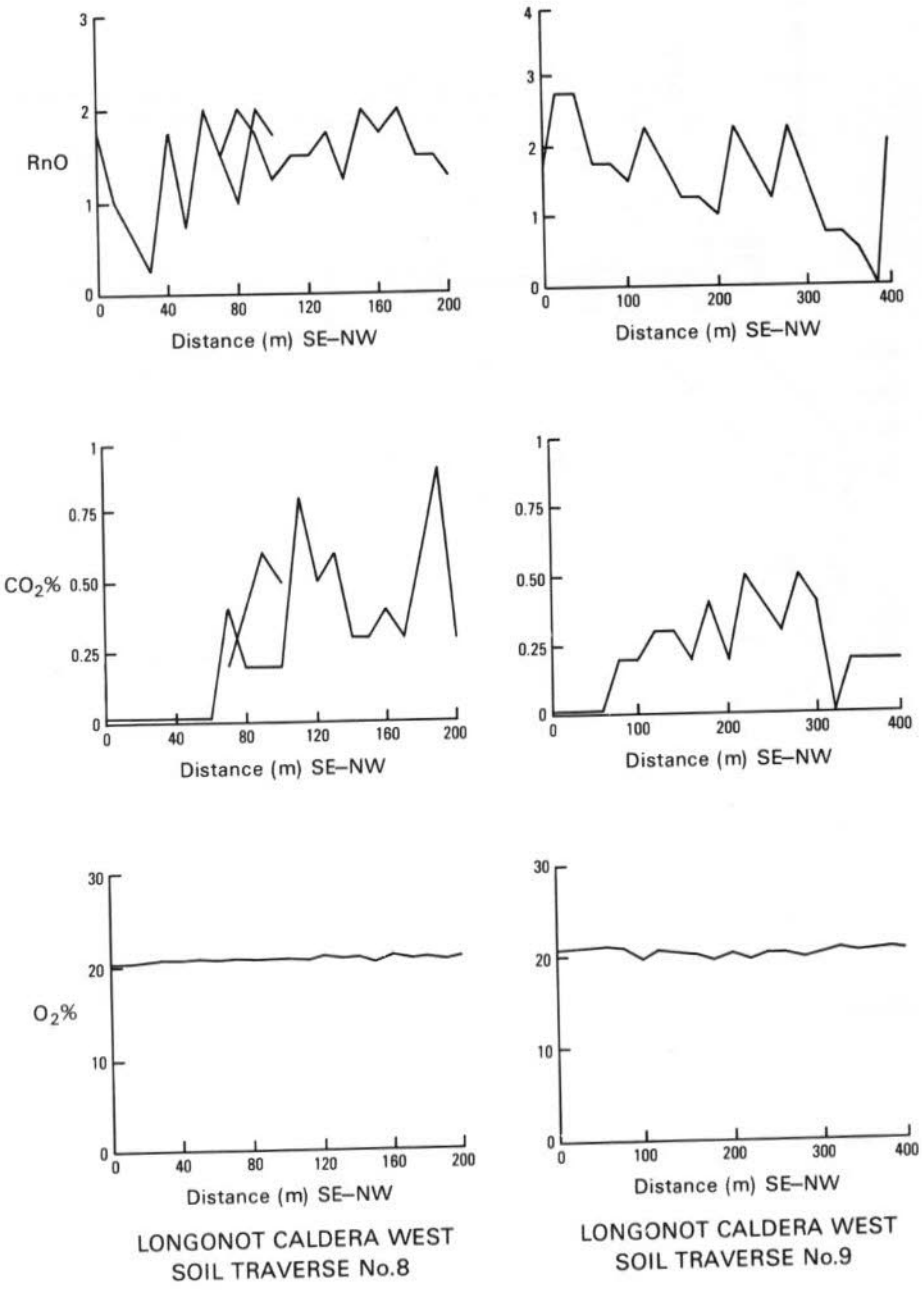

Figure 5.12 Soil gas variation across probable concealed western sector of the Longonot caldera fracture.

5.4.5 **Strategic prospecting**

5.4.5.1 Introduction

Investigations described in the previous section were undertaken to assess the possibility of hydrothermal transport along structures where the geology was reasonably well known. These can be regarded as studies of the applicability of gas geochemical methods in a tactical sense. South of Longonot there is a large low lying area where the geology is largely obscured by recent ash falls. The possibility of prospecting on a regional or strategic scale was investigated in this area. Lines had been cut for geophysical investigations. Sample sites were located at stations used for gravity surveys but with infill where appropriate.

Figure 5.14 illustrates the gas concentration profiles for line I over a distance of 16 km. Two separate zones of high values of CO_2 and Tn (Rn1 is about half the intensity of RnO) occur near the east end of the traverse and could relate firstly to a volcanic alignment (extensional axis) which has given rise to a series of fissure flows and volcanic cones extending south-east from Longonot, and secondly to active systems related to faults in the Mt Margaret area.

5.4.5.2 500 m interval soil sampling south of Olkaria and Longonot

The 500 m interval sampling programme was extended to a total of 134 line km, mainly on east–west lines surveyed previously for a gravimetric survey but with some traverses along motor tracks oblique to that direction. The extent of the lines and significant results are shown on Map 2. The limit of detection using the ORSAT is nominally 0.1% but significant results are assumed to be 0.2% or above for the purposes of the following discussion. The area surveyed may be divided into three from west to east.

Akira Ranch westwards (includes area south of Olkaria)
In general this area shows no significant occurrences of soil gas CO_2 with the exception of two adjacent values of 0.5% which lie 2.0 km south of the most southerly steam and hot water occurrences located by the GSD during shallow drilling carried out 20 years ago (Mason, 1967).

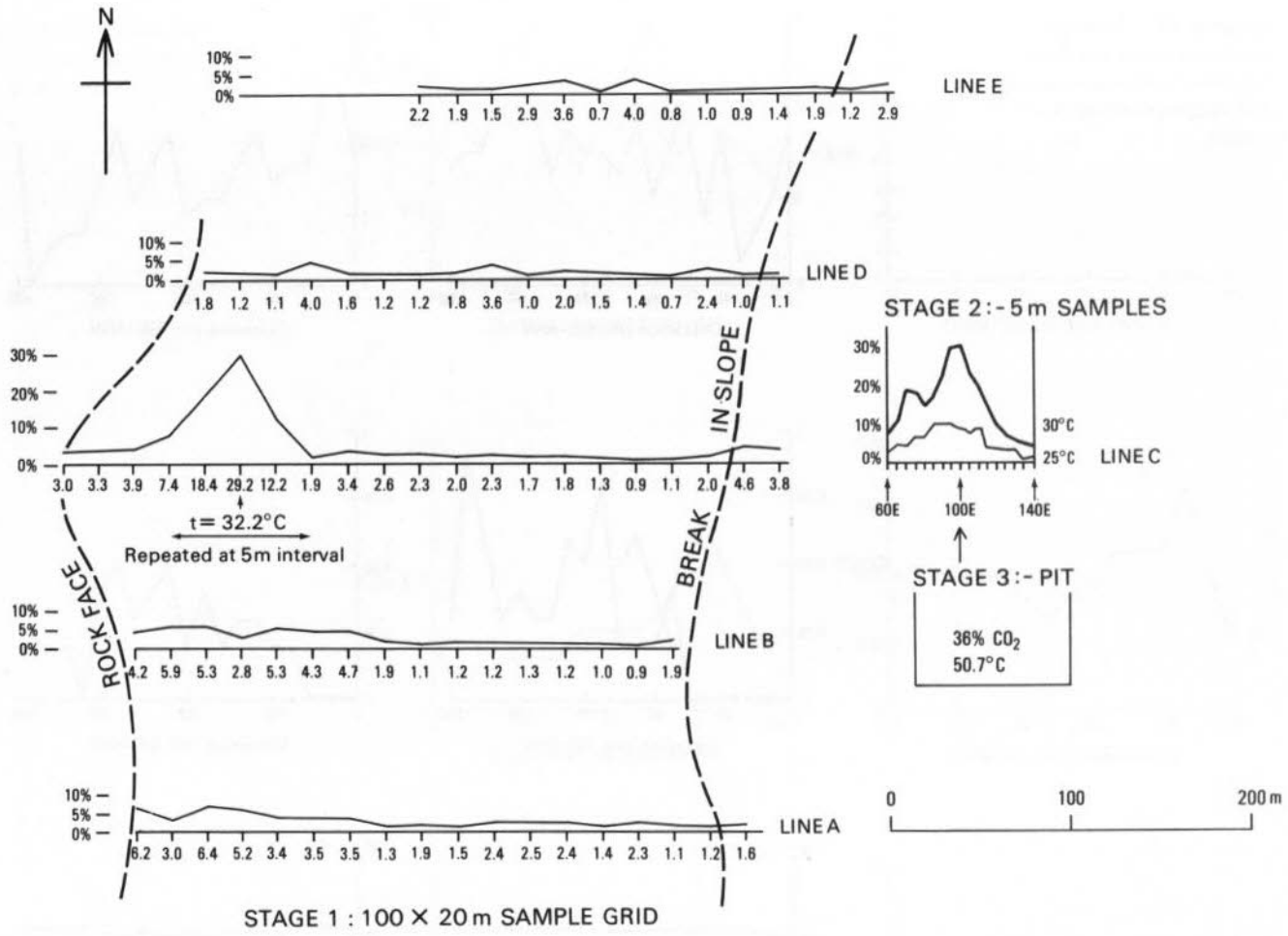

Figure 5.13 Soil gas variation near Mt Margaret

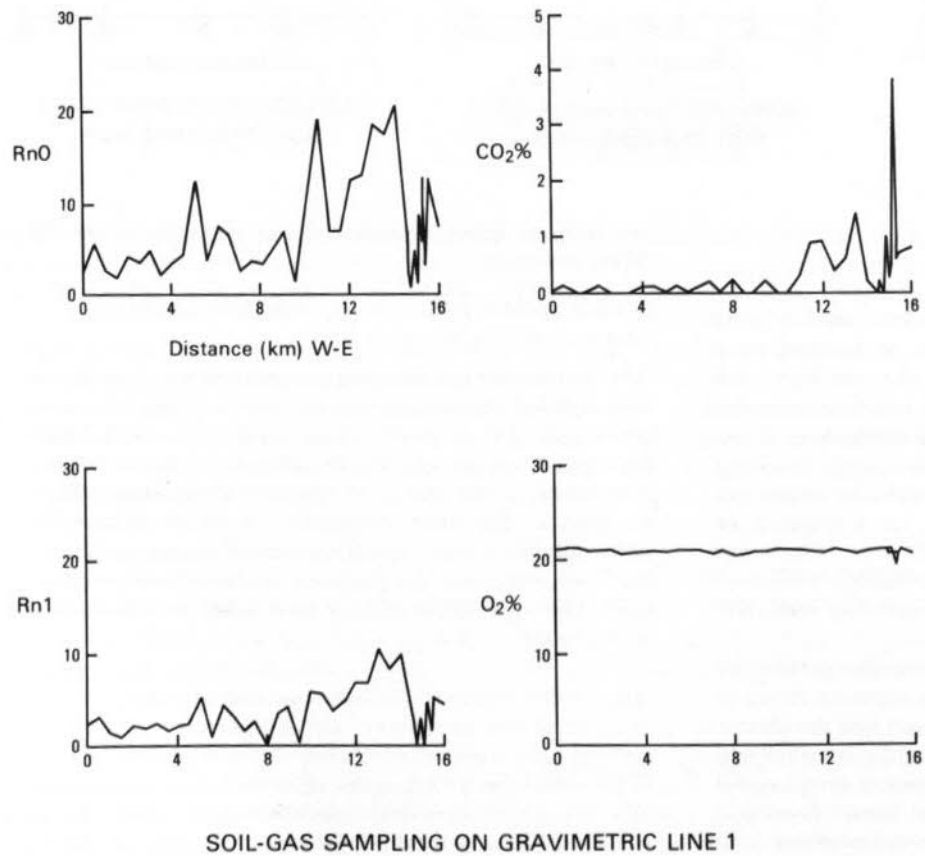

Figure 5.14 Soil gas variation at 500 m intervals on an east-west line south of Longonot.

East of Akira Ranch to the satellite station
The results show only a scatter of significant values and provide no evidence of distinct anomalous zones. This data, together with the lack of any visible faulting, provides no evidence for near surface structural links between Suswa and Longonot (however see section 5.2.1.).

East of the satellite station and around Mt Margaret
This sub-area differs markedly from the above two, in that CO_2 values are widely distributed. There are two probable controls. One is the south-south-east-trending Mlima Panya volcanic axis which is the surface expression of a fissure zone extending from the Longonot crater area. Trachytic flows and tephra have been erupted from this zone and it is still weakly geothermally active at the surface.

An important control on the occurrence of detectable CO_2 in soil gas in these areas may well be the presence or absence of thick post-caldera, Longonot-derived, airfall pyroclastics. Road cuts and shallow stream incisions often expose Longonot ignimbrite at shallow depths around Mt Margaret and between it and the Mlima Panya flow. The greater incompetence of this lithology allows more distinct fractures to develop which could well be more efficient pathways for gas emissions to reach the surface than the more competent post-caldera airfall units, within which CO_2 could be being dispersed (and diluted), before reaching the surface and soils sampled.

It may be, therefore, that the relative high soil gas CO_2 detected in the Mt Margaret area gives a false impression of the general distribution of CO_2. The latter's presence in soils could be inversely correlated with increasing thickness of blanketing post-caldera tephra, consequent on the dominantly west and south-west dispersion of the Longonot airfall plume.

Nevertheless, the coincidence of fumarolic activity, young volcanic activity, recent faulting and relatively high CO_2 occurrence suggests that the Mt Margaret area cannot be written off as a locus of possible geothermal potential. When the resistivity data for this area is examined, these geological and geochemical data should be critically reassessed.

5.4.6 Comparative alpha emission/CO_2 ratios in soil gas from Longonot and the Eastern Olkaria Domes

During the orientation study it was noted that in general the emission from Olkaria related sample sites was 1–2 orders of magnitude higher than from sites at Longonot (and Mt Margaret). This aspect has been explored further and compared with accompanying CO_2 values by means of the loglog plot, Figure 5.15.

The data used is from SG 1 and 2 (Eastern Olkaria Dome traverses) and SG 3–9 (Longonot Caldera traverses). Two mutually exclusive trends are visible confirming the much higher levels of emission in the Olkaria area. At 10% CO_2 the Olkaria area values are approximately one hundred times those at Longonot.

The low Rn component of the trachyte-derived soils and geothermal areas at Longonot enclosed in trachytes is consistent with the recent ages of the rocks. Uranium has not had time to breed in the daughter products to produce the Rn concentration that might have been expected from the moderately high U concentrations. Because of the short half-life of Tn it is likely that this component is locally derived and introduced into the hydrothermal conduits near to the surface. That CO_2 probably serves as a carrier for this gas is confirmed by the good correlation between CO_2 and Tn in the soils overlying the trachyte rocks.

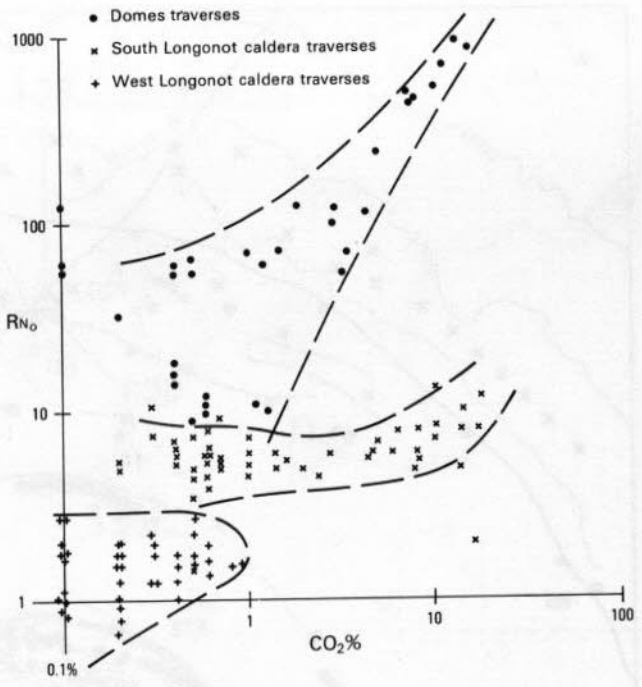

Figure 5.15 Comparison of Rn and CO_2 variation in Olkaria and Longonot soils.

This however leaves the problems of the high Rn concentration in the Olkaria area. The geological data available suggests that the rocks are of approximately the same age as those of the Longonot centre. Although the U content is slightly higher than for the the Longonot rocks, (Figure 4.8), there is no indication that the values are so high that the Rn concentration could be up to 2 orders of magnitude higher. Further work involving disequilibrium studies of whole rocks is needed but the following possibilities should be considered:

1 The Olkaria rocks are on aggregate, much older than is suggested by the radiocarbon age determinations and the relationships of the more recent pyroclastic members with the Longonot ashes.
2 There is uranium mineralisation in the area.
3 The hydrothermal circulation system accesses basement rocks which are much older than the volcanic rocks of the Olkaria complex.

Because of the short half-life of Rn it would have to travel long distances in a relatively short time. An alternative is that the immediate precursor to Rn, Ra-226 is leached from the host rock and carried to the hot area, where on conversion of the water to steam the Rn passes directly into the gas phase. With the high CO_2 content of the gas phase it is likely that radium carbonate would be most stable of the complexes in solution in the hot but not boiling water. Uranium bicarbonate and tricarbonate complexes are relatively unstable at high temperatures. It must therefore be predicted that either the hydrothermal conduits must be open, with rapid transit of the components or that radium complexes are dissolved in the ground water prior to conversion to steam when the temperature rises or pressure is decreased.

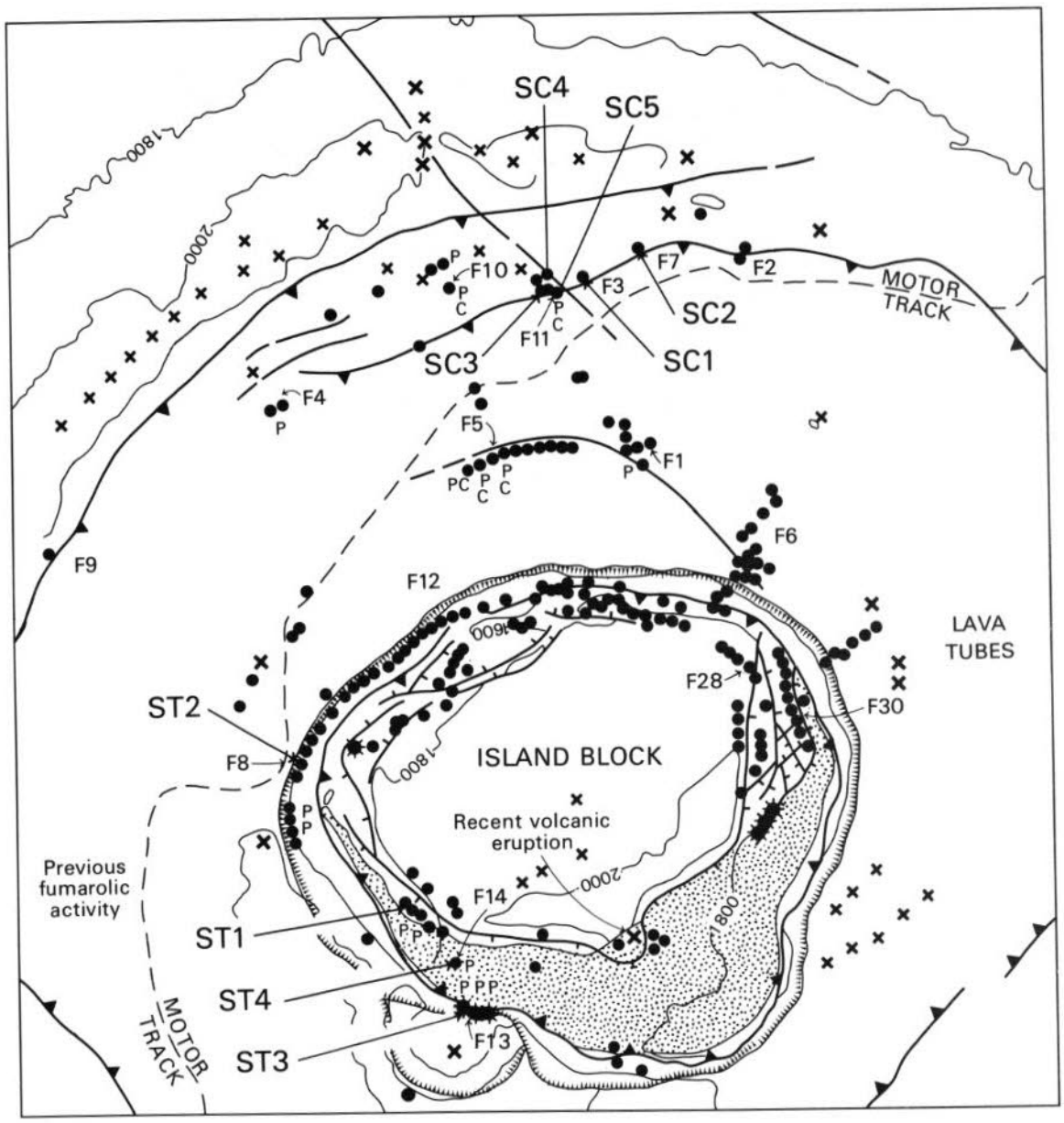

● Fumaroles (with UNDP sample no.)

✸ Fumaroles with sulphur

P Fumaroles under pressure

C Fumaroles used for condensing by Masaii

Caldera fracture

Outer limit of annular trench

× × Eruption centres

SC 1 / ST 1 Fumaroles sampled by BGS for radon and CO_2

Figure 5.16 Fumaroles sampled for Rn and CO_2 at Suswa.

5.4.7 Investigation of Rn/CO_2 ratios in fumaroles

5.4.7.1 Introduction and Location of samples

During the orientation study (section 5.4.3) it was noted that alpha emission in soils at Olkaria was much greater than in the Longonot area and that this distinction appeared to apply also to fumaroles.

It was therefore decided to investigate a larger selection of fumaroles, from Longonot Crater, additional Domes examples, Olkaria, Mt Margaret, Suswa and Eburru.

The sampling procedure was to collect fumarole products either by using a metal spike driven into moist and steaming ground or by means of a plastic funnel buried in the steaming, usually clay-rich, ground. At each fumarole area 2 or 3 sites were sampled, separated by a few metres. In each case the temperature was recorded and the gas (and steam) passed through a water-cooled condenser and condensate trap and then led to an emanometer for measurement of alpha emission (in cps), or an ORSAT apparatus, to measure CO_2 and O_2. In several cases the

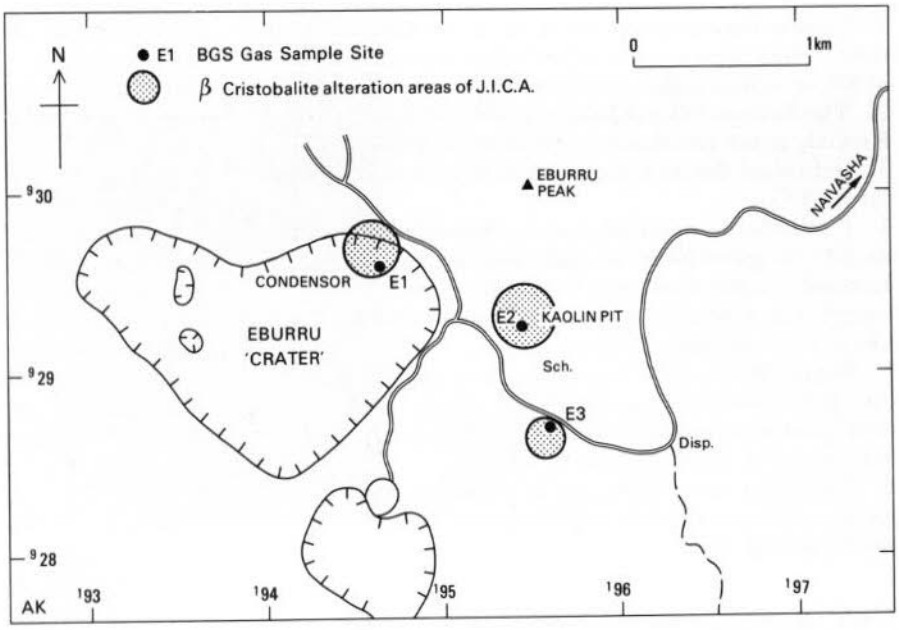

Figure 5.17 Fumaroles sampled for Rn and CO_2 at Eburru.

CO_2 content was so high that dilution of the sample with air was necessary. In other cases considerable atmospheric dilution was noticed; this variation means that comparisons using absolute values of Rn and CO_2 are less meaningful than their ratio.

Fumaroles sampled in the Olkaria, Domes, Longonot and Mt Margaret areas are located on Map 2, and are labelled GO, GD, GL and GM respectively. Those sampled at Suswa are shown on Figure 5.16 and labelled GSC (Suswa Caldera) and GST (Suswa Trench); locations at Eburru are shown on Figure 5.17.

5.4.7.2 Summary of results

The results, which essentially refer to the non-condensable fraction of the fumarole product, are given in Table 5.1. This includes sequential levels of alpha emission at 1 minute intervals, after subtracting background readings, in order to determine the approximate proportions of Rn and Tn by the method noted in section 5.4.2.

The actual values used in subsequent plots are those in the RO column, i.e. the cps recorded initially (time zero).

It is recognised that gases other than CO_2 (e.g. H_2S) may be present in the non-condensable fraction collected but these are in very low amounts compared with CO_2, according to the data listed in Table 2 of Armannsson (1987), often for the same fumaroles.

Additionally O_2 is always present and has in most cases been determined by the ORSAT. This usually represents approximately 20% of the gas present other than that absorbed by the KOH and therefore this gas is presumed to be atmospheric and not derived from the geothermal system.

It therefore follows that the absolute values of CO_2 (and Rn) determined are not significant; correction for atmospheric dilution has to be considered. This has been allowed for, assuming the CO_2 present represents the geothermal gas, by considering the ratios of Rn to CO_2 rather than their absolute amounts as determined in the field.

Figure 5.18 displays the RO and CO_2 data as a bivariant plot; in addition to the data from fumaroles, it includes higher values from the soil traverses previously made in the vicinity of SG1 and SG2 (Eastern Olkaria Domes).

The following deductions can be made by examination of Figure 5.18:

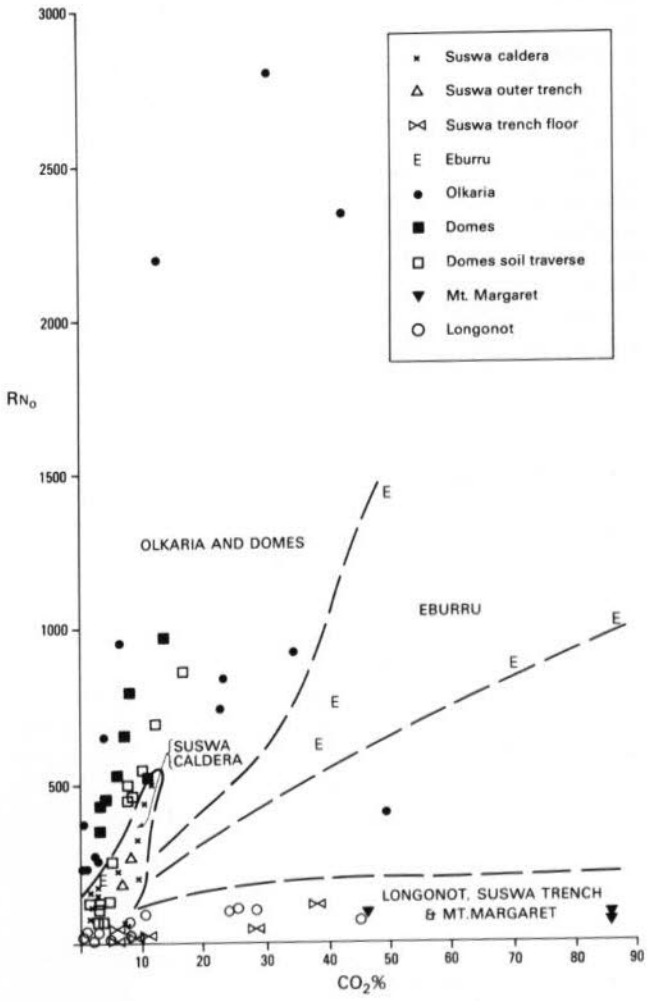

Figure 5.18 Rn/CO_2 variation between different volcanic groups.

1 Olkaria fumaroles are far richer in Rn than those from Longonot, i.e. have much higher absolute values of Rn as well as higher Rn/CO_2 ratios.
2 The Eastern Olkaria Domes have very similar Rn/CO_2 ratios and absolute values as the Olkaria data.
3 Individual domes have a very high correlation index for Rn/CO_2.
4 Fumaroles from the floor of the Suswa Trench, plus the Mt Margaret fumarole, have similar characters to Longonot Crater fumaroles in that Rn values are extremely low relative to CO_2 when compared with Olkaria and the Eastern Domes.
5 Fumaroles from the Suswa Caldera, and one from the upper outer trench wall (GST2), plot in a restricted field quite separate to those from the trench floor and have a similar Rn/CO_2 ratio to Olkaria.
6 The data from Eburru plot in a position intermediate between Olkaria and Longonot but have relatively high Rn.

5.4.8 Rn/CO_2 variation in different fumaroles compared with UNDP geochemical studies

As part of the UNDP input to the investigation of the Suswa and Longonot areas, a study of the geochemistry of the condensable and non-condensable fractions of fumarole products was made (Armannsson, 1987).

One of the main conclusions reached was that two separate reservoirs exist at Suswa, one under the trench, the other in the area of the caldera fracture—northern sector. It has already been demonstrated that a clear-cut distinction between these two areas is evident from the Rn/CO_2 data also. Armannsson's deep water 1 is associated with the higher alpha emission fumaroles of the Trench.

The UNDP model (*op. cit.*) for Longonot is more complex as two different waters are predicted to explain the geochemistry, but in general the characters of Longonot fumaroles are similar to those of Suswa Trench in that SO_4/Cl ratios and CO_2 content of steam are both high compared with fumaroles from the Domes area, and Suswa Caldera. Again, therefore, there is a close parallel with the distinctions evident from the Rn/CO_2 data groups.

5.4.9 Discussion

The following section attempts to explore possible controls on the presence and relative amounts of alpha emission (mainly Rn) at the various centres.

A large number of analyses are available of lavas and pyroclastics from Olkaria, Longonot and Suswa (Torfason, 1987, Clarke, 1987) and show that U and Th contents of volcanics from Olkaria (including Domes) are 2–4 times higher than in similar rocks from Longonot and Suswa. However, this factor does not equate with the 10–100 times greater alpha emission recorded in fumaroles of Olkaria and the Domes compared with Longonot Crater and Suswa Trench. Factors other than the average U and Th rock content must be controlling the variation in alpha emission.

It was suggested in section 5.4 that one possible reason for the great difference in alpha emission between Olkaria and Longonot could be due to differing ages: the older the age the greater the radon bred in. As the rocks exposed at the surface are of similar age in both complexes this consideration demands that alpha emission at Olkaria is associated with rocks of greater age at depth, and that the fractures (ring and linear) which constrain the fumarole distribution and young volcanics, are accessing these older rocks. If this is so it follows that the hydrothermal system at Olkaria may also be of greater age and maturity, than at Longonot.

Support for age as a control may be present at Suswa where fumaroles associated with an older fracture system, the Caldera, emit much higher levels of Rn than do fumaroles associated with younger fractures in the trench. This aspect receives no support from the Mt Margaret data, however, where very low levels of Rn are associated with this (relative to Longonot) older centre.

A paper on radon measurements at 3 New Zealand geothermal areas contains a useful discussion (Whitehead, 1980). Radon was found to be almost entirely in the gas phase, not in the condensate. Negative correlation between ^{14}C and Rn ($+CO_2$) at Wairakei and Broadlands is believed to indicate that the CO_2 and Rn originate from depth rather than from shallow ground water. This conclusion was also reached by D'Amore et al. (1975), who found strong negative correlation between radiogenic argon (from ground water) and Rn, in the Lardarello field.

At Wairakei there is a strong positive correlation between Rn and CO_2, less so at Broadlands. Amongst the conclusions reached by Whitehead are that that no unusual deposits of U and Th are necessarily present, that there is no need to postulate a magmatic origin but that the origin is deep and Rn is likely to be an indicator of permeability in the intermediate levels of a geothermal field.

A study of Rn from Lardarello wells (D'Amore et al., 1976) includes the following conclusions: Almost all the Rn values are from wells which are generally shallow and near recharge areas; Rn probably originated from the upper part of the basement; emanation of Rn is least from liquid saturated rocks. In water-dominated areas, however, they state that low gas/steam ratios are associated with high Rn, while in vapour-dominated areas high gas/steam ratios are associated with lower Rn contents.

Applying these conclusions to the present study at Olkaria and Longonot allows a tentative equation of the low Rn-high gas/steam ratio fumaroles of Longonot with a vapour-dominated geothermal regime, possibly close to an upflow zone. The high Rn-lower gas/steam ratio character of Olkaria (Domes) fumaroles may indicate a water-dominated system possibly close to a recharge area.

At Suswa the above distinction could be applied to the trench, versus caldera, fumarole groups, with the latter being equivalent to the shallow, water dominated class of D'Amore et al. In this context it is interesting, and possibly significant, that the current UNDP work concludes that the caldera fumaroles are associated with a separate shallower aquifer than those in the trench (Armannsson, 1987).

A further possible correlation is evident from comparison of the new UNDP data with that of the present study. Chloride concentrations reported by UNDP are higher in fumaroles with high Rn while the Longonot Crater and Suswa Trench fumaroles have lowest Cl and lowest Rn.

5.4.10 Conclusions

Orientation studies across zones of alteration and adjoining soils carried out in the Eastern Olkaria Domes gave high values and strong positive correlation for CO_2 and

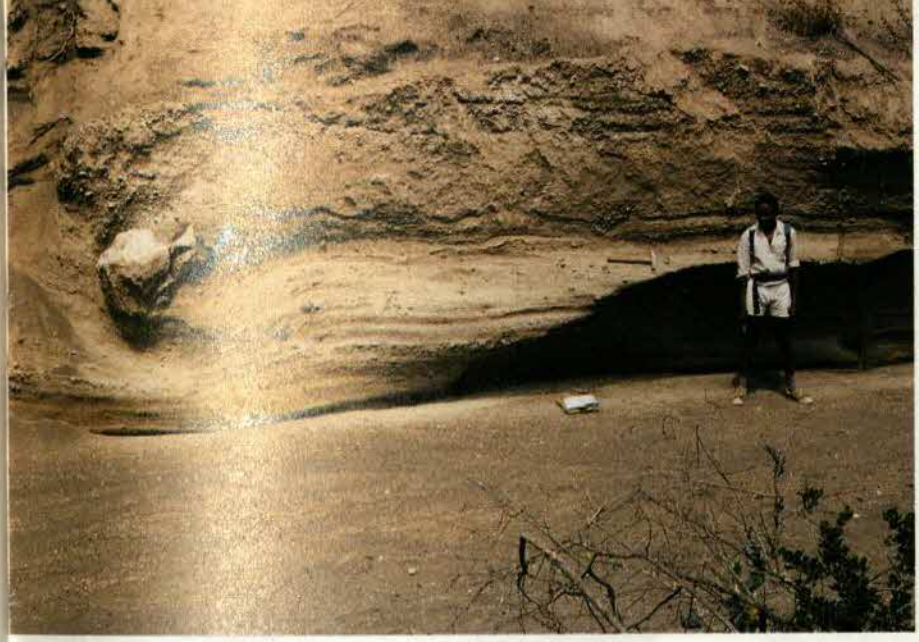

Plate 19 Ballistically emplaced comendite lava block within the surge deposit, shown in Plate 18.

Plate 20 Olkaria Volcanic Complex. Aerodynamically shaped obsidian-rimmed bomb with breadcrust-textured rind and highly vesiculated pumiceous core. The numerous bombs of this age are equated with the Olubutot Comendite Member, the youngest event recognised at Olkaria.

Plate 21 Njorowa Gorge. View of southern approaches and out across plains with basic and mixed lava scoria cone and other minor centres.

Plate 22 Closer view of basic scoria cone showing typical magmatic-style profile.

Plate 23 Mixed lava from the southern Olkaria area. Segregations of basic material being broken and dispersed by flowage within the matrix of a Middle Comendite plug.

Plate 24 Ndabibi area. Crater lake, the flooded floor of a crater within a low-angle cone of phreato-magmatic origin associated with basic magmatism.

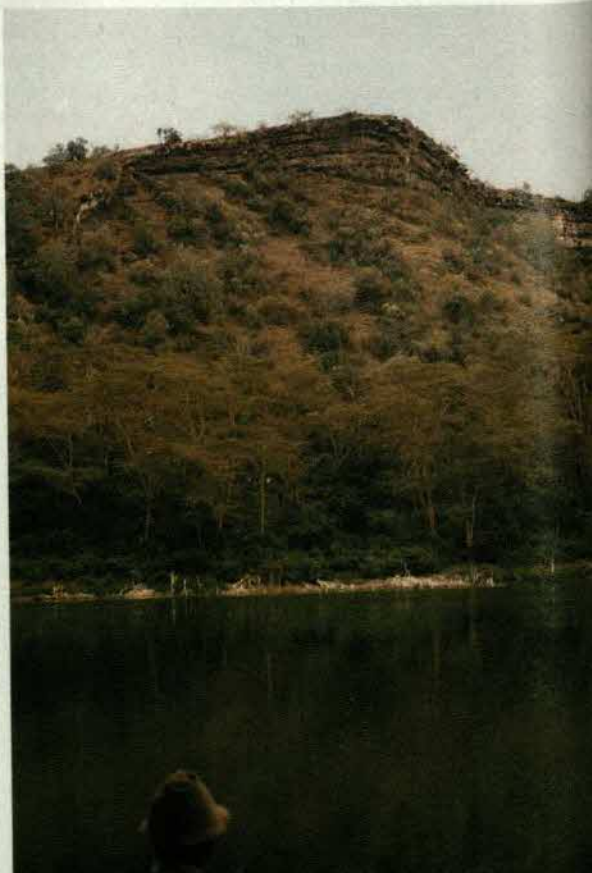

Plate 25 Lake Beds. Pumice conglomerate and overlying impure diatomaceous sediments are both products of reworking of the siliceous volcanics of the Olkaria area during times of high lake level.

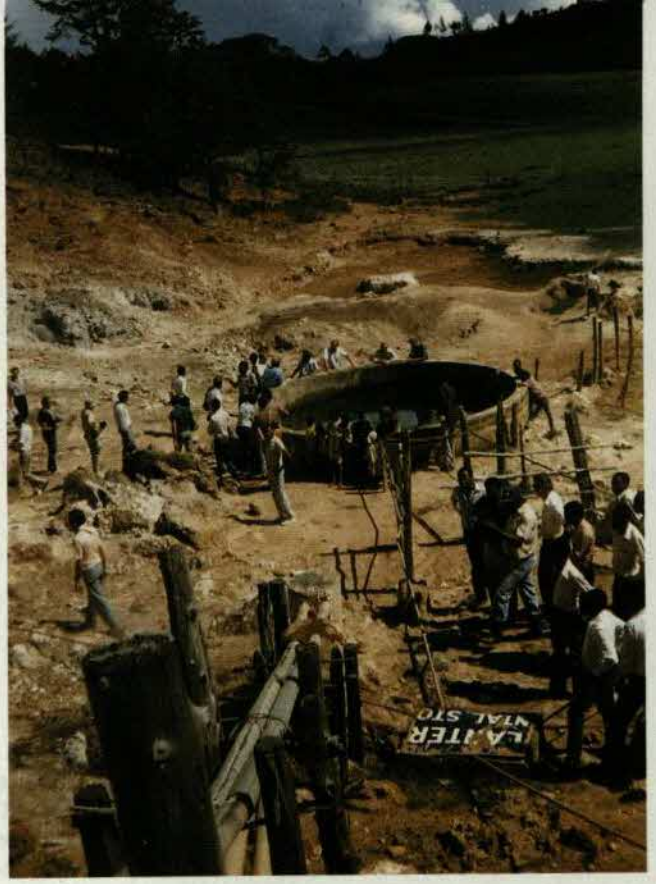

Plate 26 Eburru Volcanic Complex. Primitive steam condensors, the water from which is used for domestic and agricultural purposes.

Plate 27 Eburru Volcanic Complex. Semi-welded pumice clasts from a young pantelleritic cone from Eastern Eburru.

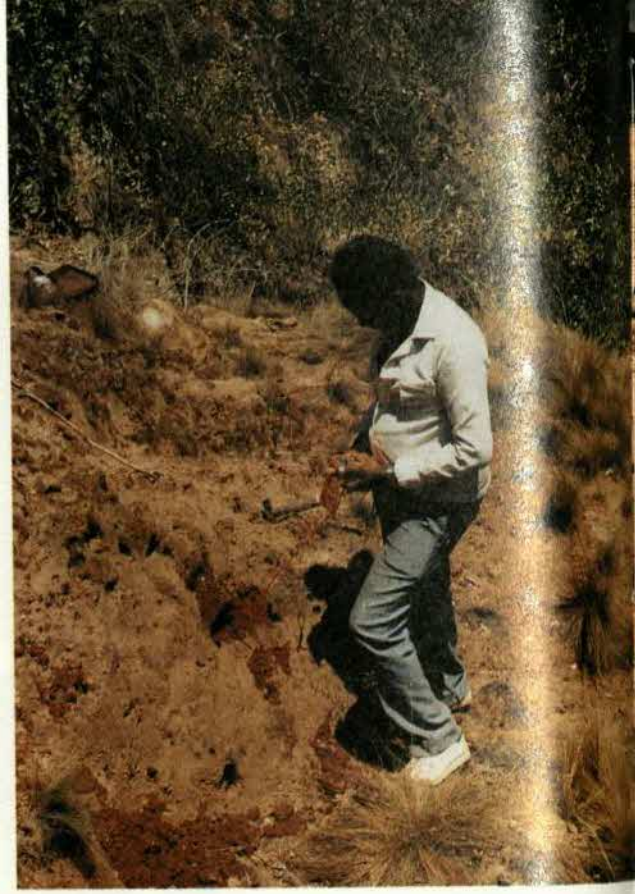

Plate 28 Checking for thermal anomalies. Temperature probes are routinely used for locating areas of weak or concealed geothermal activity. This method has revealed many previously unknown occurrences of hot ground.

Plate 29 Soilgas traversing. CO_2 (by Orsat apparatus) and radon (by Emanometer), are measured in the field as an aid to understanding the distribution of geothermal activity.

Plate 30 Measurement of the relative concentration of CO_2 in fumaroles. The fumarole gases are collected via à funnel and passed through a plastic tube to a condensor to remove most of the steam before being fed into the Orsat apparatus. A temperature probe is seen in use also.

Plate 31 Lake Magadi. Trona crust covers a considerable part of the lake surface and sometimes developes pressure ridges as seen in ice flows.

Plate 32 Lake Magadi. In parts the lake typifies many other Rift Valley saline lakes in that very shallow water with a mud bottom is present which harbours the algae so beloved by flamingoes.

Rn, (together with temperature). Similar traverses across the south Longonot Caldera Fracture were also high in CO_2 (<18%) but with alpha emission (predominantly Tn) being 1 or 2 orders of magnitude lower.

Widely distributed but low values of CO_2 (<0.8%) were found in the West Longonot Caldera where fractures are draped by thick post-caldera pyroclastics.

CO_2 soil-gas reconnaisance has been carried out over low ground between Longonot, Suswa and Olkaria where 134 linekms. were sampled at 500m intervals. The highest CO_2 found (>4%) was in the north–south faulted Mt Margaret area which also coincides with the south-east extention of the Longonot TVA. There is little other soil gas evidence of active geothermal zones, in the low ground between the 3 centres, from this wide interval CO_2 data.

The soilgas technique was adapted to make a comparative study of the alpha emission of fumaroles from different centres. Two distinct data sets were found:

1 High Rn/CO_2 and high absolute Rn: OLKARIA, DOMES, SUSWA CALDERA

2 Low Rn/CO_2 and low absolute Rn: LONGONOT, MT MARGARET, SUSWA TRENCH FLOOR.

Samples from Eburru gave high absolute values of Rn and Rn/CO_2 ratios intermediate between Longonot and Olkaria.

At Suswa the 2 major groupings show good agreement with the 2 different waters predicted by the UNDP geochemist—the higher Rn Caldera area fumaroles equating with his deep water 1 area while the low Rn Trench floor group equate with the area of his deep water 2.

The main thrust of the investigation was to study the possibility of using field analytical procedures, which had been developed for other purposes, for prospecting for, and evaluation of, geothermal energy sources. In particular the techniques have potential in recognition of weak geothermal manifestations, to examine possible extensions of known geothermal fields and to locate buried geothermal manifestations caused by permeable structures e.g. faults. The recognition of buried or diffuse geothermal activity thereby enables the geometry of potential fields to be delineated accurately at an early stage in exploration.

A preliminary assessment (see discussion above) of the wider implications of the very striking differences and groupings of the Rn/CO_2 data has begun but the full significance of these trends is not yet understood. It is hoped that presentation of this report will stimulate comment from those with more experience of the controls on Rn emission in geothermal areas.

6 Physical and chemical hydrogeological studies

6.1 INTRODUCTION

The purpose of this work was to investigate the hydrogeology of a section of the Rift Valley with particular reference to its geothermal potential. The study examined in detail an area between Lake Nakuru in the north and Lake Magadi in the south, with emphasis on the Naivasha catchment. In addition chemical sampling was undertaken as far north as Lorusio and as far west as Homa Bay, and rainfall samples were collected over an even larger area.

The cold water systems can be studied by standard hydrogeological techniques which involve the construction of piezometric maps from water level data, mainly derived from boreholes, and the assessment of the hydraulic properties of the aquifer, normally obtained from pumping tests. In the Rift Valley these techniques are restricted by the lack and poor quality of such data, but by making certain assumptions valuable insight can be obtained into directions and likely amounts of flow. In addition to the physical data, chemical and isotopic data are important in helping to identify possible recharge areas, mixing patterns and residence times of groundwaters, which in turn are used to correct and improve the physical model.

Geothermal systems are unlikely to be penetrated by boreholes, unless geothermal exploration boreholes have been drilled, and the geochemical investigation of the thermal fluids therefore assumes a greater importance. Indeed in the reconnaissance stage of exploration, before surface geophysical techniques are employed, geochemistry is by far the most valuable tool in determining the hydrodynamic nature of a geothermal system, providing information such as the nature of the geothermal fluid, temperatures at depth, mixing processes and likely areas of upflow.

By combining the model of the cold water systems, derived mainly from physical data, with that of the geothermal systems, deduced essentially from chemical data, the relationship between the two can be studied. This enables questions about the origin of the geothermal fluids, areas of recharge to, and discharge from, the geothermal fields, and availability of recharge to the exploited fields, to be addressed.

The results are presented and discussed under 5 main headings:

SURFACE HYDROLOGY,
PHYSICAL HYDROGEOLOGY,
GEOCHEMISTRY,
HYDROGEOLOGY OF THE OLKARIA FIELD
LAKE MAGADI THERMAL SPRINGS

The first three are general studies while the remaining two give more details of two individual areas.

6.2 SURFACE HYDROLOGY (Figure 6.1)

6.2.1 Nakuru–Elmenteita area

Lake Nakuru is separated from Lake Elmenteita by a low topographic divide and lies at the northern boundary of the study area, in a graben between Isirkon (2097 m) to the east and the Mau Escarpment to the west. Menengai rises to the north of the lake, and the high ground of the Mau and Eburru Forests lies to the south. The lake is alkaline and saline (sodium-bicarbonate type) as a result of evaporation and is recharged by rainfall, surface runoff and groundwater.

The rivers Njoro, Larmudiac, Makalia, and Nderit drain from the Mau Escarpment towards Lake Nakuru, but most of the flow is lost as groundwater recharge before the lake is reached. Of these rivers the Makalia and Njoro are normally perennial (McCann, 1972). The Ngosur (a permanent stream) and several minor streams flow from the Bahati uplands westwards towards Lake Nakuru, although none of them reaches the lake.

Lake Elmenteita is, like Lake Nakuru, recharged by direct precipitation, from shallow aquifers and by surface runoff. The Meroni, Mbaruk and Kariandusi streams (which flow from the Bahati Escarpment) reach the lake, but only after most of their discharge has been lost to shallow aquifers.

6.2.2 Naivasha area

The Naivasha catchment is separated from the Nakuru–Elmenteita catchment mainly by the Eburru volcanic pile which is linked to the Mau Escarpment by a ridge at an altitude of around 2600 m. Between Eburru and the Bahati Escarpment the surface drainage divide runs via Gilgil along a culmination of the Rift floor at an altitude of approximately 2000 m.

South-east of the drainage divide the perennial Gilgil and Malewa Rivers provide much of the recharge to Lake Naivasha. The Gilgil River has its headwaters high in the Bahati Forest and drains parts of the eastern slopes of the Bahati Escarpment. These slopes also provide some of the tributaries of the much larger Malewa River. Most of the discharge of the Malewa River, however, at least in its upper reaches, derives from the western slopes of the high Nyandarua Range. Further downstream the Malewa is joined by the Turasha River which is also perennial and drains the north Kinangop Plateau via deeply incised tributaries.

On the west side of the Naivasha catchment the main river draining the Mau Escarpment is the Marmonet, which flows towards the lake but fails to reach it, instead recharging the alluvium of the Ndabibi Plain. Similarly none of the numerous seasonal streams which incise the Eburru Ridge reaches Lake Naivasha.

To the south of Lake Naivasha the surface water divide runs from the Mau Escarpment in the west, via Olkaria and Longonot to the Kinangop Plateau and finally to the Nyandarua Mountains. Surface drainage in this region, at least at lower altitudes, is limited, only the River Karati

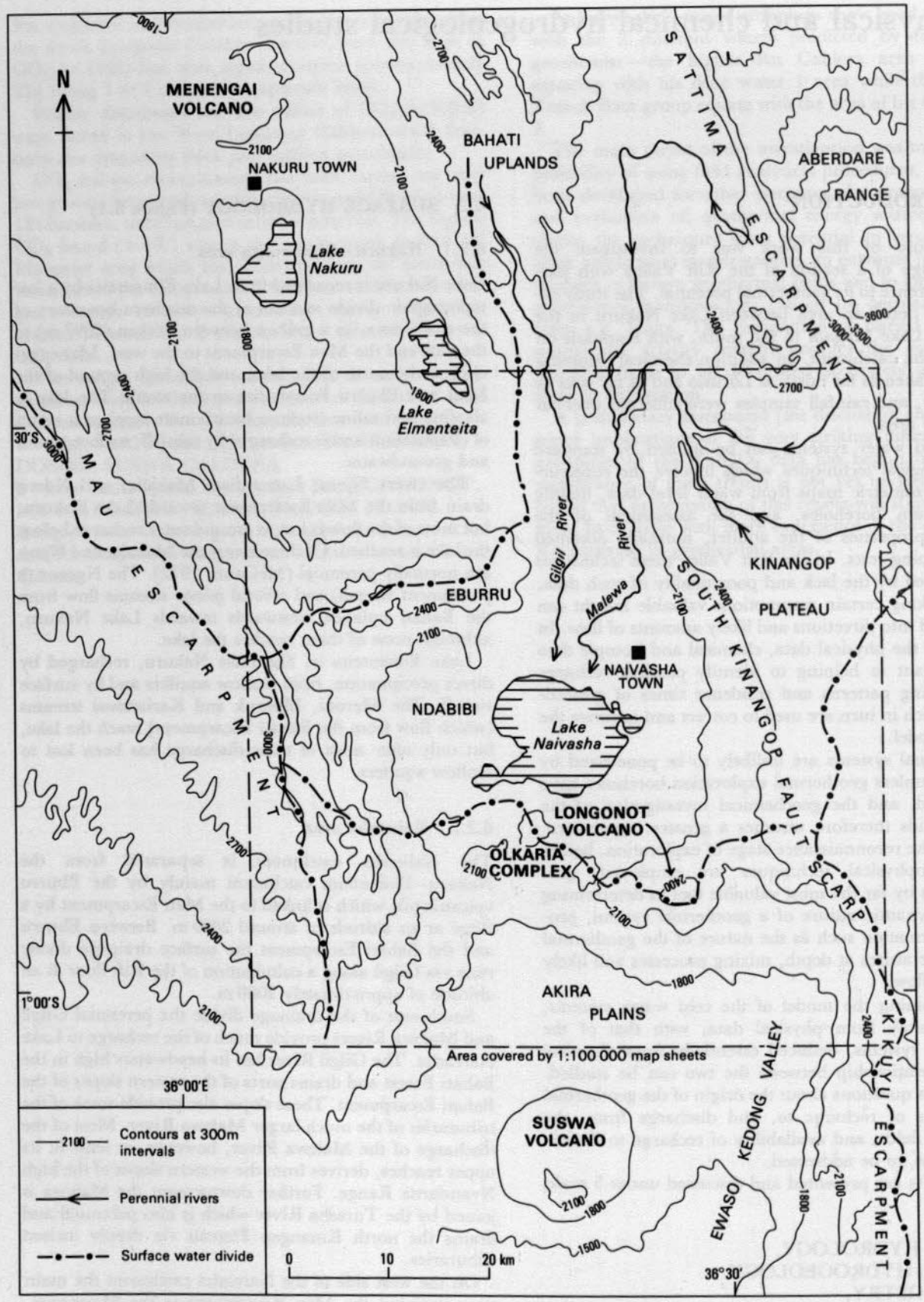

Figure 6.1 Map of the project area.

providing perennial flow in its upper reaches, and cutting a deep gully as it descends the step platforms east of Naivasha Town.

Drainage systems south of this divide originate on downfaulted platforms of the western rift margin west of the Sakutiek settlement, on the Olkaria Volcanic Complex, on Longonot Volcano, and on, and adjacent to, the southernmost part of the Kinangop Plateau. The drainage originating on the Olkaria Complex includes the Hell's Gate–Ol Njorowa Gorge. All the above drainage systems, except those from the Kinangop Plateau, terminate as alluvial fans on the Akira Plains. Braided channel systems on the central parts of these plains indicate past drainage eastwards around the northern flanks of Suswa Volcano. Well to the south of the project area this drainage merges with that from the Ewaso Kedong Valley. The Ewaso Kedong River flows southwards close to the eastern margin of the rift and most of the year is solely supplied by warm springs in the Kijabe Town and Mayers Farm areas. The headwaters are near the Magumu settlement on the Kinangop Plateau but many tributary gullies originate on, and have deeply dissected, the main rift margin fault scarp between Kijabe Hill and Kijabe Town.

6.2.3 Suswa–Magadi area

The southern part of the Rift Valley is bounded in the west by the Nguruman and Mau escarpments. In the east the boundary of the Rift is most clearly defined by the Kikuyu Escarpment at the latitude of Mt Suswa. The Nguruman Escarpment descends from a height of 1950 m via the Kirikiti Platform at 1350 m to the Rift Valley floor at 900 m in the extreme west, from where the valley floor descends by a series of ridge and trough faulted escarpments to 590 m at Lake Magadi in the centre of the Rift. The Mau Escarpment reaches a height of 2375 m to the north-west of Suswa, and the Kikuyu Escarpment 2400 m to the east.

The Rift Valley floor south of Suswa is divided into many sub-parallel ridges and troughs trending approximately north-north-east, a physiographic expression of the recent grid faulting. The valley floor slopes southwards with a gradient of approximately 1:100 from Lake Naivasha to Lake Magadi and the surfaces of the fault blocks dip similarly gently southwards.

The only perennial river in the Rift in this sector is the Ewaso Ngiro River, which has built out an extensive alluvial fan several kilometres onto the Ewaso Ngiro Plain. The river rises to the west of the Mau Escarpment and its tributaries drain the south-western slopes of the escarpment, from around the latitude of lake Naivasha southwards. The river initially flows south-east, then turns south, passing to the west of Lake Magadi and to the east of the Nguruman Escarpment, where it is joined by tributary streams draining the escarpment. The Ewaso Ngiro River finally discharges into the Engare Ngiro swamp at the north end of Lake Natron, to the south of the present project area.

There is no perennial surface drainage to, nor any outlet from, Lake Magadi. A number of springs and seepages which feed the lake occur around its margin, some of which have a significantly elevated temperature (maximum 86°C at the northern extremity of Little Magadi). As a result of extreme evaporation Lake Magadi has developed some of the most concentrated brines to be found in the alkaline saline lakes of the Rift Valley, and a layer of trona (crystalline carbonates of sodium) covers the surface.

6.2.4 Rainfall

Rainfall is concentrated into the two rainy seasons of October–November and March–May. Within the Rift mean annual rainfall is low, ranging from 430 mm at Magadi through 627 mm at Naivasha to 981 mm at Nakuru, with most of the region experiencing an average of about 750 mm (Kenya Met. Dept. data 1931–1980). The average maximum daily temperature at Magadi is 35°C (minimum 23°C), while at Naivasha, near the culmination of the Rift, it is 25°C (minimum 9°C).

Relative humidity is low throughout the Rift (less than 75% at Naivasha, less than 60% at Magadi) and potential evaporation (1600 to 1800 mm) greatly exceeds annual rainfall. Monthly averaged potential evaporation at Naivasha exceeds rainfall by a factor of 2 to 8 for every month except April when potential evaporation still exceeds rainfall except in the wettest of years. The same figures are not recorded for Magadi where the excess of evaporation over rainfall must be considerably greater. However individual storms in the two rainy seasons can be extremely heavy and in areas of permeable material some recharge is probable.

On the Rift escarpments rainfall values are much higher ranging up to around 1250 to 1500 mm annually (McCann, 1974). Also evapotranspiration rates at these altitudes are lower at about 1400 mm per year, and much less during the rainy seasons.

6.2.5 Geothermal manifestations

Geothermal manifestations in the area between Lake Nakuru and Longonot Volcano have been described in section 5 of this memoir and are shown on the accompanying 1:100 000-scale geothermal map. The most active thermal areas are associated with the volcanic complexes at Eburru, Olkaria, Longonot and Suswa. In these areas fumaroles, often controlled by linear or ring fractures, are common, although thermal springs are rare. This is in part because the volcanoes occupy high ground and are therefore in hydrological recharge areas. The infrequent hot springs associated with these areas are found in topographically lower regions such as to the north of Eburru and in Njorowa Gorge within the Olkaria Complex. The natural heat discharge from Olkaria has been estimated as 376 MW, and from Eburru as 130 MW (Glover, 1972).

The only important thermal area which is not associated with a volcanic centre (and where there are no fumaroles) is at Lake Magadi. Here the hot and warm springs surrounding the Lake discharge an estimated 250 MW (Crane, 1981). Elsewhere thermal springs are infrequent and usually occur near the Rift margins. These springs are often associated with faulting and do not reach elevated temperatures.

6.3 PHYSICAL HYDROGEOLOGY

6.3.1 Scope of the study

In general the permeability of rocks in the Rift Valley is low, although there is considerable local variation. Aquifers are normally found in fractured volcanics, or along the

weathered contacts between different lithological units. These aquifers are often confined or semi-confined and storage coefficients are likely to be low. In addition aquifers with relatively high permeabilities are found in sediments covering parts of the Rift floor (particularly around Lake Naivasha). Such aquifers are often unconfined and will have relatively high specific yields. Tectonic movements of the Rift Valley have important effects on aquifer properties, both on a small scale by creating the local fracture systems which comprise many aquifers, and on the large scale by forming regional hydraulic barriers or shatter zones of enhanced permeability.

Knowledge of the hydrogeology of the Rift Valley varies considerably over the project area (between Lake Nakuru and Lake Magadi) and depends primarily on the distribution of water supply boreholes. Around Lake Naivasha for example over 100 boreholes have been drilled since the 1930s, whereas less than 20 boreholes have been drilled in the Rift floor between Longonot volcano and Lake Magadi—a distance of nearly 100 km.

Another limitation is that boreholes can strictly only provide information concerning groundwater conditions within limited depths, and in the case of the Rift Valley boreholes this usually implies depths of less than 250 m, an important exception is the Olkaria geothermal field where borehole depths exceed 1 km. This means that to a large extent the hydrogeology of the Rift Valley at depths relevant to the recharge of geothermal fields (several kilometres) has to be inferred from information such as piezometric and chemical data. In particular the degree of connection between aquifers intercepted by boreholes on the Rift sides, and those at depth beneath the Rift is poorly known.

In this study borehole data have been used in two main ways. Firstly, they have been used to construct a piezometric map of the Rift Valley—vital in attempting to examine regional flow systems. Secondly, an attempt has been made to identify variations in aquifer properties with rock type, and with depth. After examining the effects of structure, a semi-quantitative assessment of the regional flows which may contribute to the deep geothermal systems has been made.

6.3.2 Previous work

General accounts of the hydrogeology of the project area are given in the reports of the Geological Survey of Kenya. Particularly relevant reports are; No. 78 covering the area from Gilgil to beyond the northern boundary of the area (McCall, 1967), No. 55 covering the Longonot–Gilgil area (Thompson and Dodson, 1963), No. 43 covering the Kijabe and Kinangop areas (Thompson, 1964), and No. 42 covering the Magadi area (Baker, 1958). In addition Ministry of Works Technical Report No. 3 discusses groundwater conditions in the Nakuru area (McCall, 1957).

Hydrogeological reports with specific reference to geothermal energy studies in the Rift Valley in areas north of Longonot were prepared as part of a previous UN study (McCann, 1972 and 1974), and similar investigations have recently been completed to the north of the present project area (Geotermica Italiana, 1987). Several papers and reports have been published which are relevant to the hydrogeology of the Rift Valley in the project area, and these are mentioned in the appropriate sections of this report.

6.3.3 Data collection and data base construction

Data for 596 boreholes from 32 sheets of the 1:50 000 topographic map series were abstracted from Ministry of Water Development records. The density of borehole data varies considerably; most boreholes are in the north and east of the project area, with very few in the south and west. Data for most boreholes in the Nakuru–Magadi region of the Rift were abstracted; the exceptions were generally where borehole density was high, when a representative sample was taken.

Data were initially copied from the files and were subsequently entered into a computer data base at Wallingford, listings of which are given in BGS Rep. No. SD/89/1 (Allen et al., 1989).

A problem with collecting hydrogeological data in the Rift Valley is that so few wells have access for water level measurements, either because a piston pump is installed or because the borehole is blocked. Therefore water levels are taken from borehole records. These data refer to the levels at the time of well completion, which is a period spanning over 50 years for boreholes in the project area. This introduces errors in defining piezometric contours, because of the seasonal and longer term variations in groundwater levels.

The scale of such errors may be found by comparing borehole water levels at the time of completion with levels measured recently. While differences measured are not insignificant, such variations are small when compared with the large spatial variation in surface topography and water table geometry encountered in the Rift, and can therefore be ignored when groundwater movement on the scale of the Rift is considered. They cannot however be ignored if local small-scale effects are examined.

Other errors are introduced into piezometric map construction by using borehole rest-water levels which may represent a local averaging of several piezometric surfaces where different aquifers are intersected by a borehole.

The scale chosen for the draft piezometric map of the project area was 1:250 000 with a contour interval of 100 m (with variations depending on the data quality). At this scale the regional flow systems which may contribute to geothermal recharge can be well represented, while the effects of errors such as those discussed above can be minimised. Piezometric contours were drawn using the borehole water level data, and spring data obtained from the 1:50 000 and 1:250 000 topographic map series. Where such data are scarce local topographic variations have been used as a guide to contour geometry. Figure 6.2 is a reduced version of the piezometric map.

6.3.4 Analysis of the piezometric map

In general the map shows the features expected of a valley/interfluve system, with groundwater flowing from elevated recharge areas to low-lying discharge areas, the flow occurring both laterally and longitudinally according to the Rift geometry. In the following discussion the different sub-catchments are considered separately.

6.3.4.1 Nakuru–Elmenteita

Lakes Nakuru and Elmenteita lie a little to the north-west of the culmination of the Rift floor, between Naivasha and Gilgil. Groundwater gradients and therefore flows in this area are generally directed towards the lakes, with some flow away from the area to the north-west. In more detail, groundwater flows north-east from the Mau Escarpment, south-west from the Bahati Escarpment and

northwards from Eburru. It is also probable that there is some southerly flow from Menengai towards Lake Nakuru. However at depth it is likely that flow occurs to the north-west away from the Nakuru–Elmenteita catchment towards the lower-lying area around Lake Bogoria.

6.3.4.2 Naivasha

This is the most important catchment in the project area in terms of present and near-future geothermal development. It is also the most complex hydrogeologically, because while it is lower than the Rift escarpments it is at a culmination of the Rift floor. Flows towards Lake Naivasha from the Mau Escarpment and the Kinangop Plateau are unambiguous and some of the groundwater from the western side of the Rift must eventually form part of the discharges at Olkaria and Eburru. However the longitudinal flows in this area are more difficult to assess.

To the north of Naivasha the surface water divide runs approximately east–west through Eburru, and then north through Gilgil. However there is no evidence that a groundwater divide follows this route, because the piezometric surface has an uninterrupted fall from Lake Naivasha, around the east side of Eburru, towards Lake Elmenteita, indicating flow in this direction.

The configuration of groundwater contours around Eburru is uncertain because boreholes drilled at Eburru have encountered steam. It is probable that while shallow groundwaters on the south side of Eburru move locally towards Naivasha, deeper flows are substantially northwards.

Around Lake Naivasha itself the groundwater level is between approximately 1880 and 1890 m, similar to that of the lake itself. East and west of the lake the groundwater contours rise, indicating flow towards the lake, while to the south they remain at about the same level as far as the latitude of the Longonot and Olkaria complexes. South of this region the piezometric surface must drop by several hundreds of metres because the few boreholes drilled between Longonot and Suswa have all proved to be dry, or have produced steam. The data do indicate a fall of at least 450 m in piezometric level over a distance of around 10 km (i.e. a gradient of at least 0.05 m/m). At depth a north–south pressure gradient of 11 bars/km has been reported in the Olkaria geothermal field (Bodvarsson et al., 1987) which corresponds to a freshwater head gradient of 0.1 m/m.

Groundwater certainly flows away from Lake Naivasha because the lake water is fresh, even though the lake has no outlet and lies in an area of high evaporation. The position of the lake, at a culmination of the Rift floor, suggests flow both to the north and to the south (i.e. a groundwater divide runs east–west in the vicinity of the lake). As discussed above, northerly flow may occur both via Gilgil and under Eburru (but see Section 6.4.3.). Southerly flow must also occur, following the hydraulic gradient, but the high values of the gradient suggest that values of permeability in the Olkaria-Longonot region are low. Values for subsurface discharge in the Naivasha area are discussed in Section 6.3.6.5.

6.3.4.3 Longonot–Magadi

A surface water divide runs east–west through Olkaria and Longonot but appears to have little effect on the southerly flow of groundwater from Naivasha. Between Longonot and Lake Magadi groundwater flows from the sides of the Rift towards the centre, and southwards along the Rift towards Magadi. The unknown, but very deep position of the piezometric surface in the Suswa area suggests that flow from the sides of the Rift in this area is limited, and it is very likely that the major Rift faults act as low permeability barriers to flow across the Rift. For example borehole C4971 in the Rift to the east of Suswa encountered no water at a depth of 300 m, corresponding to a maximum water level altitude of 1250 m, whereas less than 10 km to the east, on the side of the Rift, the piezometric surface is between 100 m and 200 m below the surface, at an altitude of 1900–2000 m.

Between Suswa and Lake Magadi water level data are very sparse, but the limited evidence indicates the expected flow down the topographic gradient, i.e. southwards from Suswa, south-east from Narok, south-west from the Ngong area and east from the Nguruman Escarpment, with all flows eventually coinciding in the topographic low around Lake Magadi. From hydraulic evidence there is no way of distinguishing which of these flows contributes the most to the thermal springs at Lake Magadi, but the nearby Nguruman Escarpment would seem to be a likely source because of the substantial hydraulic head gradient which it could provide.

6.3.5 **Aquifer properties**

Very little information is available concerning the variation in aquifer properties between the various rock types of the Rift Valley. The main reason for this is that the standard hydrogeological field test to determine aquifer transmissivity—a carefully monitored pumping test with observation wells—has not been undertaken when water wells have been drilled. (The Olkaria wells form a special case and will be considered later). In general, after water wells have been drilled they have been test-pumped for a few hours in order to obtain a well yield. In some cases recovery data have been recorded, but for the majority of wells only a yield, or a yield and a pumped water level at equilibrium have been noted.

These data allow only semi-quantitive values to be calculated (Table 6.1) but even so provide an insight into the relative potential of different rock types as aquifers.

The study indicates that the permeability of the volcanic rocks underlying the Rift Valley is generally low, although there is considerable local variation. Aquifers are normally found in fractured or reworked volcanics, or along the weathered contacts between different lithological units. The highest values of permeability are found in the reworked volcanics composing the sediments of the Naivasha area, where the specific capacities of wells often exceed 3 l/s/m and where estimated hydraulic conductivities of greater than 10 m/d are common. In the Rift floor to the north, where the sediment size decreases, borehole specific capacities fall, to around 0.3 l/s/m in the Elmenteita–Nakuru area (leading to an estimated average hydraulic conductivity of 2 m/d). On the Rift escarpments the permeabilities of the different rock types are uniformly low. Mean borehole specific capacities and estimated hydraulic conductivities range from 0.03 l/s/m and 0.1 m/d for the Kinangop Tuff to 0.2 l/s/m and 1.1 m/d for the Limuru Trachyte to the east of Suswa and the Mau Tuff.

These figures are only applicable to the drilled depths of the boreholes, normally less than 250 m. Below this depth permeabilities will fall, mainly as a result of the closure of fissures by overburden stresses.

The only deep boreholes drilled in the Rift are those in the Olkaria geothermal field, the hydrogeology of which is discussed in Section 6.5. The permeability of the reservoir

rocks at Olkaria is low, and recent modelling of the Eastern Olkaria borefield has produced values of 7.5×10^{-15} m^2 (7.5 mD) for the steam zone (700–800 m approximately) and 4×10^{-15} m^2 (4 mD) for the underlying liquid-dominated zone (Bodvarsson et al., 1987). The average transmissivity of the reservoir is also low, with values ranging between 1 and 5×10^{-12} m^3. The effective porosity of the liquid-dominated zone is estimated to be 2% on average, with spatial variations of 0.25–5%. In terms of well response the reservoir behaves as a dual porosity system, with both fracture and matrix porosity and permeability.

As a result of the poor transmissivity the flow rates from the Olkaria wells are low, with the average well producing only 6 kg/s of steam, which is the equivalent of 2.5 MWe (Bodvarsson et al., 1987).

Translated into cold water (20°C) terms for comparison with the water borehole values these figures indicate hydraulic conductivity and transmissivity values of around 3×10^{-3} m/d and 1–4 m^2/d respectively.

The values are significantly lower than those obtained for most water boreholes throughout the Rift, which is expected in view of the depth of the geothermal reservoir. However, it is not known how representative these values are of permeabilities elsewhere in the Rift because the geothermal reservoir is in an unusual environment where mineral alteration, dissolution or deposition can enhance or reduce rock permeability.

In the absence of other deep wells in the Rift a preliminary estimate of permeability at depth has been made by calculating the transit times of groundwater flows for a range of permeabilities and comparing these with age data from groundwater samples obtained by radioisotope analysis.

This work suggests that the average hydraulic conductivity of rocks at depth under the Rift in the Naivasha area is much less than 0.1 m/d and may in fact be of the order of 0.001 m/d as at Olkaria, although this is speculative.

6.3.6 **Groundwater flow systems**

6.3.6.1 Fault control

The structure of the Rift Valley and in particular the major marginal Rift faults and the system of grid faulting on the Rift floor undoubtedly have a substantial effect on the groundwater flow systems of the area.

In general faults are considered to have two effects on fluid flow. They may facilitate flow by providing channels of high permeability, or they may prove to be barriers to flow by offsetting zones of relatively high permeability. The hydraulic role of faults is a subject which is poorly understood because there is often little direct evidence that a particular fault behaves in a particular way. On the whole, faults are more commonly thought of as hydraulic boundaries in cold groundwater systems where horizontal flows predominate, whereas in geothermal systems where vertical flows are more important they are often considered to provide conduits for flow. However care is needed to avoid invoking either property without evidence.

In the Rift Valley the main direction of faulting is along the axis of the Rift, and this has a significant effect on flows across the Rift. It is apparent from the high hydraulic gradients which are developed across the Rift escarpments that the effect of the major faults is to act as zones of low permeability. This is particularly true of the Bahati Escarpment and the escarpment to the east of Suswa. Water flowing in the weathered zones, which are often old land surfaces and therefore sub-horizontal, and fractures of the pyroclastics and lavas forming these Rift escarpments is forced to flow downwards by the faults, and in the case of the escarpment east of Suswa the fault permeability is so low that the piezometric surface in the nearby Rift Valley is considerably depressed.

The effects of Rift faulting appear to be less in the Kinangop Plateau area where the piezometric contours are more widely spaced, and limited borehole evidence from the Mau Escarpment to the west of Naivasha suggests that flows towards the lake are not greatly affected. Borehole data are very limited on the west side of the Rift south of Longonot, but dry boreholes to the west of Suswa indicate that Rift faulting may inhibit lateral flows in this area.

Flows along the Rift are likely to be strongly affected by the substantial amount of grid faulting of the Rift floor. The effect of these faults is to channel flow along the axis of the Rift, either because the faults are open and act as conduits, or, if they are infilled, because they provide permeability barriers to lateral flow. A microseismic study of the Rift valley concluded that the grid faults, unlike the escarpment faults, are still active (Tobin, Ward and Drake, 1969) which suggests that they are open. Alternatively in a recent study of the Olkaria area (Ogoso-Odongo, 1986) it was stated that faults in the Olkaria region acted as barriers, diverting southerly flow from Eburru to the south-west, towards Suswa; however the evidence for such behaviour is slim. Within the Olkaria geothermal field no evidence has been found of hydraulic barriers (Bodvarsson et al., 1987).

In summary the effect of faulting is to cause groundwater flows from the sides of the Rift towards the centre to follow longer flow paths reaching greater depths, and to align flows within the Rift along its axis.

6.3.6.2 Groundwater flows in the Longonot–Eburru area

The Naivasha catchment between Longonot and Eburru is in a hydrogeologically complex environment, as noted in section 6.3.4.2, receiving water from direct precipitation and from the Rift flanks—either as stream flow or subsurface flow—and discharging groundwater to the north and south. The geothermal fields at Olkaria and Eburru lie at the southern and northern edges of the Naivasha catchment and the recharge of these fields is therefore intimately connected with subsurface flows within, or more precisely out of, the catchment.

Attempts to quantify groundwater flows in the Naivasha catchment comprised two types; water balance studies, and applications of Darcy's Law of groundwater flow on a regional scale. Based on water balance studies preliminary estimates of subsurface flows from the Naivasha catchment suggest that the amount contributed by Lake Naivasha is around 50×10^6 m^3/y (which is 20% of the total recharge estimated by a previous water balance study). Flow to the south via relatively shallow aquifers (i.e. at depths of less than about 500 m) may be the most significant route for water flow from the catchment, accounting for perhaps 50% to 90% of the total.

Estimates of the scale of the regional flow out of the Naivasha catchment can be attempted if certain assumptions are made concerning regional head gradients and permeabilities.

6.3.6.3 Southward flows from the Naivasha area

In Section 6.3.4.2. it was established that a north–south groundwater gradient of at least 0.05 m/m exists over the Olkaria–Longonot area, and over the Olkaria field itself the gradient has been measured as 0.1 m/m. If the latter gradient is accepted and if the estimated hydraulic conductivity of the Olkaria geothermal field (3×10^{-3} m/d— Section 6.3.5.) is taken to represent that across the Rift (with a width of 25 km), and assuming flow to occur to a depth of 5 km, below which depth fissures are unlikely to be open, then the southerly flow at depth from the Naivasha catchment is estimated to be 14×10^6 m³/y. To this figure must be added the amount of southerly flow in shallow aquifers. The hydraulic conductivity of rocks to around 500 m (the depth of the caprock) in the Olkaria–Longonot area is unknown. If, however, it is taken to be between 0.1 m/d and 1 m/d, i.e. similar to the Rift-wall rocks then, assuming the same hydraulic gradient and a saturated thickness of 300 m (that is, assuming the average depth to the water table to be 200 m) then the shallow component of southerly flow is estimated to be between 27×10^6 m³/y and 270×10^6 m³/y.

The above figures are very crude, being based on very rudimentary data, but they do indicate the order of magnitude of southerly flows from the Naivasha catchment, and suggest that the shallower aquifers may form a significant conduit for southerly flow.

6.3.6.4 Northerly flows from the Naivasha area

McCann (1974) estimated a northerly flow of 39×10^6 m³/y from the Naivasha catchment towards the Elmenteita catchment, on the basis of a transmissivity of 1000 m²/d. Data from the present study (Table 6.1) suggest values of transmissivity of less than 100 m²/d to the drilled depth of boreholes between Naivasha and Elmenteita, suggesting transmissivities of the order of 500 m²/d for shallow aquifers to 500 m, assuming water tables to be near the surface). If a mean groundwater gradient of 0.004 m/m is taken, from the piezometric map, and assuming the width of the Rift to be 15 km, an estimate of 11×10^6 m³/y is obtained for shallow northerly flow. Deep northerly flow (i.e between 500 m and 5 km) over the same cross-section is estimated as 0.3×10^6 m³/y, assuming the same permeability as at Olkaria.

6.3.6.5 Discussion

The implication of the above rough analysis is that much of the subsurface outflow from the Naivasha catchment is to the south, via Olkaria–Longonot towards Suswa, and eventually towards Magadi, although there is little evidence that such water ever reaches Magadi in an identifiable form.

In terms of relative flow amounts to the north and south, the most important, and least known value is the hydraulic conductivity of relatively shallow material between Longonot and Suswa. If the higher value of the range given above is taken, the the total flow out of the Naivasha catchment is estimated to be around 295×10^6 m³/y—a figure which agrees reasonably well with McCann's estimate of 250×10^6 m³/y—of which around 20% is lake recharge. Less than 5% of this total would flow north, and of the southerly flow only 5% would occur at depth.

If the lower estimate of hydraulic conductivity is taken, then the total estimated recharge value is 52×10^6 m³/y, virtually all of which could be lake recharge. Here northerly flow would account for about 20% of the flow from the catchment, and of the southerly flow around 25% would be at significant depths.

Concern has been expressed about the possible effect of geothermal production on the level of Lake Naivasha. According to Bodvarsson et al. (1987) the average well at Olkaria produces about 6 kg/s of steam, equivalent to around 2.5 MWe. Therefore in order to produce 45 MWe the present wellfield discharges approximately 100 kg/s of steam, equivalent to a liquid discharge rate of 3×10^6 m³/y. This is only a small proportion of even the minimum estimated total natural southerly flow from the Naivasha area (41×10^6 m³/y). It is therefore considered that any effect of present or proposed geothermal production on lake levels is likely to be masked by the effects of natural rainfall variations over the catchment.

6.4 GEOCHEMISTRY

6.4.1 Geochemical sampling and analysis

6.4.1.1 Sampling

The locations of all BGS sampled sites in the southern Rift Valley are shown on the 1:100 000-scale Geothermal

Table 6.1 Average aquifer characteristics of selected areas and lithologies from borehole data. (Figures in brackets are arithmetic means)

Area	Lithology	Arithmetic mean borehole yield l/s	Geometric mean specific capacity l/s/m	Geometric mean estimated transmissivity m²/d	Geometric mean estimated permeability m/d	No. dry boreholes	Total no. boreholes
NE Naivasha	Sediments + volcanics	9.3	2.8(11.6)	307(1170)	12(33)	0	35
SE Naivasha	Sediments + volcanics	4.4	4.6(29.2)	502(3082)	20(114)	0	22
SW Naivasha	Sediments + volcanics	5.4	2.7(8.7)	297(940)	63(196)	0	17
NW Naivasha	Sediments + volcanics	6.4	14.9(52.6)	1601(5308)	148(818)	0	26
Naivasha–Elmenteita	Sediments + volcanics	2.6	0.7(1.3)	78(143)	1.4(3.9)	1	12
Elmenteita–Nakuru	Sediments + volcanics	1.9	0.3(2.4)	32(261)	2(7)	2	31
Bahati Escarpment	Tuffs	3.4	0.1(0.4)	14(47)	1.2(3.7)	1	25
Kinangop Plateau	Tuffs	1.8	0.2(0.9)	14(106)	0.8(5)	5	32
S Kinangop	Pyroclastics	1.9	0.03(0.04)	4(5)	0.1(0.2)	3	11
E Suswa Rift Escarpment	Trachyte	2.1	0.2(2.6)	20(325)	1.1(35)	4	48
Mau Escarpment	Pyroclastics	1.3	0.2(1.6)	22(174)	1(10)	5	23
Mau Forest (W Nakuru)	Pyroclastics	1.7	0.2(1.1)	20(119)	1.1(22)	4	43

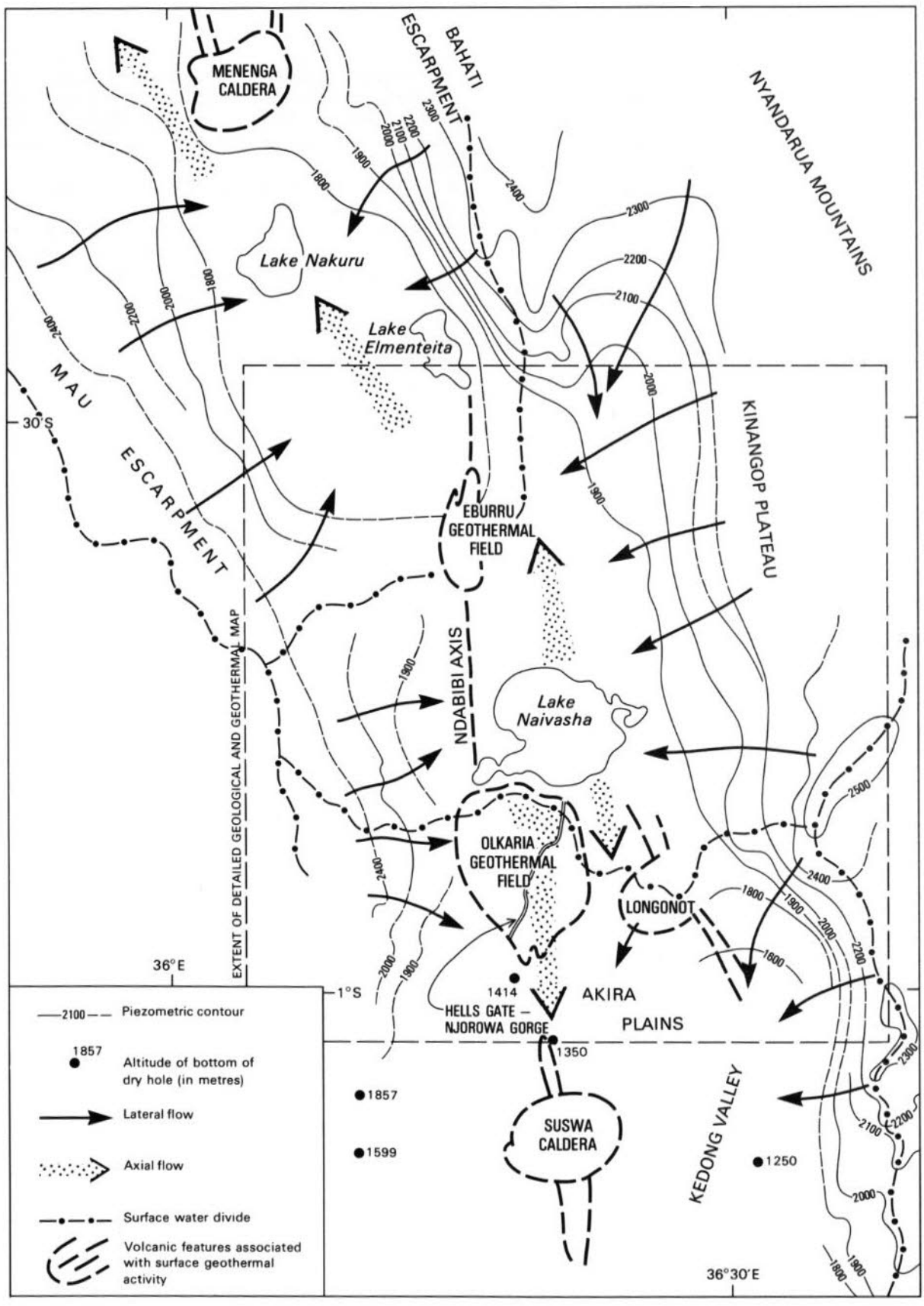

Figure 6.2 Piezometric map of the project area.

Map, sites sampled in the Rift north of Lake Nakuru are shown on Figure 6.2. Additional information on these and various UNDP sites is given in Allen et al., (1989). Water samples intended for chemical analysis were filtered through a 0.45f Millipore filter under wellhead or hand pump pressure. Two 30 ml Sterilin sample tubes were filled at each site, one being acidified with a drop of concentrated HCl (primarily to stabilise cations) and the other left unacidified to preserve original chloride and bicarbonate as far as possible. When hot springs were sampled, a third 30ml water sample was collected, diluted ten times by distilled water to prevent silica from precipitating.

Samples for O and H stable isotope analysis were collected in 30 ml glass bottles with neoprene-lined caps (McCartney-type). Waters for $\delta^{13}C$ measurement of dissolved inorganic carbon (DIC) were collected in 250 ml glass bottles and usually precipitated in the field with alkaline $BaCl_2$ solution.

Samples for tritium analysis were collected in 500 ml glass bottles. Radiocarbon analysis entailed the collection of two 60 litre water samples in aspirators at most sites except those with high bicarbonate, when one was sufficient. Field precipitation with alkaline $BaCl_2$ was carried out with $FeSO_4$ added to speed up flocculation where necessary. The resulting pairs of carbonate precipitates were eventually bulked in 2.5 litre polythene bottles.

Gas samples for chemical and isotopic analyses were collected from geothermal wells, fumaroles and one water well in 125 ml glass bulbs with side septa. Steam from the geothermal wells and fumaroles was condensed through a stainless steel coil immersed in cold water to permit the collection of these samples.

Samples for inert gas ratio and helium isotope ratio measurement were collected in copper tubes clamped at each end. Samples were collected in dissolved or gaseous form, the latter with or without a condensing coil, depending on the sampling technique used.

6.4.1.2 Measurement

Measurements of pH, temperature and in some cases Eh and alkalinity were made at the time of sampling. Eh measurements require flowing, air-free water, and these conditions were not always possible to fulfil. All other measurements were carried out in the UK. Chemical analysis (at BGS Wallingford) was by plasma emission spectrophotometry for cations and non-halides, and automated colorimetry for halides.

Stable isotope analysis was carried out at BGS Wallingford by mass spectrometry of H_2 produced by reduction of water by zinc (for δ^2H), and of CO_2 produced by equilibration with water (for $\delta^{18}O$), acid decomposition of precipitated bicarbonate ($\delta^{13}C$ DIC) or from geothermal sources after cryoseparation and drying ($\delta^{13}C$ CO_2). Gas ratio measurements were made by gas chromatography using thermal conductivity and flame ionisation detectors.

Tritium measurements were made by the DSIR Institute of Nuclear Sciences, New Zealand employing predistillation, electrolytic enrichment and liquid scintillation counting. Radiocarbon was measured by the NERC Radiocarbon Laboratory by counting benzene after conversion from CO_2 liberated by acid from $BaCO_3$ precipitated in the field (see above); this work was supervised by Dr D D Harkness.

Inert gas samples were measured at the University of Bath by static mass spectrometry. Helium isotope ratios were also determined by mass spectrometry after suitable preparation; this work was carried out at the University of Cambridge. We are grateful to Mr M J Youngman and Dr J N Andrews (Bath) and Ms E Griesshaber and Prof. R K O'Nions (Cambridge), both for measuring the samples and for discussing interpretation of the results.

6.4.2 Water chemistry

6.4.2.1 Non-thermal and slightly thermal waters: Suswa to Nakuru

This section deals with most of the waters sampled between Suswa and Nakuru. The only high-temperature waters in this area were collected from the Olkaria area, and these, together with samples from the Ol Njorowa Gorge, are treated in Section 6.5 of this report. The waters sampled fall into two main classes: modified and unmodified. The latter category includes waters whose chemical composition is derived from normal water–rock interaction at moderate temperatures, while the former comprises waters which possess evaporated or thermal components.

Unmodified waters

Results are reported in Table 6.2 and their areal distribution plotted in Figures 6.3a–g. Most unmodified groundwaters tend to be associated with the eastern and western Rift walls, i.e. sites 25–27, 85, 87, 90–92, 96, 100 and 101. Table 6.2 indicates that the waters are of sodium-bicarbonate type with a relatively high silica content. The analyses are typical of igneous terrains, where dissolution of minor carbonate provides the main anion, HCO_3^-. All waters are oversaturated with respect to SiO_2, but most have not yet reached calcite saturation. Only trace amounts of chloride and sulphate minerals are present in these rocks, hence the low amounts of these ions, and the relatively low total dissolved solids (TDS), averaging 365 mg/l. While much lower TDS values are known from groundwater in igneous rocks in temperate climates, the higher TDS in these waters is attributed in most cases to the high ambient temperature obtaining in the Rift Valley rather than to long residence time or particularly deep circulation.

Waters of similar composition are seen in some wells on the Rift floor—for example sites 37, 39, 82, 95 and 118, and it is considered that these waters too are the product of rainfall followed by limited water–rock interaction.

Other properties of these waters, such as pH and Eh (oxidation potential) measurements, also indicate that these waters are relatiely unmodified. Figure 6.3b shows that pH is similar for most of these waters, with a very few exceptions such as the alkaline Kijabe springs (site 27), and averages 7.5 pH units which is typical of dilute bicarbonate waters. Eh values were recorded at comparatively few sites (Figure 6.3b), but they all indicate that the waters are oxidising in character. Temperatures range from 18°C (site 90) to 43°C (site 27), but, as already stated, water chemistry does not indicate a former high temperature origin.

It is likely that the compositional range of the waters described above (Table 6.3) is typical of shallow waters from the Rift wall and floor for considerable distances north and south of the Suswa–Nakuru sector. Supporting evidence comes from the BGS data in the Magadi area and from the MERD data in the Bogoria area.

Modified waters

These can be divided into those north and south of the Eburru massif. The southern group are all relatively close

Table 6.2 Chemical and stable isotope data for all samples collected in the Rift Valley during the present study

Site no.	Temp	pH	Na	K	Ca	Mg	HCO_3	Cl	SO_4	Si	NO_3	B	F	δ^2H	$\delta^{18}O$
1	84.6	8.85	10000	186	.6	<.4	18900	5250	163	37.3		7.71	150	- 4	- 1.2
2	80.7	9.07	11500	197	.5	<.4	21800	5950	159	40.2		8.53	180	- 4	- 1
3	85.3		10900	185	.5	<.4	20400	5550	160	39.4		8.04	170	- 6	- .9
4	81.3		11400	195	.6	<.4		5950	159	40.2		8.67	170	- 4	- .5
5	78.6		10300	174	.5	<.4		5200	162	36.8		7.48	150	- 7	- 1.1
6	72.4		11400	176	.5	<.4	20700	155		41.4	5600	8.26	170	- 6	- 1.1
7	82	9.18	10300	158	.6	.4	19900	153		41.2	5300	7.6	160	- 6	- 1.2
8	82.6	9.13	10500	165	.4	<.4	23000	5350	141	40.2		7.77	160	- 5	- 1.2
9	45	8.82	9640	112	.7	<.4	16700	4900	204	49.2		7.7	80	- 17	- 3.1
10	43.5	8.81	9120	105	1.2	.4	16800	5100	194	47.3		6.89	90	- 20	- 3.2
11	66.6	8.96	11100	157	.6	<.4	20900	5850	134	39		7.83	130	- 7	- 1
12	60.2	9.13	12500	173	.6	<.4	23600	6900	129	40.6		9	180	- 4	- .6
13	39.5	9.56	12200	100	.6	<.4	23100	6400	160	23.8		6.83		- 16	- 2.4
14	38.5	9.56	12000	96.8	.6	<.4	22900	6550	157	22.6		6.96	140	- 16	- 2.5
15	34	9.86	7000	75.4	.6	<.4	13000	3550	52.4	16.7		2.69	70	- 16	- 1.3
17	40.5		12600	109	.6	<.4		6850	169	25		7.22	130	- 15	- 2.5
18	45.3	9.57	12300	115	.6	<.4	23400	6450	189	32		7.44	130	- 23	- 2.5
19														- 17	10.4
20	25.7	8.2	59.1	16.2	16.9	3.96	193	15	10.6	49.2	4.7	<.035	2.3	- 6	- 1.5
21	21.5	8	5.5	2.6	6.2	3.89	46	4.4	2.5	7.8	<2.2	<0.35		- 22	- 4.2
22		8.8	162	15.8	8.8	1.8	390	26	10.5	38.7	3.8	.08	20	- 25	- 4.2
23													.14	23	.5
24		7.9	40.7	23.8	22.3	7.8	195	13	.9	4.4	2.2	<.035	.8	34	5.6
25	35	7.95	100	7.1	.9	.2	251	5	2.1	36.2	<2.2	<.035	30	- 20	- 4.5
26	43.3	9.05	82.5	1.4	.2	<.15	240	53.5	1.7	19	<2.2	<.035	30	- 19	- 4.2
27	16.9	7.05	38.9	8	3.6	1.3	106	10.5	5.8	31.4	<2.2	<.035		- 18	- 4.3
28	27.9	7.9	31.5	8.4	10	2.8	201	21	4.1	30.8	6.2	<.035	.7	- 28	- 4.8
29	87.2													- 36	- 3.9
30		7.91	5.1	13.4	4.6	1.3	62	6.7	2.6	6.5	<2.2	.05		8	.6
31			<.1	<.75	<.03	<.15		<.4	<.5			<.035		- 14	- 2.2
32	22.2	7.85	23.7	11.8	8.5	1.5	78	6.9	4.6	24.8	5.3	<.035	1.4	- 12	- 2.9
33	51.2	7.25	35.6	13.6	20.9	8.6	143	15	24.2	20.7		<.035	.8	- 31	- 5.2
34	52.5	7.07	33.1	13.2	21.8	8.8	135	13.5	25.1	24.3	4.1	<.035	.14	- 27	- 5.2
35	23													- 14	- 3.7
37	30	6.46	58	20	10.5	2.7	156	50	3.4	43.8		.02		- 19	- 3.7
38	24													- 18	- 4.5
39	29	7.23	29	13	5.09	.7	90	5.5	4.9	45.2		.02		- 20	- 4.5
40	23													- 16	- 3.3
41	43	9.29	1050	35	.46	<.1	1610	490	82	58.3		.92		- 7	- 1.1
42	38	9.13	773	31	.54	.1	1190	360	68	57		.71		- 10	- 1.5
43	92													- 32	- 5.8
44	77	7.75	2180	57	3	.2	5130	290	199	36.5		.88		- 20	- 3.9
45	81	7.67	2150	57	2.95	.2	5130	295	197	35.7		.87		- 23	- 3.1
46	75.5	7.5	2100	53	2.53	.2	5020	295	195	35.5		.87		- 20	- 3.3
47	75	7.95	2100	55	2.58	.2	5200	295	196	35.5		.87		- 19	- 2.9
48	50	8.25	988	22	1.58	.6	2160	215	80	35.6		.87		- 7	- 3.5
51	50	8.12	994	23	2.48	.6	2120	210	81	36.8		.89		- 6	- .2
52														- 13	- 2.4
53	72	8.06	6430	108	160	.4	12800	1800	1630	29.7		2.28		- 16	- 3
54	35	7.98	8210	138	2.29	.3	19000	2550	2060	31.7		2.93		- 5	- 1.3
55	58.3	8.36	7140	119	2.34	.45	13900	1950	1780	32		.45		- 18	- 2.5
56	74.7	8.15	6430	74	1.49	.3	12400	1750	1590	29.9		2.25		- 14	- 3.7
57	36.3	8.16	6130	92	3.75	1.6	12300	1800	1560	28.1		2.1		- 17	- 3.6
58	25	7	16.9	4.7	6.38	3.3	103	11.5	1.9	4.8		.02		26	4.2
59	25	7	6360	74	4.68	1	15900	1060	152	59.2		.62		37	7.8
60	25	7	17	4.7	6.15	3.1	761	5.8	1.5	3.13		.02		23	4.1
61	97													1	.6
62	28.6	6.5												- 12	- 2.8
63														- 13	- 3.2
64	41.5	6												- 7	- 3.5
65														36	20
66														24	15.4
67														41	13.5
68														- 3	- 1.2
69														- 2	- 1
70	25	8.94	241	18.8	11.2	5.2	546	65	23	14.5		.15		47	8.8
71	93.7	7	832	36	.54	<.7	1960	260	40	87		1.04		7	1.3
72	36.5		544	10.7	10.9	5.9	1210	25	207	16.4		.11		- 24	- 4.8
73	62.8	0	13300	240	.5	<.7	24900	6600	132	35.2		9.24		- 2	0.1
76														36	6.6
77														- 29	- 5
78														- 38	- 6.9
79														- 62	- 9
80	20.5	7.04	56	38	46.3	10	297	20	.8	36.4		.04		18	3.7
81	22.1	7.7	212	18.7	27.5	8.3	575	30	4.9	28.3		.06		22	4.5

Table 6.2 continued

Site no.	Temp	pH	Na	K	Ca	Mg	HCO_3	Cl	SO_4	Si	NO_3	B	F	D2H	$\delta^{18}O$
82	20.5	7.45	75	14	19.1	2.1	275	7.5	4.8	37.5		.3		-24	-4.1
83	26.3	7.71	186	26	23.1	10.6	513	27	<.5	30.4		.09		32	5.6
84	20.8	7.82	275	17	11.2	108	626	60	45	31.9		.06		-11	-1.9
85	20.2	7.95	80	15	13.8	1.8	238	8.2	8.7	32.4		.02		-22	-4.4
86	26.2	7.18	122	36	52	28	480	30.5	5.8	46.5		.06		19	3.7
87	25.5	7.97	177	29	10	.6	476	16.8	12	36.3		.04		-29	-4.9
88	23.9	7.77	264	18.2	13.4	1.7	575	59	48	29.1		.06		-11	-1.9
89	24.6	8.2	341	17.7	18.2	2.1	740	100	22	29		.08		6	.3
90	18	8.13	113	14.2	8.8	.6	297	10.6	9	34		.03		-20	-4.2
91	24	7.3	23	9	3.67	.7	77	2.2	1.5	38.2		.02		-13	-3.9
92	21.9	6.99	24	9.4	4.02	.7	88	2.2	1.6	38.6		.02		-17	-3.9
93	23.2	7.47	81	29	26.3	6.1	256	39	35	44.5		.02		-17	-3.5
94	18.6	8.34	797	38	4.51	<.7	1360	390	58	29.2		.11		-8	-1.1
95	24.1	8.2	109	8.6	3.22	.3	223	29	14	20.2		<.02		-16	-3.6
96	22.6	7.01	10.9	5.9	1.71	.6	44	.6	1.1	34.1		.16		-24	-4.7
97	22.6	6.64	37	17	6.1	1.6	124	6.8	2.3	47.6		.02		-18	-4
99	25.7	7.13	98.9	4.6	120	48	308	100	31	29.7				-24	-4.1
100	26.3	6.95	64	16	5.7	.9	151	13	12.6	47		<.02		-28	-4.6
101	20	7.65	26	18	9.6	2.7	90	14	16	36		<.02		-35	-5.3
104	19.6		197	7.1	.5	.1	395	33	22	57		.04		7	4.1
106	52	3.98	97	49	5.4	.5	<1	4.3	262	<.02		.18		10	3.2
107	32.4		957	31	11	.2		900	419						
108	23		379	27	10.8	1.8	713	86	64	40		.95		2	3.5
109	72		489	6.1	3.4	<.1	183	370	299	68		.3		11	3.9
110	152	6.25	584	118	.8	<.1	57	800	30	55.1		7.14		3	2.1
111	159	6.05	265	40	.5	<.1	108	240	23	250		2.53		11	2.6
112	157	6.2	398	37	.3	<.1	334	236	86	212		2.06		13	2.7
113	148	6.2	486	74	.4	<.1	54	624	20.2	248		7.12		10	3.1
114	153	6.2	311	42	.4	<.1	183	194	34	247		2.82		13	3.6
115	152	6.2	386	53	.2	<.1	172	390	151	262		4.78		8	2.8
116	156	6.2	3.2	<.7	.7	<.1	<1	3	12.4	2.3		.95		18	3.7
118	27.9	7	68	15	12	1.3	187	13	9.5	38		<.02		-18	-2.8
121	37.1	6.95	400	48	40	1.4	1120	14	9.1	59		.05		-27	-5
122	30	7	199	32	41.6	3.3	653	13	8.6	49.4		.05		-28	-4.8
124	32.4	6.4	403	64	58	4.9	1100	55	17	61		.14		-24	-3.8
125	27.8	7.95	386	30	13	14	998	78	22	31		.1		-23	-3.5
126	50	8.13	1000	22	1.55	.5	2200	205	79	35.2		.87		-11	-2.99
127	27	8.09	1100	23	2.82	.9	2460	210	80	31.8		.9		-6	.1
128	20	7	59	23	22	15	230	8	31	23		.02			
129	25	7	187	48	38	18	586	12	8.8	43		.03		-28	-4.6

to Lake Naivasha; the furthest is some 6 km away. Seven wells were sampled (sites 80, 81, 83, 84, 86, 88 and 89) and the average and range of analyses for major elements are given in Table 6.4. If the average analysis is compared with the mean for Rift-wall groundwaters it can be calculated that the average concentration increase is by a factor of 3.4, and that most of the ions have a similar ratio to chloride in both groups (Figures 6.4). Only silica differs from this pattern, and this can be attributed to its abundance in the rocks: a similar solubility limit has been reached in both groups.

Table 6.3 Range of concentrations and average major ion values for 10 unmodified Rift-wall waters

Ion	average value mgl^{-1}	range mgl^{-1}
Na	61	11–177
K	13	1–29
Ca	8	1–19
Mg	1.5	0–3
HCO_3	190	44–476
Cl	13	1–50
SO_4	7	1–12
SiO_2	71	22–101

The rather consistent increase in concentration in the Naivasha wells can plausibly be linked to evaporation in the lake, as Glover (1972) noted. Stable isotope results (Section 6.4.3.) are very diagnostic of this process and confirm that the Naivasha wells contain up to 80% of lakewater. It is assumed that the lake is recharged by a combination of river and groundwater in the north-east, which then undergoes evaporative concentration before eventually discharging underground to the south and perhaps north of the lake, which lies at the culmination of the Rift floor. Thus mixing between lakewater and

Table 6.4 Range of concentrations and major ion values for 7 wells containing a large proportion of water from Lake Naivasha

Ion	average value mgl^{-1}	range mgl^{-1}
Na	208	56–275
K	25	17–38
Ca	27	11–52
Mg	9	2–28
HCO_3	543	297–626
Cl	47	20–100
SO_4	18	0–48
SiO_2	71	61–100

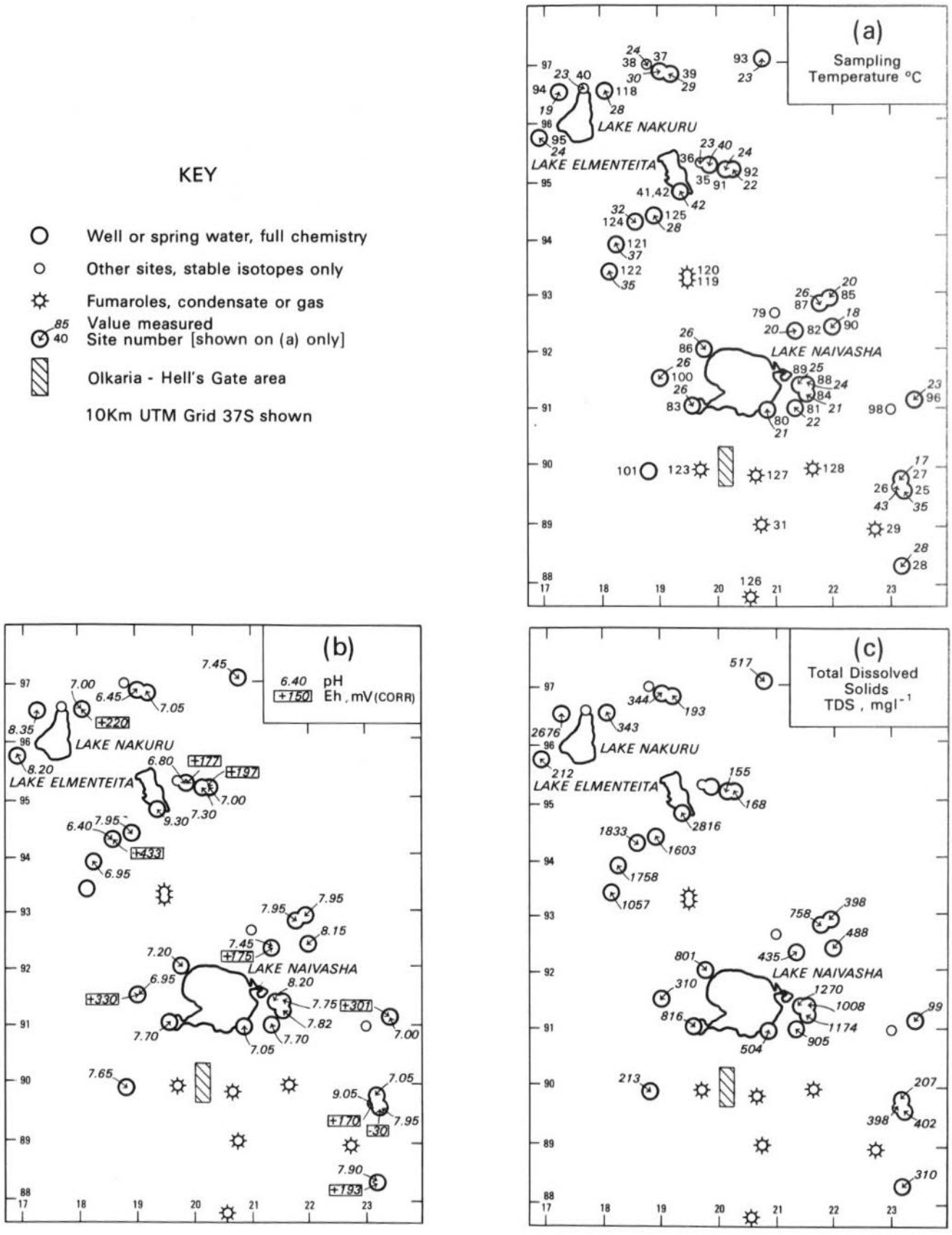

Figure 6.3 Maps of sampling, chemical and isotopic data from the Suswa–Nakuru sector.

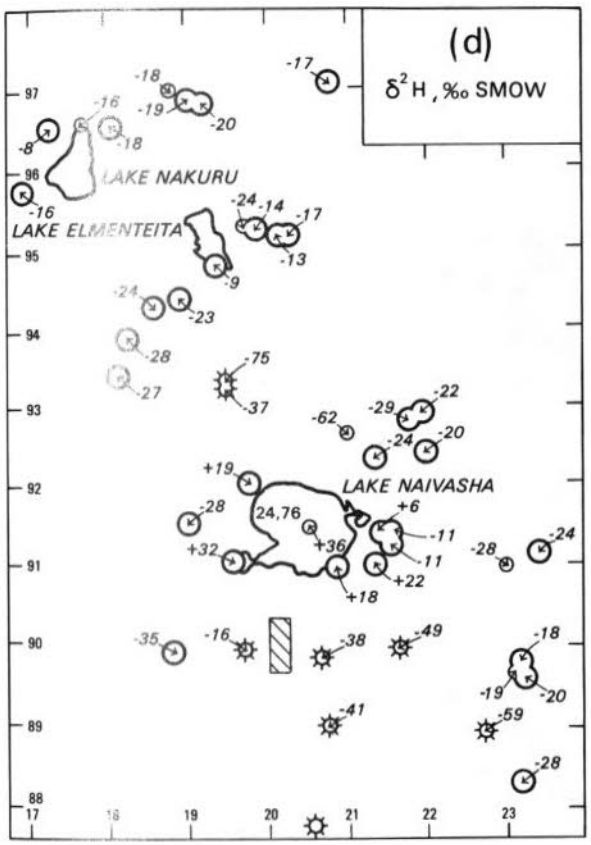
(d)
δ²H, ‰ SMOW
LAKE NAKURU
LAKE ELMENTEITA
LAKE NAIVASHA
24,76

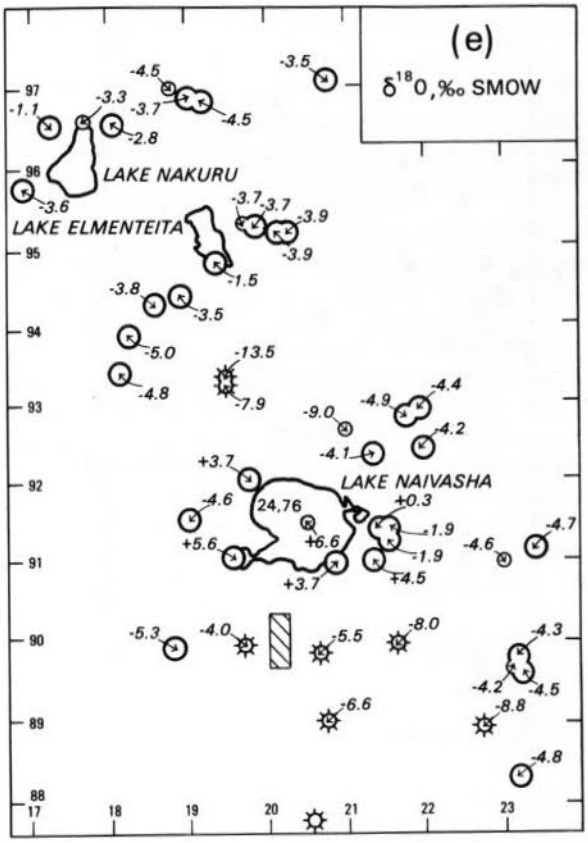
(e)
δ¹⁸O, ‰ SMOW
LAKE NAKURU
LAKE ELMENTEITA
LAKE NAIVASHA
24,76

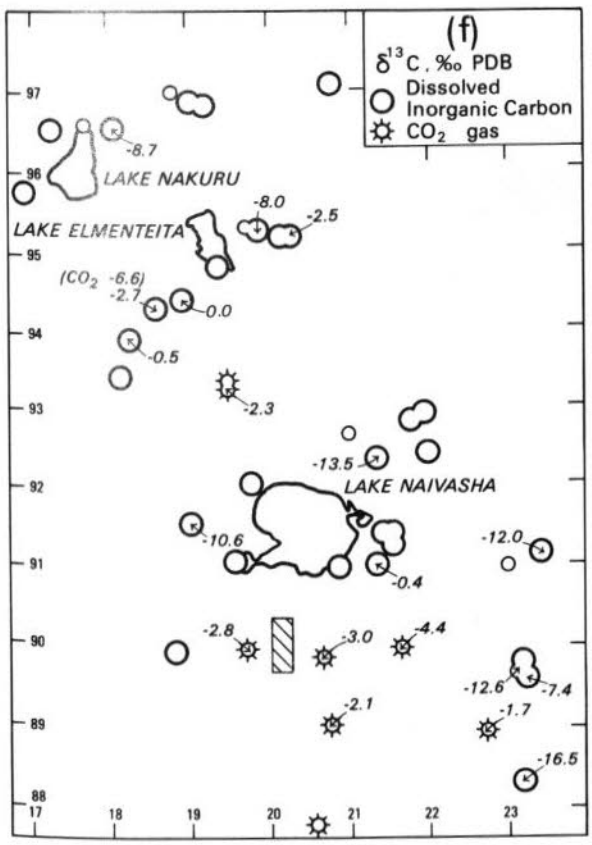
(f)
δ¹³C, ‰ PDB
Dissolved Inorganic Carbon
CO₂ gas
LAKE NAKURU
LAKE ELMENTEITA
LAKE NAIVASHA
(CO₂ -6.6)

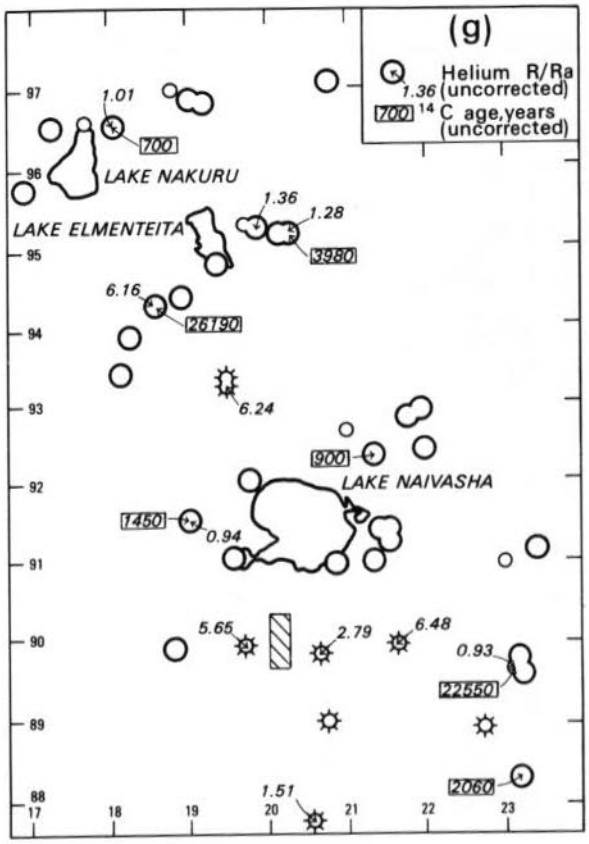
(g)
Helium R/Ra
1.36 (uncorrected)
700 ¹⁴C age, years
(uncorrected)
LAKE NAKURU
LAKE ELMENTEITA
LAKE NAIVASHA

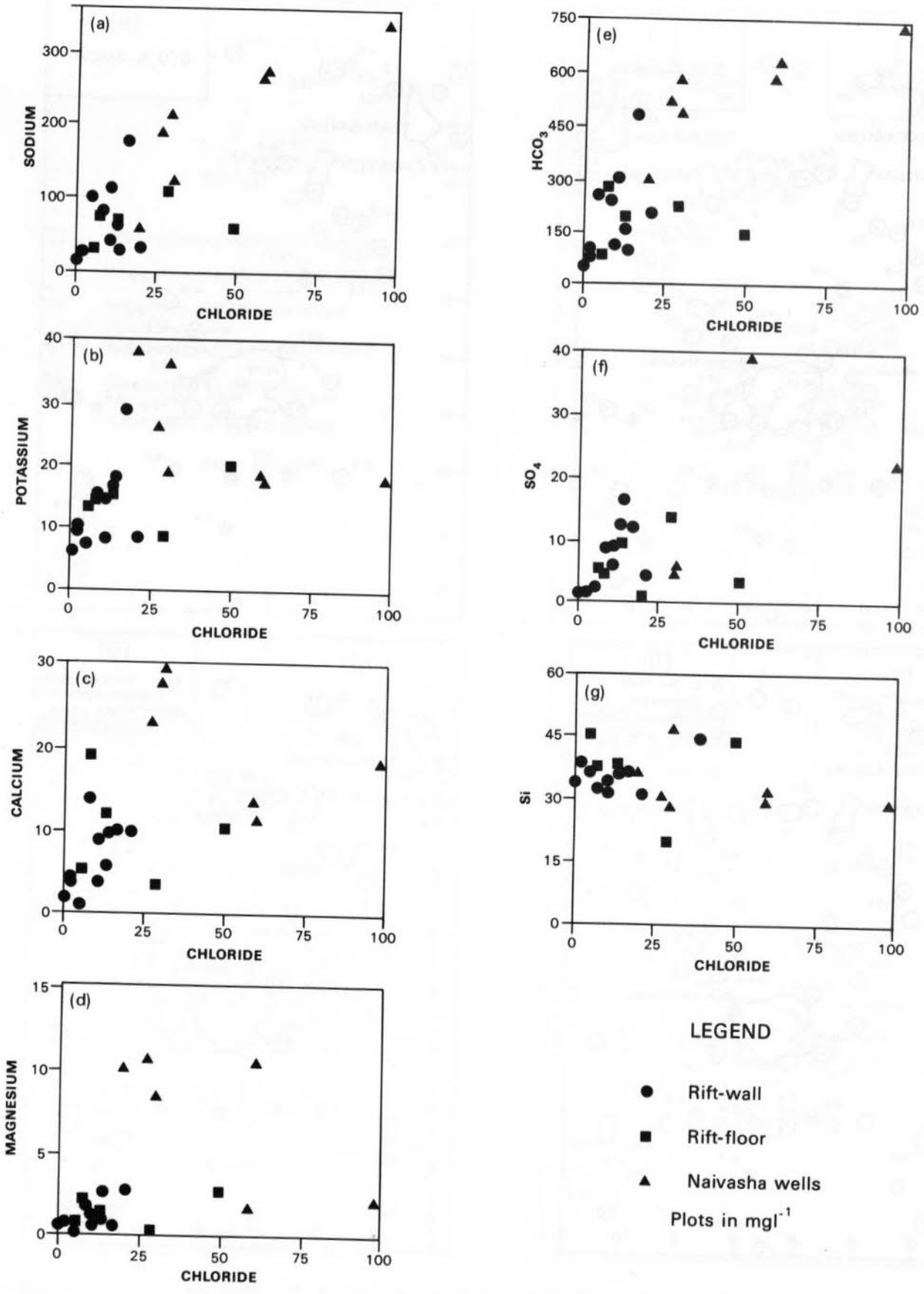

Figure 6.4 Plots of major ions versus chloride for unmodified Rift-wall and Rift-floor groundwater, and for wells with a large proportion of water from Lake Naivasha.

Table 6.5 Chemistry and isotopic composition of water from the 'Badlands' wells and warm springs of Lake Elmenteita

Property	Sample sites 122	121	124	125	41–42
Temperature, °C	35	37	32	28	42
pH	—	7.0	6.4	8.0	9.2
Na, mgl^{-1}	199	400	403	386	917
K, mgl^{-1}	32	48	64	30	33
Ca, mgl^{-1}	42	40	58	13	13
Mg, mgl^{-1}	3	1	5	14	0
HCO_3, mgl^{-1}	653	1120	1100	998	1230
Cl, mgl^{-1}	13	14	55	78	425
SO_4, mgl^{-1}	9	9	17	22	75
SiO_2, mgl^{-1}	106	126	131	66	123
TDS, mgl^{-1}	1057	1758	1833	1603	2816
δ^2H, ‰	−27	−28	−24	−23	−9
$\delta^{18}O$, ‰	−4.8	−5.0	−3.8	−3.5	−1.5

	Average Olkaria thermal water	Average Naivasha well water	41–42	Indicated lakewater contribution to 41–42
Na/Cl	0.98	4.4	2.2	35%
HCO_3/Cl	0.36	11.6	2.9	23%
SO_4/Cl	0.14	0.38	0.18	17%

shallow groundwater would occur along flowpaths away from the lake, giving rise to the chemical and isotopic properties of the Naivasha group of well waters. There is no evidence that the well waters are linked in any way to possible outflows from Olkaria or Eburru.

Waters of modified type sampled north of Eburru include four wells between the massif and Lake Elmenteita (sites 121, 122, 124 and 125), a warm spring complex at the southern end of Elmenteita (site 41/42), and a well to the north-west of Lake Nakuru (site 94). The remainder of sampling points in this area are considered to be unmodified groundwaters.

The sample from site 94 is best explained by considering it to be outflow from the highly saline Lake Nakuru, though much diluted by fresher water from the sides of the Rift (Section 6.4.3.4). The well has an ambient temperature which effectively rules out the possibility that it is some kind of thermal outflow perhaps flowing towards the lake. Although Lake Nakuru is highly saline and therefore typical of a closed basin lake, the possibility of a small amount of flow out to the northwest does exist on piezometric grounds (Section 6.3.4). In the next section it is noted that no traces of Nakuru-type water are seen in wells to the north of Nakuru.

The sequence of sites running north-east from well C431 (site 122) to the Elmenteita springs (41 and 42) is interesting as it presents the only opportunity (apart from fumaroles) of looking at the remnants of a geothermal outflow in the Suswa to Nakuru sector of the Rift. All the wells exceed the unmodified Rift-wall type of composition in terms of dissolved constituents (Table 6.5), and it is known from $^3He/^4He$ measurements at site 124 (Section 6.4.6) that a high temperature upflow must ultimately be responsible for the chemistry of much of the water flowing north from Eburru.

The increase in TDS values from about 1000 to 3000 mg/l to the north-east does not necessarily imply a greater outflow contribution. The stable isotope results (Section 6.4.3.4) imply a lakewater contribution of between 30–35% for the springs while the data for the wells to the south-west of the springs suggests a much smaller or totally absent lakewater contribution—indeed the slight increase in heavy isotopes might simply be due to steam loss from the underlying groundwater.

In view of the low chloride contents measured in the wells it is unlikely that these waters are truly representative of primary outflow from Eburru. The high bicarbonate values may be the result of condensation of CO_2 and associated gases in water which, on the basis of stable isotopes, are similar to Rift wall compositions. It is shown elsewhere (Section 6.4.3.5) that Eburru upflow water is probably very similar in isotopic terms to Rift-wall water, and therefore mixing or steam heating involving shallow and thermal waters in the Eburru outflow area is unlikely to show up isotopically. However, the likelihood that the well waters are of secondary composition is not supported by the high SiO_2 and Li results, particularly from sites 121 and 122.

Nevertheless, if the wells are considered to be secondary manifestations of thermal outflow from Eburru, then the low temperatures of the waters and the lack of evidence of secondary steam production in the 'badlands' area is an indication that the quantities of cold, shallow groundwater flowing from the Rift wall (including Western Eburru) are of sufficient volume to 'quench' steam boiling off the thermal outflow. Only where the outflow water itself is ascending towards the southern end of Lake Elmenteita and mixing with water flowing north from Lake Naivasha does the shallow groundwater temperature become higher.

If, however, the SiO_2 and Li results are given weight then it must be assumed that the Eburru upflow water is considerably lower in chloride than the thermal fluid at Olkaria. To some extent this is likely, as the Eburru system is considered on isotopic grounds to derive from the low-chloride Rift-wall water rather than the higher-chloride lakewater which feeds Olkaria. In this case it must be assumed that there is only a small upward leakage of outflow water on its journey north to Lake Elmenteita. The result appears to be a ternary mixing system between Rift-wall water, thermal outflow and Lake Naivasha water.

Despite the differences between these two models, it is clear that there must be outflow north from Eburru and also underflow from Lake Naivasha. These two sources combine to account for the apparent water supply deficiency in the Elmenteita basin noted by McCann (1972).

6.4.2.2 Surface, thermal and non-thermal waters: Nakuru to Silale

Introduction

The rather limited number of samples collected and analysed by the BGS-MERD team from this area has been supplemented by 11 samples collected between northern Lake Bogoria and Nakuru by two MERD staff members (Messrs M Arusei and J Wambugu) as part of their MSc course work at Leeds University, where the samples received chemical analysis. Isotopic analysis of these samples was performed at BGS Wallingford and the results are considered in Section 6.4.3.6 of this report. Water chemistry results are presented in Tables 6.2 and 6.6 and Figures 6.5a–d. Major element chemistry is now considered.

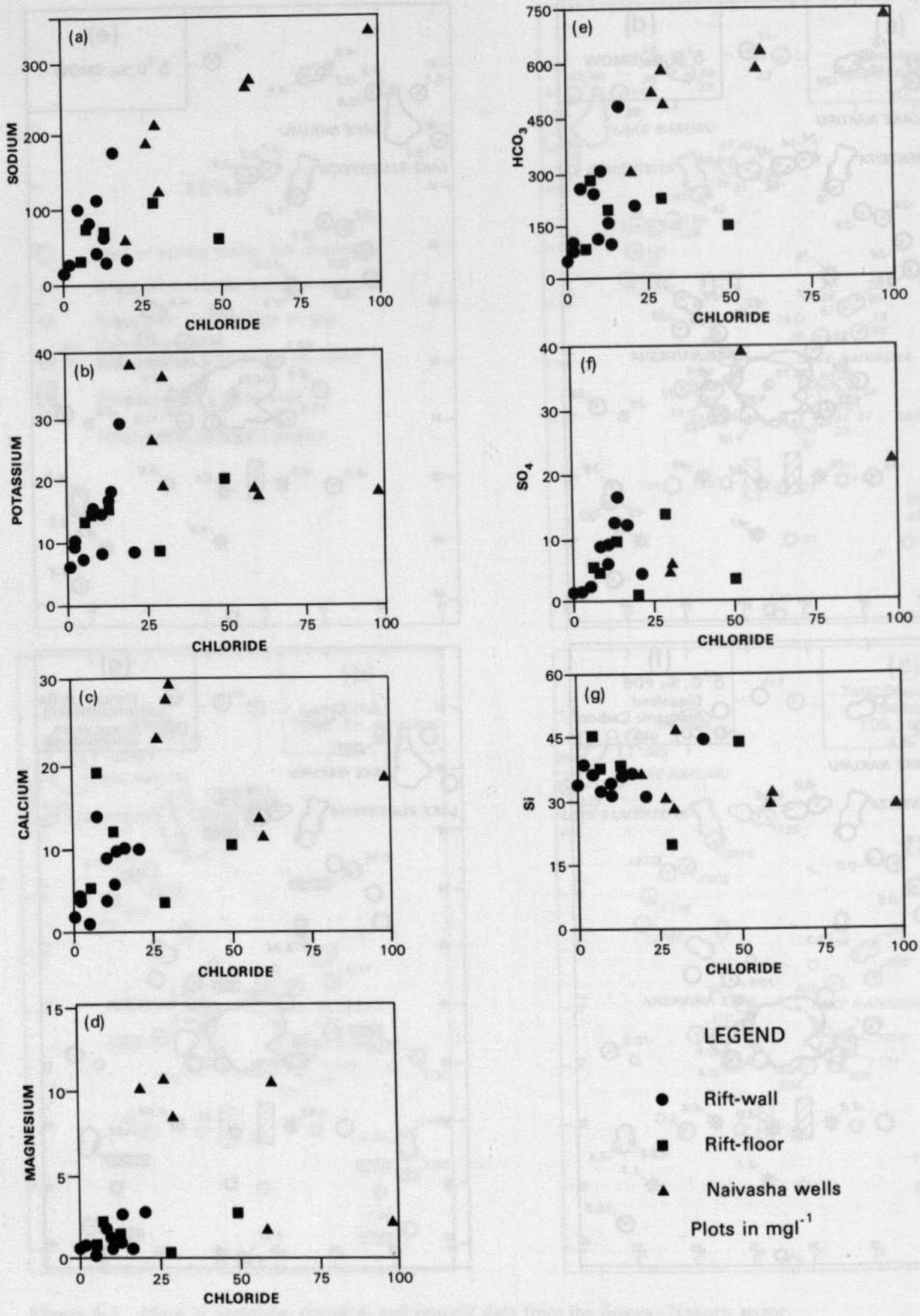

Figure 6.4 Plots of major ions versus chloride for unmodified Rift-wall and Rift-floor groundwater, and for wells with a large proportion of water from Lake Naivasha.

Table 6.5 Chemistry and isotopic composition of water from the 'Badlands' wells and warm springs of Lake Elmenteita

Property	Sample sites 122	121	124	125	41–42
Temperature, °C	35	37	32	28	42
pH	—	7.0	6.4	8.0	9.2
Na, mgl^{-1}	199	400	403	386	917
K, mgl^{-1}	32	48	64	30	33
Ca, mgl^{-1}	42	40	58	13	13
Mg, mgl^{-1}	3	1	5	14	0
HCO_3, mgl^{-1}	653	1120	1100	998	1230
Cl, mgl^{-1}	13	14	55	78	425
SO_4, mgl^{-1}	9	9	17	22	75
SiO_2, mgl^{-1}	106	126	131	66	123
TDS, mgl^{-1}	1057	1758	1833	1603	2816
δ^2H, ‰	−27	−28	−24	−23	−9
$\delta^{18}O$, ‰	−4.8	−5.0	−3.8	−3.5	−1.5

	Average Olkaria thermal water	Average Naivasha well water	41–42	Indicated lakewater contribution to 41–42
Na/Cl	0.98	4.4	2.2	35%
HCO_3/Cl	0.36	11.6	2.9	23%
SO_4/Cl	0.14	0.38	0.18	17%

shallow groundwater would occur along flowpaths away from the lake, giving rise to the chemical and isotopic properties of the Naivasha group of well waters. There is no evidence that the well waters are linked in any way to possible outflows from Olkaria or Eburru.

Waters of modified type sampled north of Eburru include four wells between the massif and Lake Elmenteita (sites 121, 122, 124 and 125), a warm spring complex at the southern end of Elmenteita (site 41/42), and a well to the north-west of Lake Nakuru (site 94). The remainder of sampling points in this area are considered to be unmodified groundwaters.

The sample from site 94 is best explained by considering it to be outflow from the highly saline Lake Nakuru, though much diluted by fresher water from the sides of the Rift (Section 6.4.3.4). The well has an ambient temperature which effectively rules out the possibility that it is some kind of thermal outflow perhaps flowing towards the lake. Although Lake Nakuru is highly saline and therefore typical of a closed basin lake, the possibility of a small amount of flow out to the northwest does exist on piezometric grounds (Section 6.3.4). In the next section it is noted that no traces of Nakuru-type water are seen in wells to the north of Nakuru.

The sequence of sites running north-east from well C431 (site 122) to the Elmenteita springs (41 and 42) is interesting as it presents the only opportunity (apart from fumaroles) of looking at the remnants of a geothermal outflow in the Suswa to Nakuru sector of the Rift. All the wells exceed the unmodified Rift-wall type of composition in terms of dissolved constituents (Table 6.5), and it is known from $^3He/^4He$ measurements at site 124 (Section 6.4.6) that a high temperature upflow must ultimately be responsible for the chemistry of much of the water flowing north from Eburru.

The increase in TDS values from about 1000 to 3000 mg/l to the north-east does not necessarily imply a greater outflow contribution. The stable isotope results (Section 6.4.3.4) imply a lakewater contribution of between 30–35% for the springs while the data for the wells to the south-west of the springs suggests a much smaller or totally absent lakewater contribution—indeed the slight increase in heavy isotopes might simply be due to steam loss from the underlying groundwater.

In view of the low chloride contents measured in the wells it is unlikely that these waters are truly representative of primary outflow from Eburru. The high bicarbonate values may be the result of condensation of CO_2 and associated gases in water which, on the basis of stable isotopes, are similar to Rift wall compositions. It is shown elsewhere (Section 6.4.3.5) that Eburru upflow water is probably very similar in isotopic terms to Rift-wall water, and therefore mixing or steam heating involving shallow and thermal waters in the Eburru outflow area is unlikely to show up isotopically. However, the likelihood that the well waters are of secondary composition is not supported by the high SiO_2 and Li results, particularly from sites 121 and 122.

Nevertheless, if the wells are considered to be secondary manifestations of thermal outflow from Eburru, then the low temperatures of the waters and the lack of evidence of secondary steam production in the 'badlands' area is an indication that the quantities of cold, shallow groundwater flowing from the Rift wall (including Western Eburru) are of sufficient volume to 'quench' steam boiling off the thermal outflow. Only where the outflow water itself is ascending towards the southern end of Lake Elmenteita and mixing with water flowing north from Lake Naivasha does the shallow groundwater temperature become higher.

If, however, the SiO_2 and Li results are given weight then it must be assumed that the Eburru upflow water is considerably lower in chloride than the thermal fluid at Olkaria. To some extent this is likely, as the Eburru system is considered on isotopic grounds to derive from the low-chloride Rift-wall water rather than the higher-chloride lakewater which feeds Olkaria. In this case it must be assumed that there is only a small upward leakage of outflow water on its journey north to Lake Elmenteita. The result appears to be a ternary mixing system between Rift-wall water, thermal outflow and Lake Naivasha water.

Despite the differences between these two models, it is clear that there must be outflow north from Eburru and also underflow from Lake Naivasha. These two sources combine to account for the apparent water supply deficiency in the Elmenteita basin noted by McCann (1972).

6.4.2.2 Surface, thermal and non-thermal waters: Nakuru to Silale

Introduction

The rather limited number of samples collected and analysed by the BGS-MERD team from this area has been supplemented by 11 samples collected between northern Lake Bogoria and Nakuru by two MERD staff members (Messrs M Arusei and J Wambugu) as part of their MSc course work at Leeds University, where the samples received chemical analysis. Isotopic analysis of these samples was performed at BGS Wallingford and the results are considered in Section 6.4.3.6 of this report. Water chemistry results are presented in Tables 6.2 and 6.6 and Figures 6.5a–d. Major element chemistry is now considered.

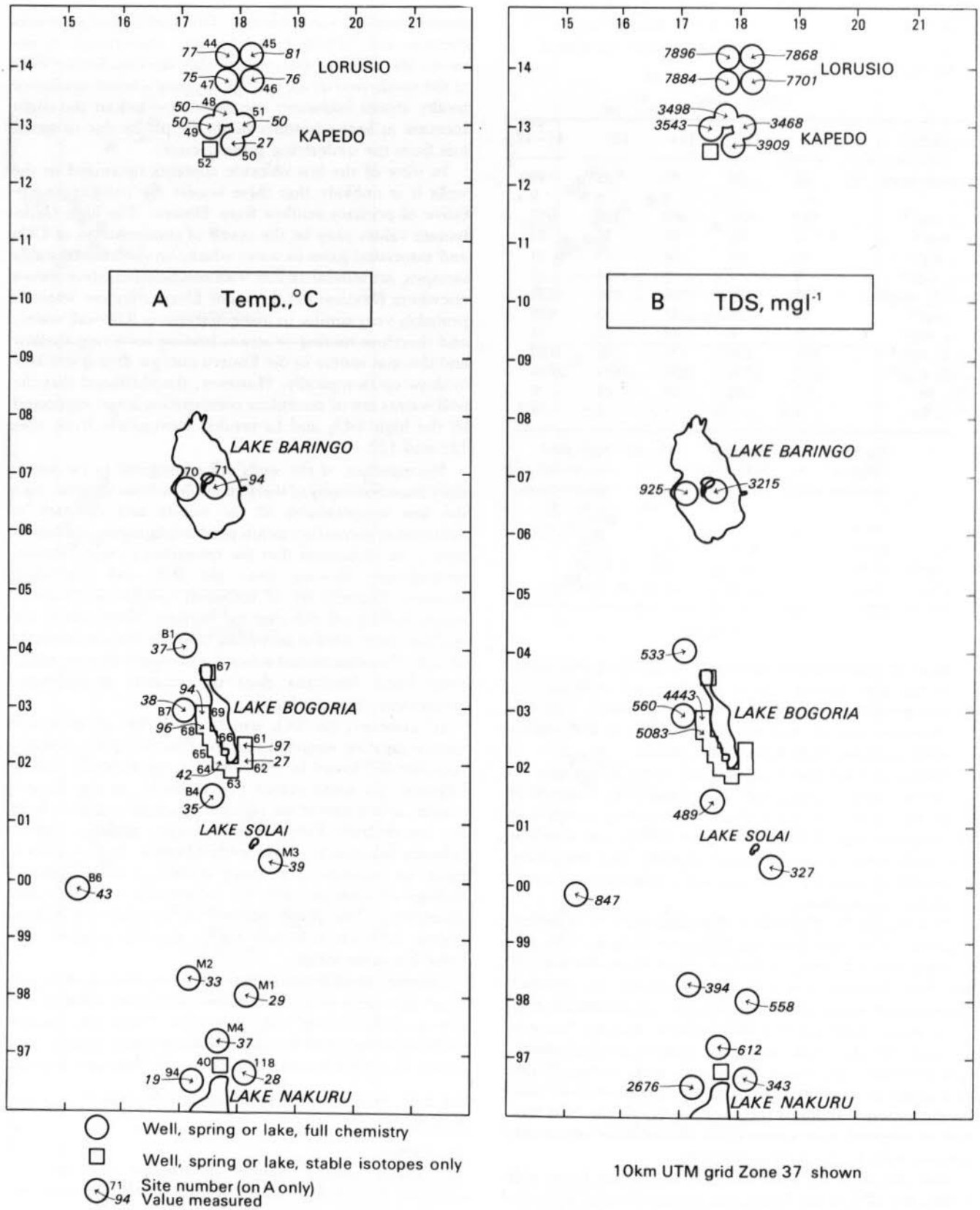

Figure 6.5 Maps of chemical and isotopic data for the Nakuru–Silale sector ('M' and 'B' numbers relate to samples collected by MERD).

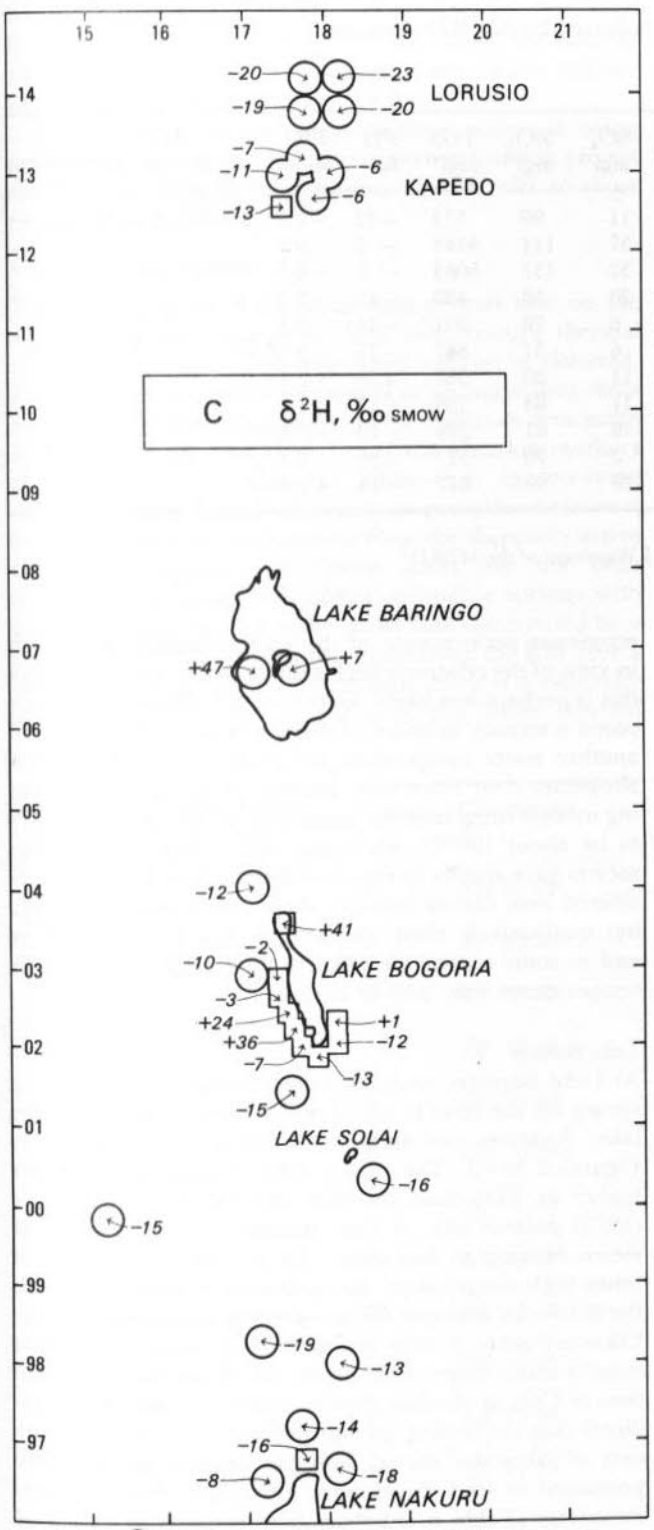

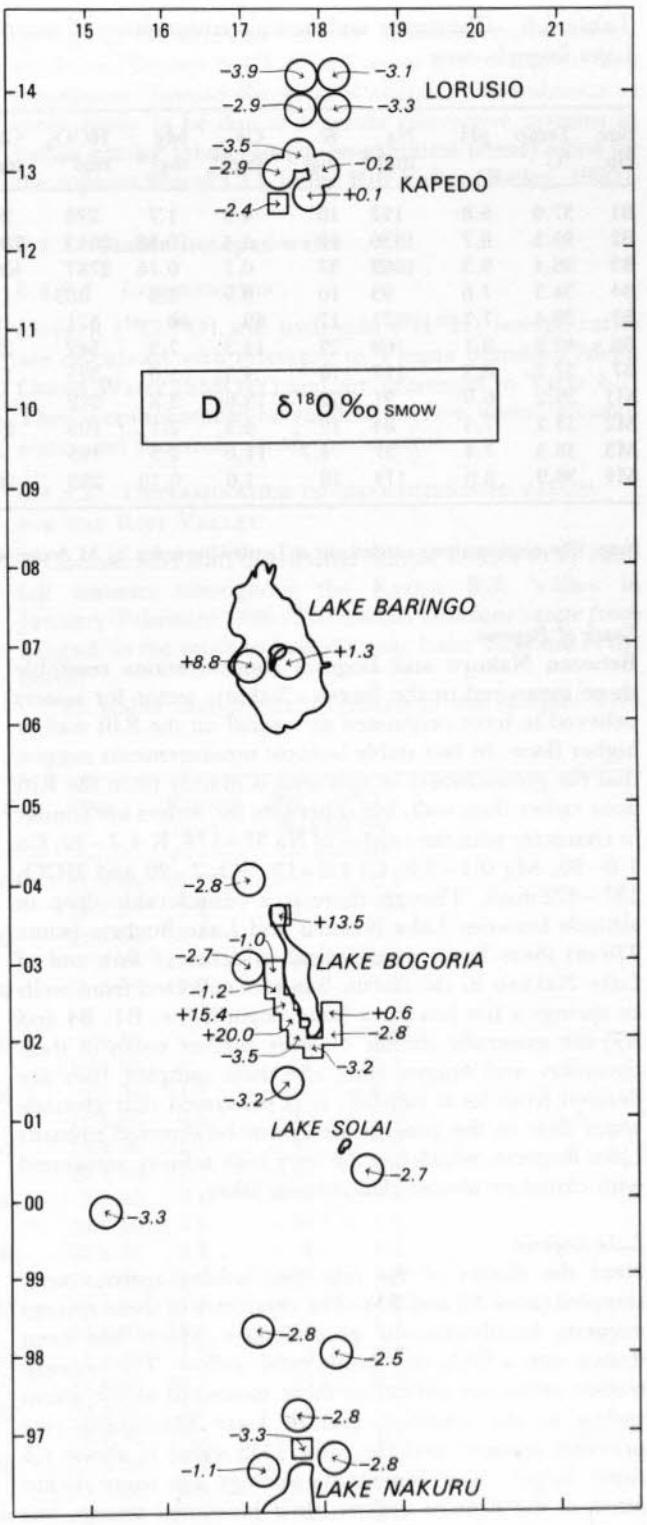

○ Well, spring or lake, full chemistry

□ Well, spring or lake, stable isotopes only

-94 Value measured

10km UTM grid Zone 37 shown

Table 6.6 Chemistry and isotopic composition of samples collected by MERD personnel in the Lake Bogoria area

Site No.	Temp °C	pH	Na mgl^{-1}	K mgl^{-1}	Ca mgl^{-1}	Mg mgl^{-1}	HCO_3 mgl^{-1}	Cl mgl^{-1}	SO_4 mgl^{-1}	SiO_2 mgl^{-1}	TDS mgl^{-1}	δ^2H ‰	$\delta^{18}O$ ‰
B1	37.0	6.8	117	10	4.9	1.7	278	20	11	90	533	−12	−2.8
B2	93.5	8.7	1336	12	1.4	0.40	2645	280	57	111	4443	− 3	−0.7
B3	96.4	9.3	1669	37	0.7	0.16	2787	400	52	137	5083	− 2	−0.5
B4	34.5	7.6	93	10	8.9	3.8	283	11.8	20	58	489	−15	−3.2
B5	29.4	7.7	121	17	49	40	671	16.5	6	70	991	−14	−3.1
B6	42.9	8.1	169	29	14.3	7.5	542	28	6	51	847	−15	−3.3
B7	37.7	6.3	117	10	4.5	1.0	325	11.8	11	80	560	−10	−2.7
M1	29.2	6.9	91	22	19.6	2.8	322	5.2	11	84	558	−13	−2.5
M2	33.2	7.5	84	10	6.3	1.1	195	21	16	61	394	−19	−2.8
M3	38.5	7.4	37	4.7	11.6	2.5	195	4.2	2	70	327	−16	−2.7
M4	36.9	8.6	174	10	1.0	0.10	283	26	20	98	612	−14	−2.8

Note: Chemical analyses carried out at Leeds University by M Arusei and J Wambugu of the MERD

South of Bogoria

Between Nakuru and Bogoria concentrations resemble those measured in the Suswa–Nakuru sector for waters believed to have originated as rainfall on the Rift wall or higher floor. In fact stable isotopic measurements suggest that the groundwater in this area is mainly from the Rift floor rather than wall, but otherwise the waters are similar in character with the ranges of Na 37–174, K 4.7–22, Ca 1.0–20, Mg 0.1–3.8, Cl 4.2–13, SO_4 2–20 and HCO_3 187–322 mg/l. Though there is a considerable drop in altitude between Lake Nakuru and Lake Bogoria (some 770 m) there is no geochemical evidence of flow out of Lake Nakuru to the north. Samples collected from wells or springs a few km from Lake Bogoria (i.e. B1, B4 and B7) are generally similar to those further south in their chemistry and suggest that, like these samples, they are derived from local rainfall. It is presumed that groundwater flow in the general area must be directed towards Lake Bogoria, which has the very high salinity associated with closed or almost closed basin lakes.

Lake Bogoria

Near the shores of the lake two boiling springs were sampled (sites B2 and B3). The chemistry of these springs suggests locally-derived groundwater which has been drawn into a CO_2-rich geothermal upflow. The concentration ratios are similar to those measured at the warm spring at the southern end of Lake Elmenteita (see previous section) and the total TDS value is about 1.5 times larger. The Elmenteita springs are some 15 km north of the Eburru upflow, their presumed source, but issue at only about 40°C compared to the boiling temperatures of the Bogoria springs. This suggests that the Bogoria springs are much closer to their upflow and may be rapidly cooling by adiabatic rather than conductive processes; the apparent steam loss identified from stable isotopic measurement supports this (Section 6.4.3.6).

The silica and alkali geothermometers give temperatures of below 150°C for the Bogoria springs; such temperatures at depth seem too low in view of the vigorous boiling of the springs. This implies that upflow is being modified by a cooler inflow at some stage. Isotopic evidence points to a small amount of lakewater contamination but suggests that steam heating is not involved; on this basis the lakewater could be contributing at various levels in the thermal circulation. Equally, non-thermal 'fresh' groundwater could be responsible for the erroneous performance of the geothermometers, though in view of the relatively high salinity of the boiling springs this is perhaps less likely. Geotermica Italiana (1987) proposed a ternary mixture of thermal water, lakewater and another water component, the origin of which was not altogether clear from their isotopic evidence. Their mixing models suggested the maximum temperature at depth to be about 190°C, while gas and isotopic geothermometers gave results in excess of 200°C. The few data considered here cannot confirm these results quantitatively, but qualitatively their similarity to the Eburru outflow and to some extent the Olkaria fluid suggests that such temperatures may well be correct.

Lake Baringo

At Lake Baringo, samples were collected from a boiling spring on the central island of Ol Kokwe, and from the lake. Analyses are given in Table 6.2 and shown in Figures 6.5a–d. The spring water is almost four times higher in TDS than the lake and therefore, as Glover (1972) pointed out, is most unlikely to be the result of steam heating of lakewater. Its chemistry is typical of other high temperature thermal waters further south in the Rift — for example there is a strong resemblance to the Olkaria fluid (e.g. very similar Cl/SO_4 ratios) except that there is much more bicarbonate, which implies condensation of CO_2 at shallow depths. Stable isotope results indicate that the boiling springs probably contain a proportion of lakewater mixed with the original groundwater presumed to feed the system. Silica and alkali geothermometers (Table 6.15) show temperatures in excess of 175°C, and it is concluded from this that lakewater must be entering the system before or during heating; if lakewater were mixing at shallow depths interference with the geothermometers would tend to result, as is apparently the case at Lake Bogoria.

Kapedo and Lorusio

Two groups of hot springs north of Lake Baringo were sampled. The results (Table 6.2, Figures 6.5a–d) show that the waters are not dissimilar in element ratios, but that the Lorusio group is twice as high in TDS and contains proportionately higher amounts of HCO_3. Silica and alkali geothermometres give rather similar temperatures at depth for each group in the range 120–150°C. Since the Lorusio group is hotter and more concentrated in TDS, it is tempting to consider that the Kapedo group

is the result of dilution of the Lorusio water, but isotopic measurements make this explanation inplausible and imply a separate origin (Section 6.4.3.6).

Further work on the origin of these waters is being undertaken during an extention of the exploration project north of the Equator and readers should refer to those results when available.

6.4.2.3 Conclusions

The consideration of chemical data reveals that on the whole large-scale mixing of high temperature thermal outflow with 'fresh' Rift-wall water cannot be detected. Few ambient or slightly warm well or spring waters show any evidence of mixing, although the badlands area north of Eburru ia an exception. Otherwise thermal outflows often appear very close to lakes—i.e. in low-lying discharge areas. Lake Naivasha is an exception because it is itself recharging, and outflow from the thermally active Olkaria, Longonot and Suswa areas has not been detected. The association of hot or boiling springs with low-lying lakes has led to the belief that there could be a general body of thermal water underlying the Rift over a large area (Mahon, 1972). Certainly there is a similarity between the chemistry of many of the hotter thermal springs as far north as Lorusio. However stable isotope evidence (Section 6.4.3 *et seq.*) tends not to support this conclusion. Instead the general chemical resemblance is more likely to be due to separate convective systems in rather similar lithologies (in geochemical terms) aided by the copious flux of CO_2 in the Rift Valley (Bailey, 1980).

6.4.3 Stable isotopes-water

6.4.3.1 Introduction

Oxygen ($^{18}O/^{16}O$) and hydrogen ($^{2}H/^{1}H$) isotope ratios are calculated with reference to Vienna Standard Mean Ocean Water (SMOW) and are presented in Table 6.2. They were measured on rainfall, surface water, groundwater and fumarole steam condensates.

6.4.3.2 Determination of characteristic values for the Rift Valley

Counterpart staff distributed sample bottles to 21 rainfall stations throughout the Kenya Rift Valley in January/February 1986. The station locations range from Magadi in the south to Lodwar near Lake Turkana in the north.

The stable isotope characteristics of the samples were

Table 6.7 Stable isotope values of rainfall in the Rift Valley

Station	Coordinates	Altitude (m)	Date	Rainfall (mm)	δ^2H ‰ SMOW	$\delta^{18}O$ ‰ SMOW
1	AH 99 91	600	21.3.86	16.3	− 7	+ 0.8
			31.3.86	2.6	+22	+ 5.4
2	BJ 16 26	600	21.3.86	8.4	− 8	− 0.3
			7.4.86	11.4	−14	− 2.1
3	BJ 37 37	1000	18.3.86	3.2	+12	+ 1.7
			—	—	—	—
4	ZP 18 30	1800	6.4.86	?	−10	− 3.2
			10.4.86	?	−64	−10.2
5	ZP 20 80	1900	5.3.86	14.3	+ 5	− 0.2
			11.4.86	6.6	−30	− 6.8
6	ZQ 16 36	2760	18.4.86	21.5	−47	− 9.0
			20.4.86	22.2	−18	− 4.8
7	BJ 31 98	2200	7.3.86	8.4	−39	− 5.8
			23.4.86	7.6	−36	− 5.6
8	AK 42 21	2550	10.3.86	8.8	− 4	− 2.3
			22.4.86	49.0	−23	− 4.9
9	BK 14 20	1920	10.3.86	22.2	− 7	− 4.2
			10.4.86	16.1	−39	− 6.4
11	BK 02 45	2000	12.4.86	4.2	− 3	− 0.3
			23.4.86	34.7	−53	− 8.2
12	AK 73 69	1850	20.3.86	2.0	− 4	− 1.4
			18.4.86	11.0	− 5	− 1.3
13	BJ 41 79	2340	21.3.86	13.7	−14	− 3.9
			23.4.86	18.4	−41	− 7.2
14	ZR 04 04	2100	18.3.86	23.3	0	− 2.0
			?	?	+ 3	− 1.9
15	AL 72 29	1150	20.3.86	10.7	+ 2	+ 0.5
			10.4.86	39.7	−11	− 0.5
16	ZR 30 06	1550	18.3.86	8.0	−20	− 5.5
			4.7.86	25.0	− 5	+ 0.7
17	AL 76 38	1000	10.4.86	17.0	−19	− 4.2
			20.4.86	19.2	− 5	− 2.8
18	ZR 05 54	2050	7.3.86	10.1	− 4	− 1.8
			10.4.86	16.8	−47	− 8.1
19	AM69 05	900	7.3.86	16.1	− 1	+ 0.1
			22.3.86	5.4	0	− 0.4
20	BM 43 21	2000	18.3.86	4.4	−31	− 4.4
			21.4.86	10.2	−16	− 2.4
21	35°40′E 2°23′N	880	5.3.86	32.3	− 7	− 2.2
			7.3.86	23.3	− 1	− 1.8
22	35°36′E 3°07′N	550	4.3.86	28.9	+19	+ 1.9
			24.4.86	33.4	−21	− 4.6

determined at Wallingford using the methods of Darling et al. (1982). $\delta^{18}O$ and $\delta^{2}H$ values are given in Table 6.7 and are plotted on Figure 6.6. Data from three rainfall samples taken in 1985 are also included in the figure. Least squares linear regression analysis was used to identify the line

$$\delta^{2}H = 5.56\,\delta^{18}O + 2.04 \quad (r2 = 0.88) \qquad (3)$$

through the data. In addition lines were fitted separately to data for the smaller and larger rainfall events to check for bias (such as that related to the 'amount effect' (Dansgaard, 1964) or to possible evaporation from rain collectors), but none was found.

Equation 3 has a smaller slope than that of the world meteoric line proposed by Craig (1963) with a slope of 8; this is probably because rain over the Rift Valley evaporates somewhat as it falls. A regression calculated for 80 Rift Valley groundwaters from Magadi to Silale (Figure 6.7) gave a slope very similar to that defined by rainfall:

$$\delta^{2}H = 5.49\,\delta^{18}O + 0.08 \quad (r2 = 0.81) \qquad (4)$$

This suggests that the rainfall line, though based on sampling over a limited period of time, is likely to be reasonably accurate. Additional support is provided by studies outside the Rift: in the Chyulu Hills of south-east Kenya the following relationship was observed for 35 samples (BGS unpublished data):

$$\delta^{2}H = 5.68\,\delta^{18}O + 6.04 \quad (r2 = 0.89) \qquad (5)$$

This indicates that rather low meteoric gradients are found in southern Kenya as a whole and are not confined to rainfall in the Rift Valley.

However, rather depleted water from the Malewa River which rises in the Nyandurua mountains is seen to fall on the world meteoric line. This implies that the modifying influences are restricted to lower altitudes.

6.4.3.3 Altitude and latitude effects

The high topographic relief of the Kenya Rift Valley makes it likely that significant variations with altitude in the mean isotopic composition of rainfall will occur. This was investigated for the rainfall samples by plotting $\delta^{18}O$ and $\delta^{2}H$ against height. Taking height as the controlled variable in each case a least squares regression line was fitted to the data sets giving:

$$\delta^{18}O = -0.0029 \times \text{altitude (m)} + 1.99 \qquad (6)$$

$$\delta^{2}H = -0.0148 \times \text{altitude (m)} + 10.82 \qquad (7)$$

Scatter in the data probably results from the limited number of samples obtained from each station. Individual rainfall events at a given station can give widely differing isotopic results, as shown in Table 6.7, because evaporation and temperature effects will be different for different rainfall events. Many samples from a given station would however be expected to have isotopic compositions which fall around a mean, dependent mainly on the altitude.

The change in $\delta^{18}O$ is estimated as $-0.29‰$ (i.e. decrease) for every 100 m of ascent from equation 6. This compares favourably with values obtained elsewhere; i.e. $-0.2‰$ for Sweden, $-0.4‰$ (French Alps), $-0.28‰$ (Czechoslovakia), $-0.26‰$ (Nicaragua), $-0.18‰$ (Cameroon), $-0.16‰$ (Greece) (figures quoted in Darling and Lardner, 1985). Few studies of deuterium variation with height are available but it is assumed that if the figure for oxygen is accepted, then the estimated variation of $-1.5‰$ per 100 m for $\delta^{2}H$ from equation 7 can also be accepted because of the close correlation between $\delta^{2}H$ and $\delta^{18}O$ described by equation 3.

The possible effect of latitude on the isotopic characteristics of the rainfall samples has been examined, however the hypothesis of a latitude dependent effect is regarded as inadequately supported by the available data. Also there was no evidence of a systematic variation in isotopic composition from one side of the Rift to the other.

6.4.3.4 Surface and low-temperature groundwater: Suswa to Nakuru

In this area a typical stable isotope value for groundwater from the side of the Rift is $-28‰$ $\delta^{2}H$, $-4.8‰$ $\delta^{18}O$, which is similar to values measured on the Kinangop plateau (Figures 6.3d and e). Slightly lighter Rift-wall waters were measured (up to $-35‰$ $\delta^{2}H$, $-5.3‰$ $\delta^{18}O$) in a few places, but there is no evidence of the highly depleted isotopic compositions presumed to exist in the Nyandarua (Aberdare) Mountains to the north-east and which are measured in the main river (River Malewa)

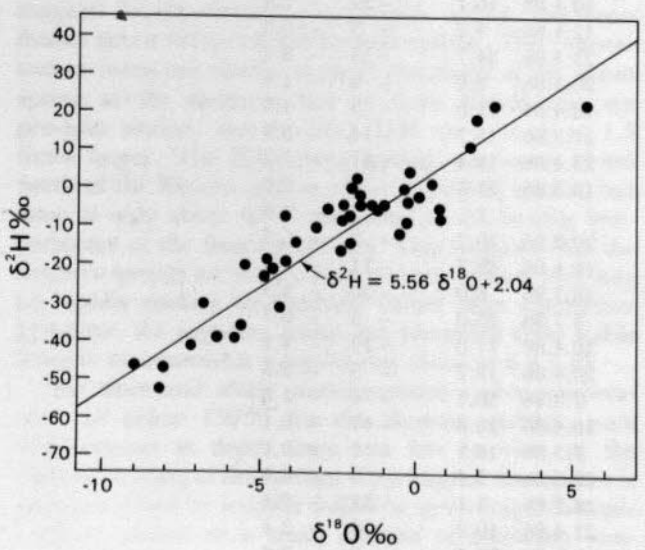

Figure 6.6 Delta-diagram of rainfall stable isotope data from collection stations in the Magadi–Silale sector.

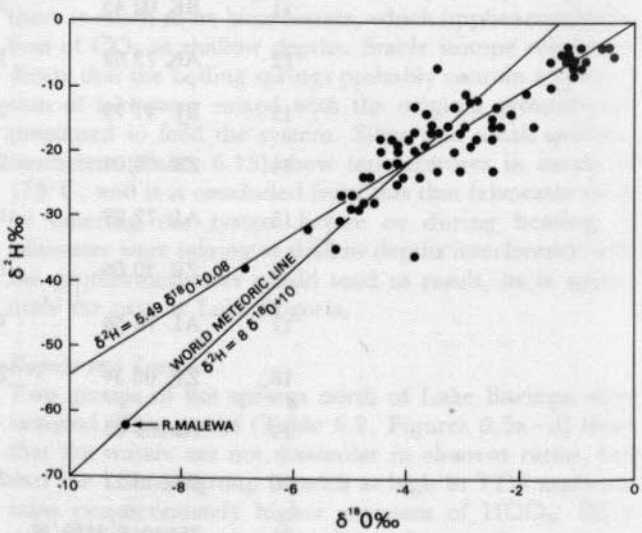

Figure 6.7 Delta-diagram of stable isotope data from unmodified groundwaters in the Magadi–Silale sector.

feeding Lake Naivasha. The implication is that the mountains are drained chiefly by surface water whose depleted composition is masked by the high evaporation acting on Lake Naivasha, the local sump for surface drainage.

The typical Rift-wall composition of $-28‰$ δ^2H, $-4.8‰$ $\delta^{18}O$ does not accord particularly well with the isotope-altitude relationships propounded in the previous section, but these are necessarily tentative and probably more important as relative indicators of altitude. In this sector of the Rift unmodified meteoric water appears to range from $-35‰$ to about $-18‰$ δ^2H, an altitude difference of some 700 m. The corresponding $\delta^{18}O$ range is -5.3 to $-3.5‰$ suggesting a difference of 600 m.

In contrast to the well waters on or near the side of the Rift, lakewaters are highly enriched in heavy isotopes owing to the great potential for evaporation. While lakes Elmenteita and Nakuru are discharge areas within an almost closed drainage basin, Lake Naivasha is a source of recharge to the Rift and provides a very effective tracer for axial groundwater movement. The typical Naivasha composition is $+35‰$ δ^2H, $+6.6‰$ $\delta^{18}O$, and it is possible to draw contours (where there are sufficient well data) showing the approximate percentage of lakewater in the mixing series between lakewater and groundwater (Figure 6.8). If certain assumptions about the production of fumarole steam are made it is possible to infer groundwater compositions beneath thermal centres; while these data have been added to Figure 6.8 their calculation is explained in the next section.

Most of the groundwater sampled in this part of the Rift can be explained in terms of unmodified rainfall or of rainfall mixed with lakewater. There is no evidence for a third source of water with thermal characteristics (for instance with a pronounced $\delta^{18}O$ shift) underlying the area at depth. The greatest mixing effects are demonstrated in the wells close to Lake Naivasha, which have an obvious lakewater contribution. Since the lake is on the topographic culmination of the Rift floor, discharge to both north and south may be expected. Unfortunately well data are concentrated on the east and west sides of the lake, and the only strong indication of the presence of lakewater elsewhere (apart from high-temperature geothermal sources) comes from the warm springs near the southern end of Lake Elmenteita some 30 km to the north. These suggest a 30% contribution from Lake Naivasha. To the north-east of the lake the River Malewa feeds a swamp which ultimately must recharge the lake, and there is accordingly no evidence of heavily evaporated water here. While the influence of the lake is seen up to 6 km to the south-south-east of the lake, data from the western side suggest that there is very little flow to the west.

The warm springs at the southern end of Lake Elmenteita show evidence of water from Naivasha, as already mentioned. A few kilometres to the north-east and south-west of the springs typical Rift-wall water compositions of $-24‰$ δ^2H are seen (sites 36 and 124). The flow of already considerably diluted lakewater to the north therefore passes through a relatively narrow constriction at this point. Beyond this well data are sparse, and the effects of discharge at the north-west end of Lake Elmenteita of considerably enriched water would in any case obliterate evidence of Naivasha water. Although Lake Nakuru is assumed (like Elmenteita) to be extremely enriched in heavy isotopes, there are only limited signs of this in wells to the north-west of the lake. The implication of this is that flow out of this basin is very small and most water is lost by evaporation. Alternatively, if there is a greater flow to the north-west from the lake it is being rapidly diluted by a comparable amount of flow from the sides of the Rift, particularly from the west.

6.4.3.5 Thermal Waters: Suswa to Eburru

Steam condensate from fumarolic discharges on Suswa, Longonot Domes, Olkaria, Eburru and surrounding areas was collected for analysis, much of it by Dr H Armannsson of the UNDP. Deep thermal fluid was sampled from some of the wells in the Olkaria geothermal field which is of extreme importance as the only location in this part of the Rift where the total geothermal fluid can be sampled.

The geochemistry of the Olkaria–Hell's Gate area is dealt with in greater detail in Section 6.5.2, but the total fluid compositions from the wells are plotted together with steam condensates from all fumaroles on Figure 6.9. The steam condensate samples form an elongate group, parallel to the meteoric line for the Rift, and covering a large range, approximately -1 to $-15‰$ $\delta^{18}O$. There is no sign of a conspicuous $\delta^{18}O$ shift in the fumarole results or the Olkaria thermal fluid.

On the basis of the steam results it is proposed that most, if not all, of the fumarole condensates are products of steam separation from a mixing series between Naivasha lakewater ($+36‰$ δ^2H, $+6.6‰$ $\delta^{18}O$) and Rift-wall groundwater ($-30‰$ δ^2H, $-5.0‰$ $\delta^{18}O$). This situation may be slightly complicated by a small $\delta^{18}O$ shift (maximum 1.5‰) suggested by the Olkaria results.

To demonstrate this hypothesis, Figure 6.10 shows a delta plot of all steam samples together with theoretical lines formed by primary steam separation from various dilutions of lakewater with Rift-wall water allowing for a small (1‰) $\delta^{18}O$ shift. The resulting temperature ranges (100–260°C) form parallel curves with a gradient somewhat steeper than the KRML, and several of the fumarole groups plot subparallel to these calculated lines, e.g. Longonot, Hell's Gate and Suswa caldera floor, suggesting that the interpretation may be justified. Samples lying outside the primary steam range are likely to be caused by local conditions, e.g. for example the fumaroles from the Eastern Olkaria wellfield appear to derive from steam heated groundwater, and the more depleted waters from Suswa may be the result of steam condensation, a process considered by Darling and Armannsson (1989). In addition, the primary steam envelope would itself be subject to possible local dilution effects and small variations in $\delta^{18}O$ shift.

The steam data from each region are now considered in terms of a lakewater mixing model. Starting with Eburru, the most northerly high-temperature manifestation in this sector of the Rift, it can be seen on Figure 6.10 that the samples obtained from EF2 lie beyond the influence of lakewater. This implies that water from Naivasha does not flow beneath Eburru during its passage northwards. Eburru EF2 shows some evidence of local dilution effects, but the presence of He and H_2 in the accompanying gases (see later sections), confirm that the steam is basically primary and derived from local Rift-wall groundwater. This is supported by the nature of the outflow from Eburru which affects the chemistry of wells at sites 121, 122, 124 and 125. These waters have a basic Rift-wall isotopic composition but their chemistry is clearly the result of thermal processes—they contain for example high silica, lithium and bicarbonate, as well as having a high gas content (mainly CO_2) and a $^3He/^4He$ ratio similar to EF2 (Table 6.12). EF13, on the other hand, is highly depleted in heavy isotopes and can only easily be

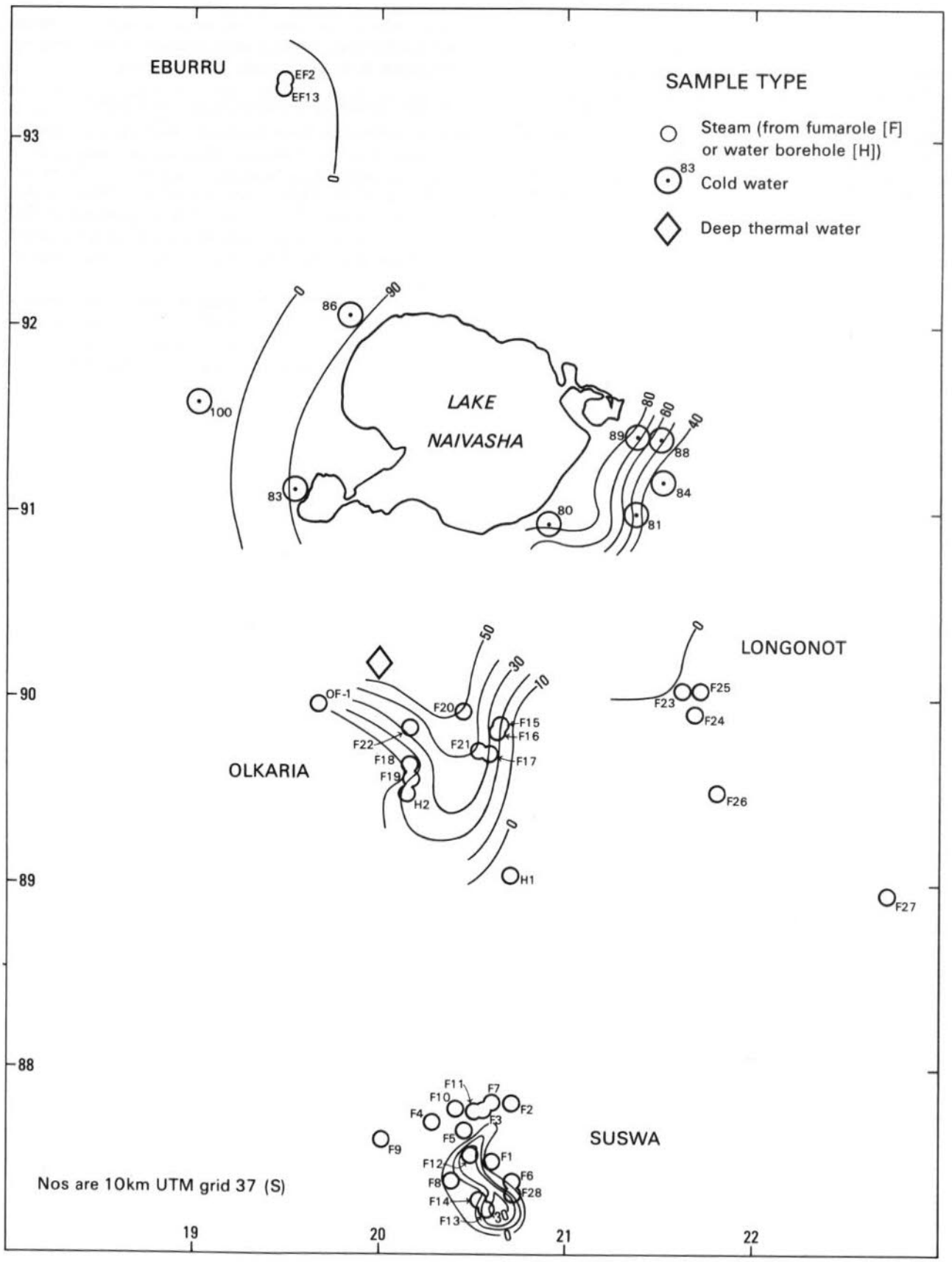

Figure 6.8 Contour map showing the contribution of Naivasha lakewater to groundwater in the Suswa–Elmenteita sector, based on geochemical evidence from wells, springs and fumaroles.

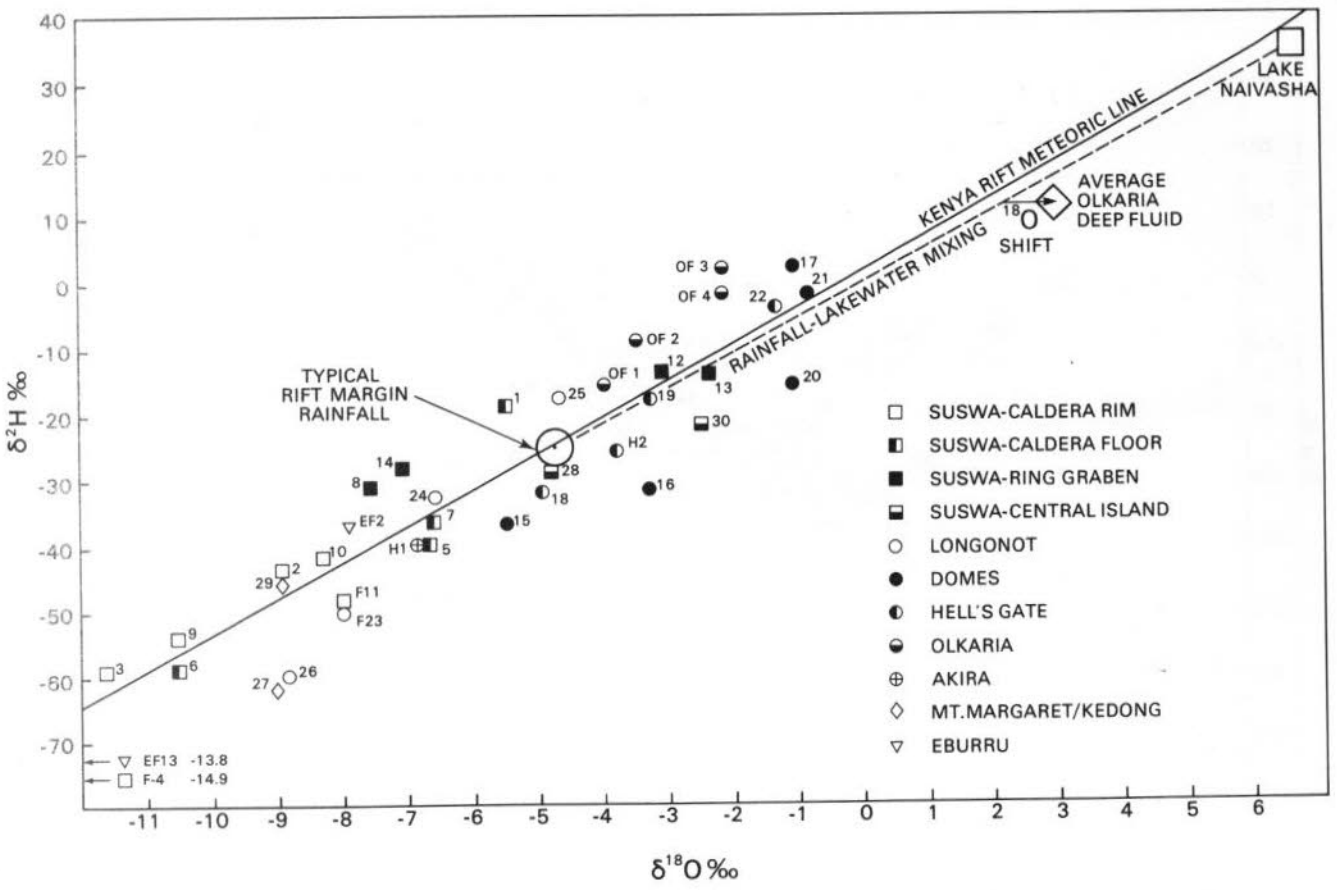

Figure 6.9 Delta-diagram of fumarole condensate isotope data from the Suswa–Eburru sector.

explained by a large degree of steam condensation below surface. The very low gas content of this fumarole (Z W Muna, personal communication) tends to confirm that it is not unmodified primary steam.

The fumaroles in the Olkaria and Hell's Gate area are treated in more detail with the Olkaria wellfield in Section 6.5, but all show the influence of lakewater to a greater or lesser extent. In the Domes area east of Hell's Gate, the fumaroles generally show compositions suggesting more than 30% lakewater in the thermal fluid. The Longonot crater fumaroles (F23–25) on the other hand imply little or no lakewater at depth, while the fumarole on the southern slopes of the volcano (F26) and those of the eastern part of the valley beyond, Mt Margaret (F27) and Kedong (F29) suggest that no lakewater reaches these areas.

The Suswa area has four different zones: caldera rim, caldera floor, ring graben and central island, and this zonation is partly reflected in the condensate stable isotope results (Figure 6.10). In general only samples from the ring graben and central island show evidence of lakewater content, with F8 and F14 showing evidence of steam heating. A small hot spring (56°C) in the ring graben, recently discovered by BGS, yielded a result of −25‰ δ^2H, −4.5‰ $\delta^{18}O$. This composition probably represents the residual water remaining after the steam heating responsible for F8 and F14, and implies that local rainfall on Suswa meets ascending steam as it percolates downwards. Caldera rim and floor samples are in general depleted and are probably the results of local dilution processes and/or (especially in the case of the most depleted samples) condensation processes; it is known from gas analyses (Section 6.4.6) that at least some of the rim fumaroles contain a component of air.

The fumarole data have been added to the contour map of lakewater dilution based on well water analyses (Figure 6.8). The fumarole data suffer some disadvantages (assumptions of origin, probable large variations in depth and tortuosity of routes to the surface) but by and large provide a plausible picture of southward flow from Lake Naivasha, perhaps largely confined in width to the East Olkaria–Domes area but large enough in volume to form up to 30% of the water beneath parts of Suswa. The fumaroles of the Suswa caldera floor and rim are on the direct path of this supposed flow to the south, yet show few signs of direct derivation from the flow. Either the steam has been much modified by dilution and/or condensation as discussed above, or perhaps less likely, a strong flow of Rift-wall water is entering the system from the west.

Owing to the lack of opportunities to sample water or steam south of Suswa it is impossible to say how far towards Lake Magadi the influence of Naivasha water may extend. Inasmuch as 30% lakewater could be present 30 km south of Naivasha it may be assumed that recharge from the Rift walls will have diluted lakewater beyond recognition at some 50 km south of the lake, so that it would be impossible to identify the influence of Naivasha water on Lake Magadi, some 100 km away.

In summary, it has been demonstrated that most fumarole isotope ratios can be explained by production of steam (suitably modified in certain cases) from a mixing series between Rift-wall meteoric water and evaporated water from Lake Naivasha. No evidence of any deeper

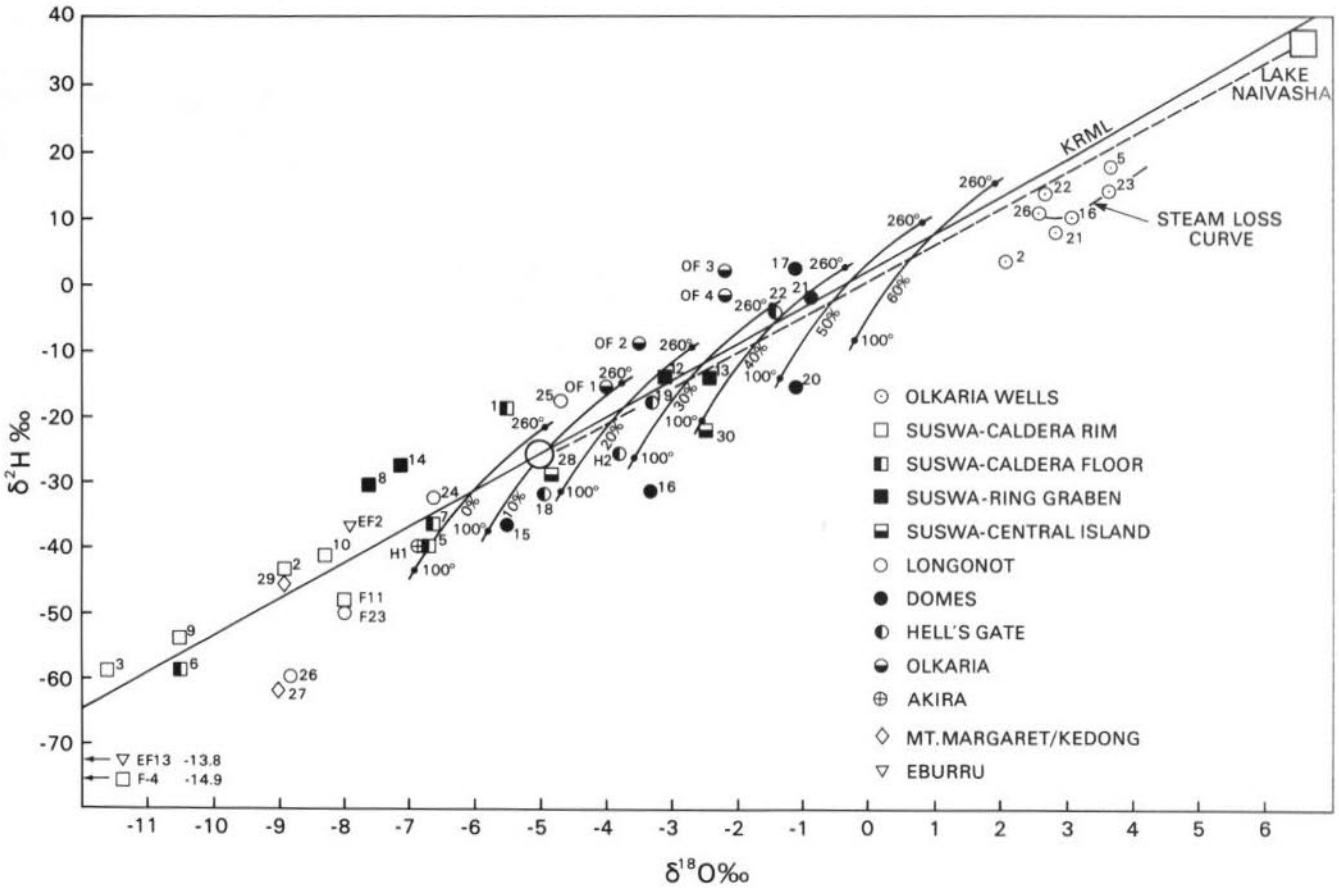

Figure 6.10 Fumarole stable isotope data shown in relation to primary steam production from a groundwater–lakewater mixing series.

reservoir of singular composition has been seen, and it appears that oxygen shifting of the dimensions commonly seen in other geothermal systems does not exist. It should be remembered that $\delta^{18}O$ shifting is dependent on a combination of residence time, initial rock and water $\delta^{18}O$ values and the porosity of the system(s). Not enough is yet known about rock $^{18}O/^{16}O$ ratios to comment on the rather low $\delta^{18}O$ shifts.

The conclusions of this study regarding the significance of fumarole isotopes are broadly similar to those of Armannsson (1987) in that he proposed mixing between unmodified Rift-wall water and a deep thermal water of an evaporated origin. Isotope data reported here (Section 6.5.2) shows that Olkaria must be considered to be part of the general hydrothermal system in the area, and that Lake Naivasha is therefore the source of this evaporated water.

6.4.3.6 Surface, thermal and non-thermal waters: Nakuru to Silale

Introduction

Various thermal and associated waters were sampled from the Nakuru area to a point some 170 km further north near the Silale volcanic centre. Stable isotope results are given in Tables 6.2 and 6.6 and are shown in Figures 6.4c and d.

As discussed in the previous section, there appears to be comparatively little outflow from the almost closed basin of Lake Nakuru. Between this lake and Lake Bogoria to the north, groundwater stable isotope values are similar to those from the valley floor further south and average $-16‰$ δ^2H, $-2.9‰$ $\delta^{18}O$. Despite the fact that some of these waters are slightly thermal (up to 43°C, Figure 6.5a) they probably all represent unmodified Rift-floor rainfall with the thermal waters similar in provenance to the Kariandusi warm spring (site 35).

Lake Bogoria

At Lake Bogoria itself a wide variation in stable isotopes is seen, ranging from unmodified Rift-floor recharge through boiling springs to highly evaporated lakewater. Figure 6.11 shows the various waters plotted on a delta-diagram. Non-thermal or slightly thermal waters cluster round the local Rift meteoric line at about $-13‰$ δ^2H, $-2.8‰$ $\delta^{18}O$ and are presumably derived from local recharge in the hills around the lake, The three boiling springs sampled have rather heavier compositions, whereas the lakewater itself is extremely enriched in heavy isotopes due to the large amount of evaporation taking place from the closed basin.

It was suggested by Glover (1972) that slightly thermal water underlying the general area reacts both with ascending steam and with lakewater, while Geotermica Italiana (1987) postulated a ternary mixing model involving local groundwater, thermal water and lakewater. The few data reported here do not support the steam heating model, but neither do they prove the ternary mixing hypothesis. Although the three boiling springs do not lie directly on a dilution between the regional cool springs and the extremely evaporated lakewater, their position is consistent with steam loss from points along this line (Figure 6.11). To this extent the contention that lakewater is involved is likely to be correct (and indeed the situation of the boiling springs on the lakeshore makes this very likely) but there is no evidence that steam with a different isotopic composition is playing a part in the process. It ap-

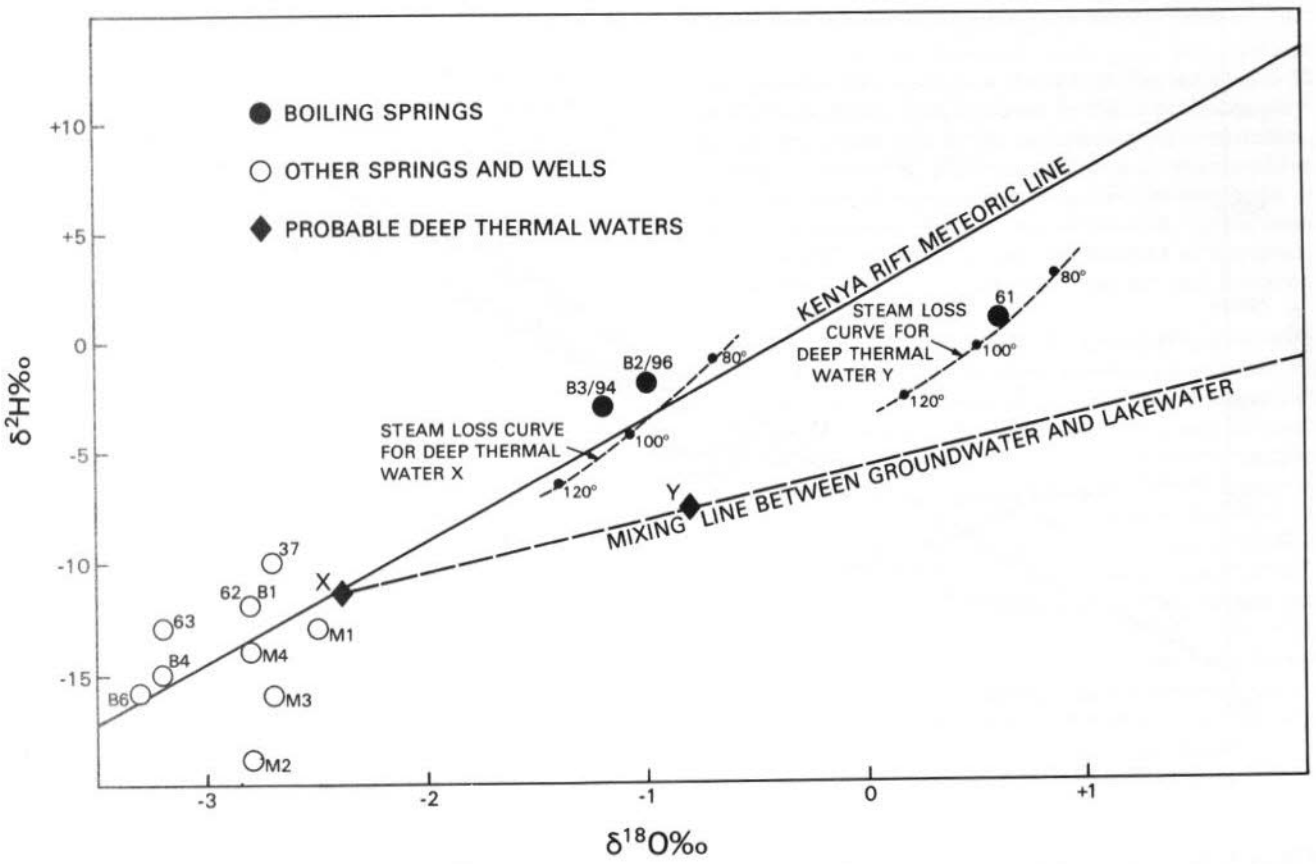

Figure 6.11 Delta-diagram of stable isotope data from groundwaters, thermal waters and lakewater of the Lake Bogoria region.

pears from the isotopic evidence that regional shallow groundwater could be suitable as a source for the thermal fluid, and that the somewhat enriched isotopic compositions seen in the boiling springs are due more to steam separation than to a lakewater contribution. There is no isotopic evidence from these results for the slightly heavier thermal water invoked by Geotermica Italiana (1987), which could probably only come from a source like Lake Baringo.

Lake Baringo

Lake Baringo is a 'freshwater' lake which in view of the lack of surface outflow must have a considerable subsurface egress. In this respect it may be compared to Lake Naivasha, though unlike that lake outflow is likely to be restricted to a northerly direction. Only two sites were sampled at the lake—a boiling spring on the central, remnant volcanic cone island of Ol Kokwe, and the lakewater itself. The results are shown on a delta-diagram in Figure 6.12. It can be seen that the lakewater is highly evaporated, though to a much lesser extent than the stagnant Lake Bogoria. The boiling spring on the central island lies on a direct dilution line between the local shallow groundwater (presumed to be similar to that of the Bogoria area) and the lakewater, and might therefore be assumed to be the product of heating a mixture of both waters by steam. However as demonstrated by the results considered in Section 6.4.3.6 (and pointed out by Glover, 1972), the boiling spring contains a much higher TDS content than the lakewater and cannot therefore be the result of steam heating of lakewater. In spite of this it seems clear that the boiling spring is related to lakewater in some way: the isotopic content of the spring water is too enriched to be simply the result of steam loss from thermal water derived from shallow Rift-floor recharge. It appears that any mixing between lakewater and shallow groundwater must take place in the deep geothermal system, with the upflow into the central island being largely unaffected by the lakewater, however unlikely this may seem at first sight.

North of Baringo—Kapedo and Lorusio

Subsurface discharge from Lake Baringo to the north should be detectable in wells, springs and perhaps fumaroles north of the lake, though only sites at Kapedo and Lorusio were sampled. These sites are some 50 and 60 km away respectively, and by analogy to the Naivasha outflow little evidence of lakewater would be likely to remain. Although two of the Kapedo group of springs show enriched isotope values (Figure 6.12) these are not on the dilution line between presumed local groundwater and lakewater, and instead are more likely to represent evaporative enrichment from the local groundwater.

The Lorusio springs are hotter than the Kapedo springs, and the average isotopic composition is shown in the delta-diagram in Figure 6.12. It is apparent that it is slightly lighter than any of the Kapedo group and may therefore be derived more from the Rift wall than the floor. Though the two groups of springs are relatively close to each other it is unlikely that Kapedo is diluted Lorusio water; not only is it difficult to see what the positive end member could be, but it would also imply a southerly flow, which is contrary to the general flow direction in this part of the Rift. On these grounds therefore it is considered that the two groups are unrelated.

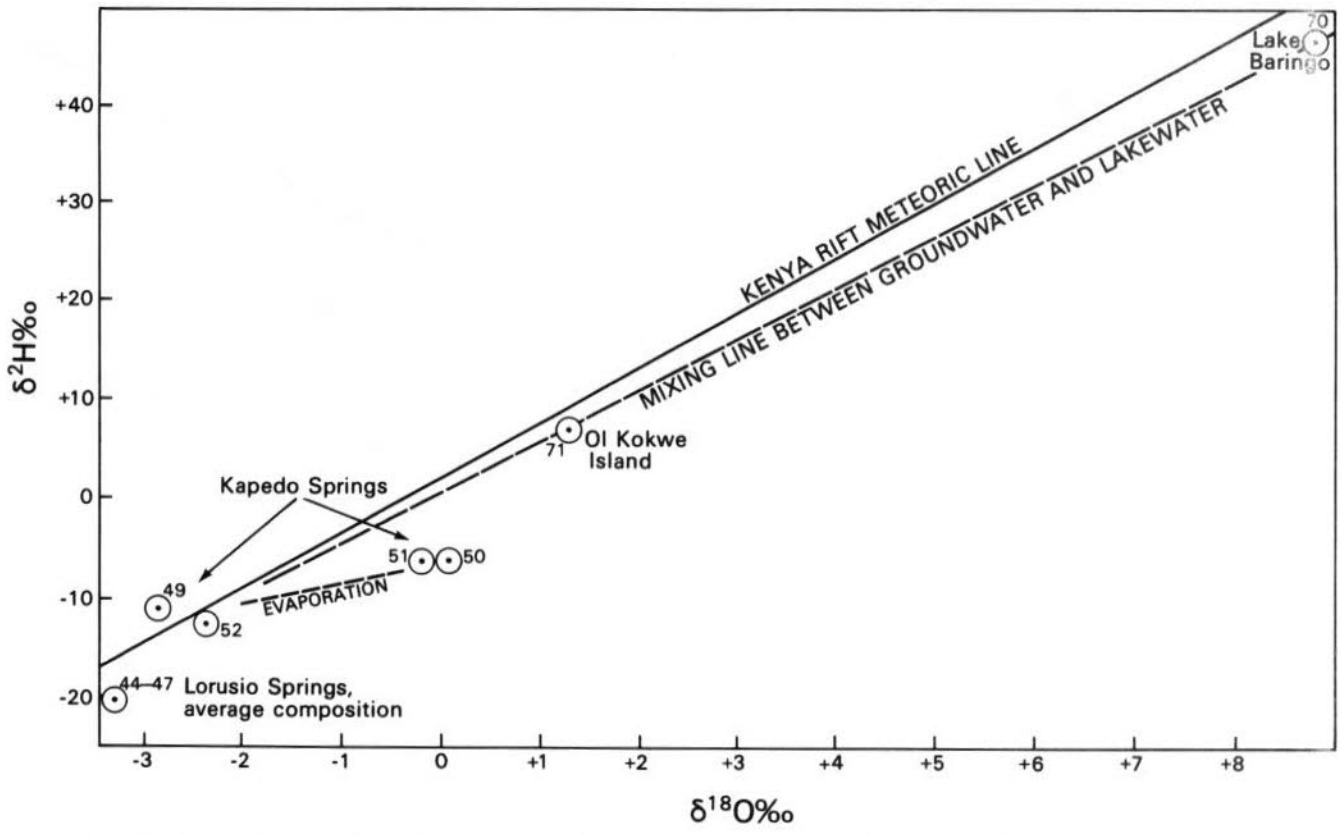

Figure 6.12 Delta-diagram of stable isotope data from thermal waters and lakewater of the Lake Baringo region.

Table 6.8 Carbon stable isotope data for Rift Valley water and gas samples

Site no.	Site name	$\delta^{13}C_{DIC}$ ‰PDB	$\delta^{13}C_{CO_2}$ ‰PDB	$\delta^{18}O_{CO_2}$ ‰SMOW
25	Kijabe RVA	− 7.4		
26	Kijabe Spr	− 12.6		
28	Mayer's Fm	− 16.5		
29	Mt Margaret		− 1.7	+ 34
31	Akira H-1*		− 2.1	+ 32.8
35	Kariandusi Spr	− 8.0		
53	Bala Springs	− 1.7		
57	Bala Springs	− 2.3		
74	Magadi NW	+ 0.9		
75	Oltepesi	− 7.4		
81	C567	− 0.4		
82	C4178	− 13.5		
92	Kanyamwi Fm	− 2.5		
96	Kinangop P65	− 12.0		
100	C1404	− 10.6		
104	Hell's Gate seep 2	− 11.0		
110	Olkaria OW2	− 10.2	− 2.7	+ 41.9
111	Olkaria OW26	− 4.8	− 2.4	+ 42.5
112	Olkaria OW22	− 7.5		
114	Olkaria OW23	− 5.1		
115	Olkaria OW21	− 7.1		
116	Olkaria OW5	− 14.6		
118	Nakuru No. 7 (Lanet)	− 8.7		
119	Eburru EF-2		− 2.3	+ 36.3
121	C431	− 0.5		
123	W Olkaria fumarole		− 2.8	+ 37.2
124	Soysambu DEL	− 2.7	− 6.6	+ 37.1
125	C1990	0.0		
127	Domes F-15*		− 3.0	+ 35.7
128	Longonot F-23		− 3.5	+ 29.5
UNDP 51	Longonot F-23		− 4.4	+ 29.5
UNDP 44	Suswa F-28		− 3.7	+ 36.6
UNDP 43	Suswa F-12		− 3.2	+ 37.8

C_{DIC} = dissolved inorganic carbon in water

C and O_{CO_2} = carbon dioxide gas

* = samples collected by UNDP

6.4.4 Stable isotopes—carbon

Differences in the $^{13}C/^{12}C$ ratio relative to that of the Pee Dee Belemnite (PDB) zero standard were measured on dissolved inorganic carbon (DIC) precipitated from water as $BaCO_3$, or directly on CO_2 gas. Results are reported in Table 6.8.

Most samples were collected from the Suswa–Nakuru sector of the Rift and the distribution of sampling points is shown in Figure 6.3f). In this area a large variation in $\delta^{13}C$ DIC is seen, ranging from around 0 to −16.5‰. The isotopic value of DIC depends primarily on the values of soil CO_2, rock carbonate, and amount and temperature of water–rock contact. The interpretation of $\delta^{13}C$ DIC can therefore be complicated in areas such as the Rift where crustal CO_2 is present in considerable amounts (Bailey 1980).

Three carbonatite samples from the Homa Bay area to the west of the Rift had $\delta^{13}C$ values of −3.0, −4.2 and −8.2‰ respectively, so −5‰ is taken as a typical value for rock carbonate. Assuming soil zone carbon dioxide to have a value of about −26‰, a minimum $\delta^{13}C$ value after stoichiometric dissolution would be around −15.5‰.

All the waters with values > −5‰ could be the product of dissolution of rock carbonate by soil-derived CO_2 followed by isotope exchange or incongruent solution. Other Rift waters are significantly heavier in $\delta^{13}C$ DIC and in cases like the 'Badlands' wells (sites 121, 124 and 125) and the Bala springs of the Homa Bay area (sites 53 and 57) magmatic CO_2 of about −3‰ is probably playing an important role in the carbon isotope systematics, tending to drive $\delta^{13}C$ DIC towards zero or even positive values because of the positive CO_2-DIC fractionation at lower temperatures. In the case of site 124, where both CO_2 and DIC were measured, the amount of fractionation (3.9‰) was exactly as predicted for the sampling temperature (Table 6.9).

At Olkaria, where both $\delta^{13}C$ CO_2 and $\delta^{13}C$ DIC were measured, equilibrium between the two phases was not well established according to the calculated separation temperatures (Table 6.9). This may be because of insufficient time for re-equilibration to occur between reservoir and wellhead, though neither OW2 or OW26 appear to be in equilibrium at reservoir temperatures (Section 6.5).

Carbon dioxide in the Suswa–Nakuru part of the Rift has a $\delta^{13}C$ of −3‰ with a standard deviation of 0.7. These may be typical volcanogenic values, but are not always associated with volcanic centres; cold CO_2 'mofettes' are known from the Rift and beyond—for example two wells at Meru, east of Mt Kenya, each gave a $\delta^{13}C$ value of −3.5‰. This tends to confirm the idea of a pervasive CO_2 flux having a deep crustal origin over a wide area (Bailey, 1980), and indicates that a $\delta^{13}C$ of

Table 6.9 Radiocarbon uncorrected and WATEQF-ISOTOP modelled Rift Valley groundwater ages, with equilibrium $\delta^{13}C$ CO_2 values

						^{14}C Corrected ages in years			
Site No.	$A^{14}C$ PMC	Unc. Age Years	$\delta^{13}C_{DIC}$ ‰ PDB	$\delta^{13}C_{CO_2}$ ‰ PDB	$\delta^{13}C_{CO_2eq}$ ‰ PDB	$\delta^{13}C_r = 0$ $pH_I = 5$	$\delta^{13}C_r = -5$ $pH_I = 5$	$\delta^{13}C_r = 0$ $pH_I = 8$	$\delta^{13}C_r = -5$ $pH_I = 8$
16	—	—	−12.6	—	−18.2	—	—	—	—
25	6.2	22500	−7.4	—	−14.2	9136	4823	16405	8249
27	—	—	−12.6	—	−18.8	—	—	—	—
28	78.6	2060	−16.5	—	−23.7	Modern	Modern	Modern	Modern
35	—	—	−8.0	—	−15.9	—	—	—	—
53	—	—	−1.7	—	−6.2	—	—	—	—
56	—	—	−2.3	—	−6.6	—	—	—	—
74	—	—	+0.9	—	−8.2	—	—	—	—
75	—	—	−7.4	—	−16.5	—	—	—	—
81	—	—	−0.4	—	−6.8	—	—	—	—
82	91.4	900	−13.5	—	−20.9	Modern	Modern	Modern	Modern
92	62.8	3980	−2.5	—	−8.9	Modern	Modern	Modern	Modern
100	86.0	1450	−10.6	—	−16.6	Modern	Modern	Modern	Modern
104	—	—	−11.0	—	−17.6	—	—	—	—
110	—	—	−10.2	−2.7	−9.7	—	—	—	—
111	—	—	−4.8	−2.4	−4.1	—	—	—	—
112	—	—	−7.5	—	−6.9	—	—	—	—
114	—	—	−5.1	—	−4.5	—	—	—	—
115	—	—	−7.1	—	−6.5	—	—	—	—
116	—	—	−14.6	—	−14.0	—	—	—	—
118	94.7	700	−8.7	—	−14.8	700	Modern	Modern	Modern
121	—	—	−0.5	—	−6.1	—	—	—	—
124	4.0	26190	−2.7	−6.6	−6.6	26190	8388	Modern	Modern
125	—	—	0.0		−6.4	—	—	—	—

A = activity
PMC = percent modern carbon
Unc = uncorrected
pH_I = initial open system pH
$\delta^{13}C_{DIC}$ = dissolved inorganic carbon
$\delta^{13}C_{CO_2}$ = measured CO_2 value
$\delta^{13}C_{CO_2}$ = calculated equilibrium CO_2 value
$\delta^{13}C_r$ = rock carbonate value

around −3‰ is not an infallible indicator of thermal activity. One methane-containing sample (from Eburru) was analysed for its $\delta^{13}C$ content—see Section 6.4.7.3.

The carbon stable isotope results can be summarised as follows. They provide a measure of the approach to equilibrium, if any, of DIC and rock carbonate, which can be broadly related to a combination of residence time and temperature, and which is essential for radiocarbon modelling purposes. They discriminate between 'normal' waters and those being affected by injection of crustal CO_2 or evaporation. Fractionations between the various carbon species are potential geothermometers, but their use appears to be rather circumscribed.

6.4.5 **Radioisotopes**

6.4.5.1 Carbon-14

The radiocarbon content of groundwater was measured at 7 representative sites (Figure 6.3g). It was considered that an indication of groundwater age would be of use as a check on the flow rates deduced from physical modelling of groundwater movement. The uncorrected ages shown on Figure 6.3g are calculated on the basis of simple ^{14}C decay and take no account of addition of 'dead' carbon to the system. In general this addition comes from the dissolution of 'dead' rock carbonate phases by 'active' carbon dioxide produced in the soil zone; if rock and dissolved inorganic carbon $\delta^{13}C$ values are known or assumed, corrections to the groundwater 'age' can be attempted. Several correcting methods are available—in this case WATEQF–ISOTOP was used.

Table 6.9 shows the results of running WATEQF–ISOTOP with two initial pH values, 5 and 8, and using two different rock carbonate $\delta^{13}C$ values. In each case soil zone CO_2 is assumed to have been −25‰ PDB. Normally rock carbonate is assumed to be marine-derived and to have a $\delta^{13}C$ of about O‰. This was used as a starting point to run the ISOTOP model, but in the Rift Valley a marine derivation for carbonate phases is unlikely. In view of the carbonatitic volcanism associated with the Rift, the model was run with a rock carbonate value of −5‰ PDB, a typical carbonatite value. In most cases the resulting ages are modern, irrespective of starting conditions. The two exceptions to this are from the DEL well on the Soysambu Estate and the Rift Valley Academy (sites 124 and 25). Both these wells have a high bicarbonate content, especially the DEL well, and it is probable that the apparent ages are an artefact caused by the addition to the carbonate system of large amounts of crustal CO_2.

Dissolved CO_2 from the DEL well was measured for ^{13}C content and the value, −6.6‰ PDB, was in exact agreement with the ISOTOP calculated equilibrium for the measured $\delta^{13}C$ DIC of −2.7‰ PDB. In reality these two waters are likely to be very much younger than the modelled ages, and by analogy with wells in similar positions within the Rift, e.g. Ndabibi C1404 (site 100) and Mayers Farm (site 28), are probably largely modern.

6.4.5.2 Tritium

The tritium content of representative groundwater was determined at Rift Valley sites (Table 6.10). In all cases except Lanet (Nakuru No. 7 well, site 118) values were well below 1 TU, suggesting that there is a negligible contribution from thermonuclear tritium and that accordingly the waters must be at least 25 years old. The slightly higher ^{3}H figure for Lanet can be compared with the ^{14}C value which gave the youngest uncorrected age of any of the Rift samples.

Table 6.10 Tritium content of groundwaters from the Suswa–Nakuru sector of the Rift Valley

Site No.	Site name	Temp °C	pH	TR	± σ
25	Kijabe RVA	35	7.95	0.09	0.14
28	Mayer's Fm	28	7.90	0.00	0.17
35	Kariandusi	39	6.6	0.34	0.16
82	Naivasha C4178	20	7.45	0.05	0.15
92	Kanyamwi Fm	24	7.30	0.34	0.16
96	Kinangop P65	23	7.00	−0.01	0.14
100	Ndabibi C1404	26	6.95	0.34	0.17
101	Kokot, Maiella	—	7.65	0.42	0.15
110	Olkaria OW2	34*	6.23*	0.19	0.14
111	Olkaria OW26	34*	6.05*	0.27	0.16
118	Nakuru No. 7, Lanet	28	7.00	1.64	0.16
124	Soysambu DEL	32	6.40	0.15	0.15

TR = Tritium ratio (1 TR ≡ 1 atom of ^{3}H in 10^{18} atoms ^{1}H)
* = cooled water phase from wellhead separator

6.4.5.3 Implications of the radioisotope data

Sites where radiocarbon and/or tritium were measured were selected on the basis of their value in identifying groundwater flow paths. Thus radiocarbon samples were taken in the western side of the Rift floor at the Ndabibi and Soysambu estates (sites 100 and 124), the central part of the Rift at Naivasha C4178 and Nakuru No. 7 (sites 82 and 118) and the eastern flanks at Mayers Farm, Kijabe RVA and Kanyamwi Farm (sites 28, 25 and 92). Mayers Farm and Kijabe RVA might particularly be expected to be associated with deep-seated faults, and Nakuru No. 7 is situated on a prominent north–south lineation on the valley floor, but none of these sites indicates long residence times (except perhaps for a small component) once radiocarbon corrections have been made. Conversely, tritium measurements show that in places where rapid flow might have been expected, especially perhaps at the Kokot water collection gallery (site 101), water was of pre-thermonuclear age.

The radioisotope measurements therefore suggest that there are no slow, deeply circulating groundwater flow paths playing a significant role in the hydrogeology of this part of the Rift Valley. A small contribution from deeper groundwater cannot however be entirely ruled out.

6.4.6 **Gases**

6.4.6.1 CO_2 and permanent gases (excluding inert gases)

During the investigations in the Rift Valley, gas samples were collected for $\delta^{13}C$ analysis. Most of these samples were taken from fumaroles and wells between Suswa and Nakuru, though samples were also drawn from gaseous springs at Bala (on the Lake Victoria arm of the Rift), Lorusio (in the Rift Valley north of Lake Baringo), and the Meru area ESE of Mt Kenya. While the isotopic results are discussed elsewhere in this report, the opportunity to carry out permanent gas analysis was taken and the results are presented in Table 6.11.

Excluding gases derived from the atmosphere, either originally or by entrainment or contamination, crustally

Table 6.11 Composition of fumarole, well and spring gas samples, excluding inert gases

Site No.	gas composition						ratios by weight		
	CO_2 %	CH_4 %	C_2H_6 vpm	H_2 %	He %	R %	CH_4/CO_2 $\times 10^{-3}$	H_2/CO_2 $\times 10^{-3}$	C_2H_6/CH_4 $\times 10^{-3}$
29/F-27	57.7	0.092	0.5	nd	nd	42.2	0.58	—	10
31/H-1	27.9	0.20	7.5	nd	nd	71.9	2.6	—	7.0
44–47	66.6	0.051	4.0	0.63	nd	33.4	0.28	0.43	15.
53–54	44.0	0.32	15*	nd	0.93	54.8	2.6	—	8.8
110	40.3	0.67	7.0	nd	nd	59.0	6.0	—	2.0
111	48.0	0.18	9.5	nd	nd	51.8	1.4	—	9.9
119	78.9	4.6	5.0	1.7	0.5	14.3	21.	0.98	0.20
123	74.4	0.37	11	nd	nd	25.3	1.8	—	5.6
124	74.3	0.001	0.5	nd	nd	25.7	0.01	—	94.
126	10.2	3 vpm	nd	nd	nd	89.8	0.01	—	—
127	17.4	0.13	2.5	nd	nd	82.5	2.7	—	3.6
127/F15	12.6	0.06	1.0	nd	nd	87.4	1.7	—	3.1
128	77.4	0.75	1.0	1.7	0.5	19.6	3.5	1.0	0.25
128/F-23	44.4	0.30	0.5	0.90	0.34	54.0	2.5	0.92	0.31
F-7	24.6	0.45	0.5	nd	nd	75.0	6.7	—	0.21
F-12	25.9	0.085	nd	nd	nd	74.0	1.2	—	—
F-28	66.0	0.41	1.0	nd	nd	33.6	2.3	—	0.46
K-1	35.8	0.010	nd	nd	nd	64.2	0.10	—	—
K-2	39.2	12 vpm	nd	nd	nd	60.8	0.01	—	—

* = Sample also contained 3 vpm C_3H_8

R = residual gases including N_2, Ar, H_2S and possibly O_2

nd = not detected

Samples with F, H and K prefixes collected by Dr H Armannsson of the UNDP

derived CO_2 dominates all samples, usually with CH_4 in second place, albeit at a much lower level. When H_2 and/or He are present, methane lies in third place. The low molecular weight gases diffuse very easily; the detection of both H_2 and He is taken as evidence of close proximity to a strong upflow, as at Eburru and Longonot, where the volcanic origins of the gas are confirmed by the helium isotope ratios. In the case of the Lorusio spring only H_2 is present; as a very similar H_2/CO_2 ratio to those of Eburru and Longonot is observed it may be that the springs are close to an upflow, though at a distance which allows escape of helium. The $^3He/^4He$ ratio was not measured for Lorusio and therefore cannot offer confirmation. At Bala He rather than H_2 was present—the He R/Ra value (next section) was not elevated much above the atmospheric level though total He was very high. On this evidence the area is unlikely to be close to an upflow.

In the absence of H_2, He and H_2S (which was not measured) methane may be the best evidence of proximity to upflow (Armannsson, 1987a) and, by implication, deep fluid temperature. The results support this in a qualitative way, with for example Mt Margaret (site 29), a relatively cool thermal area, having a much lower CH_4/CO_2 ratio than Eburru, which most other data suggest is a high temperature area. The shortcomings of CH_4/CO_2 as a geothermometer are however apparent (Section 6.4.7.2).

The ratio C_2H_6/CH_4 may be an index of a lakewater contribution, as discussed with relevance to the Olkaria area. In the Naivasha area the decline in C_2H_6/CH_4 is roughly in the order northern East Olkaria > West Olkaria > Domes > southern East Olkaria > Eburru > Longonot > Suswa, i.e. fairly consistent with increasing distance from the lake. The high ratio for the DEL well water (site 124) is likely to be an artefact of measurement at low concentrations, but Lorusio and Bala have apparently genuinely high C_2H_6/CH_4 ratios and it may be worth noting that Lorusio has been believed to derive its water ultimately from Lake Baringo (though see Sections 6.4.2.2 and 6.4.3.6), while Bala is close to the edge of Lake Victoria. By contrast the Meru (Chogoria) springs which cannot be supplied by lakewater have very low CH_4 values and undetectable C_2H_6.

6.4.6.2 Helium and inert gases

Helium and isotope ratios

The ratio $^3He/^4He$ was measured for 13 samples from the Suswa–Nakuru sector of the Rift and on one sample from the Bala springs on the edge of Lake Victoria. This latter sampling point had been chosen because a gas sample collected in 1985 indicated a high total helium content. Results are reported (Figure 6.3g, Table 6.12) in the conventional form of R/Ra, where R denotes the $^3He/^4He$ ratio of the sample and Ra the $^3He/^4He$ of air which effectively remains constant. Also shown in Table 6.12 are the He and Ne contents of each sample: He/Ne is a sensitive indicator of air contamination because the level of crustal neon is very much lower than that of air. Providing the amount of air contamination is small, a correction can be made to the original R/Ra value. This was first proposed by Craig et al. (1978) and takes the form:

$$(R/Ra)c = \frac{(R/Ra)(x-1)}{x-1}$$

where $x = \dfrac{He/Ne(sample)\ bNe}{He/Ne(air)\ bNe}$

(R/Ra)c = corrected R/Ra

bNe and bHe = Solubility coefficients for appropriate temperature

The results show that two samples possess helium contents essentially derived from air (Ndabibi C1404 and Nakuru No. 7, sites 100 and 118).

The remaining samples mostly have R/Ra values >1, indicating the presence of excess mantle helium to a greater or lesser extent. Samples collected as gas from fumaroles and geothermal wells tend to have the highest levels (corrected R/Ra values of 5.6 – 6.7 for Eburru, Longonot and Olkaria) but one water well (Soysambu DEL site 124) possesses a value in this range. Conversely two fumaroles, Suswa F3 and Domes F15 (sites 126 and 127), have lower R/Ra values, though gas analyses suggest that these fumaroles have substantial amounts of entrained atmospheric gases which may be diluting any ^3He component.

The main significance of $^3He/^4He$ ratios within this sec-

Table 6.12 Helium isotope ratios in groundwaters and gases of the Rift Valley

Site No.	Site Name	Sample Type	R/Ra	X	(R/Ra)c	He content cm^3 STP/cm^3 or cm^3 STP/g	Ne content cm^3 STP/cm^3 or cm^3 STP/g
26	Kijabe RVA	W	0.928	5	0.896	5.43×10^{-8}	4.52×10^{-8}
35	Kariandusi Spr	W	1.359	1.2	2.947	1.20×10^{-7}	4.28×10^{-7}
53	Bala Springs	W	1.446	85	1.434	2.86×10^{-3}	1.45×10^{-4}
92	Kanyamwi Farm	W	1.281	8.6	1.323	1.08×10^{-7}	5.45×10^{-8}
100	Ndabibi C1404	W	0.938	1.6	0.871	8.13×10^{-8}	2.09×10^{-7}
110	Olkaria OW2	G	5.682	383	5.694	2.67×10^{-5}	3.03×10^{-7}
111	Olkaria OW26	G	5.711	429	5.825	2.26×10^{-5}	2.29×10^{-7}
118	Nakuru No. 7, Lanet	W	1.005	0.9	1.040	3.48×10^{-8}	1.59×10^{-7}
119	Eburru EF-2	G	6.243	282	6.262	1.22×10^{-5}	1.88×10^{-7}
123	Olkaria W. field	G	5.651	881	5.623	4.12×10^{-6}	2.03×10^{-8}
124	Soysambu DEL	W	6.156	14	6.521	2.94×10^{-6}	8.96×10^{-7}
126	Suswa F-3	G	1.510	5	1.610	7.33×10^{-6}	5.80×10^{-6}
127	Domes F-15	G	2.789	17	2.921	5.16×10^{-7}	1.26×10^{-7}
128	Longonot F-23	G	6.482	32	6.656	2.96×10^{-5}	3.98×10^{-6}

W = water (well or spring)
G = gas (fumarole or geothermal well)
R/Ra = ($^3H/^4H$ sample)/($^3H/^4H$ air)
X = correction factor (see text)
(R/Ra)c = R/Ra corrected for air contamination
(samples measured at the University of Cambridge by Ms E Griesshaber)

tor of the Rift is that they do not show much evidence of transport of mantle helium up the deep faults presumed to exist at the sides of the Rift; for example Kanyamwi Farm well C570 and Kijabe Warm Spring (sites 92 and 27) have values close to atmospheric, though the Kariandusi warm spring (35) does have an elevated level (but see next section for further comments on Kijabe). Instead the high levels are all associated with volcanic centres except for the Soysambu DEL well (site 124), which on various grounds can be linked to outflow from the Eburru centre.

On a wider scale the He isotope ratios indicate an approach to a mid-ocean ridge basalt (MORB) type composition with which typical R/Ra values of 8–9 are normal. Such values and higher have been measured in Ethiopia and a hot-spot origin attributed to the values in excess of 9 (Craig, 1978b). The R/Ra values associated with Eburru, Longonot and Olkaria are consistent at around 6, suggesting that they originate from similar composition crust. The question as to whether or not there is a gradual enrichment northwards along the Rift towards MORB values may be answered by the next phase of the Geothermal Project.

As already mentioned, the total helium content of the Bala spring on the edge of Lake Victoria is very high (2.86×10^3 cc He/cc total gases). The R/Ra value of 1.446 indicates that there has either been some concentration of air-derived inert gases containing minor enrichment in ^3He (and the Ne content is high) or, less likely, that any radiogenic (^4He) and mantle (^3He) additions are largely balancing out in proportional terms. Similar gas compositions and concentrations are known from southern Africa (K O'Nions, personal communication).

Inert gases

Measurement of concentrations of dissolved inert gases were made on seven well waters and two warm spring

Table 6.13 Inert gas contents (cm^3/cm^3 H_2O at STP) and calculated recharge temperatures for selected Rift Valley groundwaters

Site No.	Site Name	He × 10^{-8}	Ne × 10^{-7}	Ar × 10^{-4}	Kr × 10^{-8}	Xe × 10^{-8}
25	Kijabe RVA	6.43	1.64	2.60	5.98	0.86
T = 35°C	Alt = 2500 m			(21.8)	(16.2)	(13.7)
28	Mayer's Farm	3.67	1.47	2.25	4.97	0.70
T = 28°C	Alt = 2100 m			(24.0)	(19.9)	(17.5)
35	Kariandusi Sp	5.47	1.64	1.94	4.16	0.58
T = 39°C	Alt = 2300 m			(>30)	(28.1)	(24.1)
82	Naivasha 4178	6.18	2.47	3.38	7.09	0.97
T = 21°C	Alt = 1900 m			(>30)	(>30)	(25.6)
92	Kanyamwi Farm	5.16	1.64	2.60	5.87	0.84
T = 27°C	Alt = 2300 m			(21.8)	(17.1)	(14.6)
96	Kinangop P65	5.69	1.67	2.84	6.42	0.91
T = 21°C	Alt = 2600 m			(17.9)	(13.9)	(12.4)
100	Ndabibi C1404	3.61	1.47	2.11	4.35	0.62
T = 21°C	Alt = 2100 m			(28.4)	(25.1)	(22.4)
118	Nakuru No. 7	3.34	1.53	2.29	5.03	0.69
T = 28°C	Alt = 2000 m			(25.4)	(21.2)	(19.5)
124	Soysambu DEL	143.0	0.87	1.05	2.12	0.30
T = 32°C	Alt = 1900 m					

Alt = sample altitude (approx)
T = sample temperature
t_r = indicated recharge temperature, °C
Figures in brackets under Ar, Kr and Xe contents are t_r

waters. Results are presented in Table 6.13 as volumes (STP) of gas in solution and in Table 6.14 as various ratios.

When the results are plotted in the form of argon versus neon content and xenon versus krypton content (Figure 6.13a), it can be seen that the inert gas ratios are wholly consistent with an atmospheric origin and, apart from one sample showing depletion, can be used to estimate recharge temperatures. These have been calculated for Ar, Kr and Xe using solubility curves in Mazor (1977), firstly on amounts of gas corrected to sea-level atmospheric pressure according to approximate altitude of collection, and secondly on amounts calculated by using a simple correction for possible atmospheric contamination of samples during sampling based on their neon content. The results (Table 6.13) are reasonably consistent with each other, though they are best considered as indicating relative rather than absolute recharge temperatures.

When the averaged inert gas-derived recharge temperatures are plotted against sampling altitude (Figure 6.14) a reasonably good correlation is seen for ffive of the surface water samples. This implies that recharge occurs fairly locally, or at least at a similar altitude to the location of sampling. The two exceptions to this are Kariandusi Spring (site 35) and Naivasha C4178 (82). The former is a warm spring, and this combined with the method of sampling employed at this site may have led to some gas loss resulting in a falsely high indication of recharge temperature. The Naivasha well indicates a recharge temperature much below that expected for its altitude, which would imply that its recharge originates from a level comparable to that recharging the Kijabe RVA and Kinangop P65 wells (sites 25 and 92). Stable isotopic evidence offers slightly equivocal support for this contention.

For free gas samples, plots of Kr content vs Ar content and Xe content versus Kr content are shown in figure 6.13b. They indicate that the gases were probably all originally derived from meteoric water, but that air contamination has affected some samples (111, 126–128). In the case of OW 26 and F 23 (111, 128) this probably occurred during sampling or storage, but there is other evidence from gas measurements (see above) that the Suswa and Domes fumaroles F-3 and F-15 (126 and 127) may already have had air entrained. The Bala sample (53) was collected from a bubbling pool, where it is sometimes difficult to avoid some air contamination (cf. Kariandusi spring, 35). However, N_2/Ar at Bala is *lower* than water, presumably due to high ^{40}Ar (see below), which indicates that this alone is responsible for the shift from the ASW (air saturated water) line. This is confirmed by the Xe vs Kr plot which shows that the Bala sample is consistent with an ASW origin. The ratio Kr/Xe suggests a recharge temperature of 10°C, and while this ratio seems liable to underestimate temperatures by 10°C or so, it does imply that this water has not been subjected to boiling at any stage, and is unlikely to be cooled outflow from a high-temperature geothermal system. This is in agreement with the chemical geothermometers (6.4.7).

The inert gas results also provide other information. They confirm that the Soysambu DEL well (site 124) has large amounts of helium and carbon dioxide in solution and also indicate that helium is enhanced in the Kijabe RVA well (site 25). A warm spring near to this particular well had a ^{3}He/^{4}He index close to that of air, so possibly radiogenic ^{4}He is offsetting a ^{3}He contribution. However, examination of the ^{40}Ar/^{36}Ar ratio (Table 6.14) indicates that in every case the value is comparable to that in air, 295.6 (Nier, 1950), and that therefore there is very little production of the radiogenic ^{40}Ar isotope which usually accompanies ^{4}He production.

6.4.6.3 Implications of the gas data

The non-inert gas data are all collected from thermal manifestations and are only interpreted in a qualitative way: presence of He and H_2 is indicative of proximity to an upflow, while the ratio C_2H_6/CH_4 may be a measure of lakewater input to a hydrothermal system. Quantitative interpretation of gas data from the Suswa, Longonot and Domes areas has been provided by Armannsson (1987b).

The inert gas and helium isotope data however have relevance to both thermal and non-thermal hydrogeology. There appears to be little evidence of the enhancement of radiogenic He and Ar isotopes which usually occurs in waters with long residence times. In this respect the data support the conclusion of ^{14}C measurement. Where high helium is encountered it appears to be due to a ^{3}He component which is the consequence of close association with volcanic centres. There is from the work so far no real indication that mantle helium is encountered in association with deep faulting. The recharge temperatures gained from consideration of amounts of inert gases in solution tend to confirm the pattern of recharge inferred from chemical and isotopic data: that much recharge is essentially local to the sampling points with flowpaths usually short. It is unlikely, at least in the cases where inert gases indicate sensible temperatures, that waters have circulated to great depths and have then cooled again during travel to the surface as this would have upset the inert gas ratios.

The foregoing evidence (particularly the ^{3}He/^{4}He and inert gas radioisotope data) points to the fact that there is no sign shown by groundwaters of mixing with a deep, long residence component. Only groundwaters closely associated with volcanic centres (e.g. at site 124) show large He enhancement, and even this seems to be caused by volcanic gas inflow rather than long residence of water.

Table 6.14 Dissolved gas ratios from mass spectrometric measurement of Rift Valley groundwaters

(Samples measured at the University of Bath by Mr M J Youngman)

Site	Site name	^{40}Ar/^{36}Ar ratio	±	N_2/Ar ratio	±	CO_2/Ar ratio	±
25	Kijabe RVA	294.1	1.3	37.8	0.2	20.9	1.5
28	Mayer's Fm	294.1	1.0	39.9	0.2	97.3	1.3
35	Kariandusi Spr	295.4	0.5	49.8	0.7	93.3	1.2
82	Naivasha C4178	296.4	2.2	42.4	0.2	62.5	1.1
92	Kanyamwi Fm	294.9	2.0	39.3	0.2	41.3	1.5
96	Kinangop P65	296.8	0.9	39.1	1.0	61.0	3.7
100	Ndabibi C1404	296.6	0.8	57.9	0.4	39.2	0.9
118	Nakuru No. 7 (Lanet)	293.7	1.3	40.2	1.3	35.5	0.7
124	Soysambu DEL	297.0	2.7	35.2	0.3	972.0	87.0

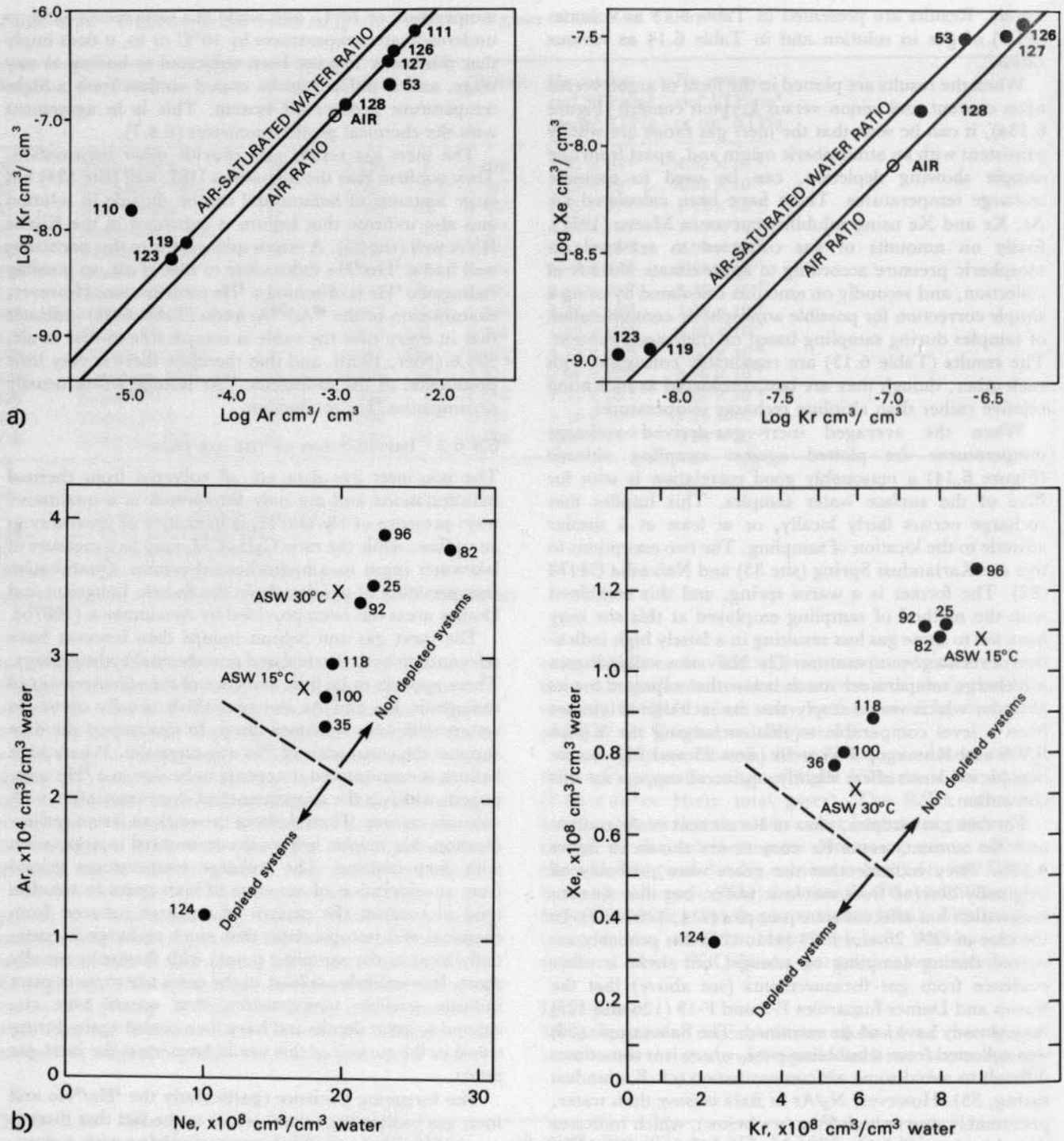

Figure 6.13a Plots of argon versus krypton and xenon versus krypton contents of selected fumaroles in the Suswa–Nakuru sector.
b Plots of argon versus neon and xenon versus krypton for selected groundwaters in the Suswa–Nakuru sector.

6.4.7 Geothermometry

6.4.7.1 Water chemistry

These geothermometers involve consideration of the effect of temperature either on solubility of a species (normally a form of silica) or on the amount of exchange of various cations (the alkali and alkaline earth metals). In older rocks and at temperatures above 150°C quartz is likely to be the controlling mineral phase for the silica geothermometer, but in rocks of Rift age below 150°C control is likely to be by cristobalite or chalcedony. The original basic alkali geothermometer of Na/K (White, 1965), which assumes cation exchange with alkali feldspar, has been supplemented by versions including Ca and Mg (Truesdell, 1975, Fournier and Potter, 1979) and a correction for low temperature waters (Paces, 1975). Table 6.15 shows the results of nine geothermometer calculations based on these various premises for all the Rift Valley Geothermal Project samples for which appropriate chemical data exist. These are now discussed with reference to the various sectors of the Rift studied during the project—Magadi, Suswa–Nakuru, north of

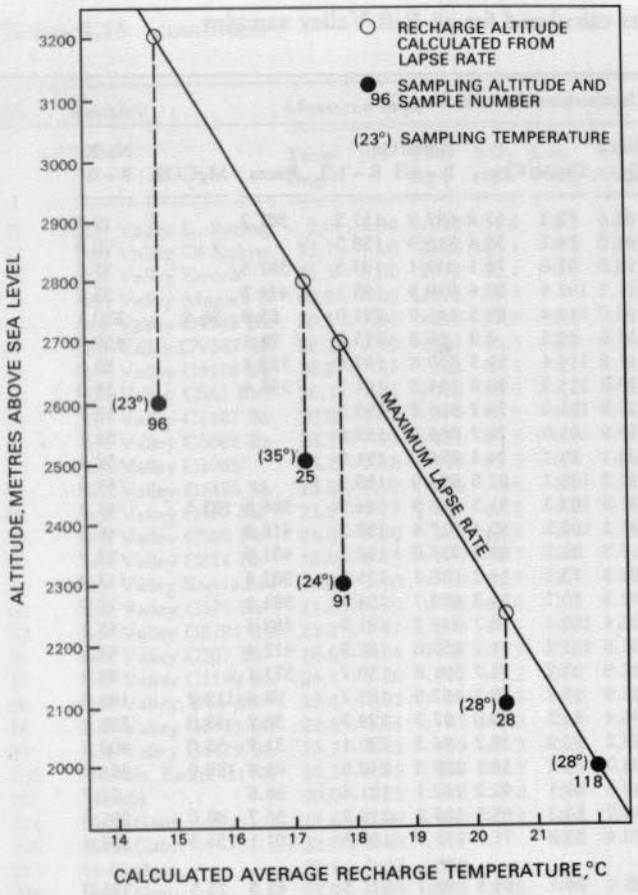

Figure 6.14 Plot of enert gas-derived recharge temperatures versus sampling altitude for selected groundwaters in the Suswa–Nakuru sector.

Menengai, and north eastern margins of Lake Victoria.

The Magadi hot springs have surface temperatures of up to 85°C and TDS values rising to over 40 000 mg/l (Section 6.6). As a consequence of the highly alkaline chemistry of the springs the simple Na/K geothermometer gives unrealistically low temperatures, while low levels of Ca and Mg make use of the corrected versions inappropriate. Indeed most of the more obviously thermal waters in the Rift are low in Ca and Mg as a consequence of various mineral controls. Of the SiO_2-based geothermometers, amorphous silica can be ruled out, as it can be in the whole of the Rift. Cristobalite gives results often little different from the sampling temperatures, but both chalcedony and quartz give reasonably steady temperatures well in excess of sampled temperatures which suggests that these warm springs have a single source at a temperature between 100°C and 130°C variously affected by cooling and/or mixing processes (Section 6.6). Two boreholes between Magadi and Suswa—Oltepesi and Mosiro (sites 22 and 129)—have medium TDS waters of ambient temperature which on chemical and isotopic grounds show little evidence of a thermal origin. The lowest temperatures suggested by geothermometers for the two sites are 76°C (cristobalite) and 58°C (Mg corrected alkali) respectively, but it seems unlikely that these well waters haye ever reached such temperatures.

The same is probably true for most of the groundwaters in the Suswa–Nakuru sector of the Rift (with the obvious exception of the Olkaria–Hells Gate area, which is considered separately) where for most of the waters the alkali geothermometers are excessive and even the silica-based ones are rather high. It is unlikely, for example, that borehole waters of ambient temperature (i.e. around 20°C) in the vicinity of Lake Naivasha have been raised to over 65°C then cooled again during their passage from recharge to discharge. Such waters are characterised by low TDS values, virtually precluding mixing with thermal components. The chemical geothermometers are therefore also unconvincing in this sector of the Rift, with the exception of the wells north of Eburru and the warm spring on the edge of Lake Elmenteita (sites 121–125 and 41–42) which are considered on other grounds to have a thermal component.

The sampled waters of the Bogoria–Silale area are generally hot (up to boiling) and the quartz and CO_2-corrected alkali geothermometers suggest a source for Kapedo and Lorusio waters at a temperature of 120–160°C, probably at the lower end of this range. The boiling spring of Ol Kokwe Island in Lake Baringo (site 71) yields a higher-temperature set of results of which quartz and CO_2-corrected alkali geothermometers agree well (about 175°C) though cristobalite at 152°C is also plausible.

The Bala hot springs of the Homa Bay area of north-east Lake Victoria range in temperature from 35°C to 75°C. Only the quartz geothermometer gives a credible temperature range, 112°C to 118°C. The appropriate Na/K/Ca geothermometer gives a rather high temperature.

Various factors affect the performance of geothermometers. Steam separation can affect silica concentrations, owing to adiabatic rather than conductive cooling, but this is only likely to apply to large, vigorously boiling springs, which are uncommon in the Rift. More importantly, amounts of silica in cooler Rift groundwaters may be raised to levels in excess of cristobalite or chalcedony equilibrium concentrations by release of silica from alteration of silicate minerals, e.g. by influx of CO_2 (Fournier, 1981). The ubiquity of of CO_2 in the Rift (Bailey, 1980) is consistent with this interpretation. As mentioned earlier the alkali geothermometers can be affected by high Mg contents, but this element is almost always present at very low levels in Rift Valley groundwaters.

The overall impression given by the geothermometer results is that those based on cations must be used cautiously in the Rift Valley. Of the silica-based geothermometers, quartz and chalcedony appear to be useful for hot springs, but for cooler waters, although chalcedony is the least oversaturated SiO_2 species and therefore theoretically most likely to tend towards the actual maximum temperature achieved at depth, it still produces temperature estimates which appear to be excessive. In this respect cristobalite is more reasonable, although it also often appears to overestimate temperatures at depth.

6.4.7.2 Gas geothermometers

These depend on temperature-controlled gas–mineral equilibria being achieved in the reservoir(s) which feed the fumarole, well or spring. Various versions exist, some using single gases and some gas ratios (Arnorsson and Gunnlaugsson, 1985). Carbon dioxide, hydrogen and hydrogen sulphide are the most suitable gases to use for geothermometry because the reactions controlling them seem to approach equilibrium over a large temperature range, but H_2 and H_2S are often only present (if at all) below detection limit in Rift Valley fumarole gases. Methane, although usually second only to CO_2 as a 'geothermal' gas, is more loosely related to reservoir temperatures owing to departures from the controlling reactions (Arnorsson and Gunnlaugsson 1985), the main one of which may be the Fischer-Tropsch reaction be-

Table 6.15 Various SiO_2 and alkali cation geothermometers calculated for all Rift Valley samples

Site	Locality	Measured data						Geothermometers, in Deg C							
		Temp DegC	pH	TDS mg/l	SiO_2 mg/l	Log PCO_2	Amphs	Silica Qz	Chalc	Crist	Na/K/Ca B = 4/3	Na/K/Ca B = 1/3	Paces	MgCOR	Na/K B = 0
16	Magadi Bird 1	40.8	9.58	45228	54.8	-2.2	- 8.4	108.4	77.3	57.8	697.9	157.2	387.7		19.7
17	Magadi Bird 2	40.5	0.00	19728	53.5		-10.5	106.0	74.7	55.4	718.9	158.5			20.0
1	Little Mag 1	84.6	8.85	34499	79.8	-1.2	7.7	126.8	97.6	76.1	857.1	195.3	382.5		57.7
2	Little Mag 2	80.7	9.07	39606	86.0	-1.4	11.5	131.1	102.4	80.4	939.9	195.1	424.3		53.2
20	R. Ewasongiro	25.7	8.20	315	105.2	-2.9	19.5	140.0	112.4	89.5	115.7	221.0	65.8	96.2	330.1
21	R. Oloibortot	21.5	8.00	71	16.7	-3.3	-51.5	57.0	22.5	7.9	50.8	215.9	21.1		450.8
9	Mag NW Lag 1	45.0	8.82	31556	105.2	-1.6	21.1	141.8	114.4	91.3	679.8	167.6	339.4		33.5
10	Mag NW Lag 2	43.5	8.81	31321	101.2	-1.6	19.1	139.6	111.9	89.0	584.5	161.7	298.4		33.0
3	Little Mag 3	85.3	0.00	37195	84.3		10.4	129.9	101.0	79.2	908.8	193.5			52.7
4	Little Mag 4	81.3	0.00	17704	86.0		10.4	129.9	101.0	79.2	884.5	192.8			53.1
5	Little Mag 5	78.6	0.00	15836	78.7		6.2	125.1	95.7	74.4	874.9	191.9			52.4
6	R. Little Mag	72.4	0.00	32431	88.6		12.6	132.3	103.7	81.6	894.9	188.9			47.6
7	Little Mag 7	82.0	9.18	30512	88.1	-1.5	12.2	131.9	103.3	81.3	806.9	184.9	386.5	183.5	47.3
8	Little Mag 8	82.6	9.13	39156	86.0	-1.4	11.5	131.1	102.3	80.4	917.4	190.5	418.0		48.6
18	L. Magadi S 1	45.3	9.57	42454	68.4	-2.2	1.1	119.3	89.2	68.6	735.0	162.1	401.9		23.4
13	L. Magadi E 1	39.5	9.56	41960	50.9	-2.2	-11.6	104.8	73.3	54.2	698.1	155.5	387.8		17.7
14	L. Magadi E 2	38.5	9.56	41704	48.3	-2.2	-13.7	102.3	70.7	51.8	688.7	154.5	384.1		17.0
11	Mag NE Lag 2	66.6	8.96	38141	83.4	-1.4	10.0	129.4	100.4	78.7	814.2	181.9	383.4		43.1
12	Mag NE Lag 2	60.2	9.13	43302	86.8	-1.6	12.2	131.8	103.2	81.2	859.8	182.9	412.4		42.0
15	L. Magadi E 3	34.0	9.86	23678	35.7	-2.8	-25.9	87.9	55.2	37.7	591.8	159.7	371.1		29.9
22	Oltepesi Bh	0.0	8.80	615	82.8	-3.3	7.8	126.9	97.7	76.3	147.9	185.7	98.9	112.2	185.1
33	Majiyamoto 1	51.2	7.25	261	44.3	-1.9	-18.8	96.4	64.2	46.0	97.3	229.3	36.2	53.9	398.3
34	Majiyamoto 2	52.5	7.07	251	52.0	-1.7	-12.5	103.7	72.2	53.2	94.3	230.1	31.7	55.0	408.2
32	R. Ewasongiro	22.2	7.85	135	53.0	-3.0	-11.6	104.7	73.2	54.1	109.3	248.6	61.8	139.0	464.9
26	Kijabe Spr	43.3	9.05	379	40.6	-3.5	-22.0	92.5	60.1	42.2	142.1	121.6	98.6		52.7
27	Kijabe Str	16.9	7.05	174	67.2	-2.1	- 1.7	116.2	85.8	65.5	123.2	210.3	56.7	88.0	281.3
25	Kijabe Rva	35.0	7.95	366	77.4	-2.5	4.7	123.4	93.8	72.7	175.8	180.3	101.1	155.3	153.6
29	Mt. Margaret	87.2													
28	Mayers Farm	27.9	7.90	279	65.9	-2.6	- 2.5	115.2	84.7	64.5	96.1	211.5	45.5	75.5	325.0
31	Akira Ranch	0.0	0.00	-2		0.0									
30	Mt. Suswa	0.0	7.91	96	13.9	-3.2	-56.7	50.6	15.9	1.8	110.2	357.4	67.2	190.6	1683.6
24	L. Naivasha	0.0	7.90	303	9.4	-2.7	-67.0	37.6	2.6	-10.4	118.7	261.9	65.0	82.7	512.2
35	Rift Valley, Karian	23.0	0.00	0		0.0									
37	Rift Valley Merorony	30.0	6.46	301	93.7	-1.2	13.7	133.6	105.1	82.9	137.7	241.2	52.5	117.6	375.6
38	Rift Valley Merorony	24.0	0.00	0		0.0									
39	Rift Valley Chamuka	29.0	7.03	148	96.7	-2.0	15.2	135.3	107.1	84.7	129.8	252.1	60.9	181.2	437.0
40	Rift Valley R. Ngosor	23.0	0.00	0		0.0									
41	Rift Valley Elmenteita	45.0	9.29	3107	124.7	-3.0	28.6	150.0	123.7	99.6	401.6	188.0	269.9		93.6
42	Rift Valley Elmenteita	38.0		2313	121.9		27.3	148.6	122.1	98.2	364.1	191.2	-245.8		106.7
43	Rift Valley Eburru	92.0													
44	Rift Valley Lorusio	77.0	7.75	7559	78.1	-0.7	5.4	124.2	94.7	73.6	344.9	171.2	155.4		77.7
45	Rift Valley Lorusio	81.0	7.67	7412	76.4	-0.6	4.4	123.1	93.4	72.4	345.5	171.8	152.7		78.6
46	Rift Valley Lorusio	75.5	7.50	7086	75.9	-0.5	4.1	122.8	93.1	72.1	347.7	170.2	151.2		75.5
47	Rift Valley Lorusio	75.0	7.95	7489	75.9	-0.9	4.1	122.8	93.1	72.1	350.2	172.0	164.3		77.8
48	Rift Valley Kapedo S	50.0	8.25	3307	76.1	-1.8	4.1	122.7	93.0	72.0	274.3	155.2	148.2	140.3	68.0
49	Rift Valley Kapedo S	50.0	8.13	3238	75.3	-1.7	3.5	122.1	92.4	71.4	275.6	155.0	146.1	145.1	67.3
50	Rift Valley Kapedo S	27.0	8.09	3647	68.0	-1.8	- 1.0	117.0	86.7	66.3	251.2	149.3	133.3	128.4	64.3
51	Rift Valley Kapedo N	50.0	8.12	3251	78.7	-1.7	5.6	124.4	94.9	73.8	254.9	153.6	133.6	142.4	70.3
53	Homa Bay Bala S2	72.0	8.06	22328	63.5	-0.7	- 3.1	114.5	84.0	63.9	214.5	135.7	88.3		52.1
54	Homa Bay Bala S2	35.0	7.98	31961	67.8	-0.8	0.1	118.3	88.1	67.6	548.8	173.8	246.0	168.9	52.1
55	Homa Bay Bala S3	58.3	8.36	24092	68.4	-1.1	0.2	118.3	88.2	67.7	512.3	170.6	245.3		51.7
56	Homa Bay Bala S3	74.7	8.15	22046	64.0	-0.8	- 2.9	114.8	84.3	64.2	479.5	154.1	218.3		33.0
57	Homa Bay Bala S4	36.3	8.16	20987	60.1	-1.1	- 5.6	111.7	80.9	61.1	422.3	158.8	205.5	151.5	46.2
58	Homa Bay Bala Lime	0.0	0.00	148	10.3	0.0	-64.8	40.4	5.4	- 7.8	79.4	206.0		52.0	332.7
59	Kisumu Lake Simbi	0.0	10.04	23036	126.6	-3.1	30.5	152.1	126.1	101.7	380.2	145.5	258.0		33.5
60	Homa Bay Lakeshore	0.0	0.00	799	6.7	0.0	-75.3	27.2	-8.1	-20.2	80.2	206.1		53.2	331.6

Table 6.15 continued

Site	Locality	Measured data						Geothermometers, in Deg C							
		Temp DegC	pH	TDS mg/l	SiO_2 mg/l	Log PCO_2	Amphs	Silica Qz	Chalc	Crist	Na/K/Ca B = 4/3	Na/K/Ca B = 1/3	Paces	MgCOR	Na/K B = 0
70	Rift Valley L. Baring	0.0	8.94	910	31.0	−3.3	−31.7	81.0	47.7	31.0	154.8	178.6	104.4	57.0	162.5
71	Rift Valley Ol Kokwe	93.7	7.00	3128	186.1	−0.8	51.9	175.1	152.6	125.4	383.3	197.0	177.1		112.3
72	Rift Valley Emerit	36.5	0.00	2013	35.1	0.0	−27.4	86.2	53.3	36.0	142.0	126.2		40.1	60.8
73	Rift Valley Magadi N	62.8	0.00	45172	75.3		5.5	124.3	94.8	73.7	1045.2	201.0			56.0
80	Rift Valley C4989 Bh	20.5	7.04	212	77.9	−2.5	4.9	123.7	94.1	73.0	122.3	272.2	62.7	118.1	561.6
81	Rift Valley CV567 Bh	22.1	7.70	367	60.5	−2.9	− 6.2	111.0	80.2	60.4	125.7	174.9	73.3	63.2	174.7
82	Rift Valley C4178 Bh	20.3	7.45	363	80.2	−2.1	6.3	125.3	95.9	74.6	109.9	200.9	47.9	135.6	266.6
83	Rift Valley C563 Bh	26.3	7.71	328	65.0	−3.0	− 3.1	114.6	84.0	63.9	143.3	199.8	87.5	50.6	227.0
84	Rift Valley C1487 Bh	20.8	7.82	574	68.2	−3.1	− 1.0	117.0	86.7	66.3	152.1	168.6	97.1		141.2
85	Rift Valley C5002 Bh	20.2	7.95	151	69.3	−3.6	− 0.3	117.7	87.5	67.1	122.1	205.7	83.5	134.6	267.3
86	Rift Valley C1063	26.2	7.18	336	99.5	−2.4	16.7	136.9	108.8	86.3	127.6	229.3	65.4	38.7	344.0
87	Rift Valley C1488 Bh	25.5	7.97	290	77.6	−3.3	− 4.8	123.6	94.0	72.9	175.4	217.0	119.6	199.8	248.0
88	Rift Valley C467 Bh	23.9	7.77	469	62.2	−3.0	− 5.0	112.4	81.7	61.8	149.0	172.0	92.1	128.0	150.9
89	Rift Valley C580 Bh	24.6	8.20	582	62.0	−3.3	− 5.1	112.2	81.5	61.6	142.2	159.4	93.8	122.2	126.5
90	Rift Valley C814 Bh	18.0	8.13	186	72.7	−3.7	1.8	120.2	90.2	69.5	137.5	193.3	98.1	169.1	213.8
91	Rift Valley Kanyamwi	24.0	7.30	48	81.7	−3.4	7.2	126.2	96.9	75.6	120.4	240.8	77.7	150.2	403.8
92	Rift Valley C570 Bh	21.9	6.99	50	82.6	−3.1	− 7.6	126.8	97.5	76.1	120.2	240.8	72.0	154.9	404.0
93	Rift Valley C3784 Bh	23.2	7.47	239	95.2	−3.1	14.5	134.4	106.1	83.8	132.0	240.9	82.1	107.5	383.8
94	Rift Valley C307 Bh	18.6	8.34	1436	62.5	−3.2	− 4.8	112.6	81.9	62.0	257.0	181.7	178.4		119.7
95	Rift Valley C1190 Bh	24.1	8.20	192	43.2	−3.8	−19.7	95.3	63.0	44.9	144.6	176.1	105.3	156.8	163.6
96	Rift Valley, P65 Bh	22.6	7.01	27	72.9	−3.2	2.0	120.3	90.4	69.7	113.9	255.3	70.0	125.6	488.7
97	Rift Valley C3955 Bh	22.6	6.64	87	101.8	−2.4	17.8	138.2	110.3	87.6	139.9	257.6	75.0	139.5	443.3
99	Rift Valley C4179 Bh	25.7	7.13	469	63.5	−2.3	− 4.1	113.4	82.8	62.8	39.1	121.7	− 0.9		117.8
100	Ndabibi Estate C1404	26.3	6.95	263	100.5	0.0	17.2	137.5	109.5	86.9	147.5	228.5		162.2	313.5
101	Maiella	20.0	7.65	176	77.0	0.0	4.4	123.1	93.5	72.5	124.2	274.3		123.9	568.8
104	Hells Gate	19.6	0.00	655	121.9	0.0	27.2	148.5	122.0	98.1	211.2	161.9		158.8	99.0
106	Hells Gate	52.0	3.98	417		0.0					218.1	292.1	0.0	275.8	
107	Hells Gate	32.4	0.00	2318							207.6	157.2			91.6
108	Hells Gate	23.0	0.00	1282	85.6	0.0	9.4	128.7	99.7	78.1	182.4	182.2		133.0	153.9
109	Kenya Rift	72.0	0.00	1350	145.5		37.0	159.2	134.2	109.3	150.3	114.1			36.9
110	Olkaria Well 2	152.0	6.25	1590	117.9		25.5	101.2	69.4	50.7	122.8	241.6		35.9	278.6
111	Olkaria Well 26	159.0	6.05	676	534.7		134.9	146.6	119.8	96.1	489.8	292.1			236.9
112	Olkaria 22	157.0	6.20	1091	453.5		119.2	257.8	253.7	214.3	358.6	254.6			180.1
113	Olkaria Well 16	148.0	6.20	1258	530.5		134.1	242.9	234.9	197.9	403.5	235.9			238.1
114	Olkaria Well 23	153.0	6.20	764	528.3		133.7	257.1	252.8	213.5	479.8	273.5			222.6
115	Olkaria Well 21	152.0	6.20	1152	560.4		139.6	256.7	252.3	213.0	386.2	253.1			224.7
116	Olkaria Well 5	156.0	6.20	17	4.9	0.0	−82.2	262.3	259.4	219.2	487.6	268.4			208.3
121	ADC Farm B/h C431	37.1	6.95	1632	126.2	−0.8	29.1	18.2	−17.0	−28.5					
122	Well C1798	0.0	0.00	950	105.7	0.0	19.7	150.6	124.4	100.2	167.7	200.4	64.2	189.8	245.4
124	Soysambu Estate B/h	32.4	6.40	1702	130.5	−0.3	31.0	140.3	122.7	89.7	136.0	203.6		156.4	243.7
125	Soysambu Estate B/h C19	27.8	7.95	1541	66.3	−2.0	− 2.2	152.6 115.6	126.7 85.2	102.3 64.9	169.8 181.8	213.9 185.6	56.8 94.1	164.8 23.8	162.1
128	Lanet Nakuru No. 7	27.9	7.00	306	81.3	−1.7	6.9	126.0	96.6	75.3	123.7	213.8	51.2	153.2	292.5
129	Mosiro B/h	0.0	0.00	898	92.0	0.0	12.8	132.6	104.0	82.0	156.7	233.0		57.8	318.2

tween CO_2 and molecular H_2.

Armannsson (1987b) dealt with the application of gas geothermometers to the Suswa, Longonot and Domes areas. This study has used the CO_2/H_2 geothermometer to estimate temperatures at depth, but this has been possible at only two sites (Table 6.16). Methane/carbon dioxide ratios from these and other sites have been applied to the theoretical CH_4/CO_2-temperature curve of Ellis and Giggenbach presented in Glover (1972). The results are also given in Table 6.16.

While the CO_2/H_2 geothermometer gives apparently plausible results for Longonot and Eburru, the CH_4/CO_2 temperatures seem too high. Arnorsson and Gunnlaugsson (1985) warn that these cannot necessarily be interpreted as equilibrium temperatures preserved from greater depths.

6.4.7.3 Isotope geothermometers

Various isotope fractionations can in principle yield information on temperatures at depth. The fractionation of water can itself reveal information on boiling temperatures if certain assumptions are made; this subject has been mentioned in Section 6.4.3. Differences between $\delta^{18}O$ values in steam condensate and accompanying CO_2 from fumaroles could also be used since isotopic exchange ceases in the vapour phase, but rapid re-equilibration at condensation temperatures can only be prevented with sophisticated sampling techniques such as cryotrapping. Another possible geothermometer is the fractionation of $\delta^{13}C$ between DIC and CO_2 gas, but since this requires a sample of liquid from which to obtain the DIC the exercise is usually academic. However, it may be noted that at the Soysambu DEL well (site 124) the $\delta^{18}O$ CO_2-H_2O and $\delta^{13}C$ DIC-CO_2 equilibria are in exact agreement with the measured temperature (Table 6.9).

Other geothermometers which have been used in geothermal systems elsewhere are the H_2-H_2O (Arnason, 1977) and the $\delta^{13}C$ CO_2-CH_4 fractionation (Hulston, 1977). Insufficient sample volumes were collected to attempt isotopic measurement of H_2 or CH_4 except at Eburru, where $\delta^{13}C$ CH_4 was measured on a sample from site 119. This gave the very enriched result of $-6.7‰$ which indicates a very high temperature and may be incorrect, though it is worth noting that samples collected previously from Eburru fumaroles gave unexpectedly high $\delta^{13}C$ CH_4 values averaging $-14.7‰$ corresponding with measured $\delta^{13}C$ CO_2 values to temperatures of around 500°C (Glover, 1972).

However the $\delta^{13}C$ CO_2-CH_4 geothermometer may not be universally applicable, depending as it does on the attainment of equilibrium for the Fischer-Tropsch reaction mentioned above, for example, at Olkaria this geothermometer indicates temperatures well in excess of 300°C (Glover, 1972), while subsequent well drilling has yielded fluid of significantly lower temperature. In view of the strong indications from stable isotopes that water from Lake Naivasha reaches Olkaria and perhaps some of the other high temperature areas in the Suswa–Eburru zone, the presence of biogenic methane produced from organically rich lake water cannot be excluded. Such methane would upset any isotopic geothermometer on the Fischer-Tropsch equilibrium.

6.4.7.4 Geothermometers — summary

The application of chemical geothermometers to ambient and warm groundwaters in the Rift Valley is often inappropriate. Most ambient groundwaters are local and will not have been raised to much higher temperatures or mixed with thermal waters during their travel, but many give excessive alkali and Si geothermometer temperatures, for reasons explained above. In hot springs and geothermal wells, however, both alkali and quartz temperatures are plausible unless, as at Magadi, local conditions are such that the Na/K/Ca geothermometer is rendered useless.

There are however comparatively few opportunities for sampling hot water in the Rift — most areas of thermal upflow appear as fumarolic discharges. The gas geothermometers are potentially useful here, though the ratio types, CO_2/H_2 and CO_2/H_2S, which are perhaps easiest to measure accurately, cannot often be applied because of the scarcity of H_2S and H_2 in Rift fumarole gases. CH_4/CO_2 ratios, though available for all gases, are a rather unreliable geothermometer both on account of the controlling reactions and the possibility of a biogenic component. The straightforward CO_2 geothermometer may be the most universally applicable one in the Rift, though Armansson (1987a) points out that cold CO_2 wells exist inside and outside the Rift where the CO_2 geothermometer cannot sensibly be applied. This is despite the indications from carbon isotope measurements that all the CO_2 has a similar origin

Isotope fractionations are by and large not particularly good geothermometers. Oxygen and hydrogen isotope fractionations between liquid and vapour phases only indicate the temperature of separation, which in fumaroles can be much cooler than reservoir temperature. The CH_4-CO_2 isotope geothermometer suffers from the same problems as the CH_4/CO_2 gas geothermometer. Other potential isotope geothermometers require difficult collection techniques (e.g. $\delta^{18}O$ liquid-CO_2 gas) or collecting large amounts of gas (e.g. δ^2H liquid-H_2 gas) and may only serve to indicate separation temperatures.

6.5 HYDROGEOLOGY OF THE OLKARIA GEOTHERMAL FIELD

6.5.1 Introduction and previous work

Geothermal exploration at Olkaria started in the 1950s, and the first exploration well, X1, was drilled in 1956, followed by X2 in 1958. However these wells failed to produce steam and exploration drilling was abandoned until the 1970s when several successful wells were drilled (Noble and Ojiambo, 1975).

During the last decade production drilling has been carried out at Olkaria, and a 45 MWe power station has been constructed in the eastern part of the field. By early 1987 34 wells had been drilled at Olkaria of which 25 are in the East Olkaria production field which covers an area of approximately 2 km^2. Well depths generally range from 1000 m to 1600 m with the deepest well reaching 2484 m (Bodvarsson et al., 1987).

The subsurface stratigraphic sequence in the area comprises intercalated rhyolite, trachyte and basalt lavas with pyroclastic beds (Browne, 1981). A thick trachyte extends from 200 m to 400 m below which basalts and rhyolites predominate to 900 m. At greater depths trachytes form the main rock type (Bodvarsson et al.,1987).

A basaltic caprock between 500 m and 700 m is thought to confine the geothermal reservoir at Olkaria. A steam zone, between 50 m and 100 m thick at a pressure of 3.5 MPa and with a temperature of 240°C underlies the caprock. Below the steam zone is a liquid-dominated reservoir which follows a boiling point for depth relationship with a temperature of 300°C at a depth of 1500 m

(Bodvarsson et al., 1987). Above the caprock are shallow aquifers containing cool saline waters.

Zones of high permeability (feed zones) exist both in the steam zone and in the underlying liquid-dominated reservoir. These are few in number with normally one major feed in the steam zone and one or two in the liquid zone. There is no good correlation between rock type and permeability although it has been suggested that the pyroclastics may be more permeable (Browne, 1981). Permeability values are discussed in Section 6.3.5.

The East Olkaria field shows a substantial north–south pressure gradient of 1.1 MPa/km from which it has been inferred that an upflow zone exists to the north of the present field (Bodvarsson et al., 1987). Well temperature measurements (Haukwa, 1986) and the distribution of epidote (Browne, 1984) also indicate that the hottest, upwelling part of the field is to the north. Southerly flow beneath the caprock may then have created the steam zone by phase separation (Grant and Whittome, 1981). In a recent interpretation of reservoir hydrology (Barnett et al., 1987) it has been suggested that a major fault running east–west across the field—the Olkaria Fault—acts as a conduit for hot upwelling fluid, and that at shallow levels the upflow is perturbed by cooler fluids associated with a major north–south structure, the Ololbutot Fault.

In recent years exploration drilling has discovered extensions of the field to the west and north. Wells in the west Olkaria field have in general lower temperatures than those in the east, but they have encountered mainly liquid (and therefore their mass output is potentially higher). Permeability values in this area are similar to those in the east (Haukwa, 1984).

6.5.2 Geochemistry

The Olkaria geothermal field has already been mentioned as the only locality in the Rift where deep thermal fluid can be sampled, and as such has provided useful information, particularly isotopic, about flow southwards from Lake Naivasha. In addition to this larger scale picture, the relatively high density of sampling points in the eastern wellfield and the Hell's Gate (Ol Njorowa) Gorge permits closer analysis of the relationship between the wellfield and possible outflow in the gorge.

Figures 6.15a–l show locations of sampling sites in the wellfield (oblongs) and gorge (circles) with chemical and isotopic values indicated. It is apparent that there are changes in chemical and isotopic species, and also that there are similarities and dissimilarities in various species between the wellfield and gorge sampling sites. While the geochemistry of the Olkaria geothermal field has been investigated in considerable detail by other workers (Arnorsson et al, in preparation), a brief description of the changes across the wellfield is now given . Total dissolved solids (TDS) rise north to south from 676 to 1590 mg/l, an increase of some 2.4 times. Individual ions show fairly even increases of this order, except for SO_4 which does increase but is low in the southernmost well (OW2), HCO_3 which rises then declines again, and Si which is constant except for a lower level in OW2.

This general increase in TDS content across the eastern wellfield from north to south fits the regional model of southerly flow from Lake Naivasha deduced from isotopic evidence: water at the southern end of the wellfield has been in residence longer than water in the north and has thus had more time for reaction with the reservoir rock at high temperature. Clearly the water has achieved supersaturation in some species before others; silica values hardly change across the wellfield. Isotopic changes across the wellfield are not regular (Figures 6.15j and 6.15k). The southernmost well (OW2) is comparatively depleted, and if this represents a local dilution effect it may also explain the drop in Si and SO_4 already noted above. Otherwise, the variations between wells may be due to steam loss (a loss curve from OW26 is shown in Figure 6.10), though is more likely to be due to a combination of variable water–rock $\delta^{18}O$ shifting and local dilution. If the total fluid compositions are considered to derive from mixing of Rift-wall groundwater and Naivasha water, a 55 to 75% lakewater contribution is suggested.

The relationship of the three northern Hell's Gate (Ol Njorowa) water sampling points to the geothermal field seems fairly straightforward. The only sample from the western side of the gorge (site 107) has a very high TDS (>2000 mg/l) and most probably represents natural outflow or artificial effluent from the field. Although the temperature of this manifestation is only 32°C, the enrichment in dissolved solids is probably due to steam loss/evaporation. Sites 108 and 109, on the eastern side of the gorge opposite the wellfield, have a chemistry much closer to wellfield values which suggests that they are sampling relatively unmodified outflow. The higher TDS level in 109 shows that evaporation is likely to have occurred which, as for site 107, is likely to be related to steam heating because SO_4/Cl ratios are higher than in the deep fluids. Simple evaporation would tend to cause isotopic enrichment, and 109 with a higher TDS and temperature is accordingly slightly heavier than 108.

South of these sites, on the eastern side of the gorge, four sampling sites possess stable isotopic values similar to those from the wellfield. In terms of chemistry, however, these sites are very much lower in TDS which implies that they are not directly derived from deep fluid. Instead they are probably the result of condensation of steam which was separated from an Olkaria-type deep fluid which is undergoing progressively greater dilution with Rift-wall water as it flows to the south. In some cases the sampled springs or seeps are clearly associated with nearby fumaroles while in others the connection with a steam source is less obvious, but similar mechanisms seem to apply in each case.

The end result is that although sites 103–106 have similar isotopic values to the wellfield and sites 108 and 109, they are actually produced from lighter waters. Figure 6.16 shows the primary steam line for a 20% lakewater component. This line passes near F18, F19 and H2, suggesting that their steam shares a common origin. Site 103 appears to result from surface (or near-surface) condensation of F18, and an evaporative slope connects the fumarole with the seep. Similarly sites 105 and 106 are associated with F22 along a trend of similar gradient, while the fumarole itself lies near the 30% lakewater primary steam line. Site 104, which is situated about halfway between F18 and F22, has no obvious steam source, but an evaporative line sub-parallel to the other two would suggest that the source is around 25% lakewater, in accordance with the progressive southward dilution.

Fumaroles 01 to 03 were sampled in the wellfield itself. These samples lie outside the range of likely primary steam composition (Figure 6.10) and are probably the consequence of steam heating of cooler, more diluted lakewater overlying the Olkaria reservoir with values of about 0‰ δ^2H, 0‰ $\delta^{18}O$. A fumarole in the western Olkaria field could possibly be related to this process but may alternatively be a product of primary steam separa-

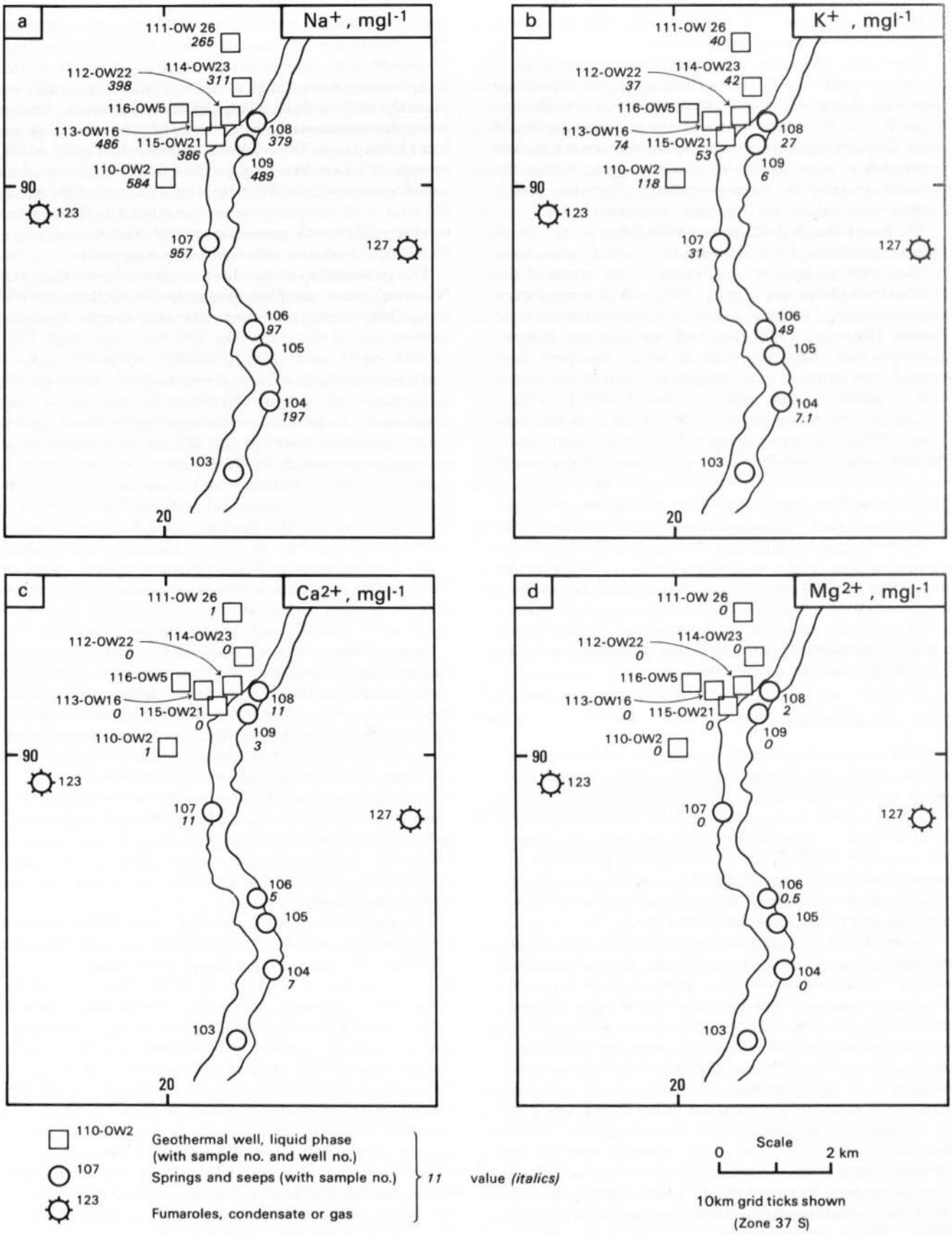

Figure 6.15a–l Maps of chemical and isotopic data fro the Olkaria–Ol Njorowa (Hell's Gate) geothermal area.

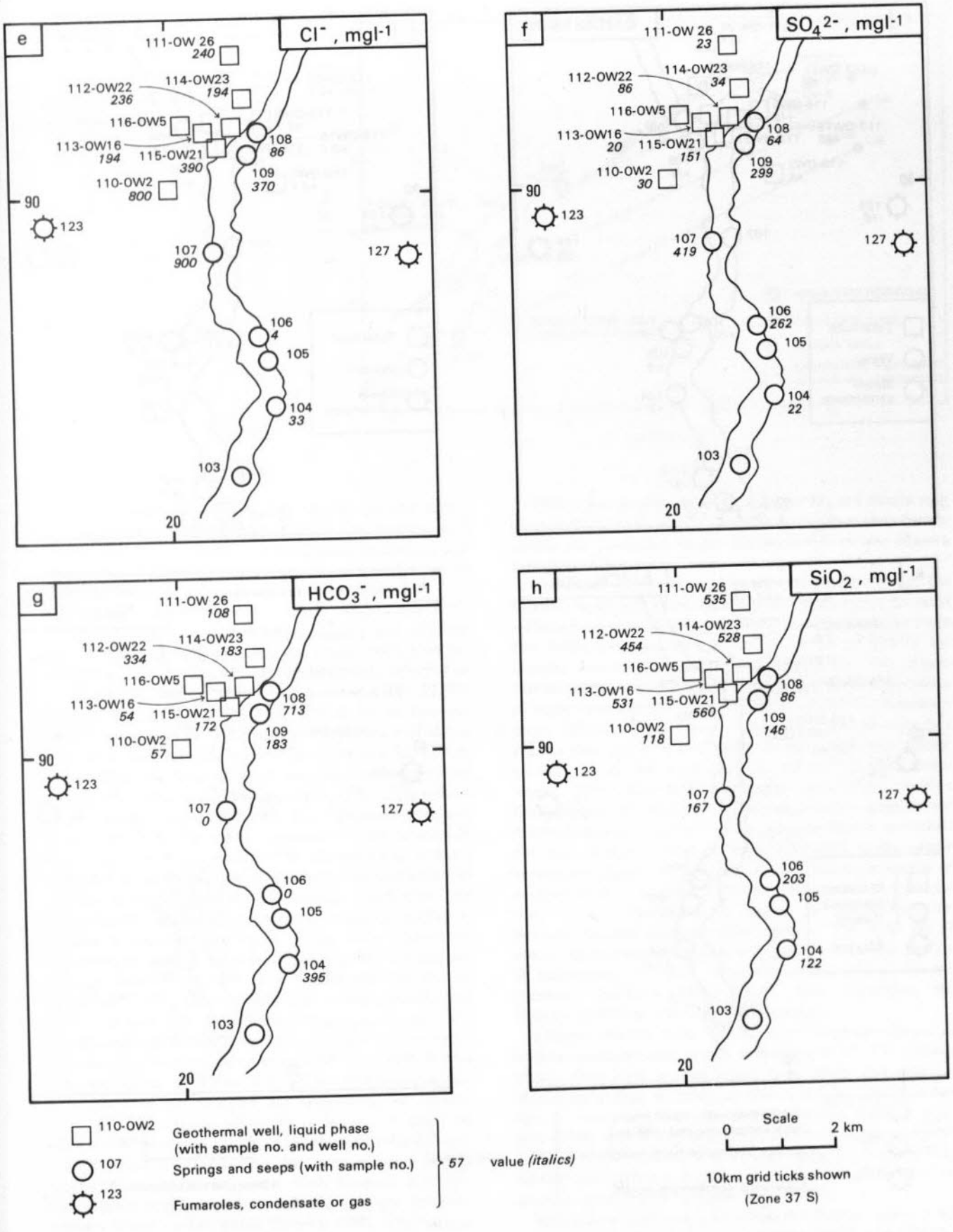
e
Cl⁻ , mgl-1
111-OW 26
240
112-OW22
236
114-OW23
194
116-OW5
113-OW16
194
115-OW21
390
110-OW2
800
108
86
109
370
90
123
107
900
127
106
4
105
104
33
103
20
f
SO4 2- , mgl-1
111-OW 26
23
112-OW22
86
114-OW23
34
116-OW5
113-OW16
20
115-OW21
151
108
64
110-OW2
30
109
299
90
123
107
419
127
106
262
105
104
22
103
20
g
HCO3⁻ , mgl-1
111-OW 26
108
112-OW22
334
114-OW23
183
116-OW5
113-OW16
54
115-OW21
172
108
713
110-OW2
57
109
183
90
123
107
0
127
106
0
105
104
395
103
20
h
SiO2 , mgl-1
111-OW 26
535
112-OW22
454
114-OW23
528
116-OW5
113-OW16
531
115-OW21
560
108
86
110-OW2
118
109
146
90
123
107
167
127
106
203
105
104
122
103
20
110-OW2
Geothermal well, liquid phase (with sample no. and well no.)
107
Springs and seeps (with sample no.)
123
Fumaroles, condensate or gas
57
value (italics)
Scale
0
2 km
10km grid ticks shown
(Zone 37 S)

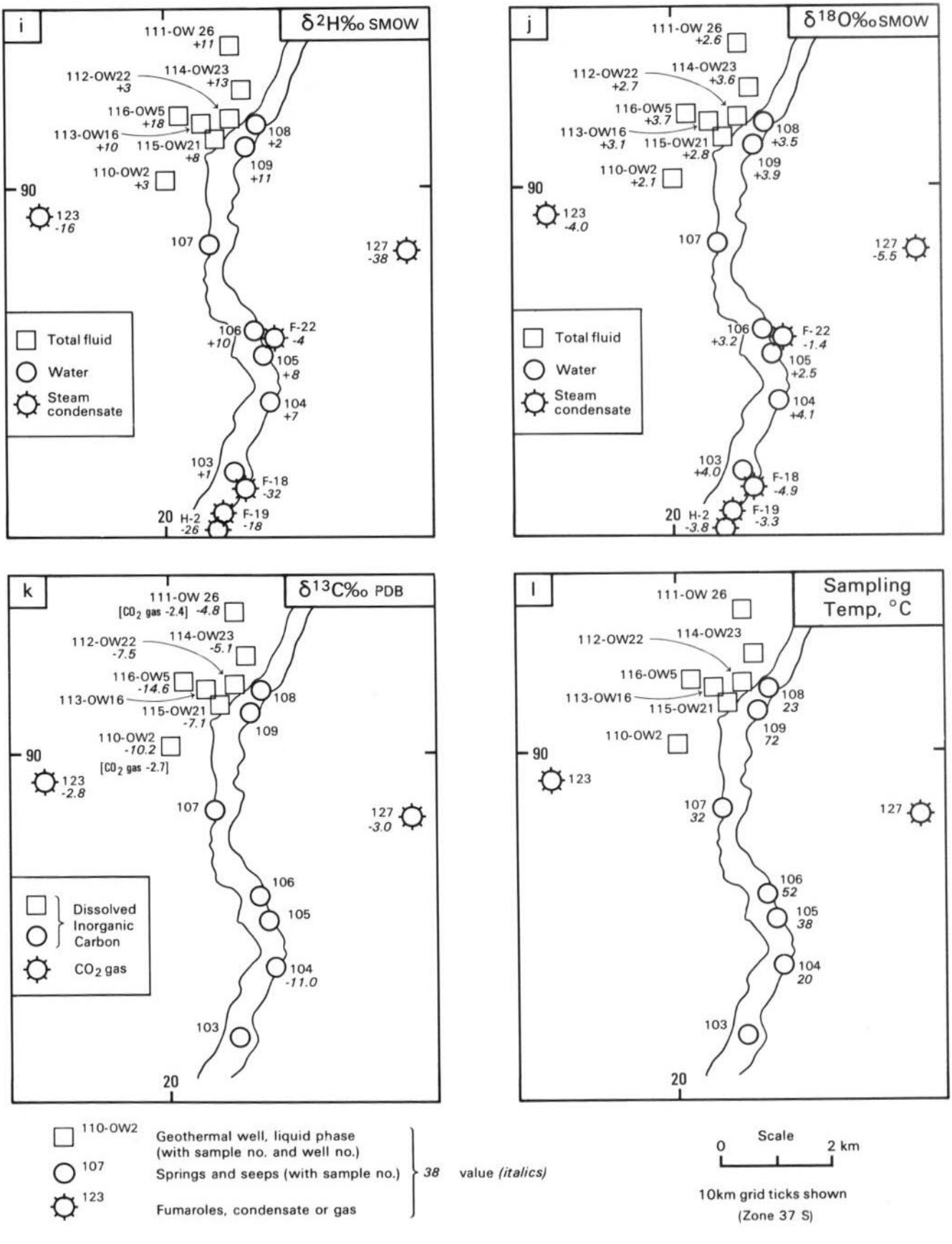
i
δ2H‰ SMOW
111-OW 26 +11
112-OW22 +3
114-OW23 +13
116-OW5 +18
113-OW16 +10
115-OW21 +8
110-OW2 +3
108 +2
109 +11
90
123 -16
107
127 -38
Total fluid
Water
Steam condensate
106 +10
F-22 -4
105 +8
104 +7
103 +1
F-18 -32
20
H-2 -26
F-19 -18
j
δ18O‰ SMOW
111-OW 26 +2.6
112-OW22 +2.7
114-OW23 +3.6
116-OW5 +3.7
113-OW16 +3.1
115-OW21 +2.8
110-OW2 +2.1
108 +3.5
109 +3.9
90
123 -4.0
107
127 -5.5
Total fluid
Water
Steam condensate
106 +3.2
F-22 -1.4
105 +2.5
104 +4.1
103 +4.0
F-18 -4.9
20
H-2 -3.8
F-19 -3.3
k
δ13C‰ PDB
111-OW 26 [CO2 gas -2.4] -4.8
112-OW22 -7.5
114-OW23 -5.1
116-OW5 -14.6
113-OW16
115-OW21 -7.1
110-OW2 -10.2 [CO2 gas -2.7]
108
109
90
123 -2.8
107
127 -3.0
Dissolved Inorganic Carbon
CO2 gas
106
105
104 -11.0
103
20
l
Sampling Temp, °C
111-OW 26
112-OW22
114-OW23
116-OW5
113-OW16
115-OW21
110-OW2
108 23
109 72
90
123
107 32
127
106 52
105 38
104 20
103
20
110-OW2 Geothermal well, liquid phase (with sample no. and well no.)
107 Springs and seeps (with sample no.)
123 Fumaroles, condensate or gas
38 value (italics)
Scale
0
2 km
10km grid ticks shown
(Zone 37 S)

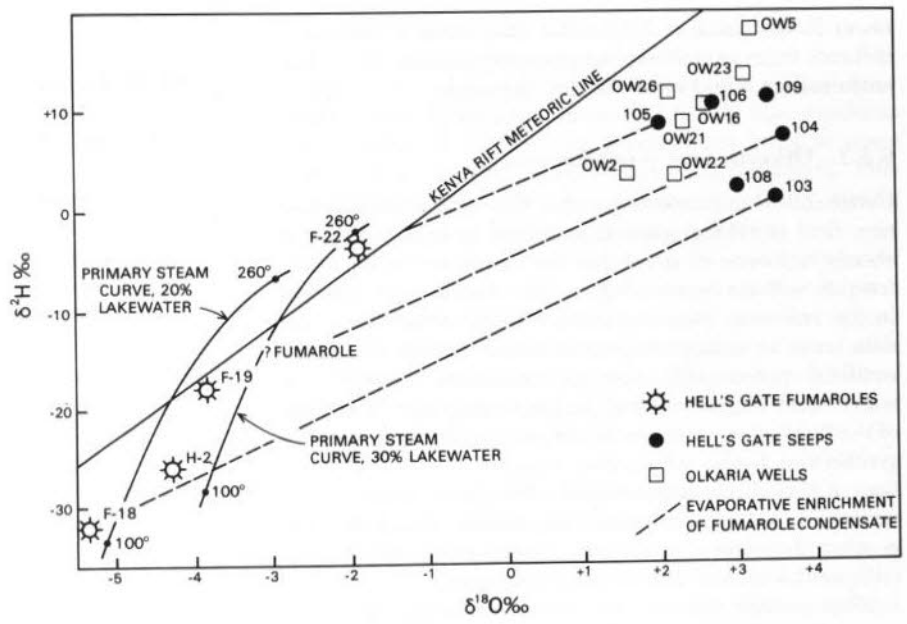

Figure 6.16 Delta-diagram of stable isotope data from the Olkaria–Ol Njorowa (Hell's Gate) geothermal area.

tion from a more dilute reservoir. In view of the major north-south fault (Ololbutot) dividing the eastern and western wellfields the latter is a tempting conclusion, but more western wellfield fumarole and/or wellfield data are required to confirm or refute this interpretation.

Carbon isotope ratios show a steady depletion in $\delta^{13}C$ DIC southwards across the geothermal field (Figure 6.15k). On the other hand, CO_2 gas from OW2, OW26, F15 and the western Olkaria fumarole already referred to are remarkably similar ($\delta^{13}C$ −2.4 to −3.0‰ PDB). Although HCO_3^- and CO_2 may almost be in isotopic equilibrium for OW26, indicating a temperature of about 200°C, they are completely out of equilibrium for OW2. This is unlikely to be a result of sampling technique; the fact that $\delta^{13}C$ DIC depletion is steady, $\delta^{13}C$ CO_2 values remain constant and bicarbonate concentration does not correlate with $\delta^{13}C$ depletion suggests that the explanation lies elsewhere. Changes in the $\delta^{13}C$ of well CO_2 in other geothermal fields have been attributed to the precipitation of calcite caused by near-well boiling conditions. As discussed below, there is no evidence for this occurring in the Olkaria wells on the basis of the water chemistry presented here, and in any case $\delta^{13}C$ CO_2 does not appear to change. In addition there is no reason why this should affect the $\delta^{13}C$ CO_2-DIC equilibrium, which would be expected to re-establish itself during transit to the surface. In the absence of further data the question remains open.

Gas samples were collected from OW2 and OW26 and results are given in Table 6.10. The geothermometric aspects of these gas samples are considered in Section 6.4.7.2 of this report, where it is suggested that the presence of a large percentage of lakewater in the Olkaria reservoir could be responsible for a proportion of the methane measured in the gases. Such biogenic methane would render unreliable chemical and isotopic geothermometers based on inorganic thermal CH_4. The ethane values from OW2 and OW26 appear to indicate a lakewater rather than a thermogenic origin: OW26 has the highest C_2H_6/CH_4 ratio of any gas sample collected while OW2, situated downflow, is lower. By contrast a very strong upflow like Longonot F23 (indicated by the presence of He and H_2, has a low C_2H_6/CH_4 ratio. On this rather tenuous evidence, the West Olkaria fumarole sampled may have a larger lakewater contribution than its H and O isotopic values suggest.

The lack of readily detectable He or H_2 at Olkaria suggests that the wells are further from an upflow than for example the Longonot crater fumarole F23 or the Eburru fumarole EF2.

Chemical geothermometers give good results for the Olkaria wellfield. There is reasonable agreement for most wells between the quartz and Na/K results. Samples from five wells give an average temperature of 255°C for quartz, and 240°C for Na/K (Table 6.15). The results can be compared with the average main feed temperature of eight (unidentified) Olkaria wells of 242°C (Armannsson, 1987b). In the same report, CO_2 geothermometry results were reported averaging 245°C, and it was assumed that calcite was a primary control of CO_2 concentrations. The WATEQF-calculated saturation indices though not as ideal for high-temperature geothermal systems as some specific codes, suggest that it is indeed the case. Calcite, although undersaturated, is the major carbonate phase, though not so very much in excess of magnesite and nahcolite. This undersaturation of calcite may be a consequence of cooling by conduction, or perhaps limited dilution, after upflow. The wells do of course show supersaturation with respect to quartz and, it is interesting to note, magadiite—a sodium silicate mineral, $NaSi_7O_{13}(OH)_3.3H_2O$, first identified by Eugster (1970) in the Lake Magadi area.

Tritium results from OW2 and OW26 are identical within measurement error, averaging 0.23 TU (Table 6.10). This level implies either that inflow has been in transit for at least 40 years, or that it is older than this but has a small amount of thermonuclear tritium (i.e. post-1954) as a result of leakage from the surface. Alternatively the ^3H content might result from the decay of ^6Li, though this process is probably of most significance in granitic rocks (Andrews and Kay, 1982).

Helium isotope ratios of corrected R/Ra values 5.69 and 5.83 (Table 6.12) were noted for OW2 and OW26. The values are close to those of Longonot F23 and Eburru EF2. The fact that they are slightly lower is presumably due to the fact that they are not directly situated over the local Olkaria upflow. A very similar R/Ra value of 5.62 was noted for the West Olkaria fumarole sampled. While this does not necessarily imply that the western wellfield is intimately linked to the eastern, it does suggest a similar proximity to an upflow. The Domes fumarole F15 gave a

lower R/Ra value of 2.92—this may suggest increasing distance from an upflow, but gas analyses indicate that air entrainment could have affected the ratio.

6.5.3 Olkaria area—conclusions

Geochemical indications are that flow across the production field is taking place from north to south. While it should be borne in mind that the chemistry of the water fraction will not be identical to that of total fluid at depth in the reservoir (due to steam and gas separation), the data serve to indicate a general rise in solutes across the wellfield presumably due to increasing amounts of water–rock interaction and perhaps steam loss. The TDS of the fluid is however low by the standards of many other geothermal fields, which may suggest a relatively short flow path and/or residence time, though the latter is constrained as to its lower limit by the tritium data. Chemical geothermometers give reliable results where they can be compared with well-bottom temperatures.

Water stable isotopes indicate a decreasing lakewater contribution to the deep fluid in a southerly direction. They also show that only a limited $\delta^{18}O$ shift is presently occurring: this implies a system of some antiquity where rock is approaching isotopic equilibrium with original water values after a large amount of throughflow. The alternative explanation, a younger but very 'wet' geothermal system seems less likely from the preliminary interpretation of the local water balance presented in this report. Core material obtained from some Olkaria wells will be subjected to stable isotope analysis to see what light can be shed on the field's history.

Gas data suggest that eastern Olkaria is not situated directly over an upflow since He and H_2 are only present at lower concentrations. Although the R/Ra values are relatively high these are not infallible indicators of proximity to upflow—for example the DEL well (site 124) on the Eburru outflow has a very similar R/Ra to EF2, even though it is situated some 10 km away.

The relationship between $\delta^{13}C$ CO_2 and $\delta^{13}C$ DIC is problematic, but the hydrocarbon gas ratios appear to confirm that substantial amounts of lakewater are present at Olkaria.

6.6 LAKE MAGADI THERMAL SPRINGS

6.6.1 Introduction

As a result of extreme evaporation of the alkaline lake brine (Na^+, HCO_3^{2-} + CO_3^{2-} type; salinity 290 000 mg/l), Lake Magadi contains a deposit of crystalline trona up to 40 m thick (Jones et al., 1977). This is composed of crystalline carbonates of sodium (principally sodium sesquicarbonate $Na_2CO_3.NaHCO_3.2H_2O$]) which is dredged by the Magadi Soda Company and treated before being calcined in large kilns to produce soda ash.

The lake is fed by groups of alkaline springs with temperatures varying between 34°C and 86°C which occur at several points around the periphery of the lake (Figure 6.17), adapted from Baker, 1958). In general the hottest springs are the most dilute and occur in the north, and the cooler more saline springs are found to the south of the lake. The values of discharge of the springs are very variable. Some are only seepages rising in the mud and shingle of the lake shore (for example those at Bird Rock). Others such as the main hot springs feeding Little Magadi are much larger, with flows of several litres/second.

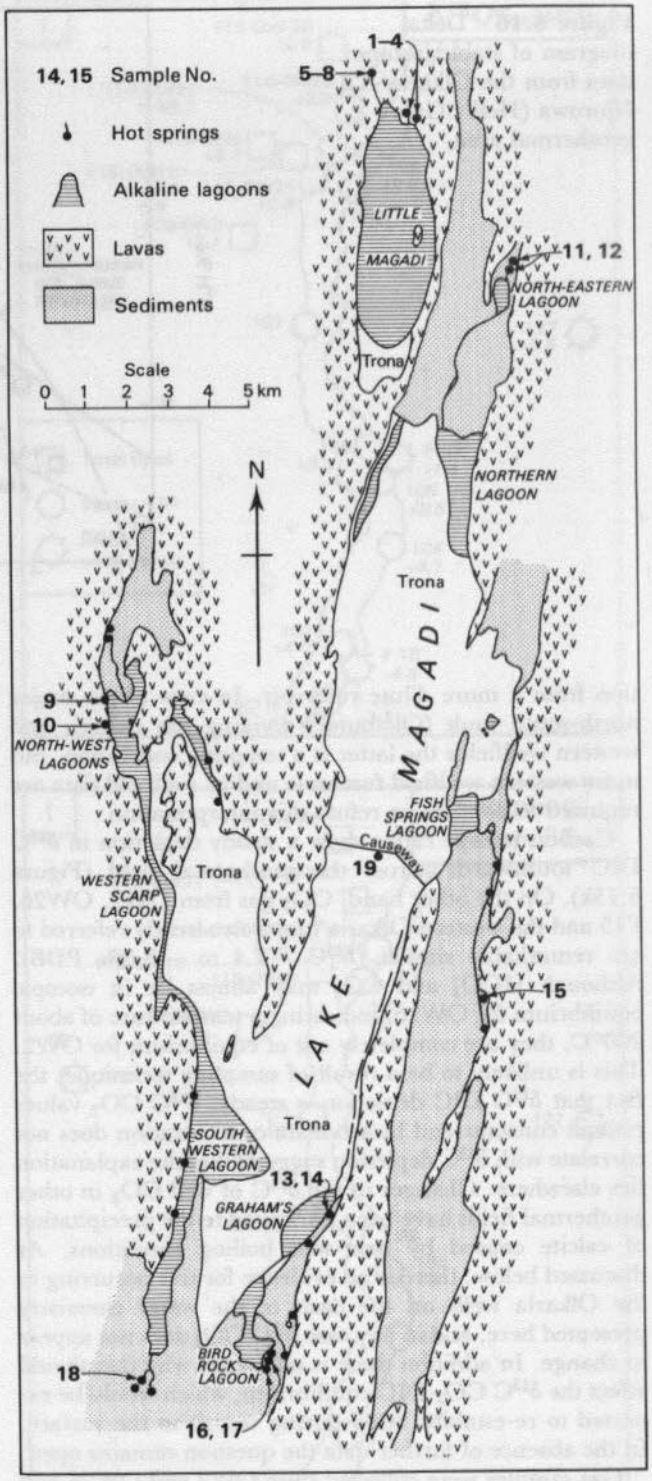

Figure 6.17 Location map of the Magadi hot springs.

According to Baker (1958) most springs issue from scree at the base of the fault escarpments bounding the lake and nearly all the spring waters then find their way into the stagnant lagoons that border the main trona bed at lake level. During and immediately after the rainy seasons the lagoons are connected with the shallow brine body covering the lake surface (Jones et al., 1977). This brine body vanishes during the dry seasons exposing a porous but firm trona deposit. As a result of the economic and scientific importance of Lake Magadi a number of studies have been carried out, usually aimed at determining the origin of the solutes forming the trona. These studies are reviewed here together with new data.

6.6.2 Origin of the hot springs—previous work

Early ideas concerning the origin of the springs are discussed by Baker (1958). He considers three hypotheses, namely Parkinson's, Stevens' and the re-circulation hypothesis.

Parkinson's hypothesis (1914) was that the spring water is of juvenile origin. The water, he suggested, contains magmatic CO_2 and reacts with the sodium silicates in the lavas through which it passes, forming sodium carbonate and silica. This hypothesis may be dismissed on the basis of the isotope evidence which proves the water to be meteoric in origin-although the chemical reaction suggested is valid.

Gregory in 1921 (cited in Baker, 1958) raised the possibility that the lake was an evaporating pan in which trona, leached from adjacent lavas by percolating waters was deposited, but he rejected the idea in favour of Parkinson's hypothesis.

Stevens (1932) concluded that the greater part of the lake salts at Magadi must be derived from spring solutes and he suggested that the constancy of the carbonate/chloride ratio in the springs implied a common source for them all, which he considered to be a large body of 'mother liquor' at depth. Later, in 1951, Guest and Stevens, having estimated the flows of the springs (by considering the rate of lake evaporation) concluded that the rate of solute addition to the lake was too great to account for its age (Guest and Stevens, 1951). They therefore reasoned that a proportion of the lake liquor must recirculate, with heavy liquor descending and becoming mixed with ascending hot spring water.

Bakers own hypothesis (1958) was that groundwater in the Rift Valley leaches salt from igneous silicates over a large area. These salts become concentrated by repeated evaporation of lake water, and re-leaching in the numerous pans between fault escarpments in the southern Rift Valley. Such waters would ultimately accumulate as alkaline groundwater in the Magadi basin at the lowest point in the Rift Valley, and would provide trona by evaporation of the spring waters.

More recently Eugster and others have proposed a detailed model for brine evolution at Magadi involving evaporative concentration as the main process for solute acquisition (Eugster, 1970; Jones, Eugster and Rettig, 1977; Eugster, 1980).

The basis for the model is that, according to Eugster, the Na/Cl ratios of stream waters on the sides of the Rift are similar to those of groundwaters, and for the springs bordering the lake. Eugster therefore proposes that the increase in solute concentration observed between the peripheral streams and the lake brines is principally a result of surface evaporation, and can be followed by using NaCl as a tracer (assuming that NaCl remains in solution until very late in the concentration process). Eugster argues that constituents such as Ca, Mg, HCO_3 and CO_2, SiO_2 and K which are not concentrated to the same degree as NaCl are lost during brine evolution, chiefly by precipitation (or in the case of CO_2, by degassing).

The main mechanism for evaporative concentration proposed by Eugster is the dissolution of efflorescent crusts. These crusts are formed either by the evaporation of runoff, or by capillary evaporation of shallow groundwater. Once formed, only the more soluble constituents of the crusts are dissolved by subsequent contact with dilute rainwater. Thus for example, NaCl and Na_2CO_3 dissolve, while calcite, magnesium calcite, dolomite, silica and silicates remain.

Eugster's postulated circulation system "involves inflow from dilute rim streams descending into the Rift Valley and ephemeral runoff within the valley floor feeding local dilute groundwater bodies. It also stipulates the presence of a hot saline groundwater body at some depth within the trachyte lavas under Lake Magadi]. This body is inferred from the constancy of the spring temperatures over 40 years" (Eugster, 1980).

In order therefore to arrive at the various spring concentrations, composition and temperatures Eugster postulates three sources which are mixed in different proportions for each spring: shallow groundwater (cold, dilute), deep groundwater (hot, saline) and recirculated surface brine (cold, more saline, high pH). The solutes in all three sources originate ultimately by evaporative concentration.

Recently Hillaire-Marcel and Casanova (1987) have used Eugster's model and with the addition of isotopic data have attempted to identify the different types of water in the model. The authors obtained δ^2H and $\delta^{18}O$ values for the lake, for several of the surrounding springs, and for local precipitation.

Hillaire-Marcel and Casanova found a linear relationship between the δ^2H and $\delta^{18}O$ values for the springs and the interstitial lake brine which indicated evaporation. By regressing this line to the World Meteoric Line they obtained an intersection value which they considered to represent the value of deep thermal water. This value is significantly depleted isotopically with respect to the average value for present day recharge and, the authors suggest, represents recharge during the last humid episode in Kenya. This period was determined by Hillaire-Marcel and Casanova as 12 000–10 000 years BP from stromatolite dating, when the lake level was significantly higher than at present.

A study by Crane (1981) has concentrated more on the geothermal aspects of the springs. She compiled thermal, seismic and rainfall data collected over periods of up to 60 years and attempted to correlate spring temperature variation with volcanic, tectonic and meteoric activity.

Crane found that the southern cooler springs have a rapid temperature response to rainfall fluctuations over several decades. She concluded that these springs therefore have a shallow source and, following Eugster's model, that they therefore recirculate lake brines rapidly.

No such relation between temperature and rainfall was evident for the northern springs leading Crane to conclude that these arise from a deep-seated saline water body. She did however attribute temperature variations in the northern springs partially to volcanic activity in Tanzania and suggested that this inferred a greater hydraulic connection with the Rift to the south than with the north. Other temperature variations were postulated by Crane to have been caused by local seismic activity affecting circulation patterns.

The total heat output of the Magadi region was estimated by Crane to be around 900 MW, based on aerial infra-red measurements.

Additional hydrochemical work in the Magadi area was carried out by Glover (1972) who favoured an origin for the springs as locally steam-heated groundwater, and a limited number of stable isotopic analyses (mainly $\delta^{18}O$) have been reported by Panichi and Tongiorgi (1974) and Bwire-Ojiambo (1984).

6.6.3 Sampling

Samples for chemical and isotopic analysis were taken from all the main groups of springs and from several of the minor groups, as shown in Figure 6.17. Samples 1–4 and 5–8 were taken from two groups of hot springs to the north-east and north respectively of Little Magadi. These groups contain the hottest springs found around Lake Magadi, with temperatures of up to 85.3°C. Flow rates of individual springs range up to an estimated 6 l/s. The springs are mainly associated with fault scarps, and some occur within the lagoon.

Samples 9 and 10 were taken from a series of springs and seeps spread over a distance of over a kilometre to the west of the North-West Lagoons. The temperature of the sampled springs, 45°C, was significantly lower than that of the Little Magadi springs and flow rates were also lower, ranging up to 2 l/s for individual springs.

Samples 11 and 12 were obtained from a group of three springs and seep zones on the east side of a small graben to the north of the North-East Lagoon. Spring temperatures were intermediate to the previous groups at 65–67°C and spring discharges totalled 5 l/s.

A small spring group on the edge of Graham's Lagoon producing water at 38–39.5°C was sampled (samples 13 and 14), as was a group of springs further north with low discharge rates and the lowest temperatures recorded—34°C (sample 15).

At the southern end of Lake Magadi by the Bird Rock Lagoon, a group of seeps and small springs (flow rates less than 1 l/s) with temperatures of 40.5–40.8°C were sampled (samples 16 and 17). To the west sample 18 was taken from a powerful set of springs with an estimated total discharge of 100 l/s and a temperature of 45.3°C.

Finally a sample of lake liquor was taken from a point near the causeway (sample 19).

In addition to springs and lakewater samples were taken from the Ewaso Ngiro and Oloibortoto rivers to the west (samples 20 and 21) and from boreholes at Oltepesi and Emerit, about 40 km to the north-east of Magadi, (samples 22 and 23).

6.6.4 Isotopic characteristics

Isotopic determinations ($\delta^{18}O$, $\delta^{2}H$) are listed in Table 6.2 and illustrated in Figure 6.18, which includes for reference the standard World Meteoric Line of Craig (1963) and the Kenya Rift Meteoric Line determined previously (Section 6.4.3).

Ambient water samples

Three samples from rivers near to Magadi are shown in Figure 6.18. Two of the samples were taken from the Ewaso Ngiro River which is the only perennial river in the area; one sample was from the upper reaches of the

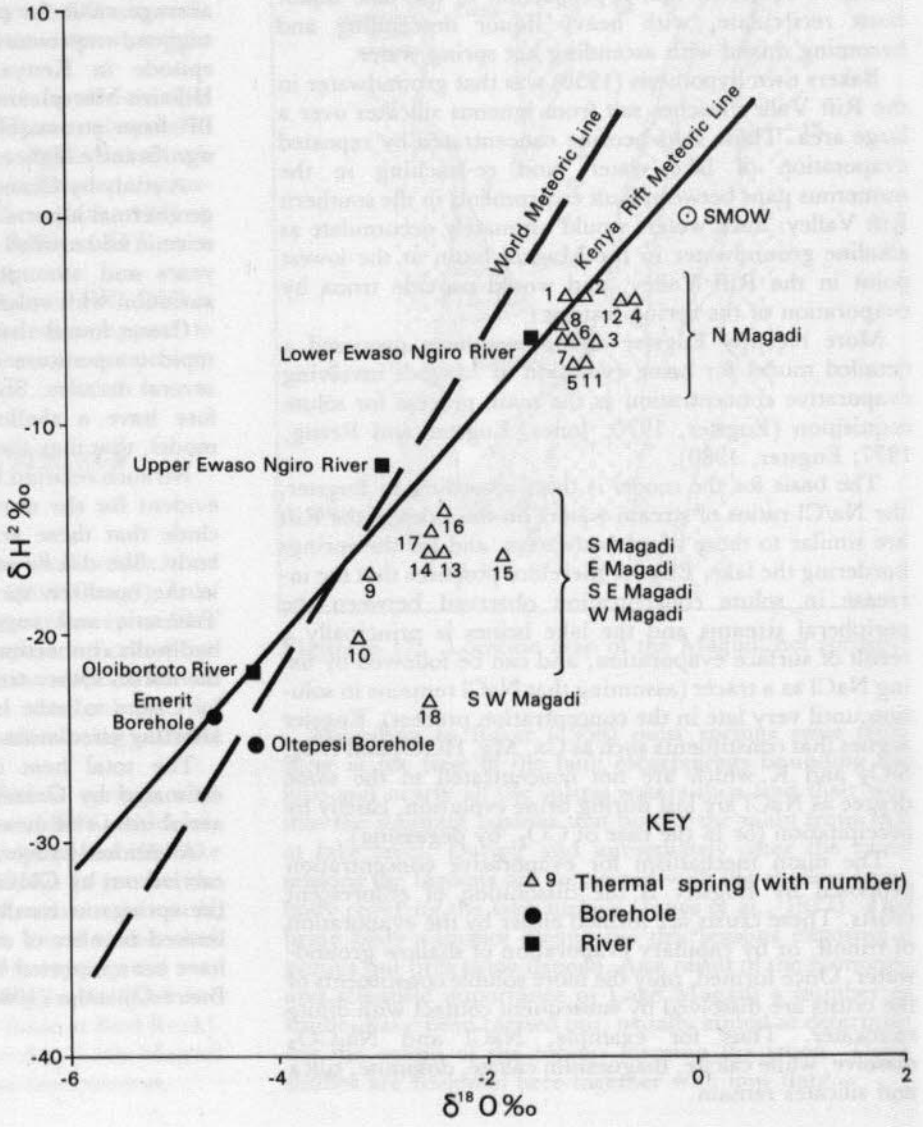

Figure 6.18 Stable isotope characteristics of waters in the Magadi area.

river, near Narok, and the other was taken where the river reaches the Ewaso Ngiro plain at the base of the Nguruman Escarpment. The slope of 4.3 between the two samples' isotopic compositions suggests that evaporation has occurred between the upper and lower reaches of the river, and this is supported by the higher concentration of solutes found in the lower sample.

Thermal springs

The isotopic characteristics of the thermal springs (Figure 6.18) fall mainly into two groups. The northern, hotter springs from the north shores of Little Magadi and the North-Eastern Lagoon form a tight cluster about the local meteoric line, with an average value of $-5‰$ δ^2H and $-1‰$ $\delta^{18}O$ (samples 1–8, 11–12). The cooler spring groups of the North-West Lagoon (samples 9–10) and the spring groups to the east and south east of the lake (samples 13–17) form a looser, more isotopically more depleted cluster near the meteoric line with an average vale of around $-17‰$ δ^2H, $-2.5‰$ $\delta^{18}O$. Sample 18, taken from a powerful warm spring at the southern end of the lake may not form part of this second cluster, being slightly more depleted in deuterium and enriched in ^{18}O.

Many thermal waters throughout the world exhibit a significant increase in $\delta^{18}O$ as a result of interaction with silicates or carbonates at depth, an effect known as the 'oxygen shift'. However the Magadi spring samples show very little evidence of any shift and in fact the hottest springs fall closest to the meteoric line whereas these would be expected to be the most shifted. Hillaire-Marcel and Casanova (1987) suggest that the oxygen shift has indeed occurred, but that isotopically depleted CO_2, associated with the carbonatitic volcanism of the Oldoingo Lengai volcano to the south of Magadi, has mixed with the springwaters and has resulted in depletion by isotopic exchange. However, while it is true that the waters around Magadi are CO_2-rich, the above hypothesis is unnecessary and unproven. Apart from the unlikelihood of waters being shifted away from the meteoric line and then fortuitously back onto it (in the case of the hottest springs) the quantities of CO_2 required to exchange with the springwaters would be enormous. A simpler explanation is that little or no shift has occurred, probably because flow paths and groundwater residence times of the springwaters are too short for exchange to occur.

Another possible mechanism which may have affected the isotopic compositions of the springwaters is evaporation, such as the trend suggested by Hillaire-Marcel and Casanova (1987) and discussed in Section 6.6.2. In general terms it is possible that all values which lie to the right of the Kenya Rift Meteoric Line on Figure 6.18 may indeed lie on an evaporative trend even though they are close to the meteoric line. This is because the Kenya Meteoric Line is itself a reflection of evaporative effects, which is why it departs from the World Meteoric Line.

However the data do not support Hillaire-Marcell and Casanova's contention that all the springs lie on an evaporative trend because the most enriched samples (which would be expected to be the most evaporated) lie closest to the local meteoric line. Also the cooler springs, which according to Hillaire-Marcel and Casanova have mixed with recirculated (and therefore highly evaporated) lake brines should therefore be further along the evaporation trend than the hot brines, which they are not.

Eugster's hypothesis concerning spring evolution depends on evaporation for solute concentration but this is not supported by a plot of Cl^- v. $\delta^{18}O$ (Figure 6.19)

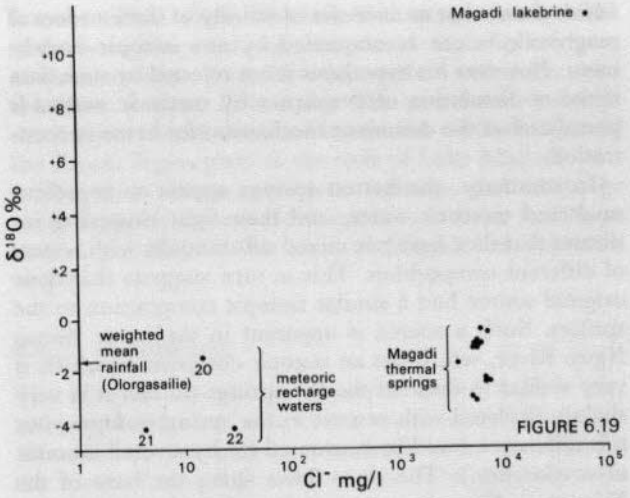

FIGURE 6.19

Figure 6.19 Variation of chloride with $\delta^{18}O$ for Magadi water samples.

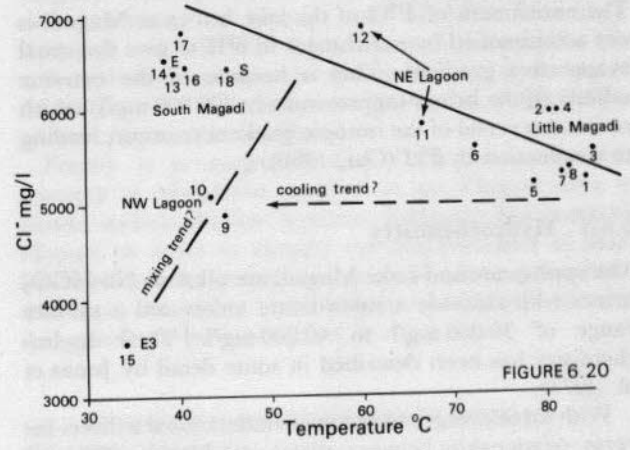

FIGURE 6.20

Figure 6.20 Variation of chloride with temperature for Magadi spring samples.

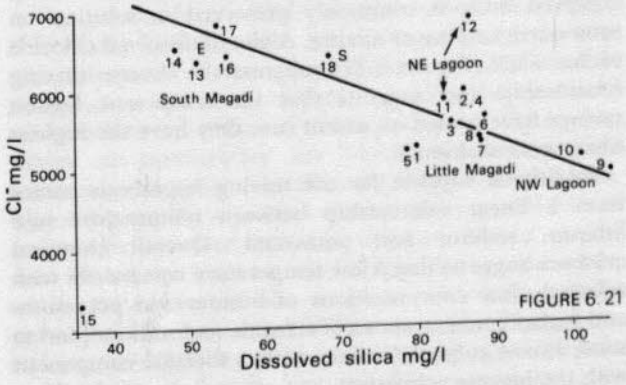

FIGURE 6.21

Figure 6.21 Variation of chloride with silica for Magadi spring samples.

which shows that an increase of salinity of three orders of magnitude is not accompanied by any isotopic enrichment. However his hypothesis is not rejected by such data if the re-dissolution of evaporites by meteoric waters is postulated as the dominant mechanism for brine concentration.

In summary, the hottest springs appear to represent unaltered meteoric water, and their tight clustering indicates that they have not mixed substantially with waters of different composition. This in turn suggests that their original source had a similar isotopic composition to the springs. Such a source is apparent in the lower Ewaso Ngiro River, which has an isotopic composition which is very similar to those of the hot springs (in fact it is very slightly depleted with respect to the spring isotopes, but this difference could be accounted for by a small amount of evaporation). The river flows along the base of the Nguruman Escarpment approximately 20 km to the west of Lake Magadi and is perennial. The postulated recharge mechanism would therefore be via the river alluvium on the Ewaso Ngiro plain.

Lake water

The enrichment of $\delta^{18}O$ of the lake brines at Magadi is not accompanied by enrichment in $\delta^{2}H$ to give the usual evaporative gradient. This is because of the extreme salinity of the brines (approximately 300 000 mg/l) which causes a reversal of the isotopic gradient to occur, leading to a reduction in $\delta^{2}H$ (Gat, 1980).

6.6.5 **Hydrochemistry**

The springs around Lake Magadi are alkaline Na-HCO_3 brines with chloride a subordinate anion and a salinity range of 30 000 mg/l to 40 000 mg/l. Their hydrochemistry has been described in some detail by Jones et al. (1977).

With three exceptions the present data show a direct inverse relationship between dissolved chloride Cl^-, and discharge temperature (Figure 6.20). Sample 15 is interpreted as a local spring at ambient temperature unrelated to the thermal system. This linear relationship between Cl^- and temperature implies that the Magadi springs discharge a mixture of two components. A thermal relatively less saline component appears to mix in varying proportions with a cooler saline component prior to discharge. Samples 9 and 10 which do not appear to conform with this view may be on a cooling trend or a mixing trend.

The dependence of silica solubility on temperature controls the levels of SiO_2 in solution above about 100°C and dissolved SiO_2 is commonly preserved in solution on subsequent cooling or mixing. A plot of dissolved chloride versus silica (Figure 6.21) supports the inverse mixing relationship and suggests that the north-west lagoon springs have cooled on ascent (i.e. they have the highest silica concentrations).

Additional support for the mixing hypothesis comes from a linear relationship between temperature and lithium, sodium and potassium. Overall chemical evidence suggests that a low temperature component with relatively low concentrations of lithium and potassium and higher concentrations of chloride and sodium (and to some extent sulphate) mixes with a thermal component with the inverse properties.

6.6.6 **Discussion**

Lake Magadi lies at the lowest point of the southern Kenya Rift Valley and is therefore the point to which all groundwaters in the Rift from Lake Naivasha southwards are directed. This in turn means that the region is a discharge area and a terminus for solutes leached from the rocks composing the Rift by circulating groundwaters, and the presence of evaporites and saline springs in the area is therefore to be expected, as discussed by Baker (1958).

Various attempts have been made to explain more precisely the mechanism for solute concentration and trona formation, and by far the most detailed and most widely accepted in the literature is that of Eugster et al., based on evaporative concentration.

Eugster's hypothesis hinges on the assumption that Na/Cl ratios remain constant from marginal streams to lake brines. This assumption is well supported by data for the sequence from springs to trona formation; but there are few data for the sequence from marginal streams through groundwaters to springs. Eugster proposes surface and capillary evaporation and dissolution of efflorescent crusts as mechanisms of evaporative concentration (Eugster, 1980). The results of the present study indicate that if Eugster's hypothesis is to be accepted only the dissolution of efflorescent crusts by meteoric waters is a possible mechanism for solute concentration.

Of greater importance to the present study, however are Eugster's proposals, supported by Hillaire-Marcel and Casanova (1987) and Crane (1981) regarding the sources of the waters supplying the Magadi thermal springs. Eugster proposes two cool components (Section 6.6.2) mixing with the thermal component and Crane cites evidence that the cool meteoric component is a relatively shallow system. Data from the present study however indicate essentially a two-component mixing series, with one cool saline end-member and a hot less saline end-member. Also, whereas one of Eugster's cool components is recirculated lake brine the present study indicates that the cool end-member shows little of the evaporation that characterises the true lake brines. On the other hand the interstitial lake brines are so saline (with chloride contents ranging between 37 000 mg/l and 96 000 mg/l [Eugster, 1980]) that the ratio of groundwater to lakewater would be high to obtain the salinity of the warm springs (c.7500 mg/l). Eugster's model and the two component mixing model are not necessarily incompatible therefore if a body of ambient groundwater with a salinity of around 7500 mg/l chloride is postulated to exist in the sediments underlying the lake formed by a mixture of meteoric water and either recirculated lakewater or perhaps dissolved evaporites.

Some evidence for the existence of a saline groundwater body is that a borehole drilled to 297 m encountered brines with a salinity of 20 000 mg/l chloride in the lavas beneath the lake (Eugster, 1980). This borehole was stated as being artesian (i.e. indicating upward flow within the lavas towards some discharge area) but no temperature data were given.

The third and geothermally significant component of Eugster's spring model is the proposed hot saline groundwater body with a composition similar to the hottest springs at Little Magadi (i.e. with a chloride content of around 5000 mg/l and a TDS of around 30 000 mg/l). Eugster's evidence for such a body is the constancy of spring temperatures and chemistry over several decades. Paradoxically Crane (1981) presents data of variations in

spring temperature over several decades but concludes that as the hot spring temperatures do not vary with changes in rainfall then they must originate in a deep reservoir.

Data from the present study support Eugster's hot spring source. The chemical data suggest a single end-member source for the hot springs and the clustering of the isotopic data indicate that the hottest springs have not mixed significantly with other waters and therefore represent the hot end-member of the mixing series. If this is so then silica geothermometry may be used to estimate the temperature of the springs at depth (other cation geothermometers cannot be used because of the origin of the solutes). Table 6.15 shows that these temperatures are low, never reaching 150°C. (The highest temperatures estimated by silica geothermometry are in fact those for the two north-west Lagoon samples, which do not fall in the same isotope cluster on Figure 6.18 as the other hot springs, for reasons which are unknown).

An alternative interpretation of the data is raised by Mahon's (1972) suggestion that much of the Rift is underlain by a hot body of water containing a few hundred parts per million of chloride. This view was based on similarities in the chemistry of fluids at Olkaria and hot springs further north near lakes Elmenteita, Bogoria and Baringo. If it were assumed that a hot end-member of the Magadi mixing series existed with a chloride content of 450 mg/l (similar to that found at Olkaria) then this body of water would, from Figure 6.20, have a temperature slightly in excess of 200°C. There is however no direct evidence for any such water in the Magadi area and the hypothesis is regarded as unlikely.

The best indications of the likely source of the Magadi thermal water are provided by the stable isotope data. These show (Figure 6.18) that the water is meteoric but more enriched than the sampled groundwaters (although these were obtained from a significant distance to the north-west). From the available data, the most likely source is the Ewaso Ngiro River which runs along the base of the Nguruman Escarpment some 25 km to the west of Lake Magadi. In this area the Ewaso Ngiro River has undergone some evaporation and is somewhat enriched isotopically, compared with its headwaters. Figure 6.18 shows that its isotopic composition is in fact very close to that of the northern Magadi hot springs and the very small difference in composition could readily be attributed to further evaporation and some mixing with local groundwaters. (Mixing could also explain the displacement of the north-west Lagoon springs from the main hot spring cluster).

It has sometimes been suggested that the Magadi hot springs could have their origin in the groundwater recharge from Lake Naivasha, but this may be refuted on two accounts. Firstly the hot spring stable isotope data show no connection with the highly enriched samples obtained from Lake Naivasha. Secondly isotopic evidence from groundwaters around Lake Naivasha indicates that the lakewater becomes significantly diluted by mixing with local groundwaters within a short distance of the lake, and dilution would increase as the lakewater flowed south. Therefore, while some lakewater may eventually reach the Magadi springs, it would be so diluted as to be unrecognisable.

A more pertinent question therefore is whether the Magadi hot springs have their origin in the mix of waters flowing from the north, or from essentially local sources such as the Ewaso Ngiro and the Nguruman Escarpment, and in the absence of other data the isotopic evidence favours a local origin. The lack of an oxygen isotope shift in the hot springs also suggests a local origin by implying a short contact time between water and rock, and therefore a short flow path. The postulated recharge mechanism would therefore be via the river alluvium of the Ewaso Ngiro plain to the west of Lake Magadi.

The short distance between recharge and discharge areas suggests a convective cell driven by a local heat source probably to the west of Magadi. of unknown origin.

6.6.7 Conclusions

The Magadi hot springs appear to derive from a hot, saline groundwater body with a temperature of between 100–150°C. Recharge is considered to be provided by the lower Ewaso Ngiro River and local groundwaters derived from the sides of the Rift, with cold waters percolating through the river alluvium and underlying volcanics and rising, after being heated, via active grid faults around Lake Magadi. The heat source for the springs is probably local and lies to the west of Lake Magadi. Although the heat output of the springs is significant (estimated as greater than 250 MW from their discharge, and 900 MW from infra-red analysis) the low indicated reservoir temperature would rule out the use of the resource for electrical power generation unless binary systems were to be considered.

Finally it is suggested that if further geothermal research is considered justified in the Magadi area it should include shallow borehole drilling to the north of Magadi in order to identify the characteristics of fluid flowing from the north, and geophysical work/borehole drilling to the west of Little Magadi to attempt to identify the postulated thermal upflow in this area.

6.7 SUMMARY OF HYDROGEOLOGICAL OBSERVATIONS

On a regional scale the Rift Valley between Lakes Nakuru and Magadi broadly exhibits the hydrogeological features expected of a Valley–interfluve system with lateral groundwater flows from the Rift escarpments to discharge areas on the Rift floor, and axial groundwater flows away from the Rift floor culmination at Lake Naivasha. This model is modified by the presence of the major Rift faults, which act as barriers to lateral flow, leading to longer, deeper, flow paths, and by the grid faulting in the Rift floor which tend to align flow paths within the Rift along its axis.

The permeabilities of the volcanic rocks underlying the Rift Valley are generally low, although there is considerable local variation. Aquifers are normally found in fractured or reworked volcanics, or along the weathered contacts between different lithological units. The highest values of permeability are found in the reworked volcanics composing the sediments of the Naivasha area, where the specific capacities of wells often exceed 3 l/s/m and where estimated hydraulic conductivities of greater than 10 m/d are common. In the Rift floor to the north, where the sediment size decreases, borehole specific capacities fall, to around 0.3 l/s/m in the Elmenteita-Nakuru area (leading to an estimated average hydraulic conductivity of 2 m/d). On the Rift escarpments the permeabilities of the different rock types are uniformly low. Mean borehole specific capacities and estimated hydraulic conductivities range from 0.03 l/s/m and

Table 6.16 Gas geothermometer temperatures for fumaroles in the Suswa, Longonot, Olkaria-Domes and Eburru sector of the Rift Valley

Site No.	Locality	t CO_2/H_2	t CO_2/CH_4	t CO_2[1]
29/F-27	Mt Margaret	—	330	423
31/H-1	Akira Ranch	—	314	246
44–47	Lorusio Springs[2]	246	338	—
53–54	Bala Springs[2]	—	314	—
110	Olkaria OW2	—	308	—
111	Olkaria OW26	—	322	—
119	Eburru EF-2	256	296	—
123	W. Olkaria	—	400	—
124	Soysambu DEL[2]	—	319	—
126	Suswa, rim	—	384	324
127	Domes	—	313	316
127/F-15	Domes	—	320	
128	Longonot, crater	256	311	409
128/F-23	Longonot, crater	255	315	
F-7	Suswa, caldera floor	—	307	303
F-12	Suswa, ring graben	—	324	298
F-28	Suswa, central island	—	316	370
K-1	Meru, Chogoria	—	315	—
K-2	Meru, Chogoria	—	383	—

1 Figures from Armannsson (1987b) for directly-calculated CO_2 geothermeter
2 Gas samples collected from water
Samples with F, H and K prefixes collected by Dr H Armannsson of the UNDP

0.1 m/d for the South Kinangop Pyroclastics to 0.2 l/s/m and 1.1 m/d for the Rift Escarpment Trachyte to the east of Suswa and the Mau Forest pyroclastics.

These figures are only applicable to the drilled depths of the boreholes, normally less than 250 m. Below this depth permeabilities will fall, mainly as a result of the closure of fissures by overburden stresses. The only available data for permeability at depth are from the Olkaria Geothermal Field where values of around 5 mD have been found, equivalent to a cold water hydraulic conductivity of about 3×10^{-3} m/d. Simple modelling in the present study has suggested an upper limit of 0.1 m/d for rocks at depth in the Naivasha area.

Preliminary estimates of subsurface flows from the Naivasha catchment suggest that the amount contributed by Lake Naivasha is around 50×10^6 m^3/y (which is 20% of the total recharge estimated by a previous water balance study). Flow to the south via relatively shallow aquifers (i.e. at depths of less than about 500 m) may be the most significant route for water flow from the catchment, accounting for perhaps 50 to 90% of the total.

Chemical data obtained during the present study have enabled the model of the ambient flow systems to be refined. Stable isotope determinations on samples of rainfall taken over a wide area have enabled an isotopic meteoric line for the Rift to be constructed which is similar to the trend for ambient and slightly thermal groundwaters. In addition an approximate correlation of isotopic composition with height has been found. This correlation suggests that much of the groundwater in the Naivasha–Nakuru area is relatively local in origin, an interpretation which is supported by inert gas data (which indicates recharge temperatures similar to local ambient values) and recent ^{14}C ages. The implication is that deep components of flow are not important in the shallow hydrology of the Rift floor, and therefore supports the contention that permeabilities at depth are low.

The most important result of the chemical analyses with regard to ambient (and geothermal) water flows in the Study Area of the Rift is the tracing of water from Lake Naivasha using stable isotope data. River water entering the Lake has a very depleted composition indicative of its origin at high altitudes (principally in the Nyandarua Mountains). Meteoric water entering the lake directly has a less-depleted composition similar to that of local groundwaters. However the lake itself is highly enriched by virtue of the intense evaporation to which it is subjected. Enriched lakewater flowing both to the north and to the south can therefore be detected in groundwater and geothermal fluid samples by stable isotope analysis. By this method it has been shown that Lake Naivasha water flows northwards via Gilgil—but not apparently under Eburru—at least as far as Lake Elmenteita, where it is estimated to form 30% of the discharge of warm springs bordering the lake.

To the south a component of Naivasha lakewater has been detected as far as Suswa, but there is no evidence that it reaches Lake Magadi in an identifiable form.

The interpretation of geochemical analyses of geothermal fluids from Eburru, Olkaria, Longonot and Suswa has led to the important conclusion that all the fluids can be explained in terms of a mixing series between Rift-wall meteoric water and water from Lake Naivasha and that there is no evidence of a unique deep thermal water. At Eburru, analysis of fumarole condensates and gases indicates that the steam is basically primary and is derived from local Rift-wall groundwater; well and spring-waters to the north of Eburru show evidence of outflow of geothermal fluids in this direction. At Olkaria the wellfield shows evidence of a 55–75% lakewater component mixing with Rift-wall groundwater; fumaroles in the Domes area further east indicate a smaller but significant (>30%) lakewater contribution, and fumaroles in Longonot crater, east of the Domes, show only traces of lakewater. Between Longonot and Mt Margaret, fumaroles show no evidence of lakewater influence. The Suswa area shows evidence of lakewater, but only in fumaroles in the ring graben and central island (where however a substantial contribution (30%) of lakewater has been detected).

Further south, at Magadi, the hot springs are considered to derive from a hot saline groundwater body, originating as a mixture between recharging waters from the lower Ewaso Ngiro River and local groundwaters. No evidence of the presence of Naivasha lakewater has been found.

Further north, geochemical sampling of the Lake Bogoria and Lake Baringo thermal systems tends to con-

firm that lakewater mixing is involved, although at Baringo this appears to take place in an unexpected manner. The Kapedo and Lorusio springs north of Lake Baringo are not obviously affected by subsurface outflow from the lake.

There is no evidence in any of the geothermal fluids sampled of a $\delta^{18}O$ shift of the magnitude commonly seen in other geothermal systems. This could be due to rapid transit times, or to equilibration of rock and water $\delta^{18}O$ values, but too little is yet known of rock $^{18}O/^{16}O$ values to understand which process is involved.

Gases in the geothermal fluids are dominated by crustally derived CO_2 usually followed by CH_4—although at a much lower level. (There is also evidence of a pervasive CO_2 flux over much of the Rift which is unrelated to specific geothermal fields). The presence of He and H_2—regarded as indicators of upflow conditions—has been confirmed at Eburru and at Longonot. High $^3He/^4He$ ratios, taken to represent evidence of the transport of mantle helium, are found at Eburru, Longonot and Olkaria. The ratio of C_2H_6/CH_4 may be an index of lakewater contribution to groundwaters and geothermal fluids and is found to vary with distance from Lake Naivasha, thus supporting the mixing model.

The use of chemical geothermometers in the Rift has met with variable success. In the Olkaria geothermal field quartz, alkali and gas geothermometers give plausible temperatures. However in the other thermal areas there are few opportunities to sample hot water, and the gas geothermometers are often problematic; the ratio types commonly cannot be used because of the scarcity of H_2 and H_2S in fumarolic gases. At Magadi the highly alkaline nature of the springs precludes the use of the alkali geothermometers, although those based on quartz seem to be reliable. Ambient or slightly thermal waters elsewhere in the study area often give excessive indications of temperature which are unsupported by other evidence.

Two thermal areas, Olkaria and Magadi were examined in some detail during the study. At Olkaria the results support the conclusion of other workers that the present wellfield is situated somewhat to the south of a thermal upflow. Also there are indications that short flow paths may be involved, and that the system may be quite old. At Magadi it is concluded that the thermal springs are formed by a two-component mixing series, probably with a local heat source, and that the hot end member is at a temperature of 100–130°C.

With regard to the warm springs found at various points along the Rift margins, there is no indication that these are anything other than local phenomena associated with Rift faults and result from deep groundwater circulation under ambient geothermal gradients. The geothermal potential of these springs is therefore low.

7 CONCLUSIONS

In summary, the main conclusions of this study are that the geothermal areas at Eburru, Olkaria-Domes, Longonot, Suswa and Magadi are individual fields where local heat sources set up convective cells which circulate fluids which originate as mixtures of ambient groundwaters and Naivasha Lakewater (or in the case of Magadi, probably a mixture of groundwater and recharging river water). There is no evidence of a deep thermal fluid pervasive over large areas of the Rift—chemical similarities between geothermal fluids from different areas are caused by similar groundwaters reacting with similar rock types. Thermal areas north of Nakuru (Bogoria, Baringo, Kapedo and Lorusio) though sampled in much less detail during this study, are considered to have a fundamentally similar mode of origin.

It is also tentatively concluded from the limited available data that recharge into the Naivasha catchment should be ample to sustain production from geothermal fields bordering the catchment—however a thorough water balance study would be needed to be certain of this. Further south, groundwater conditions around Suswa are virtually unknown, and therefore the availability of recharge is speculative. There are indications however of at least some hydraulic connection with the Naivasha catchment.

It is recommended therefore that future exploration should concentrate on areas where high temperatures and thermal upflow conditions are expected, and present data suggest that these are to be found principally at Olkaria, Longonot and probably Suswa. Magadi appears to have limited potential in view of the low temperatures indicated—although the heat output from the area is high. Areas of outflow from the fields, that is to the north of Eburru and to the south of Olkaria, Longonot and Suswa are expected to possess less significant geothermal potential, as are areas between the fields.

The most likely areas for the discovery of new resources are within or adjacent to large ring structures.

ACKNOWLEDGEMENTS

The BGS residential and short term experts greatly benefitted from the presence of UNDP and Government of Italy personnel working on adjacent areas under the coordination of Mr G Gislason. The support of Mr J K Kinyariro, counterpart Team Leader, is also gratefully acknowledged. The Kenyan technical assistants Mr B Macharia and Mr P Mwangi are especially thanked for their unfailing support at all times.

REFERENCES

ACRES. 1987. Kenya National Power Development Plan 1986–2006. Prepared for joint world bank/UNDP energy sector management assisstance programme by Acres International Ltd. June 1987.

ALLEN, D J, DARLING, W G, and BURGESS, W G. 1989. Geothermics and hydrogeology of the southern part of the Kenya Rift Valley with emphasis on the Magadi–Nakuru area. *British Geological Survey Research Report*, SD/89/1.

ANDREWS, J N, and KAY, R L F. 1982. Natural production of tritium in permeable rocks. *Nature, London*, Vol. 298, 361–363.

ARMANNSSON, H. 1987a. Geochemistry of steam in the Suswa and Longonot geothermal areas. Technical Report. Project KEN/82/002. United Nations Department of Technical Co-operation for Development.

— 1987b. Studies on the geochemistry of steam in the Suswa and Longonot areas and water in the Lake Magadi, Kedong Valley and Lake Turkana areas, Rift Valley, Kenya. Final Technical Report. Project KEN/82/002. United Nations Department of Technical Co-operation for Development.

ARNASON, B. 1977. The hydrogen and water isotope thermometer applied to geothermal areas in Iceland. *Geothermics*, No. 5, 125–151.

ARNORSSON, S, and GUNNLAUGSSON, E. 1985. New gas geothermometers for geothermal exploration—calibration and application. *Geochimica et Cosmochimica Acta*, Vol. 49, 1307–1325.

ASE, L E, SERNBO, K, and PER, S. 1986. Studies of Lake Naivasha, Kenya, and its drainage area. Stockholms Universitet Naturgeografiska Institutionen 106 91 Stockholm.

BAILEY, D K. 1980. Volcanism, Earth degassing and replenished lithosphere mantle. *Philosophical Transactions of th Royal Society London*, A297, 309–322.

BAKER, B H. 1958. Geology of the Magadi Area. *Report Geological Survey of Kenya*, No. 42.

— MOHR, P A, and WILLIAMS, L A J. 1972. Geology of the Eastern Rift System of Africa. *Geological Society of America Special Paper*, No. 136. 67 pp.

— WILLIAMS, L A J, MILLER, J A, and FITCH, F J. 1971. Sequence and geochronology of the Kenya Rift volcanics. *Tectonophysics*, Vol. 11, 191–215.

— and MITCHELL, J H. 1976. Volcanic stratigraphy and geochronology of the Kedong-Olorgesaile area and the evolution of the South Kenya rift valley. *Journal of the Geological Society of London*, Vol. 132, 467–484.

— — and WILLIAMS, L A J. 1988. Stratigraphy, geochronology and volcano-tectonic evolution of the Kedong–Naivasha–Kinangop region, Gregory Rift Valley, Kenya. *Journal of the Geological Society of London*, Vol. 145, 107–116.

BONE, B D. 1988. The geological evolution of the SW Naivasha Volcanic Complex, Kenya. Unpublished PhD thesis, University of Reading.

BENNION, D W, and GRIFFITHS, J C. 1966. A stochastic model for predicting variations in reservoir rock properties. *Transactions American Institute of Mining Engineers*, Vol. 237, 9–16.

BLISS, C M. 1979. Geology and petrochemistry of the Naivasha area, Kenya Rift Valley. Unpublished PhD thesis, University of Lancaster.

BODVARSSON, S, PRUESS, K, STEFANSSON, V, BJORNSSON, S, and OJIAMBO, S B. 1987. East Olkaria Geothermal Field, Kenya. 1: History Match With Production and Pressure Data Decline. *Journal of Geophysical Research*, Vol. 92, No. B1, 521–539.

BROWNE, P R L. 1984. Subsurface stratigraphy and hydrothermal alteration of the eastern section of the Olkaria Geothermal Field, Kenya. *Proceedings 6th New Zealand Geothermal Workshop, Auckland, N.Z.*, 33–41.

BURKE, K, and DEWEY, J F. 1973. Plume generated triple junctions—key indicators in applying plate tectonics to old rocks. *Journal of Geology*, Vol. 81, 406–433.

BUTZER, K W, ISAAC, G L, RICHARDSON, J L, and WASHBOURNE-KAMAU, C. 1972. Radiocarbon dating of East African lake levels. *Science*, No. 175, 1069–1076.

BWIRE-OJIAMBO, S. 1984. Isotope hydrogeochemistry of Lakes Elmenteita and Naivasha catchment areas. Unpublished paper to Olkaria review meeting, Nairobi December 1984. 8 pp.

CLARKE, M C G. 1987. Compilation and interpretation of rock geochemical data for the Longonot Volcano and the greater Olkaria Volcanic Complex. *BGS Rep. Genken/5.*

CRAIG, H. 1963. 17–53 in '*Nuclear geology on geothermal areas*', (E Tongiorgi, editor). (Consiglio Nazionale della Richerche, Lab. di Geol. Nucl. Pisa.)

— LUPTON, J E, and HOROWITZ, R M. 1977. Isotope geochemistry and hydrogeology of geothermal waters in the Ethiopean Rift Valley. Scripps Institute of Oceanography. Ref. No. 77–14. University of California, San Diego.

— 1978. Helium isotope variations: evidence for mantle plumes at Yellowstone, Kilauea, and the Ethiopian Rift Valley. EOS, Transactions American Geophysical Union, 59, 1194. Helium isotope ratio in Yellowstone and Lassen Park volcanic gases. *Geophysical Research Letters*, No. 5, 897–900.

CRANE, K. 1981. Thermal variations in the Gregory Rift of southern Kenya. *Tectonophysics*, Vol. 74, 239–262.

D'AMORE, F, FERRARA, G C, NUTI, S, and SABROUX, J C. 1987. Variations in radon-222 content and its implications in a geothermal field. International Congress on Thermal Waters, Athens, Oct. 1975. 184–200.

— 1976. Radon-222 survey in Larderello Geothermal Field, Italy (Part 1). *Geothermics*, Vol. 4, No. 1–4.

DANSGAARD, W. 1964. Stable isotopes in precipitation. *Tellus*, No. 16, 436.

DARLING, W G, and ARMANNSSON, H. In preparation. Stable isotopic aspects of fluid flow in the Krafla, Namafjall and Theistareykir geothermal systems of north-east Iceland.

— BATH, A H, and BRUNSDON, A P. 1982. Revised procedures for the measurement of $^{2}H/^{1}H$ and $^{18}O/^{16}O$ in water samples. *BGS Hydrogeology Group Stable Isotope Technical Report*, No. 16.

— and LARDNER, A J. 1985. The effect of altitude on the stable isotope composition of rainfall in the Balquhidder research catchments. *BGS Hydrogeology Research Group Stable Isotope Technical Report*, No. 27.

EUGSTER H P. 1970. Chemistry and origin of the brines of Lake Magadi, Kenya. *Mineralogical Society of America Special Paper*, No. 3, 215–235.

— 1980. Lake Magadi, Kenya, and its precursors. In '*Developments in sedimentology*', 28, Hypersaline brines and evaporitic environments. A. Nissenbaum (editor). (Elsevier.)

FAIRHEAD, J D. 1976. The structure of the lithosphere beneath the eastern rift, East Africa. Deduced from gravity studies. *Tectonophysics*, No. 30. 269–298.

— 1986. Geophysical controls on sedimentation within the African Rift systems. 19–27 in Sedimentation in the African Rifts. *Special Publication of the Geological Society of London*, No. 25.

FISHER, R V. 1979. Models for pyroclastic surges and pyroclastic flows. *Journal of Volcanology and Geothermal Research*, Vol. 6, 305–318.

— and SCHMINCKE, H-U. 1984. Pyroclastic rocks. (Berlin: Springer-Verlag.)

FITTON, I, and UPTON, B G J. 1987. Alkaline igneous rocks. *Special Publication of the Geological Society of London*, No. 30.

FORTEY, N J, BEDDOE-STEPHENS, B, MILODOWSKI, A, and NANCARROW, P H A. 1986. Petrography of lithic clasts and other rocks from Longonot, Kenya. *BGS Mineralogy and Petrology Report*, No. 86/30. Nov. 1986.

FOURNIER, R O, and POTTER, R W. 1979. Magnesium correction to the Na-K-Ca chemical geothermometer. *Geochimica et Cosmochimica Acta*, Vol. 43, 1543–1550.

FREEZE, R A, and CHERRY J A. 1979. Groudwater. 604 pp. (Prentice-Hall.)

GAT, J R. 1980. Isotope hydrology of very saline lakes. Chapter 1 *in* 'Hypersaline brines and evaporitic environments.' NISSENBAUM, A (editor). *Developments in Sedimentology*, No. 28.

GENZL. 1986. Olkaria and Eburru Geothermal Development. Unpublished report prepared for the Kenya Power Company Ltd., by Geothermal Energy New Zealand Ltd., Nov. 1986.

GEOTERMICA ITALIANA SRL. 1987. Geothermal Reconnaissance Survey in the Menengai-Bogoria Area of the Kenya Rift Valley. Final Draft Report Part IV —Hydrogeology. TCD CON 7/85 KEN 82/002.

GLOVER, R B. 1972. Chemical characteristics of water and steam discharges in the Rift Valley of Kenya. Unpublished Report to the UNDP. 56 pp.

GRANT, M A, and WHITTOME, A J. 1981. Hydrology of Olkaria Geothermal Field. *Proceedings 3rd New Zealand Geothermal Workshop, Auckland N.Z.*, 125–129.

HAUKWA, C B. 1984. Recent measurements within Olkaria East and West Fields. Paper for Kenya Power Company Scientific and Technical Review Meeting. 13 pp.

— 1986. Interpretation of well measurements for exploration areas and reservoir changes in Olkaria East Field. Paper for Kenya Power Company Scientific and Technical Review Meeting. 11 pp.

HEALEY, J. 1972. Technical Review. Rept. to UN/EAPL Geothermal Resources Exploration Project Review Meeting. Dec. 1972. (Unpublished.)

HILLAIRE-MARCEL, C, and CASANOVA, J. 1987. Isotopic hydrology and paleohydrology of the Magadi (Kenya) – Natron (Tanzania) basin during the late Quaternary. *Palaeogeography, Palaeoclimatology, Palaeoecology*, Vol. 58, 155–181.

HULSTON, J R. 1977. Isotope work applied to geothermal systems at the Institute of Nuclear Sciences, New Zealand. *Geothermics*, Vol. 5, 89–96.

JICA. 1983. Pre-feasibility study report for the Rift Valley Geothermal Development Project in the Republic of Kenya. Japan international cooperation agency unpublished report.

JONES, B F, EUGSTER, H P, and RETTIG, S L. 1977. Hydrochemistry of the Lake Magadi basin, Kenya. *Geochimica et Cosmochimica Acta*, Vol. 44, 53–72.

KAGASI. 1983. The volcanic petrology and geological structures of Mt.Margaret–Kijabe Hill area, Kenya Rift Valley. Unpublished MSc thesis, University of Nairobi.

KAMAU, C. 1974. The Lake Naivasha Basin. Report Geography Department Nairobi University.

KHAN ET AL. 1988. Geology today.

KING, B.C. 1978. Structural and volcanic evolution of the Gregory Rift Valley. 29–54 in *Geological background to fossil man.* W W Bishop (editor). (Scottish Acad. ress.)

LEAT, P T, MACDONALD, R, and Smith, R L. 1984. Geochemical evolution of the Menengai Caldera Volcano, Kenya. *Journal of Geophysical Research*, Vol. 89 (B10), 8571–8592.

LE BAS, M J. 1978. *Carbonatite–nephelinite volcanism.* 347 pp. (John Wiley and Sons.)

— — ET AL. 1986. A chemical classification of volcanic rocks based on the total alkali-silica diagram. *Journal of Petrology*, Vol. 27, Pt. 3, 745–750.

LOGAN, J. 1964. Estimating transmissibility from routine production tests of water wells. *Groundwater*, Vol. 2, No. 1, 35–37.

MACDONALD, R. 1974. Nomenclature and petrochemistry of the peralkaline oversaturated extrusive rocks. *Bulletin of Volcanology*, Vol. 38, 498–516.

— DAVIES, G R, BLISS, C M, LEAT, P T, BAILEY, D K, and SMITH, R L. 1987. Geochemistry of high silica peralkaline rhyolites, Naivasha, Kenya Rift valley. *Journal of Petrology*, Vol. 28, Pt. 6, 979–1008.

— and BAILEY, D K. 1973. Chemistry of igneous rocks, Part 1. The chemistry of the peralkaline oversaturated obsidians. *Professional Paper, US Geological Survey*, No. 440, N1–37.

MAHON, W A J. 1972. The general geochemistry of the Rift Valley of Kenya, Lake Baringo to Lake Magadi, and the geochemistry of Olkaria, Eburru and Lake Hannington geothermal prospects. Technical Review Meeting Report. United Nations Geothermal Resources Exploration Project.

MASON, J E. 1967. Geothermal occurrences and investigations in the central Rift valley, Kenya. Unpublished Report of the Mines and Geology Dept., Kenya.

MAZOR, E. 1977. Geothermal tracing with atmospheric and radiogenic noble gases. *Geothermics*, Vol. 5, 21–36.

McCall, G.J.H. 1957. Geology and groundwater conditions in the Nakuru area. Ministry of Works (Hydraulic Branch) Technical Report No. 3.

MCCALL, G J H. 1967. Geology of the Nakuru-Thompson's Falls-Lake Hannington area. *Report Geological Survey of Kenya*, No. 78.

MCCANN, D L. 1972. A preliminary hydrogeologic evaluation of the long-term yield of catchments related to the geothermal prospect areas in the Rift Valley of Kenya. Unpublished UN Report. 23 pp.

— 1974. Hydogeologic investigation of the Rift Valley catchments. Unpublished UN Report. 47 pp.

NAYLOR, W I. 1972. Geology of the Eburru and Olkaria Geothermal prospects. Unpublished UNDP/EAPL Geothermal Exploration Project Report.

NDOMBI, J M. 1981. The structure of the shallow crust beneath Olkaria geothermal field, Kenya, deduced from gravity studies. *Journal of Volcanology and Geothermal Research*, Vol. 9, 237–251.

NIER, A O. 1950. A redetermination of the relative abundances of the isotopes of carbon, nitrogen, oxygen, argon and potassium. *Physics Review*, Vol. 77, 789.

NOBLE, J W, and OJIAMBO, S B. 1975. Geothermal exploration in Kenya. *Second U.N. Symposium, Development and use of Geothermal Research, San Francisco, California, U.S.A.*, Vol. 1. 189–204.

ODONGO, M E O. 1982. Petrogaphy of well samples from the Olkaria Geothermal Field—its use as a tool in geothermal resource development. Proceedings of the Regional Seminar on Geothermal Energy in E and S Africa. 15–21. Nairobi. UNESCO/USAID 76–79.

— 1984. Geology of Olkaria Geothermal field. The Kenya Power Co. Ltd Geothermal Project, Kenya. Report No. GL/OW/020.

OGOSO-ODONGO, M E. 1986. Geology of the Olkaria geothermal field. *Geothermics*, Vol. 15, No. 5/6, 741–748.

PACES, T. 1975. A systematic deviation from the Na-K-Ca geothermometer below 75 C and above 10^{-4} atm P_{CO2}. *Geochemica et Cosmochimica Acta*, Vol. 39, 541544.

PANICHI, C, and TONGIORGI, E. 1974. Isotopic study of the hot water and steam samples of the Rift Valley, Kenya. Unpublished report to the U.N.D.P. 56 pp.

PARKINSON, J. 1914. The East African Trough in the neighbourhood of the soda lakes. *Geographical Journal*, Vol. 44, 33–49.

PULFREY, W. 1960. Shape of the submiocene erosion bevel in Kenya. *Bulletin Geological Survey of Kenya*, No. 3.

RICHARDSON, J L. 1966. Changes in level of Lake Naivasha, Kenya, during postglacial times. *Nature, London*, Vol. 209, No. 5020, 290–291.

RICHARDSON, J L. 1972. Palaeolimnological records from Rift Valley lakes in central Africa. 131–136 in *Palaeoecology of Africa, the surrounding Islands and Antarctica.* Zinderen Bakker Sr (editor). (Cape Town: E.M. van Balkema.)

SCOTT, S C. 1977. The volcanic geology and petrology of Mt. Longonot, central Kenya. Unpublished PhD Thesis, University of Reading.

— 1980. The geology of Mt. Longonot Volcano, central Kenya; a question of volumes. *Philosophical Transactions of the Royal Society, London*, Vol. 296, (A.1420), 437–465.

— 1982. Evidence from Longonot volcano, central Kenya, lending further support to the argument for a coexisting CO_2 rich vapour in peralkaline magma. *Geological Magazine*, Vol. 119, No. 2, 215–217.

— and BAILEY, D K. 1986. Coeruption of contrasting magmas and temporal variations in magma chemistry at Longonot Volcano, central Kenya. *Bulletin of Volcanology*.

SHACKLETON, R M. 1951. A contribution to the geology of the Kavirondo Rift Valley. *Quarterly Journal of the Geological Society of London*, Vol. 106, 345–389.

STEVENS, J A. 1932. Lake Magadi and its alkaline springs. Unpublished report to the Magadi Soda Co. Ltd., Kenya.

SUTHERLAND, D S. 1974. Petrography and mineralogy of the perakaline silicic rocks. *Bulletin Volcanology*, Vol. 38. 517–547.

TANNER, A B. 1964. Radon migration in the ground: a review. 161–190 in *The natural radiation environment.* Adams, J A S, and Lowder, W M (editors). (Chicago University Press.)

THIEM, G. 1906. *Hydrologische Methoden*. 56 pp. (Leipzig: Gebhardt.)

THOMPSON, A O. 1964. Geology of the Kijabe Area. *Report of the Geological Survey of Kenya*, No. 67.

— and Dodson, R G. 1963. Geology of the Naivasha area. *Report Geological Survey of Kenya*, No. 55.

TOBIN, D G, WARD P L, and DRAKE, C L. 1969. Micro-earthquakes in the Rift Valley of Kenya. *Geological Society of America Bulletin*, Vol. 80, 2043–2046.

TOLE, M P. 1986. Investigation of low enthalpy occurrences in Kenya. Unpublished UNDP report, Nairobi.

TORFARSON, H. 1987. Geothermal and geological survey of Mt Suswa, Kenya. Final Technical Report. DTCD-UNDP Exploration for geothermal energy project.

TRUESDELL, A H. 1975. Geochemical techniques in exploration. 53–86 *in* Proceedings of the Second United Nations Symposium on the development and use of Geothermal Resources, Vol. 1.

VOGEL, A I. 1961. A tetbook of quantitative inorganic analysis (3rd. edition). (London: Longmans.)

WARREN, J E, and PRICE, H S. 1961. Flow in heterogeneous porous media. *Journal Society of Petroleum Engineers*, Vol. 1, 153–169.

WASHBOURNE-KAMAU, C. 1970. Late quaternary lakes in the Nakuru-Elmenteita Basin, Kenya. *Geographical Journal London*, Vol. 137, 522–535.

WENDLANDT, R F, and MORGAN, P. 1982. Lithosphere thinning associated with rifting in East Africa. *Nature, London*, Vol. 298, 734–736.

WHITEHEAD, N E. 1980. Radon measurements at three New Zealand geothermal areas. *Geothermics*, Vol. 9, 279–286.

WILLIAMS, L A J. 1978. The volcanological development of the Kenya Rift. In *Petrology and geochemistry of Continental rifts.* N R Neumann, and I Ramberg (editors). NATO adv. study series. D Reidel, Dordrecht, Holland. Wohletz and Sheridan, 1983.

WINDLEY, B F. 1984. *The evolving continents* (2nd edition). (Chichester: Wiley.)

MINISTRY OF ENERGY

Minister: Hon. K. N. K. Biwott

Permanent Secretary: Mr C. N. Mutitu

This report presents the results of a joint Kenya–British technical co-operation project carried out in 1985–88 for the Kenya Government by staff of the Kenya Ministry of Energy and for the British Government by the British Geological Survey funded by the British Overseas Development Administration. The project is part of an ongoing programme of exploration for geothermal energy being undertaken by the Kenya Government.

MINISTRY OF ENERGY

BRITISH GEOLOGICAL SURVEY

Printed in England by Derry and Sons Limited,
Nottingham